

## **INFORMATION TO USERS**

This manuscript has been reproduced from the microfilm master. UMI films the text directly from the original or copy submitted. Thus, some thesis and dissertation copies are in typewriter face, while others may be from any type of computer printer.

**The quality of this reproduction is dependent upon the quality of the copy submitted.** Broken or indistinct print, colored or poor quality illustrations and photographs, print bleedthrough, substandard margins, and improper alignment can adversely affect reproduction.

In the unlikely event that the author did not send UMI a complete manuscript and there are missing pages, these will be noted. Also, if unauthorized copyright material had to be removed, a note will indicate the deletion.

Oversize materials (e.g., maps, drawings, charts) are reproduced by sectioning the original, beginning at the upper left-hand corner and continuing from left to right in equal sections with small overlaps.

**ProQuest Information and Learning  
300 North Zeeb Road, Ann Arbor, MI 48106-1346 USA  
800-521-0600**

**UMI<sup>®</sup>**

**DISSERTATION**

**STUDIES TOWARDS THE SYNTHESIS OF TREHALAMINE AND  
THE EFFECT OF ADJACENT CHIRAL TERTIARY AND QUATERNARY  
CENTERS ON THE METAL-CATALYZED ALLYLIC SUBSTITUTION REACTION**

**Submitted by**

**Holly Lynn Sebahar**

**Department of Chemistry**

**In partial fulfillment of the requirements**

**for the Degree of Doctor of Philosophy**

**Colorado State University**

**Fort Collins, Colorado**

**Summer 2002**

UMI Number: 3064011

**UMI<sup>®</sup>**

---

UMI Microform 3064011

Copyright 2002 by ProQuest Information and Learning Company.  
All rights reserved. This microform edition is protected against  
unauthorized copying under Title 17, United States Code.

---

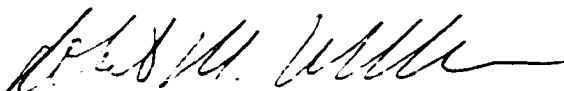
ProQuest Information and Learning Company  
300 North Zeeb Road  
P.O. Box 1346  
Ann Arbor, MI 48106-1346

COLORADO STATE UNIVERSITY

March 26, 2002

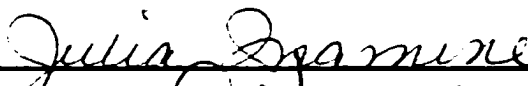
WE HEREBY RECOMMEND THAT THE DISSERTATION PREPARED UNDER OUR SUPERVISION BY HOLLY LYNN SEBAHAR ENTITLED STUDIES TOWARDS THE SYNTHESIS OF TREHALAMINE AND THE EFFECT OF ADJACENT CHIRAL TERTIARY AND QUATERNARY CENTERS ON THE METAL-CATALYZED ALLYLIC SUBSTITUTION REACTION BE ACCEPTED AS FULFILLING IN PART REQUIREMENTS OF THE DEGREE OF DOCTOR OF PHILOSOPHY.

Committee on Graduate Work











Advisor



Department Head

## ABSTRACT OF DISSERTATION

### STUDIES TOWARDS THE SYNTHESIS OF TREHALAMINE AND THE EFFECT OF ADJACENT CHIRAL TERTIARY AND QUATERNARY CENTERS ON THE METAL-CATALYZED ALLYLIC SUBSTITUTION REACTION

Studies were conducted towards advancing a *trans*-epoxy alcohol, derived from an amino-substituted cyclobutanone, to trehalamine. Efforts to manipulate the epoxy alcohol under standard conditions were hindered by the extraordinary propensity of the system to undergo the Payne rearrangement and the steric environment shielding both the hydroxyl group and the epoxide.

Metal-catalyzed allylic substitution reactions of allylic esters containing chiral quaternary and tertiary centers adjacent to the allyl system were examined. Reaction with stabilized nucleophiles led to exclusive attack at the less hindered allylic terminus and the stereoselectivity varied with the bidentate ligand used but favored retention. The yields and reaction times were improved with the use of microwaves. Application of standard conditions for transmetallation afforded starting material or decomposition. Conversely, vinyl and phenylstannatranes reacted cleanly and gave the opposite regio- and stereoselectivity than was observed with stabilized anions. Catalysts containing metals other than palladium were completely unreactive and led to recovered starting material.

Holly Lynn Sebahar  
Department of Chemistry  
Colorado State University  
Fort Collins, CO 80523  
Summer 2002

## ACKNOWLEDGEMENTS

I would like to thank Professor Hegedus for his patience and for the freedom to work independently on problems I found interesting. Thank you to the past and present members of the Hegedus group, especially Xin Wen and Brian Brown, who were invaluable mentors at the beginning of my studies, and Kazuhiro Yoshida, with whom I had the pleasure of working with on the allylic substitution project. Also, many thanks to the Williams group for sharing generously of their equipment and chemicals, helpful discussions, and much comic relief. Throughout college and graduate school I have valued the support and advice of my professors from UMM: Nancy Carpenter, Roger Echols, Jim Togeas, Jim Olson. They continue to inspire me with their generosity, honesty and kindness.

Thank you to all of the great friends I have made at CSU. I will always remember the fun times fishing, camping, cheering for Rams football and basketball and just hanging out. Thank you to my parents and grandparents for their endless love, support, and humor and for ensuring that I was never hitting the books too hard. Finally, I would like to thank my husband Paul for standing by me through all of the tough times and for making it so that the good days far outnumber the bad ones. Your love and support mean the world to me.

## TABLE OF CONTENTS

### CHAPTER ONE

#### Studies Towards the Synthesis of Trehalamine

I.	Introduction and Background	1
II.	Rationale	13
III.	Results and Discussion	16
IV.	Future Studies	29
V.	Experimental Section	30
VI.	References	44

### CHAPTER TWO

#### Effect of Adjacent Chiral Tertiary and Quaternary Centers on the Metal-Catalyzed Allylic Substitution Reaction

I.	Introduction and Background	48
	A. Palladium-Catalyzed Reaction	51
	B. Molybdenum-Catalyzed Reaction	62
	C. Tungsten-Catalyzed Reaction	72
	D. Rhodium-Catalyzed Reaction	75
	E. Iridium-Catalyzed Reaction	79
II.	Rationale	82
III.	Results and Discussion	83
IV.	Conclusions	103
V.	Experimental Section	104
VI.	References	125

### APPENDIX

	X-ray crystal structure data for compounds <b>119b</b> , <b>299a</b> , and <b>322b</b>	133
--	----------------------------------------------------------------------------------------	-----

# Chapter One

## Studies Towards the Synthesis of Trehalamine

### I. Introduction and Background

Oligosaccharides play an integral role in energy storage and cell surface recognition and serve as structural elements in the cell walls of bacteria and plants.<sup>1</sup> The ability to inhibit these functions has far-reaching biological effects. Both natural and synthetic inhibitors of glycosidases, enzymes which have a role in the biosynthesis of oligosaccharides, are useful in agriculture and medicine.<sup>2</sup> One family of such inhibitors is the aminocyclopentitols (Figure 1.1). As well as displaying effective inhibition of their respective enzymes, they also possess an interesting structural framework and have thus drawn a great deal of attention in the last decade.<sup>2</sup>

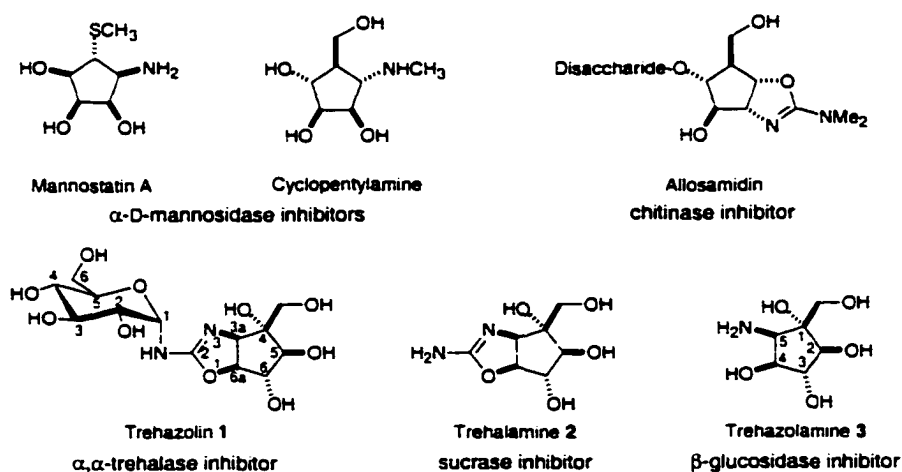


**Figure 1.1**

Trehazolin 1 was isolated in 1991 by Ando and coworkers from the culture broths of *Micromonospora* sp. SANK 62390 and *Amycolatopsis* sp. SANK 60791.<sup>3</sup> This unique

pseudodisaccharide displays specific and potent inhibition of  $\alpha,\alpha$ -trehalase ( $IC_{50} = 52$  nm versus the silkworm trehalase). Trehazolin is thought to mimic the natural substrate for the enzyme,  $\alpha,\alpha$ -trehalose **4** (Figure 1.2). Trehalose is the primary blood sugar of insects and because it is not found in vertebrates, inhibition of trehalase is attractive for insecticide development.

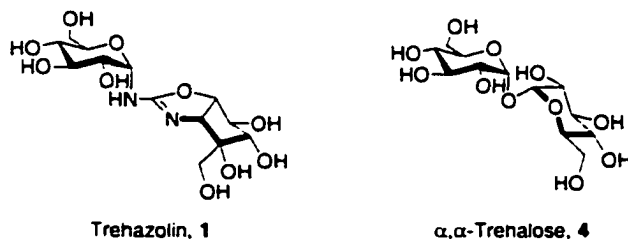


**Figure 1.2**

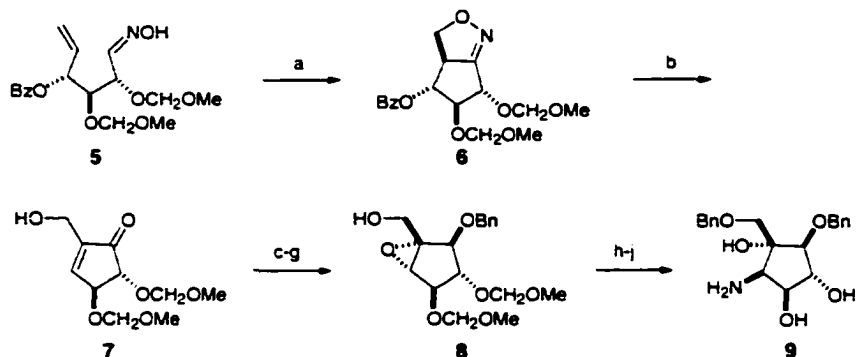
The aglycon trehalamine **2** was also isolated from the aforementioned strains and is thought to have a close relationship to trehazolin on the biosynthetic pathway. Although trehalamine and the aminocyclopentitol **3** displayed decreased trehalase inhibition ( $180\ \mu\text{M}$ , and  $>500\ \mu\text{M}$  respectively) they were more active towards other glycosidases (trehalamine **2**:  $68\ \mu\text{M}$ , trehazolin **1**:  $170\ \mu\text{M}$  versus rat sucrase: aminocyclitol **3**:  $5.6\ \mu\text{M}$ , trehazolin **1**:  $> 500\ \mu\text{M}$  versus sweet almond  $\beta$ -glucosidase).<sup>3</sup>

Because of their interesting structure and biological activity, trehazolin, trehalamine, and the aminocyclopentitol **3** have been the subject of many synthetic endeavors and have served as templates for the design of new, more-potent glycosidase inhibitors.<sup>2</sup> The syntheses were accomplished with a variety of strategies. Numerous routes utilized the stereochemistry present in natural sugars and [3+2]-cycloaddition, reductive cyclization, and olefin metathesis were employed in carbocycle formation. Shiozaki, Ogawa, and Carreira completed total syntheses of trehazolin and in each case

the aminocyclopentitol core was accomplished first, then coupled with a glucopyranosyl derivative. The coupled product then underwent ring closure to give the natural product. Therefore, construction of the aminocyclopentitol core constitutes a formal synthesis of trehazolin.

Shiozaki completed the first total synthesis of trehazolin (Scheme 1.1) and concomitantly determined the absolute stereochemistry.<sup>4</sup> The synthesis began with D-glucose, which was converted in five steps to oxime **5**. Upon treatment with 5% aqueous sodium hypochlorite and a catalytic amount of triethyl amine, the olefinic oxime **5** underwent a [3+2]-cycloaddition, which gave the isoxazoline **6**. Hydrogenolysis with Raney nickel and hydrogen was followed by in situ hydrolysis of the intermediate imine with boric acid and elimination of the benzyloxy group. Protection of the primary hydroxyl group then reduction using Luche conditions provided a 1:2.5 ( $\alpha$ : $\beta$ ) mixture of separable alcohols favoring the desired epimer. Following protecting group manipulation asymmetric epoxide formation was accomplished using Sharpless conditions. Benzyl protection of the primary hydroxyl group afforded **8**, which underwent regioselective ring opening with sodium azide to set the final stereogenic center. Reduction of the azido group and removal of the methoxymethyl groups gave the aminocyclopentitol **9**.

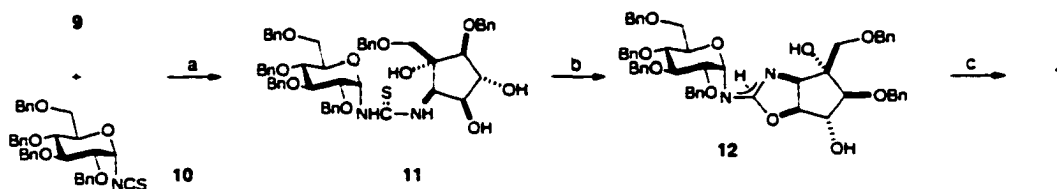
### Scheme 1.1



(a) aq 5% NaOCl, cat. NEt<sub>3</sub>, CH<sub>2</sub>Cl<sub>2</sub>/H<sub>2</sub>O, 0 °C, 60%. (b) H<sub>2</sub>, Raney Ni, B(OH)<sub>3</sub>, 72%. (c) TBDMSCl, 88%; (d) NaBH<sub>4</sub>, CeCl<sub>3</sub>·7H<sub>2</sub>O, 53%, (e) BnBr, NaH, (f) Bu<sub>4</sub>NF, 58%, (g) Ti(O<sup>i</sup>Pr)<sub>4</sub>, L-DIPT, *t*-BuOOH, 94%. (h) BnBr, NaH, 98%, (i) NaN<sub>3</sub> (12 equiv), NH<sub>4</sub>Cl (12 equiv), DMF/HO(CH<sub>2</sub>)<sub>2</sub>OH, 125 °C, 78%, (j) 4 equiv LAH, then 5% HCl, MeOH.

Aminocyclopentitol **9** was coupled with isothiocyanate **10** to give the thiourea **11** (Scheme 1.2). Cyclization to the aminooxazoline **12** was accomplished using Mukaiyama's reagent and deprotection provided trehazolin **1**.

### Scheme 1.2

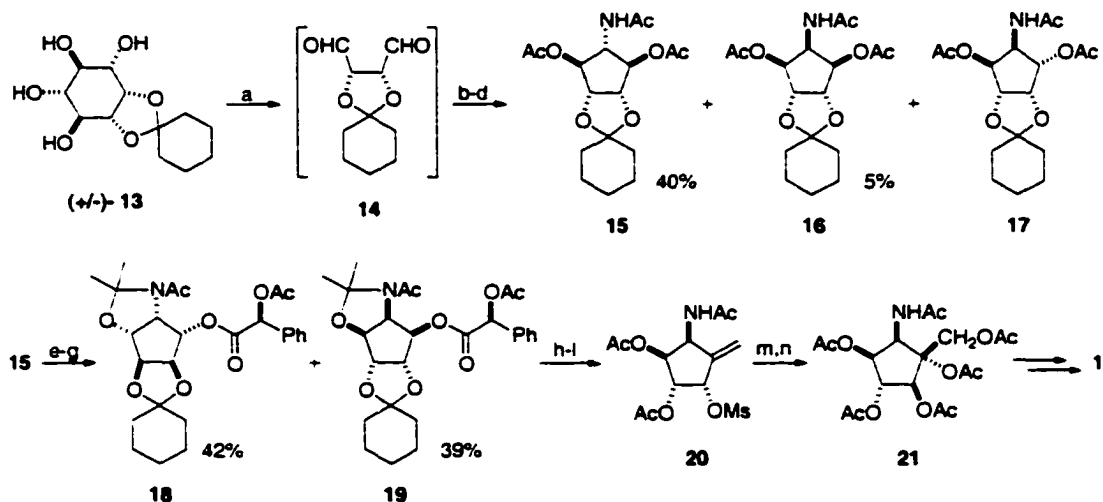


(a) 15 equiv NEt<sub>3</sub>, 60%. (b) 17 equiv 2-chloro-3-ethylbenzoaxazoline tetrafluoroborate, then NEt<sub>3</sub>, 68%. (c) H<sub>2</sub>, Pd(OH)<sub>2</sub>/C, 44%.

Soon after isolation of the natural products, Ogawa and coworkers completed a racemic synthesis of the aminocyclopentitol core **3** which helped confirm the relative stereochemistry.<sup>5</sup> More recently an enantioselective approach was developed (Scheme 1.3).<sup>6</sup> Oxidative cleavage of protected *myo*-inositol **13** gave an intermediate dialdehyde **14** which underwent base-catalyzed nitromethane cyclization. Reduction and acetate

protection gave a mixture of products, including only 5% of the desired cycloadduct **16**. Although the major isomer **15** was transformed into **16** in five steps, the low yield of this key transformation limited the utility of the synthesis. However, isomers **15** and **17** were useful in preparing many analogs. Selective deacetylation followed by ketalation of the *meso*-compound **16** and formation of the chiral mandelate esters allowed for separation with column chromatography. Deesterification of **19**, installation of the exomethylene, and protecting group manipulation gave the olefin **20**. Nucleophilic displacement of the mesylate with sodium acetate, osmium tetroxide-catalyzed dihydroxylation and acetylation afforded intermediate **21**, which was advanced to trehazolin following Shiozaki's protocol.

### Scheme 1.3

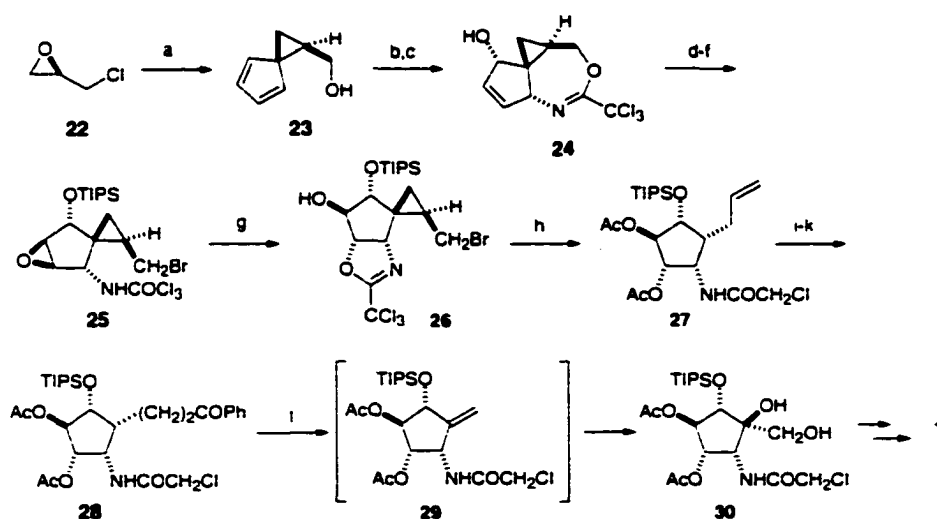


(a)  $\text{NaIO}_4$ ; (b)  $\text{MeNO}_2$ ,  $\text{MeONa}$ ,  $\text{MeOH}$ , then  $\text{AcOH}$ , 60%; (c) glacial  $\text{AcOH}$ ,  $\text{H}_2$ , Adam's catalyst; (d)  $\text{Ac}_2\text{O}$ ,  $\text{py}$ ; (e)  $\text{MeONa}$ ,  $\text{MeOH}$ ; (f)  $\text{Me}_2\text{C}(\text{OMe})_2$ ,  $p\text{-TsOH}$ , 87%; (g) (*S*)-acetylmandelic acid,  $\text{DCC}$ ,  $\text{DMAP}$ , 81%; (h)  $\text{MeONa}$ ,  $\text{MeOH}$ , 92%; (i)  $\text{PCC}$ , 98%; (j)  $\text{CH}_2\text{N}_2$ ,  $\text{DMSO}/\text{Et}_2\text{O}$ , then  $\text{P}(\text{OMe})_3$ ,  $130^\circ\text{C}$ , 45%; (k) 80% aq  $\text{AcOH}$ ; (l)  $\text{MsCl}$ , then  $\text{Ac}_2\text{O}$ , 65%; (m)  $\text{NaOAc}$ , 66%; (n)  $\text{OsO}_4$ ,  $\text{NMO}$ , then  $\text{Ac}_2\text{O}$ , 85%.

Carreira and coworkers reported one of the most novel syntheses which began with optically active epichlorohydrin **22** (Scheme 1.4).<sup>7</sup> The addition of lithium

cyclopentadienylide to epichlorohydrin in the presence of sodium hydride led to epoxide-opening then cyclization which gave the spirocyclopropane **23** in 91% ee. Trichloroacetimidate formation followed by iodocyclization and in situ hydrolysis gave the tricycle **24**. Ring opening of the imidate was accomplished using  $\text{Li}_2\text{NiBr}_4$  and epoxidation with dimethyldioxirane. Lewis acid-promoted intramolecular epoxide-opening gave the desired oxazoline **26**. Treatment of **26** with free radical conditions converted the spirocyclopropane moiety into the terminal olefin and partially reduced the trichloromethyl group. Following hydrolysis of the oxazoline and protection of the secondary alcohol, the olefin underwent hydroboration then oxidation to the aldehyde. Treatment with phenylmagnesium bromide then Swern oxidation gave the ketone which underwent Norrish type II cleavage to the exomethylene of intermediate **29**. Dihydroxylation afforded **30**, which was advanced to trehazolin using chemistry similar to that described by Shiozaki.

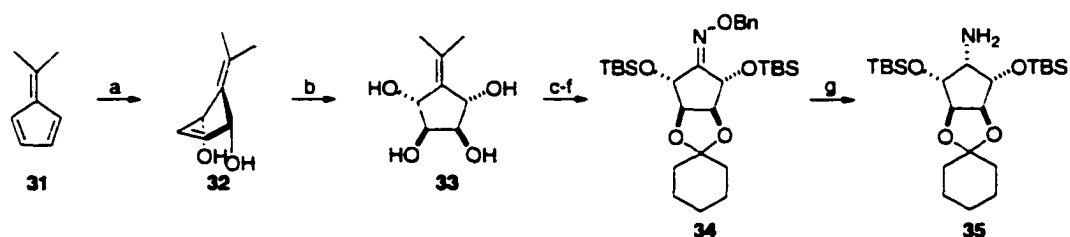
#### Scheme 1.4



(a)  $\text{CpLi}$ ,  $\text{NaH}$ , 60%; (b)  $\text{NaH}$ ,  $\text{Cl}_3\text{CCN}$ , 95%; (c)  $l(\text{sym-collidine})_2\text{ClO}_4$ ,  $\text{NaHCO}_3$ , aq MeCN, 61%; (d)  $t\text{-Pr}_3\text{SiOTf}$ , 2,6-lutidine, 95%; (e)  $\text{Li}_2\text{NiBr}_4$ , 80%; (f) DMDO, 95% (g)  $\text{BF}_3 \cdot \text{Et}_2\text{O}$ , 87%; (h)  $\text{Bu}_3\text{SnH}$ ,  $\text{Et}_3\text{B}$ ,  $\text{NaBH}_4$ ,  $\text{EtOH}$ , 75%; (i) PPTS, aq MeCN, then  $\text{Ac}_2\text{O}$ , 77%; (j)  $\text{Chx}_2\text{BH}$ ,  $\text{H}_2\text{O}_2$ , 83%; (k)  $(\text{COCl})_2$ , 83%; (l)  $\text{PhMgBr}$ ,  $\text{LiBr}$ , then  $(\text{COCl})_2$ , 60%; (m) *iv*, then  $\text{OsO}_4$ , NMO, 79%.

Ganem and coworkers also utilized a cyclopentadiene in their racemic synthesis of **35**,<sup>8</sup> an intermediate in Ogawa's synthesis of trehazolin<sup>6</sup> (Scheme 1.5). The key step involved the [4+2]-cycloaddition of fulvene **31** with singlet oxygen. In situ reduction of the peroxide gave the diol **32**. Dihydroxylation occurred preferentially on the face opposite the 1,4-diol. Protection of the *cis*-vicinal diol, ozonolysis, oxime formation and protection provided intermediate **34**. The large cyclohexylidene ketal directed the reduction of the oxime and a 6:1 mixture was observed, favoring the desired amine, **35**.

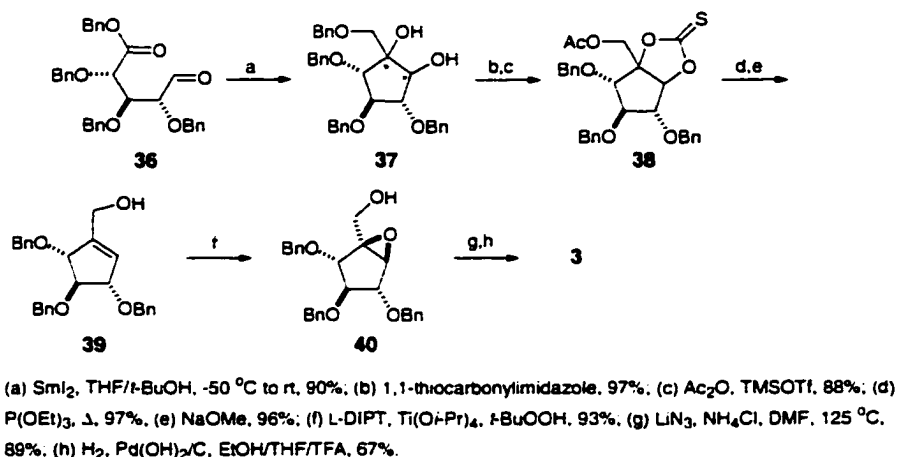
### Scheme 1.5



(a) O<sub>2</sub>, rose bengal, thiourea, NaOAc, 78%; (b) OsO<sub>4</sub>, NMO, 70%; (c) 1,1-diehoxycyclohexane, *p*-TsOH, 62%; (d) O<sub>3</sub>; (e) NH<sub>2</sub>OBn; (f) TBSCl, 92%; (g) 15 equiv BH<sub>3</sub>-THF, 89%, 6:1  $\alpha$ : $\beta$ .

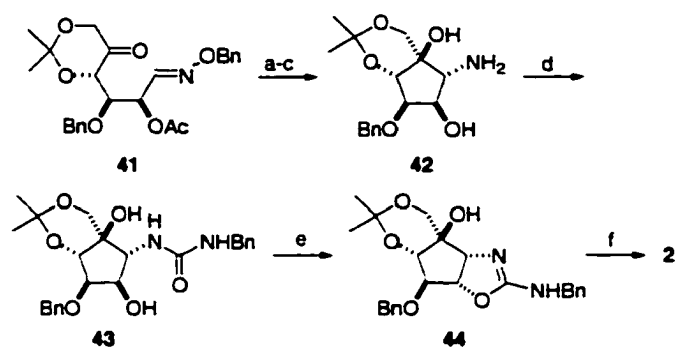
Two groups utilized reductive cyclizations to form the cyclopentane skeleton. In 1998 Chiara published a route to trehazolamine **3** featuring the reductive carbocyclization of diketone **36** (Scheme 1.6).<sup>9</sup> The diketone was available from glucose in four steps, and upon treatment with samarium iodide underwent cyclization to a 1:1 mixture of *syn*-diols **37**. In order to utilize both diastereomers, the mixture was transformed to the diastereomeric thiocarbonates and the primary hydroxyl groups were selectively reprotected. Heating the mixture **38** with triethyl phosphite converted both isomers to the common cyclopentene **39**. The completion of the synthesis paralleled Shiozaki's route to the aminocyclopentitol.

## Scheme 1.6



Although the above route fixed three of the five stereogenic centers of the aminocyclopentitol efficiently, setting the final two centers proved laborious. To improve this, a keto-oxime ether derived from *D*-mannose was used in the reductive cyclization. The substrate featured a cyclic ketal which controlled the stereochemistry at the quaternary center (Scheme 1.7).<sup>10</sup> Treatment of keto-oxime ether **41** with excess samarium iodide led to cyclization and reduction of the hydroxylamino group. Hydrolysis of the ester gave **42**, which contained the desired configuration at four of the five stereogenic centers. The synthesis was completed effectively beginning with formation of the *N*-benzyl urea **43**. Upon treatment with triflic anhydride and pyridine, intramolecular  $\text{S}_{\text{N}}2$  displacement of the triflate ester by the carbonyl oxygen of the urea took place to form the oxazoline ring of **44** with the desired stereochemistry. Deprotection afforded trehalamine, **2**.

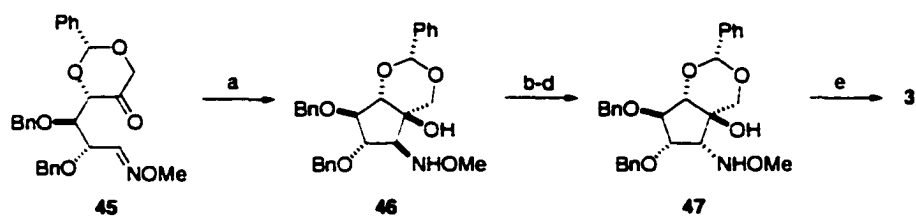
### Scheme 1.7



(a)  $\text{SmI}_2$ , THF/*t*-BuOH,  $-30\text{ }^\circ\text{C}$ ; (b)  $\text{H}_2\text{O}$ ; (c) LiOH,  $\text{H}_2\text{O}$ , 98%; (d)  $\text{BnNCO}$ , 93%; (e)  $\text{Ti}_2\text{O}$ , py,  $-20\text{ }^\circ\text{C}$ , 99%; (f)  $\text{Pd}(\text{OH})_2/\text{C}$ ,  $\text{H}_2$ , EtOH/TFA, 85%.

Using similar methodology, Giese and coworkers have synthesized trehazamine with impressive efficiency (Scheme 1.8).<sup>11</sup> Stereoselective, reductive cyclization of the *D*-glucose derived keto-oxime ether **45** afforded cyclopentane **46**. Similar to Chiara's strategy, the cyclic acetal directed the intermediate ketyl radical anion to adopt the chair conformation which led to the aminocyclitol with the desired stereochemistry at the quaternary carbon. An oxidation/reduction sequence inverted the stereochemistry at the carbon bearing the *O*-methylhydroxyamino group and deprotection delivered trehazamine **3**.

### Scheme 1.8

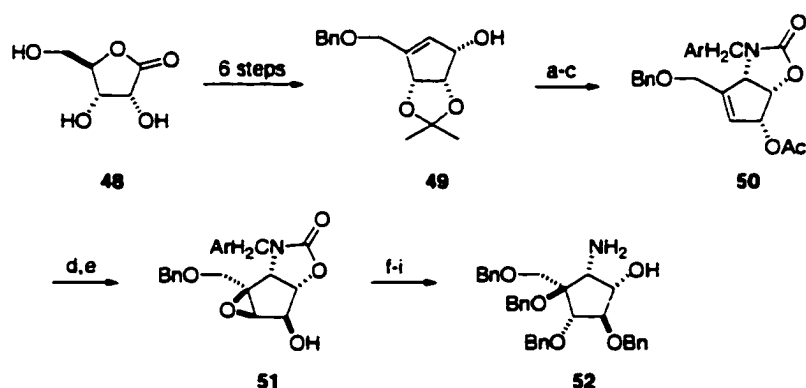


(a)  $\text{SmI}_2$ , THF/*t*-BuOH,  $-78\text{ }^\circ\text{C}$  to rt, 84%; (b)  $\text{Ac}_2\text{O}$ ; (c)  $\text{Pb}(\text{OAc})_4$ , 44%; (d)  $\text{K}_2\text{CO}_3$ , MeOH; (e)  $\text{LiAlH}_4$ , MeONa, 67%; (e) Na,  $\text{NH}_3$ , 90%.

*D*-Ribolactone **48** also served as a building block for the construction of the aminocyclopentitol core (Scheme 1.9). Knapp and coworkers converted the lactone into

cyclopentene **49** in six steps.<sup>12</sup> Treating **49** with benzyl isocyanate followed by iodide led to oxazolidinone formation, resulting from a rare anti-Markovnikov iodocyclization. The pathway for the cyclization was presumably determined by the kinetic preference for formation of the five- over six-membered ring and the fused rather than bridged system. Reduction of the iodide also led to elimination of the ether and gave **50**. Mitsunobu inversion and Sharpless asymmetric epoxidation afforded the epoxy alcohol **51**. Sodium benzoate regioselectively opened the epoxide and the resulting alcohol was benzyl protected. Removal of the PMB group and hydrolysis of the oxazolidinone gave **52**, a protected form of trehazolamine **3**.

### Scheme 1.9

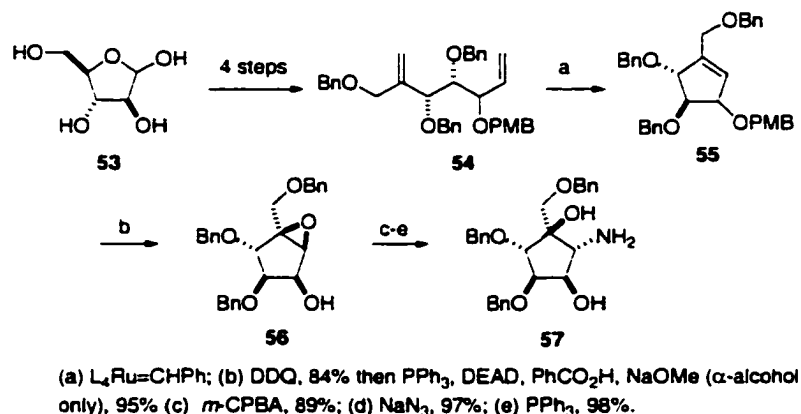


(a) NaH, ArCH<sub>2</sub>NCS, MeI; (b) I<sub>2</sub>, Na<sub>2</sub>CO<sub>3</sub>, Na<sub>2</sub>SO<sub>3</sub>, 82%; (c) Ac<sub>2</sub>O, H<sub>2</sub>SO<sub>4</sub>, Zn, 90%; (d) K<sub>2</sub>CO<sub>3</sub>, aq MeOH, PhCO<sub>2</sub>H, DEAD, PPh<sub>3</sub> then Na<sub>2</sub>CO<sub>3</sub>, aq MeOH, 83%; (e) CF<sub>3</sub>CO<sub>3</sub>H, Na<sub>2</sub>CO<sub>3</sub>, 90%; (f) PhCO<sub>2</sub>Na, aq DMF, 100 °C, 89%; (g) NaH, BnBr, Bu<sub>4</sub>Ni; (h) CAN, 86%; (i) 2N KOH, EtOH, reflux.

The most recent synthetic efforts featured ring-closing metathesis to construct the cyclopentane skeleton. Seepersaud and Al-Abed published the first such strategy which began with diene **54** derived from arabinose **53** (Scheme 1.10).<sup>13</sup> Ring-closing metathesis of **54** with Grubb's catalyst gave the cyclopentene **55** as a mixture of diastereomeric allylic ethers. Oxidative removal of the PMB group, Mitsunobu inversion of the

undesired  $\alpha$ -alcohol and chelation-controlled epoxidation gave the epoxy alcohol **56**. Nucleophilic opening of the epoxide with sodium azide followed by reduction under Staudinger conditions provided the amino alcohol **57**, an advanced intermediate in Chiara's synthesis of trehazolamine **3**.

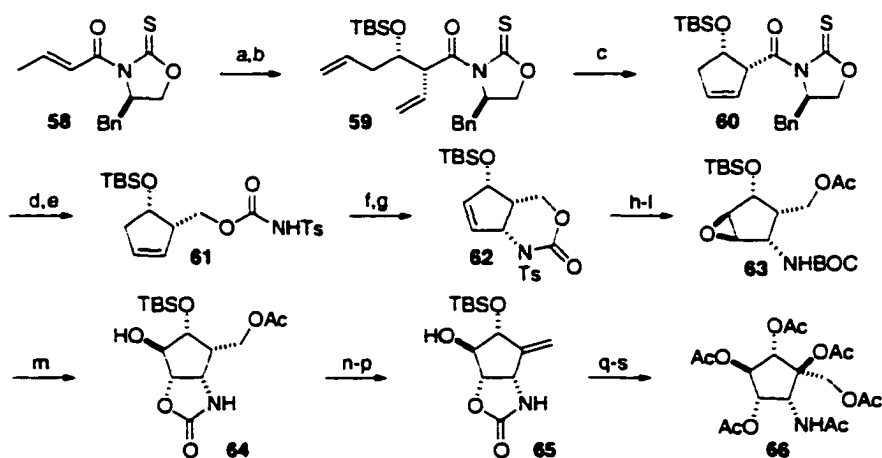
### Scheme 1.10



The latest synthesis was completed by Crimmins and Tabet and featured an asymmetric aldol reaction and olefin metathesis for construction of the cyclopentane skeleton (Scheme 1.11).<sup>14</sup> Enolization of the *N*-acyloxazolidinethione **58** with  $TiCl_4$  and (-)-sparteine followed by addition of 3-butenal provided the *syn*-aldol product in good yield. To prevent coordination of the homoallylic alcohol to the metal during the metathesis reaction, it was protected as the silyl ether **59**. Grubb's catalyst efficiently promoted ring-closing metathesis which gave cyclopentene **60** in 85% yield. Removal of the chiral auxiliary with lithium borohydride was followed by formation of carbamate **61**. Iodocyclization followed by elimination of the iodide delivered the oxazolidinone **62**. Protecting group manipulation, hydrolysis of the oxazolidinone and epoxidation on the side opposite the three large groups set epoxy carbamate **63** up for intramolecular

epoxide-opening. Camphorsulfonic acid-catalyzed attack of the carbamate carbonyl oxygen on the epoxide resulted in the bicycle **64** with the desired stereochemistry at four of the five centers. Introduction of the quaternary center was achieved via exomethylene formation then dihydroxylation. Finally base-catalyzed hydrolysis of the oxazolidinone and exhaustive acetylation gave the aminocyclopentitol **66**.

**Scheme 1.11**



(a)  $\text{TiCl}_4$ , (-)-sparteine, 3-butenal, 75%; (b) TBSOTf, 2,6-lutidine; (c)  $\text{L}_4\text{Ru}=\text{CHPh}$ , 91%; (d)  $\text{LiBH}_4$ , 75%; (e)  $\text{TsNCO}$ ; (f)  $\text{I}_2$ ,  $\text{K}_2\text{CO}_3$ , 77%; (g) DBU, 91%; (h) Na naphthalenide; (i)  $(\text{Boc})_2\text{O}$ , 88%; (j)  $\text{Cs}_2\text{CO}_3$ , MeOH, 94%; (k)  $\text{Ac}_2\text{O}$ , 95%; (l) DMDO, acetone, 74%; (m) CSA,  $\text{CH}_2\text{Cl}_2$ , 83%; (n)  $\text{K}_2\text{CO}_3$ ; (o)  $\text{o-NO}_2\text{C}_6\text{H}_4\text{SeCN}$ , *n*- $\text{Bu}_3\text{P}$ , 71%; (p)  $\text{H}_2\text{O}_2$ ; (q)  $\text{OsO}_4$ , NMO, 75%; (r) 2N KOH, EtOH; (s)  $\text{Ac}_2\text{O}$ , 86%.

A number of analogs of both trehalamine and trehazolin have also been synthesized in the search for more-potent glycosidase inhibitors. Both the sugar moiety and the aminocyclopentitol core have been modified with limited success. A small sample of analogs with the most notable activity are shown below (Figure 1.3). The 5a'-carbatrehazolin **67**, in which the ring oxygen of the sugar was replaced by a carbon, demonstrated similar inhibitory activity to trehazolin ( $\text{IC}_{50} = 49$  nm for silkworm trehalase) but was more stable towards isomerization. The simplified cyclic phenyl isoureas **68** and **69** also displayed strong specific inhibition of  $\alpha$ -glucosidases ( $\text{IC}_{50} = 29$

nm and 7.6 nm respectively against yeast  $\alpha$ -glucosidase). Attempts to modify the linkage position on the sugar to the 4- or 6-position caused a dramatic decrease in activity. Deoxygenation at one or more positions of the sugar or aminocyclitol portion resulted in inactive compounds. Similar results were observed when stereogenic centers were inverted on either half of trehazolin.

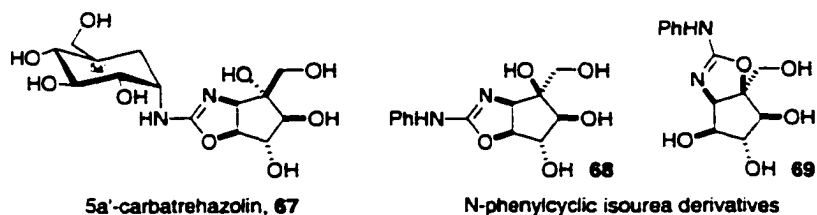
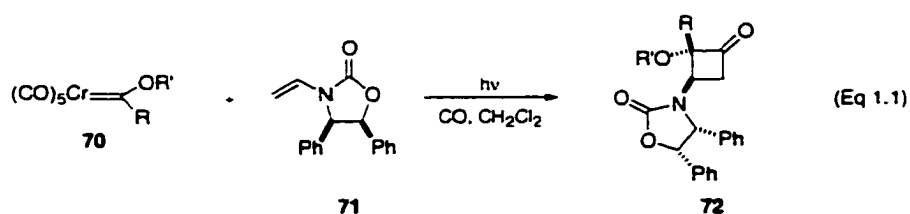


**Figure 1.3**

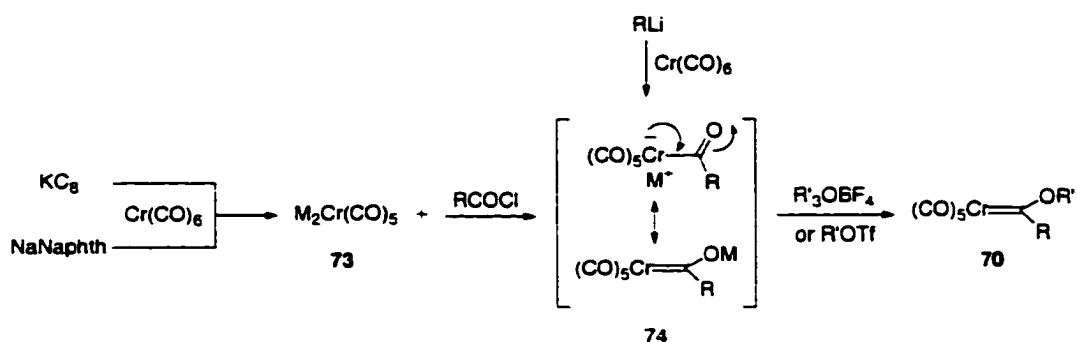
## II. Rationale

Trehazolin **1**, trehalamine **2**, and the aminocyclitol **3** display important biological activity, but more importantly serve as templates for the synthesis of more-potent inhibitors. They also present a significant synthetic challenge due to their dense functionalization and five contiguous stereogenic centers. For these reasons, it is of interest to develop an efficient and versatile synthetic route to this class of molecules. The Hegedus group has previously established methodology for the stereoselective formation of functionalized cyclobutanones via photolysis of heteroatom-stabilized chromium carbene complexes with chiral, electron-rich olefins (Eq 1.1).<sup>15</sup> The appropriately substituted cyclobutanone could serve as a building block for the synthesis of trehalamine **2**.



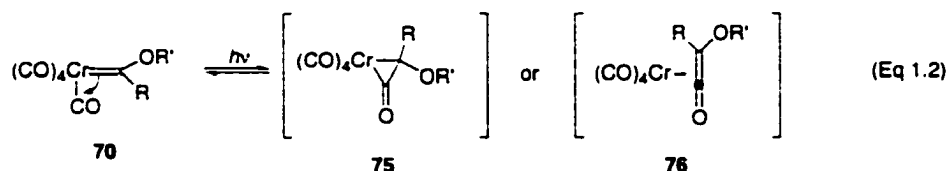
A wide range of substituents, which are subsequently transferred to the cyclobutanone, can be incorporated into the carbene complex. The traditional way to synthesize heteroatom-stabilized carbene complexes (Fischer carbene complexes, **70**) involves attack of an organolithium reagent on one of the CO ligands of a metal hexacarbonyl (Scheme 1.12). The resulting “ate” complex is then trapped by a hard alkylating agent.<sup>16</sup> The range of functionality available by this method was limited to groups available as organolithiums. Therefore, a complementary method was developed involving the generation of a pentacarbonyl dianion **73** from a metal carbonyl and sodium naphthalene or potassium/graphite laminate. Subsequent nucleophilic attack of the dianion on a carboxylic acid chloride followed by alkylation gave the alkoxy carbene complex **70**.<sup>17</sup>

### Scheme 1.12



Fischer carbene complexes undergo a wide variety of reactions. Although research originally focused on the thermal transformations,<sup>18</sup> more recently the utility of

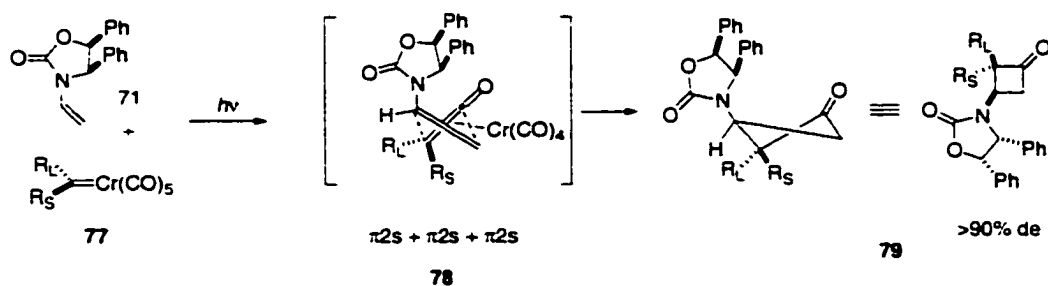
the photochemical reactions has been realized.<sup>19</sup> Irradiation of a carbene complex into the metal-to-ligand charge transfer band (350–450 nm) causes promotion of an electron from the metal to the carbene carbon. This formal, reversible, one-electron oxidation of the metal was proposed to drive a reversible insertion of CO into the chromium-carbon bond to yield a metallacyclopropanone **75** / metal-bound ketene **76** intermediate (Eq 1.2).<sup>20</sup>



Although no direct evidence for these intermediates exists, ketene-like reactivity is observed upon irradiation of carbene complexes.<sup>18</sup> Because the ketene is formed in low concentrations and is bound to the chromium, side reactions normally associated with ketenes such as dimerization are not observed.

The [2+2]-cycloaddition of the photogenerated chromium-bound ketene **78** and an electron-rich alkene (such as **71**) is very highly regio- and stereoselective. The use of an optically active alkene results in nearly complete diastereoselectivity (Scheme 1.13).<sup>14</sup>

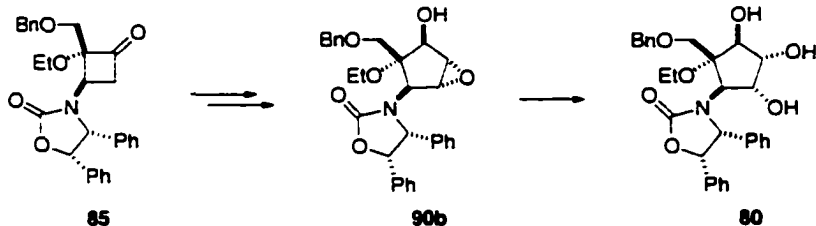
### Scheme 1.13



Preliminary studies conducted in this group revealed that cyclobutanone **85** could be advanced to epoxy alcohol **90b**, which contained the basic framework and four of the

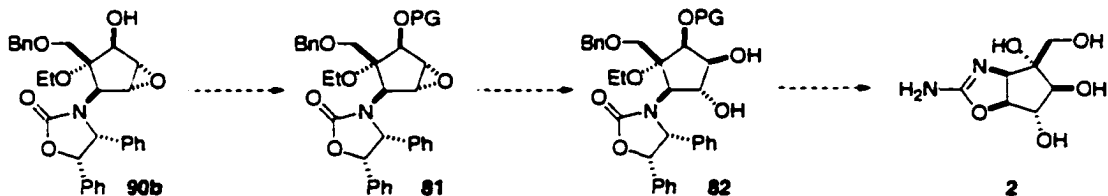
five stereogenic centers of trehazolamine (Scheme 1.14).<sup>21</sup> However, attempted epoxide-opening with aqueous TFA in dioxane gave triol **80**, which resulted from initial Payne rearrangement then epoxide hydrolysis.

**Scheme 1.14**



Protection of the alcohol would suppress the undesired Payne rearrangement. Regioselective epoxide-opening, installation of the isoxazoline unit, and exhaustive deprotection would afford trehalamine **2** (Scheme 1.15).

**Scheme 1.15**

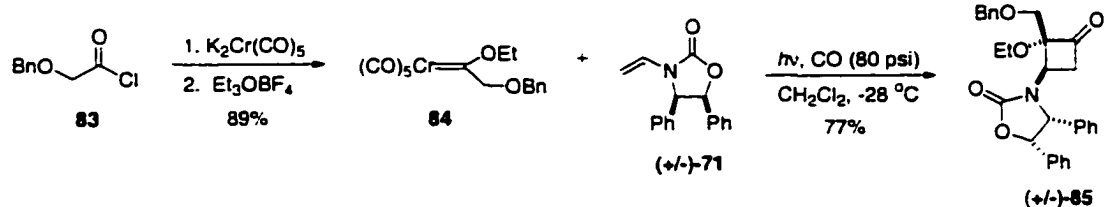


### III. Results and Discussion

Cyclobutanone **85** was synthesized following the protocol developed earlier in the Hegedus Group (Scheme 1.16).<sup>22</sup> Chromium carbene complex **84** was available in 89% yield from the potassium dianion of chromium carbonyl, benzyloxycetyl chloride **83** and triethyloxonium tetrafluoroborate. Irradiation of the carbene complex **84** with vinyl

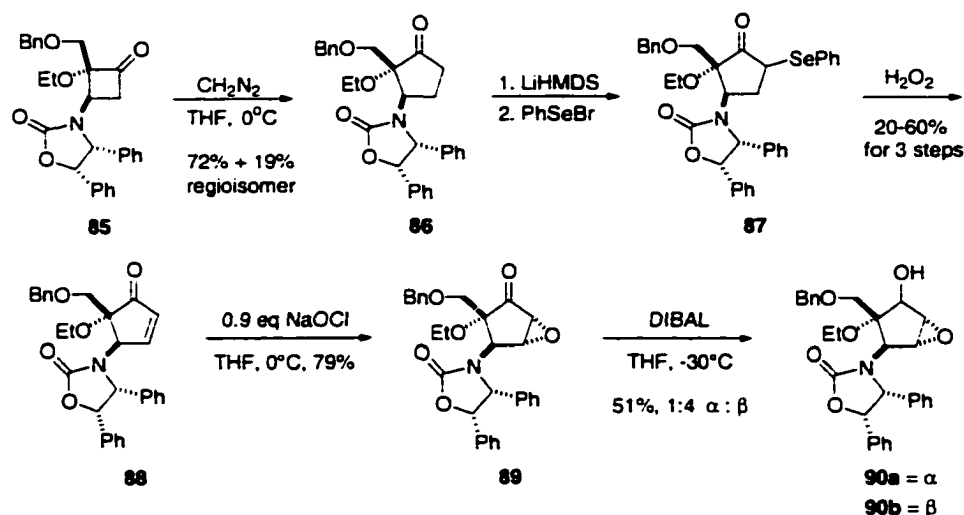
carbamate **71**<sup>23</sup> at  $-28\text{ }^{\circ}\text{C}$  for six days provided cyclobutanone **85** in 77% yield with >20:1 diastereoselectivity.

**Scheme 1.16**



Originally, cyclobutanone **85** was advanced to the epoxy alcohol **90** following the previously reported route (Scheme 1.17).<sup>21</sup> Ring expansion of cyclobutanone **85** with diazomethane gave a 4:1 mixture of regioisomers favoring **86**. The  $\alpha$ -selenide **87** was then formed as a mixture of diastereomers, which, upon oxidation with hydrogen peroxide underwent spontaneous elimination to cyclopentenone **88** in variable yields (20-60%). Treating the enone **88** with less than one equivalent of sodium hypochlorite resulted in epoxidation on the face opposite the oxazolidinone in 79% yield. Reduction with DIBAL in THF gave a 4:1 mixture of epimeric alcohols, favoring the desired isomer **90b**. Former attempts to improve the selectivity of the reduction were unsuccessful.<sup>21</sup> A standard method for *anti*-epoxy alcohol formation is the use of NaBH<sub>4</sub> and CeCl<sub>3</sub>.<sup>24</sup> However application of these conditions to substrate **89** gave the *cis*-epoxy alcohol **90a** exclusively. Complex mixtures were observed when epoxy ketone **89** was treated with Bu<sub>3</sub>SnH/TBAF and NaBH<sub>4</sub>.

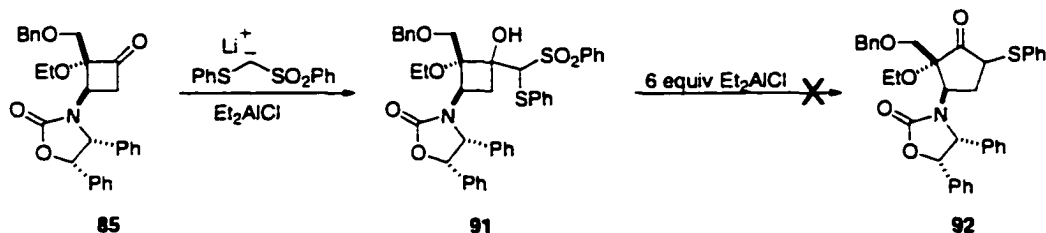
### Scheme 1.17



The previously established route to epoxy alcohol **90b** contained two problematic steps. Conversion of cyclopentanone **86** to cyclopentenone **88** gave variably low yields and the selectivity for reduction of the epoxy ketone **89** was poor. Attention was focused on optimization of these two transformations, beginning with formation of cyclopentenone **88**. Attempted dehalogenation<sup>25</sup> of the  $\alpha$ -bromide derived from cyclopentanone **86** led to decomposition. Cyclopentanone **86** was then converted to the silyl enol ether. However, application of Saegusa's conditions ( $\text{Pd}(\text{OAc})_2$ )<sup>26</sup> to mediate oxidation to cyclopentenone **88** resulted in recovery of the cyclopentanone. Trost and coworkers have developed a protocol for ring expansion of cyclobutanones to  $\alpha$ -phenylthiocyclopentanones.<sup>27</sup> Application of this methodology to cyclobutanone **85** would provide a direct route to the  $\alpha$ -substituted thioether **92** and eliminate the use of potentially explosive diazomethane (Scheme 1.18). Oxidation of **92** and elimination would deliver the cyclopentenone **88**. Treatment of cyclobutanone **85** with the lithium anion of phenylthiomethyl phenylsulfone and various Lewis acids led to complex mixtures. Because the carbonyl was sterically hindered due to the adjacent quaternary

center approach of the anion may have been prevented. Also, the cyclobutanone may not have been stable to the required Lewis acidic conditions.

### Scheme 1.18

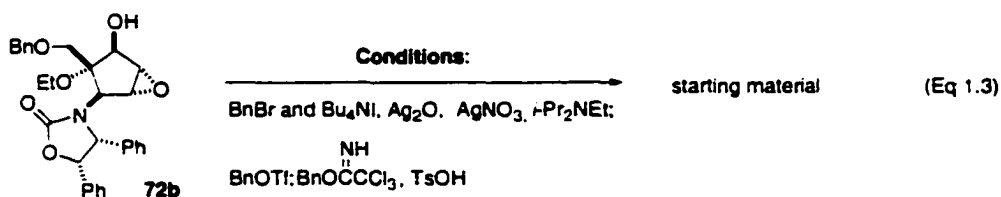


Highly variable yields were observed previously for oxidation of the  $\alpha$ -selenide **87** with aqueous hydrogen peroxide. Additionally, Reich and coworkers have reported a prevalence of undesired side reactions for this type of transformation including selenoxide-mediated decomposition of hydrogen peroxide and conjugate addition of PhSeOH, a byproduct of the elimination, to the enone product.<sup>28</sup> Therefore, focus shifted to finding an alternative oxidant. Oxidation of the  $\alpha$ -selenide **87** with the Davis oxaziridine and pyridine reproducibly afforded cyclopentenone **88** in 60% yield. A number of factors contributed to the observed improvement. The addition of pyridine proved beneficial because amine bases react with the PhSeOH to suppress addition to the olefin. Also, the use of 2-sulfonyloxaziridine excludes the need for water. The presence of water in the oxidation by hydrogen peroxide inhibits the desired *syn* elimination and side reactions predominate.<sup>29</sup>

Improving the selectivity for reduction of the epoxy ketone **89** was also explored. Attempted chelation-controlled reduction with  $\text{Zn}(\text{BH}_4)_2$ <sup>30</sup> in ether: $\text{CH}_2\text{Cl}_2$  (1:1) at 0 °C led to a 55% yield of a 1:1 mixture of epimers **90a:90b**. Selectivity for the *cis*-epoxy alcohol **90a** was increased by cooling the reaction mixture to -78 °C (10:1 **90a:90b**) and

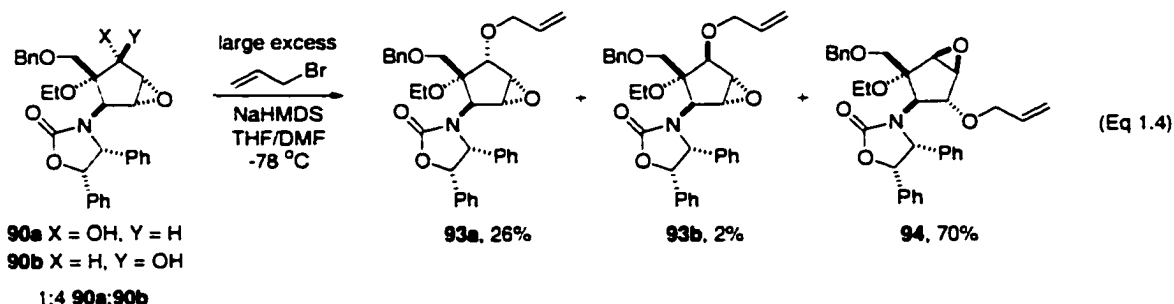
by using THF (100:0) or CH<sub>2</sub>Cl<sub>2</sub> (6:1). LiAl(OBu)<sub>3</sub>H and both L- and K-selectrides gave **90a** exclusively. Conversely, employing a solution of DIBAL in *hexanes* produced the desired selectivity (1:10 **90a**:**90b** in 53%). The less polar solvent may have allowed for improved chelation with the epoxide, which favored attack from the bottom face of the molecule.

Having developed a more efficient preparation of the *anti*-epoxy alcohol **90b**, attention was focused on its protection. Installation of the protecting group selected to suppress the Payne rearrangement must proceed under neutral conditions. Additionally, the protecting group must be stable towards the planned acid-catalyzed epoxide-opening. With these requirements in mind, initial efforts focused on formation of the benzyl ether. Unfortunately, a wide range of neutral conditions led to recovered starting material (Eq 1.3). Presumably, the steric hindrance at this neopentyl center was too great for approach of the large benzyl group.



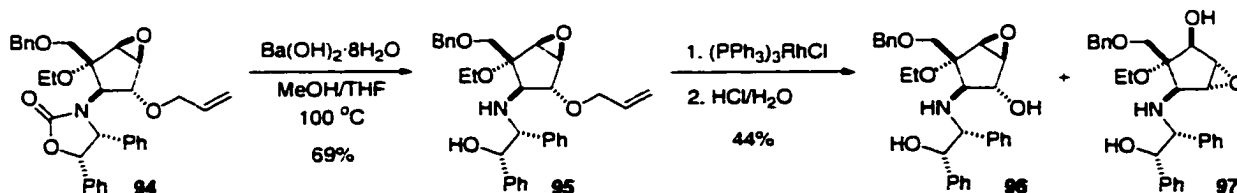
Focus then shifted to formation of the allyl ether, which is also acid-stable but less bulky. Neutral conditions led to recovered starting material. However, subjecting the mixture of alcohols **90a** and **90b** (1:4) to a large excess of allyl bromide and NaHMDS at -78 °C gave three products (Eq 1.4). The major product, **93**, resulted from initial Payne rearrangement of **90b** followed by allylation. Compound **93a** was readily identified by comparison with material prepared from **90a**. Distinguishing between **93b** and **94** was more difficult because they are regioisomeric and have very similar <sup>1</sup>H and <sup>13</sup>C spectra.

Extensive NMR studies ( $^1\text{H}$ ,  $^{13}\text{C}$ , DEPT, COSY, HMBC, HMQC, NOE) were performed. Finally, assignment of structure **94** was based on a 1% NOE interaction between the methine proton on the carbon bearing the oxazolidinone with the methylene proton on the *O*-allyl group.



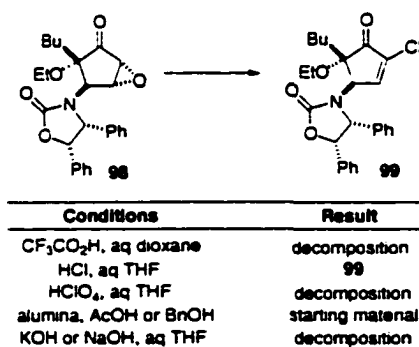
Attempted acid-catalyzed hydrolysis of this rearranged epoxide **94** ( $\text{HClO}_4$ , TFA) led to complex mixtures. Alternatively, barium hydroxide gave the amino alcohol **95** resulting from hydrolysis of the oxazolidinone (Scheme 1.19). Removal of the allyl group via rhodium-catalyzed isomerization to the enol ether followed by hydrolysis with aqueous hydrochloric acid gave a 44% yield of a 1:1 mixture of regioisomeric epoxy alcohols **96** and **97**. Attempts to promote acid- (CSA, TsOH, AcOH) and base-catalyzed ( $\text{NaHMDS}$ , *t*-BuOK) intramolecular epoxide-opening of the mixture of **96** and **97**, which would guarantee the desired regioselectivity, led to recovered starting material or decomposition.

### Scheme 1.19

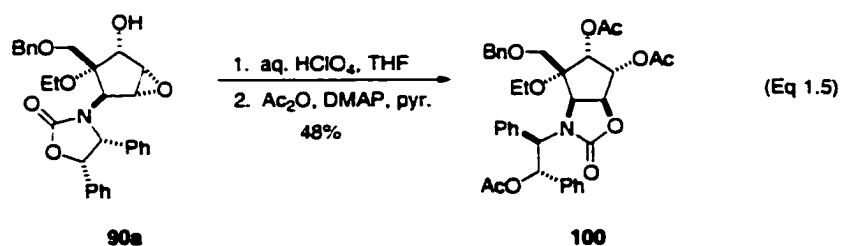


Next, an attempt was made to open the epoxide prior to reduction of the ketone. This study was performed on a model system in which the benzyloxy methyl group was replaced by a butyl group (**98**) (Scheme 1.20).<sup>20</sup> Unfortunately, neither acidic nor basic conditions led to the desired *trans*-diol. Aqueous hydrochloric acid-mediated ring opening with chloride ion followed by elimination of water afforded cyclopentenone **99**.

**Scheme 1.20**



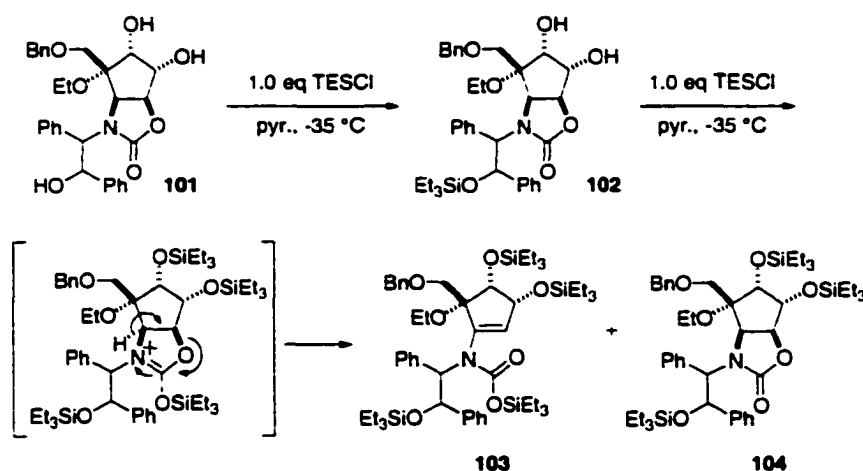
Regioselective epoxide-opening without promoting the Payne rearrangement had become a major challenge. Previously, it was observed that reaction of the *cis*-epoxy alcohol **90a** with aqueous perchloric acid had led to the desired epoxide-opening followed by transacylation with the oxazolidinone.<sup>21</sup> Acetylation gave oxazolidinone **100** (Eq 1.5). To date, this was the only example of the desired epoxide-opening. Epimerization of C2 would give the desired stereochemistry at each position. To utilize



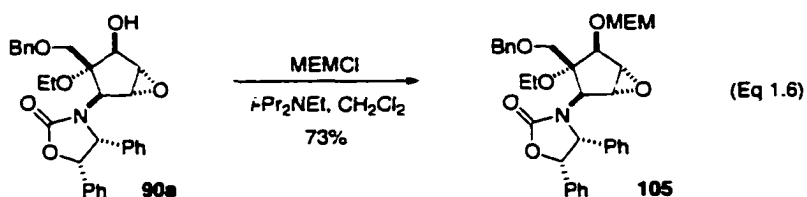
this ring-opening, selective di-protection of the triol and Mitsunobu inversion or oxidation/reduction of the remaining alcohol would be required. Steric hindrance surrounding the neopentyl alcohol should allow for selective protection of the other alcohols.

Clean mono-protection was observed when triol **101** was treated with one equivalent of TESCI (Scheme 1.21). However, addition of a second equivalent of TESCI led to isolation of the tetra- and trisilylated products (**103** and **104**). Possibly, silylation of the carbamate carbonyl oxygen followed by ring opening resulted in cyclopentene **103**. Over-protection was also observed with BnBr and TBSCl so this strategy was abandoned.

**Scheme 1.21**

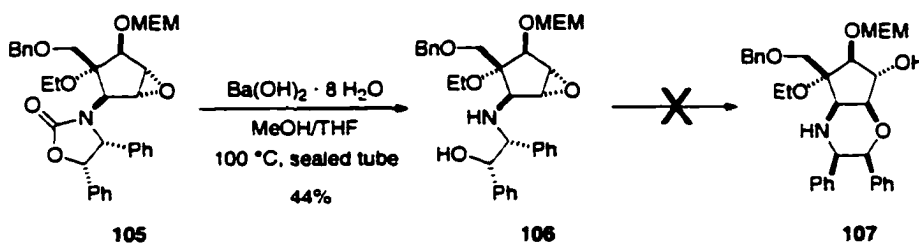


Attention returned to protection of the neopentyl alcohol under neutral conditions. Alcohol **90a** was treated with methoxyethoxymethyl chloride (MEMCl) and Hunig's base which gave the MEM ether **105** in 73% yield (Eq 1.6). Unfortunately, although MEM ethers are traditionally relatively stable to acidic conditions, **105** did not withstand the conditions required for hydrolysis of the epoxide. With protic ( $\text{HClO}_4$ , TFA) and Lewis acids ( $\text{Sc}(\text{OTf})_3/\text{H}_2\text{O}$ ) decomposition along with the free alcohol and recovered starting



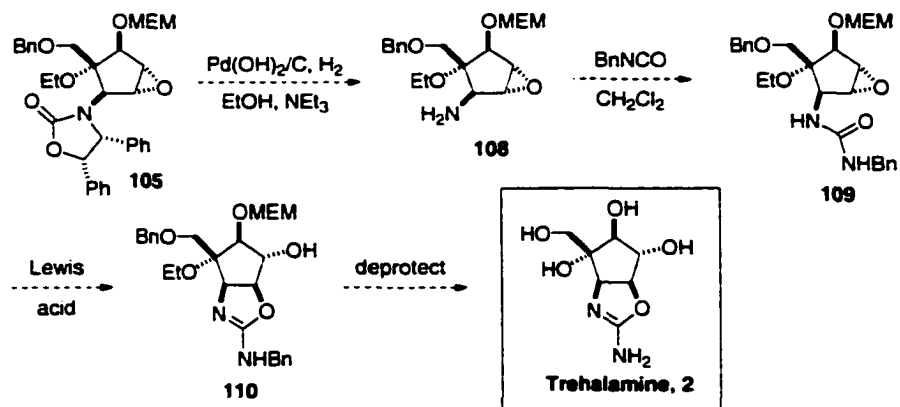
material was observed. Potassium superoxide and sodium hydroxide decomposed **105**. Alternatively, barium hydroxide gave a low yield of amino alcohol **106** (Scheme 1.22). Intramolecular epoxide-opening with the newly formed secondary alcohol would deliver the desired stereochemistry. However, treatment of the amino alcohol **106** with CSA, TsOH, and NaHMDS led to recovered starting material.

### Scheme 1.22



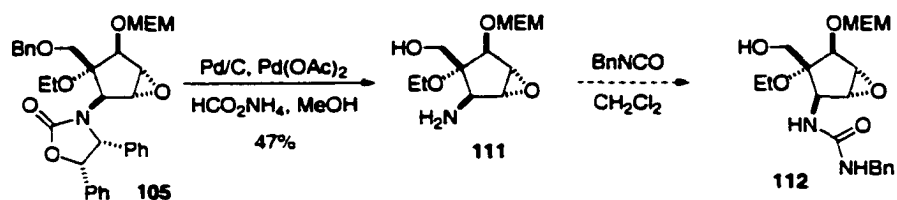
Chiara and coworkers demonstrated that intramolecular displacement of a triflate with the carbonyl oxygen of a urea was an efficient method for introducing the oxazoline portion of trehalamine **2** (Scheme 1.7). Substituting a pendant urea for the side chain containing the secondary alcohol of **106** may facilitate epoxide-opening due to the increased nucleophilicity of the oxygen. Therefore, attention was shifted to free amine formation (**108**) followed by installation of the urea (**109**). Lewis acid-catalyzed intramolecular epoxide-opening followed by exhaustive deprotection should provide trehalamine **2** (Scheme 1.23).

### Scheme 1.23



On a similar structure, hydrogenolysis of the oxazolidinone in the presence of the benzyl ether was observed.<sup>31</sup> The corresponding results were not achieved reproducibly with substrate **105**. Hydrogenolysis of the *O*-benzyl linkage of the oxazolidinone occurred under mild conditions [Pd/C or Pd(OH)<sub>2</sub>/C, H<sub>2</sub> (40 psi)]. Alternatively, conditions required to cleave the *N*-benzyl linkage cleaved the benzyl ether as well. The free amino alcohol **111** was obtained reproducibly with transfer hydrogenation conditions (Scheme 1.24). Unfortunately, treating **111** with benzyl isocyanate led to decomposition, possibly due to interference by the free alcohol. Therefore, protection of the alcohol in the presence of the free amine was required.

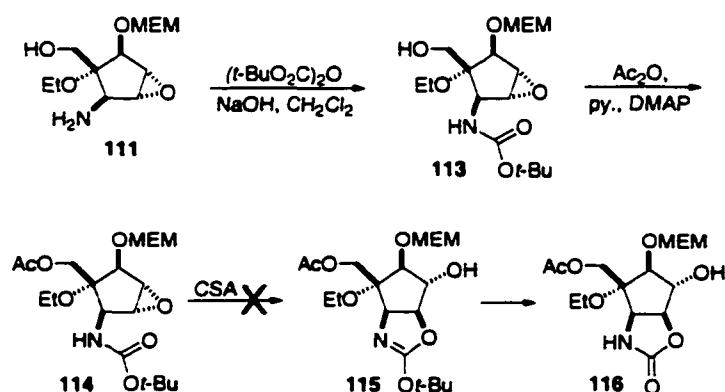
### Scheme 1.24



Regio- and stereoselective epoxide-opening with a neighboring carbamate<sup>32</sup> or trichloroacetate<sup>33</sup> have been featured in a variety of syntheses including Crimmins' route

to aminocyclitol **66** (Scheme 1.11).<sup>13</sup> Installation of a *t*-butylcarbamate in the presence of the free alcohol of **111** should be possible using Schotten-Baumann conditions. Indeed, reaction of **111** with di(*t*-butyl)dicarbonate with aqueous sodium hydroxide in CH<sub>2</sub>Cl<sub>2</sub> gave the carbamate **113** in 60% yield (Scheme 1.25). Protection of the primary alcohol gave acetate **114** which was set up for intramolecular epoxide-opening. However, treatment with acid (CSA, TFA) gave complex unidentifiable mixtures.

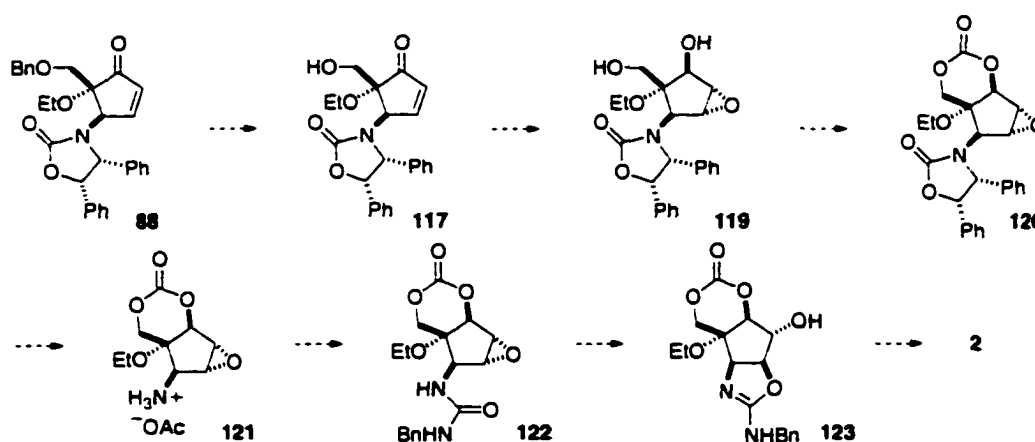
**Scheme 1.25**



Only minor differences existed between *t*-butyl carbamate **114** and the substrate which had undergone successful acid-catalyzed intramolecular epoxide-opening in Crimmins' synthesis (**63**). Substrate **114** contained the quaternary center and the protecting groups at C2 differed (MEM ether in **114** versus TBS ether in **63**). It appeared that one of these factors had interfered with the desired oxazolidinone formation. The quaternary center of **114**, which may have caused the molecule to adopt a conformation unfavorable to intramolecular ring-opening, had been installed in the key [2+2]-cycloaddition and therefore was not targeted for manipulation. Alternatively, the highly oxygenated methoxyethoxymethyl ether may have sequestered the catalytic acid required for ring opening and *t*-butyl ether cleavage.

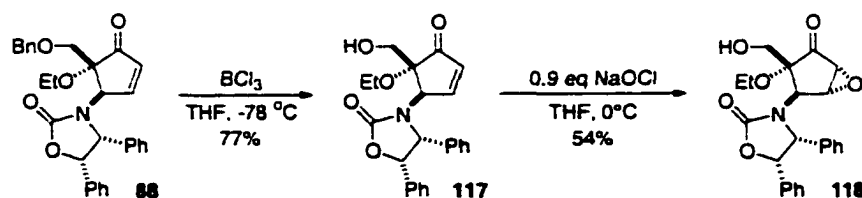
To circumvent the supposed problems associated with the MEM ether, an alternative protecting group strategy was devised (Scheme 1.26). Deprotection of the primary alcohol of **88** followed by epoxidation and reduction would give a diol **118** which could be protected as the cyclic carbonate (**119**). Hydrogenation under acidic conditions would minimize attack of the free amine on the carbonate carbonyl. Because the primary alcohol would be protected at this stage, formation of the urea should be facile.

**Scheme 1.26**



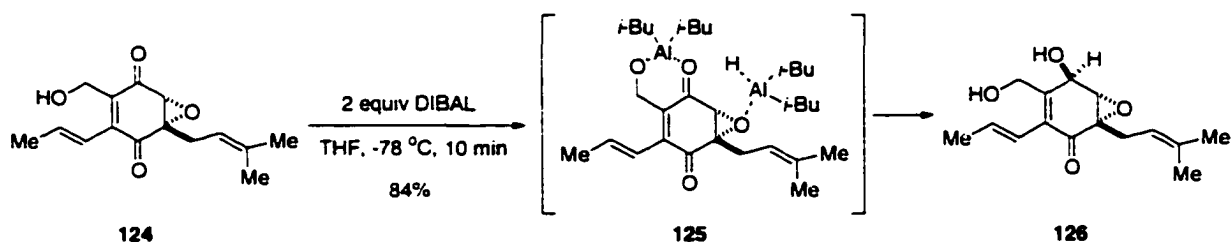
Boron trichloride-mediated deprotection of the primary alcohol followed by epoxidation on the face opposite the oxazolidinone gave epoxy ketone **118** (Scheme 1.27). Attempts to cleave the benzyl ether at a later stage led to decomposition.

**Scheme 1.27**

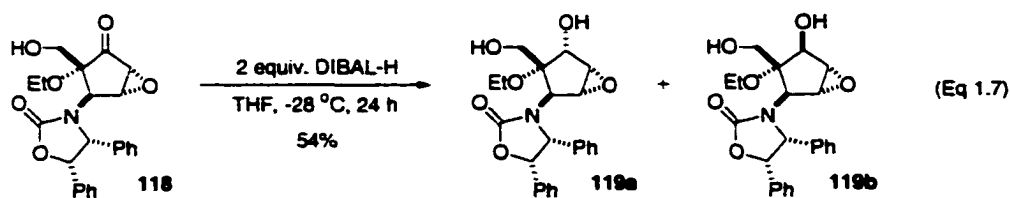


Porco and coworkers accomplished a hydroxyl-directed reduction resulting in *anti*-epoxy alcohol formation in their synthesis of (-)-jesterone (Scheme 1.28).<sup>34</sup> Chelation of one equivalent of DIBAL to the hydroxyl group and carbonyl followed by chelation of a second equivalent to the epoxide (**125**) and delivery of hydride from the same face as the epoxide led to complete selectivity.

**Scheme 1.28**



A similar chelation-controlled reduction with the epoxy alcohol **118** should be possible. Treatment of **118** with two equivalents of DIBAL in THF at  $-28\text{ }^{\circ}\text{C}$  led to a 2:1 mixture of epimeric alcohols **119a**:**119b** (Eq 1.7). Unfortunately, formation of the *cis*-epoxy alcohol was favored.<sup>35</sup> Attempts to promote the desired chelation-controlled reduction by cooling the reaction mixture to  $-78\text{ }^{\circ}\text{C}$  (no reaction), using a less polar solvent ( $\text{CH}_2\text{Cl}_2$ ), and increasing the concentration did not improve selectivity. Luche conditions ( $\text{NaBH}_4$ ,  $\text{CeCl}_3$ ) gave epoxy alcohol **119a** exclusively as did  $\text{NaBH}_4$  alone. The combination of  $\text{NaBH}_4$  and  $\text{Me}_2\text{BOEt}$  afforded a 6:1 mixture of **119a**:**119b** and additional side products. The low yield of the required epoxy alcohol **119b** prevented further investigation of this route.



#### IV. Future Studies

The great propensity for Payne rearrangement and dense functionalization of epoxy alcohol **90b** prevented successful advancement to trehalamine **2**. The presence of the large benzyloxymethyl group and oxazolidinone presumably inhibited manipulation of the epoxide under standard conditions due to steric interactions. Also, installation of the quaternary center at such an early stage in the synthesis may have greatly affected the conformation of the molecule. In previous syntheses the quaternary center was installed near the end. Eliminating the possibility of Payne rearrangement and changing the order for introduction of the functional groups and stereogenic centers may improve the strategy. A better starting material may be cyclopentenone **120**, available via an alternative ring expansion/elimination sequence developed previously in the group (Figure 1.4).<sup>36</sup> In this case the tertiary hydroxyl group and neopentyl alcohol would be easily accessed by epoxidation on the face opposite the large oxazolidinone followed by regioselective hydrolysis. Steric interactions would be minimized and Payne rearrangement would not be an issue as the *cis*-epoxy alcohol would be required. A potential problem may be oxidizing the carbon alpha to the carbonyl without eliminating the oxazolidinone.

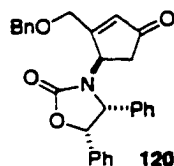
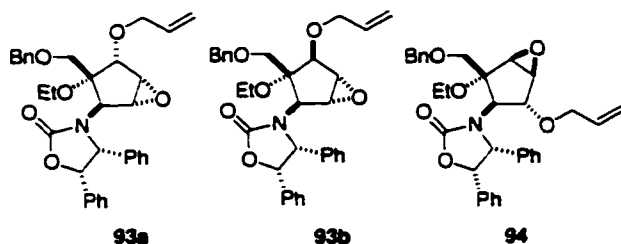


**Figure 1.4**

## V. Experimental Section

**Materials.** The following compounds were prepared according to literature procedures: diazomethane,<sup>37</sup> (+/-)-2-benzenesulfonyl-3-phenyloxaziridine (Davis' oxaziridine),<sup>38</sup> (PPh<sub>3</sub>)<sub>3</sub>RhCl,<sup>39</sup> Zn(BH<sub>4</sub>)<sub>2</sub>,<sup>40</sup> and LiAl(OBu)<sub>3</sub>,<sup>41</sup> Alumina (W200 neutral, ICN Pharmaceuticals) was used as received.

**General Procedures.** THF and Et<sub>2</sub>O were distilled from sodium-benzophenone ketyl; CH<sub>2</sub>Cl<sub>2</sub>, HMDS, pyridine, Ac<sub>2</sub>O, *i*-Pr<sub>2</sub>NEt and Et<sub>3</sub>N were distilled from CaH<sub>2</sub>; DMF was distilled from MgSO<sub>4</sub>. Pd(OAc)<sub>2</sub> was recrystallized from benzene. <sup>1</sup>H (300 and 400 MHz) and <sup>13</sup>C NMR (75 and 100 MHz) spectra were recorded in CDCl<sub>3</sub>, and chemical shifts (δ) were given in ppm relative to CHCl<sub>3</sub>. Flash column chromatography was performed with ICN 32-63 μm, 60 Å silica gel. Preparative thin layer chromatography was performed using Silica Gel 60 F<sub>254</sub>, 250 μm. Elemental analyses were performed at M-H-W Laboratories, Phoenix, AZ. All reactions were performed under an atmosphere of Ar.

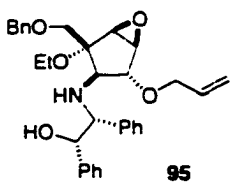


**Allyl ethers (93a, 93b, 94).** A 1:4 mixture of epimeric alcohols **90a,b**<sup>21</sup> (130 mg, 0.25 mmol) was dissolved in THF (3.0 mL) and cooled to -78°C. Allyl

bromide (0.22 mL, 2.50 mmol), NaHMDS (1.0 M in THF, 0.37 mL, 0.37 mmol), and DMF (0.2 mL) were added. The reaction mixture stirred at -78°C to 20°C over 17 h. The reaction mixture was quenched with saturated aqueous NH<sub>4</sub>Cl. The aqueous and

organic layers were separated and the aqueous layer was extracted with  $\text{CH}_2\text{Cl}_2$  (4x). The combined organic layers were washed with brine, dried with  $\text{MgSO}_4$ , filtered and concentrated in vacuo. Flash chromatography with hexane/ $\text{CH}_2\text{Cl}_2$ /EtOAc (15/1/1) gave **93a** (2 mg, 2%), **93b** (37 mg, 26%), and **94** (98 mg, 70%) as clear oils. **Allyl ether 93a**:  $^1\text{H}$  NMR  $\delta$  6.9-7.4 (m, 14H); 6.60 (m, 1H), 5.93 (m, 1H), 5.40 (d,  $J = 7.6$  Hz, 1H), 5.30 (m, 2H), 5.06 (d,  $J = 7.6$  Hz, 1H), 4.69 (s, 1H), 4.66 (d,  $J = 12.0$  Hz, 1H), 4.54 (d,  $J = 12.0$  Hz, 1H), 4.28 (ddt,  $J = 1.2, 5.2, 12.8$  Hz, 1H), 4.19 (ddt,  $J = 1.2, 6.0, 12.8$  Hz, 1H), 3.80 (s, 1H), 3.68 (dd,  $J = 10.0, 16.8$  Hz, 2H), 3.65 (m, 1H), 3.60 (m, 1H), 3.17 (d,  $J = 2.0$  Hz, 1H), 2.74 (d,  $J = 2.0$  Hz, 1H), 1.18 (t,  $J = 7.0$  Hz, 3H);  $^{13}\text{C}$  NMR  $\delta$  158.1, 137.8, 137.2, 134.7, 133.9, 128.7, 128.6, 128.2, 128.1, 126.0, 117.4, 90.4, 81.6, 80.7, 74.2, 73.2, 66.2, 63.3, 59.0, 57.7, 56.4, 56.1, 15.9; IR (thin film):  $\nu$  1750  $\text{cm}^{-1}$ ; HRMS  $m/z$  (M+H) calcd for  $\text{C}_{33}\text{H}_{36}\text{NO}_6$ : 542.2543, found: 542.2558. **Allyl ether 93b**:  $^1\text{H}$  NMR  $\delta$  7.48 (m, 5H), 7.00 (m, 6H), 6.47 (d,  $J = 6.6$  Hz, 2H), 6.07 (m, 1H), 5.42 (dd,  $J = 1.5, 17.4$  Hz, 1H), 5.31 (dd,  $J = 1.2, 10.2$  Hz, 1H), 4.86 (s, 1H), 4.75 (d,  $J = 7.8$  Hz, 1H), 4.68 (m, 2H), 4.67 (d,  $J = 1.6$  Hz, 1H), 4.34 (d,  $J = 5.7$  Hz, 2H), 4.07 (d,  $J = 9.9$  Hz, 1H), 3.82 (m, 1H), 3.72 (d,  $J = 9.3$  Hz), 3.63 (m, 1H), 3.47 (s, 1H), 2.92 (d,  $J = 2.7$  Hz, 1H), 1.23 (t,  $J = 6.9$  Hz, 3H);  $^{13}\text{C}$  NMR  $\delta$  158.8, 137.7, 136.9, 135.4, 134.0, 129.1, 128.6, 128.5, 128.0, 127.9, 127.8, 126.0, 117.8, 84.4, 80.7, 79.1, 74.4, 71.8, 70.6, 64.9, 59.8, 57.4, 57.2, 52.8, 16.5; IR (thin film):  $\nu$  1750  $\text{cm}^{-1}$ ; HRMS  $m/z$  (M+H) calcd for  $\text{C}_{33}\text{H}_{36}\text{NO}_6$ : 542.2543, found: 542.2531. **Allyl ether 94**:  $^1\text{H}$  NMR  $\delta$  6.5-7.5 (m, 15H), 5.61 (m, 1H), 5.34 (d,  $J = 7.6$  Hz, 1H), 4.99 (m, 2H), 4.89 (d,  $J = 7.2$  Hz, 1H), 4.78 (d,  $J = 12.0$  Hz, 1H), 4.59 (d,  $J = 12.0$  Hz), 4.53 (s, 1H), 3.85 (m, 1H), 3.84 (d,  $J = 10.0$  Hz, 1H), 3.76 (ddt,  $J = 1.4, 5.6, 11.4$  Hz), 3.74 (dd,  $J$

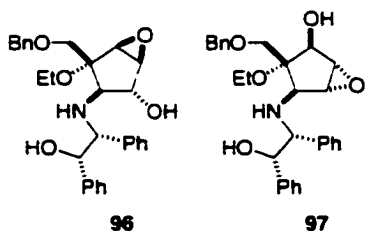
= 1.0, 2.2 Hz, 1H), 3.67 (m, 1H), 3.64 (d, J = 1.2 Hz, 1H), 3.63 (d, J = 10.0 Hz, 1H), 3.54 (ddt, J = 1.2, 5.6, 12.4 Hz, 1H), 3.38 (d, J = 2.4 Hz, 1H), 1.22 (t, J = 7.2 Hz, 3H);  $^{13}\text{C}$  NMR  $\delta$  158.4, 138.0, 136.9, 133.9, 133.8, 128.8, 128.7, 128.4, 128.1, 128.0, 127.9, 126.1, 117.9, 86.9, 81.0, 78.8, 74.1, 71.0, 67.7, 64.2, 63.6, 60.0, 59.2, 56.9, 16.0; IR (thin film):  $\nu$  1750  $\text{cm}^{-1}$ ; HRMS  $m/z$  (M+H) calcd for  $\text{C}_{33}\text{H}_{36}\text{NO}_6$ : 542.2543, found: 542.2550.



**95**

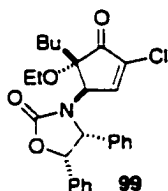
**Amino alcohol, 95.** The allyl ether **94** (0.14 g, 0.25 mmol) was dissolved in THF (1.2 mL) and MeOH (2.0 mL) in a 10 mL pressure tube and  $\text{Ba}(\text{OH})_2 \cdot 8\text{H}_2\text{O}$  was added (0.78 g, 2.50 mmol). The reaction mixture was sealed and heated to  $100^\circ\text{C}$  for 24 h. The reaction mixture was cooled to room temperature and additional  $\text{Ba}(\text{OH})_2 \cdot 8\text{H}_2\text{O}$  (0.10 g, 0.32 mmol) was added. The pressure tube was sealed and heated for an additional 24 h at  $100^\circ\text{C}$ . The reaction mixture was cooled to room temperature and quenched with saturated aqueous  $\text{NH}_4\text{Cl}$  and diluted with  $\text{CH}_2\text{Cl}_2$ . The aqueous and organic layers were separated and the aqueous layer was extracted with  $\text{CH}_2\text{Cl}_2$  (4x). The combined organic layers were washed with brine, dried with  $\text{MgSO}_4$ , filtered, and concentrated in vacuo. Flash chromatography with hexane/ $\text{CH}_2\text{Cl}_2$ /EtOAc (15/1/1) gave the amino alcohol **95** as a clear oil (36 mg, 0.07 mmol, 28%) and recovered starting material **94** (80 mg, 0.14 mmol, 56%). **Amino alcohol 95:**  $^1\text{H}$  NMR  $\delta$  7.2-7.4 (m, 15H), 5.79 (m, 1H), 5.20 (d, J = 17.2 Hz, 1H), 5.16 (m, 2H), 4.60 (dd, J = 0, 9.0 Hz, 2H), 4.52 (d, J = 4.8 Hz, 1H), 3.84 (d, J = 3.9 Hz, 1H), 3.81 (d, J = 5.1 Hz, 1H), 3.76 (d, J = 8.4 Hz, 1H), 3.66 (d, J = 8.1 Hz, 1H), 3.59 (d, J = 1.8 Hz, 1H), 3.55 (s, 1H), 3.47 (d, J = 2.1 Hz, 1H), 3.29 (m, 1H), 2.92 (m,

1H), 2.66 (s, 1H), 2.28 (bs, 1H), 1.45 (bs, 1H), 0.92 (t,  $J = 5.1$  Hz, 3H);  $^{13}\text{C}$  NMR  $\delta$  140.4, 139.3, 138.6, 134.7, 129.0, 128.6, 128.5, 128.4, 128.3, 128.0, 127.8, 127.1, 117.4, 85.5, 82.0, 78.1, 73.8, 70.5, 68.7, 67.4, 62.8, 60.5, 58.2, 57.3, 15.9; IR (thin film):  $\nu$  3456  $\text{cm}^{-1}$ ; HRMS  $m/z$  (M+H) calcd for  $\text{C}_{32}\text{H}_{38}\text{NO}_5$ : 516.2745, found: 516.2744.



**Amino diols 96, 97.** The amino alcohol **95** (38 mg, 0.07 mmol) was dissolved in ethanol (95%, 1.0 mL) and  $\text{RhCl}(\text{PPh}_3)_3$  (3 mg, 0.003 mmol) then DABCO (2 mg, 0.01 mmol) were added and the red solution was heated at reflux for 3 h. The reaction mixture was cooled to room temperature then poured into water (10 mL) and diluted with  $\text{CH}_2\text{Cl}_2$ . The layers were separated and the aqueous layer was extracted with  $\text{CH}_2\text{Cl}_2$  (4x). The combined organic layers were washed with brine, dried with  $\text{MgSO}_4$ , filtered and concentrated in vacuo to a clear oil. The oil was dissolved in  $\text{CH}_2\text{Cl}_2$  (4mL), 1N HCl (0.1 mL) was added, and the mixture was heated at reflux. After 24 h 6 drops of conc. HCl was added and the mixture continued to heat at reflux. After 24 h the mixture was neutralized with saturated aqueous  $\text{NaHCO}_3$  and diluted with  $\text{CH}_2\text{Cl}_2$ . The layers were separated and the aqueous layer was extracted with  $\text{CH}_2\text{Cl}_2$  (4x). The combined organic layers were dried with  $\text{MgSO}_4$ , filtered and concentrated in vacuo to a dark yellow oil. Preparative thin layer chromatography with hexane/EtOAc (2/1 x 3) gave **96** (7 mg, 22%) and **97** (7 mg, 22%) as clear oils. **Amino diol 96:**  $^1\text{H}$  NMR ( $\text{CDCl}_3$ ,  $\text{D}_2\text{O}$ )  $\delta$  7.2-7.6 (m, 15H), 4.68 (d,  $J = 16.4$  Hz, 1H), 4.62 (d,  $J = 16.0$  Hz, 1H), 4.54 (d,  $J = 7.2$  Hz, 1H), 3.90 (d,  $J = 6.9$  Hz, 1H), 3.87 (d,  $J = 11.4$  Hz, 1H), 3.83 (s 1H), 3.76 (d,  $J = 11.4$  Hz, 1H), 3.68

(s, 1H), 3.50 (s, 1H), 3.43 (m, 1H), 3.10 (m, 1H), 2.52 (s, 1H), 1.00 (t, J = 6.9 Hz, 3H);  $^{13}\text{C}$  NMR ( $\text{CDCl}_3$ )  $\delta$  140.5, 139.3, 138.2, 129.1, 128.6, 128.5, 128.4, 128.3, 128.1, 127.1, 86.0, 78.2, 73.9, 73.7, 67.7, 67.3, 63.9, 58.6, 58.2, 57.3, 15.8; IR (thin film):  $\nu$  3441  $\text{cm}^{-1}$ ; HRMS  $m/z$  (M+H) calcd for  $\text{C}_{29}\text{H}_{34}\text{NO}_5$ : 476.2437, found: 476.2434. **Amino diol 97**:  $^1\text{H}$  NMR ( $\text{C}_6\text{D}_6$ )  $\delta$  7.0-7.4 (m, 15 H), 4.77 (d, J = 6.3 Hz, 1H), 4.39 (dd, J = 6.9, 8.1 Hz, 1H), 4.33 (d, J = 6.0 Hz, 1H), 4.14 (d, J = 8.1 Hz, 1H), 4.05 (s, 2H), 3.81 (t, J = 5.7 Hz, 1H), 3.72 (d, J = 12.4 Hz, 1H), 3.63 (d, J = 12.4 Hz, 1H), 3.24 (d, J = 4.8 Hz, 1H), 3.13 (m, 2H), 2.12 (bs, 2H), 1.34 (bs, 1H), 0.90 (t, J = 6.9 Hz, 3H);  $^{13}\text{C}$  NMR  $\delta$  140.9, 139.5, 137.2, 129.0, 128.8, 128.5, 128.3, 128.2, 128.1, 127.9, 127.2, 84.2, 81.5, 77.9, 74.5, 74.0, 67.7, 66.8, 66.1, 65.7, 59.2, 16.1; IR (thin film):  $\nu$  3441  $\text{cm}^{-1}$ ; HRMS  $m/z$  (M+H) calcd for  $\text{C}_{29}\text{H}_{34}\text{NO}_5$ : 476.2437, found: 476.2445.



**$\alpha$ -chlorocyclopentenone 99.** Epoxy ketone **98** (14 mg, 0.03 mmol) was

dissolved in THF (0.8 mL) and water (0.4 mL). Hydrochloric acid (conc.,

1 drop) was added and the reaction mixture was refluxed overnight. After

cooling to room temperature the reaction mixture was quenched with saturated aqueous

$\text{NaHCO}_3$ . The layers were separated and the aqueous layer was extracted with  $\text{CH}_2\text{Cl}_2$

(3x). The combined organic layers were dried with  $\text{MgSO}_4$ , filtered and concentrated.

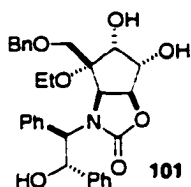
Flash column chromatography with hexane/EtOAc/ $\text{CH}_2\text{Cl}_2$  (4/1/1) gave the

cyclopentenone **99** as a white solid (4 mg, 0.01 mmol, 28%). **Cyclopentenone 99**:  $^1\text{H}$

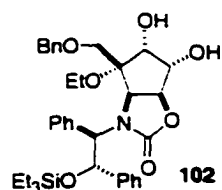
NMR  $\delta$  7.17 (m, 3H), 7.11 (m, 3H), 6.99 (m, 2H), 6.89 (bs, 2H), 6.63 (d, J = 3.0 Hz, 1H),

5.85 (d, J = 7.2 Hz, 1H), 5.24 (d, J = 3.0 Hz, 1H), 4.76 (d, J = 7.5 Hz, 1H), 3.38 (m, 2H),

1.86 (m, 2H), 1.44 (m, 2H), 1.26 (m, 2H), 1.14 (t,  $J = 6.9$  Hz, 3H), 1.00 (t,  $J = 7.5$  Hz, 3H); IR (thin film):  $\nu$  1752  $\text{cm}^{-1}$ ; LRMS  $m/z$  (M+H) calcd for  $\text{C}_{26}\text{H}_{29}\text{ClNO}_4$ : 454.2, found: 454.2.

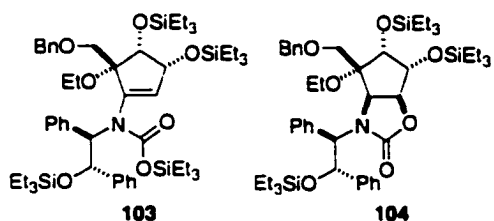


**Triol 101.** To epoxy alcohol **90a** (0.13 g, 0.26 mmol) in THF (4.0 mL) was added aqueous  $\text{HClO}_4$  (44%, 2.0 mL) and the reaction mixture was refluxed overnight. The mixture was cooled to room temperature and diluted with water. The layers were separated and the organic layer was washed with water (2x), dried with  $\text{MgSO}_4$ , filtered and concentrated in vacuo. Flash column chromatography with hexane/ $\text{CH}_2\text{Cl}_2$ /EtOAc (4/1/1 to 1/1/1) gave **101** as a white solid (0.11 g, 0.21 mmol, 80%). **Triol 101:**  $^1\text{H}$  NMR  $\delta$  7.63 (m, 2H), 7.47 (m, 2H), 7.35 (m, 9H), 7.15 (m, 2H), 5.57 (d,  $J = 8.4$  Hz, 1H), 4.40 (d,  $J = 8.1$  Hz, 1H), 4.20 (d,  $J = 9.0$  Hz, 1H), 4.07 (m, 4H), 3.55 (m, 3H), 3.21 (d,  $J = 11.4$  Hz, 1H), 3.16 (d,  $J = 11.4$  Hz, 1H), 2.97 (bs, 1H), 2.60 (m, 2H), 1/15 (t,  $J = 6.9$  Hz, 3H);  $^{13}\text{C}$  NMR  $\delta$  158.7, 141.2, 138.0, 137.1, 129.6, 128.8, 128.7, 128.6, 128.2, 127.8, 126.9, 86.4, 82.9, 76.2, 73.9, 73.6, 73.5, 70.1, 68.9, 68.0, 61.1, 16.3; IR (neat)  $\nu$  3415, 1732  $\text{cm}^{-1}$ ; HRMS  $m/z$  (M+H) calcd for  $\text{C}_{30}\text{H}_{33}\text{NO}_7$  520.2335, found 520.2330.



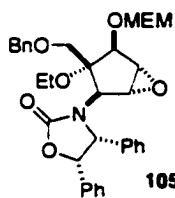
**Monosilyl ether 102.** Triol **101** (15 mg, 0.04 mmol) was dissolved in pyridine (0.25 mL) and cooled to  $-35$   $^{\circ}\text{C}$ . TESCl (0.005 mL, 0.03 mmol) was added dropwise. After 30 min the reaction mixture was quenched with brine at  $-35$   $^{\circ}\text{C}$  then allowed to warm to room temperature. Dichloromethane was added and the layers were separated. The aqueous layer was

extracted with  $\text{CH}_2\text{Cl}_2$  (3x), dried with  $\text{MgSO}_4$ , filtered and concentrated. Flash column chromatography with hexane/ $\text{CH}_2\text{Cl}_2$ /EtOAc (30/1/1 to 10/1/1) gave **102** as a clear oil (14 mg, 0.02 mmol, 57%). **Monosilyl ether 102**:  $^1\text{H}$  NMR  $\delta$  7.63 (m, 2H), 7.66 (m, 2H), 7.29-7.43 (m, 11H), 7.16 (m, 2H), 5.65 (d,  $J = 6.9$  Hz, 1H), 4.45 (d,  $J = 6.9$  Hz, 1H), 4.18 (m, 3H), 4.09 (d,  $J = 8.7$  Hz, 2H), 4.01 (m, 1H), 3.56-3.70 (m, 2H), 3.19 (m, 1H), 3.07 (s, 2H), 2.63 (s, 1H), 1.22 (t,  $J = 6.9$  Hz, 3H), 0.89 (t,  $J = 8.1$  Hz, 9H), 0.56 (q,  $J = 7.8$  Hz, 6H);  $^{13}\text{C}$  NMR  $\delta$  158.6, 141.1, 138.1, 137.3, 130.1, 128.6, 128.5, 128.3, 128.1, 128.0, 126.9, 85.9, 84.3, 73.9, 73.8, 71.0, 69.5, 68.1, 61.5, 16.2, 6.7, 4.6; HRMS  $m/z$  (M+H) calcd for  $\text{C}_{36}\text{H}_{48}\text{NO}_7\text{Si}$  634.3200, found 634.3208.



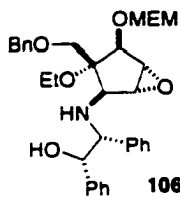
**Tetra- and trisilyl ethers 103, 104.** The monosilyl ether **102** (14 mg, 0.02 mmol) was dissolved in pyridine (0.19 mL) and cooled to  $-35$   $^{\circ}\text{C}$ . TESC1 (0.004 mL, 0.02 mmol) was added dropwise. After 20 min the reaction mixture was quenched with water and diluted with  $\text{CH}_2\text{Cl}_2$ . The layers were separated and the aqueous layer was extracted with  $\text{CH}_2\text{Cl}_2$  (3x). The combined organic layers were dried with  $\text{MgSO}_4$ , filtered and concentrated. Preparative thin layer chromatography with hexane/EtOAc (2/1) gave the tetrasilyl ether **103** (4 mg, 0.004 mmol, 18%) and trisilyl ether **104** (3 mg, 0.003, 13%). **Tetrasilyl ether 103**.  $^1\text{H}$  NMR  $\delta$  7.84 (m, 2H), 7.55 (m, 2H), 7.33 (m, 9H), 7.10 (m, 2H), 5.64 (d,  $J = 9.9$  Hz, 1H), 3.8-4.1 (m, 5H), 3.51 (m, 3H), 2.87 (s, 2H), 1.18 (t,  $J = 7.2$  Hz, 3H), 0.85 (m, 24H), 0.54 (m, 27H), 0.20 (m, 9H);  $^{13}\text{C}$  NMR  $\delta$  158.1, 142.8, 140.5, 137.5, 130.3, 128.8, 128.51, 128.46, 128.2, 127.93, 127.88, 127.0, 110.0, 85.6, 83.6, 73.8, 73.5, 71.3, 70.9, 70.0, 61.1, 16.3,

6.7, 6.6, 4.6. **Trisilyl ether 104**:  $^1\text{H NMR}$   $\delta$  7.79 (dd,  $J = 1.9, 7.4$  Hz, 2H), 7.57 (m, 2H), 7.31(m, 9H), 7.04 (m, 2H), 5.61 (d,  $J = 9.6$  Hz, 1H), 4.20 (d,  $J = 3.2$  Hz, 1H), 4.09 (d,  $J = 9.6$  Hz, 1H), 3.98 (d,  $J = 12.0$  Hz, 1H), 3.94 (d,  $J = 11.6$  Hz, 1H), 3.85 (dd,  $J = 2.8, 4.4$  Hz, 1H), 3.78 (dd,  $J = 5.2, 10.4$  Hz, 1H), 3.37 (m, 3H), 2.88 (d,  $J = 11.6$  Hz, 1H), 2.70 (d,  $J = 11.6$  Hz, 1H), 1.14 (t,  $J = 6.8$  Hz, 3H), 0.86 (m, 18H), 0.54 (m, 21H), 0.20 (m, 6H);  $^{13}\text{C NMR}$   $\delta$  158.4, 142.9, 140.2, 137.6, 130.2, 128.4, 128.3, 128.2, 128.1, 127.84, 127.78; 127.2, 84.9, 83.2, 77.7, 75.2, 74.0, 73.4, 72.1, 70.7, 69.4, 60.5, 16.2, 7.1, 6.8, 6.5, 5.5, 4.6, 4.5.

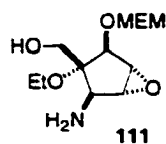


**Mem ether 105.** The epoxy alcohol **90b** (0.16 mg, 0.31 mmol) was dissolved in  $\text{CH}_2\text{Cl}_2$  (5.0 mL) then Hunig's base (0.16 mL, 0.92 mmol) and MEMCl (0.11 mL, 0.96 mmol) were added and the reaction mixture was stirred at room temperature overnight under argon. The reaction mixture was quenched with water and diluted with  $\text{CH}_2\text{Cl}_2$ . The aqueous layer was extracted with (5x). The combined organic layers were dried with  $\text{Na}_2\text{SO}_4$ , filtered and concentrated in vacuo to an orange oil. Flash column chromatography with hexane/EtOAc (2/1) gave the MEM ether **105** as a clear oil (0.14 g, 0.24 mmol, 77%). **MEM ether 105**:  $^1\text{H NMR}$   $\delta$  7.42 (m, 5H), 6.9-7.3 (m, 7H), 6.77 (m, 2H), 6.52 (bs, 1H), 5.36 (d,  $J = 7.2$  Hz, 1H), 4.92 (d,  $J = 7.2$  Hz, 1H), 4.81 (d,  $J = 12.0$  Hz, 1H), 4.63 (d,  $J = 12.0$  Hz, 1H), 4.58 (s, 1H), 4.43 (d,  $J = 7.2$  Hz, 1H), 4.36 (d,  $J = 7.2$  Hz, 1H), 3.87 (m, 3H), 3.78 (m, 1H), 3.71 (m, 1H), 3.67 (d,  $J = 10.0$  Hz, 1H), 3.58 (m, 2H), 3.46 (m, 3H), 3.35 (s, 3H), 1.26 (t,  $J = 7.2$  Hz, 3H);  $^{13}\text{C NMR}$   $\delta$  158.3, 138.0, 136.5, 133.8, 128.8, 128.4, 128.2, 128.1, 128.0, 126.8, 126.2, 95.8, 94.6, 86.8, 81.1, 78.4, 77.5, 74.1, 71.7, 67.5, 67.4, 64.7, 64.2, 60.1, 59.2, 59.1,

57.1: IR (neat)  $\nu$  1750  $\text{cm}^{-1}$ ; HRMS  $m/z$  (M+H) calcd for  $\text{C}_{34}\text{H}_{39}\text{NO}_8$  590.2754, found 590.2749.

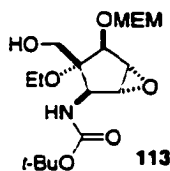


**Amino alcohol 106.** MEM ether **105** (48 mg, 0.08 mmol) was combined in a pressure tube with THF (1.6 mL) and MeOH (3.4 mL).  $\text{Ba}(\text{OH})_2 \cdot 8\text{H}_2\text{O}$  (0.26 mg, 1.15 mmol) was added to the white suspension and the pressure tube was sealed then heated to 100 °C for 48 h. The reaction mixture was then cooled to room temperature, diluted with  $\text{CH}_2\text{Cl}_2$ , and brought to pH 7 with saturated aqueous  $\text{NH}_4\text{Cl}$ . The layers were separated and the aqueous layer was extracted with  $\text{CH}_2\text{Cl}_2$  (5x). The combined organic layers were dried with  $\text{MgSO}_4$ , filtered and concentrated. Flash column chromatography with hexane/EtOAc/ $\text{CH}_2\text{Cl}_2$  (10/1/1 to 3/1/1) gave the amino alcohol **106** (9 mg, 0.02 mmol, 20%) and recovered **105** (11 mg, 0.02 mmol, 22%). **Amino alcohol 106:**  $^1\text{H}$  NMR  $\delta$  7.1-7.4 (m, 15H), 4.62 (m, 4H), 3.3-3.9 (m, 13H), 2.95 (m, 2H), 2.68 (s, 1H), 2.31 (bs, 1H), 0.96 (t,  $J = 6.9$  Hz, 3H);  $^{13}\text{C}$  NMR  $\delta$  140.3, 139.3, 138.5, 129.0, 129.0, 128.6, 128.5, 128.4, 128.3, 128.2, 128.0, 127.8, 127.1, 94.4, 85.5, 79.8, 78.2, 77.8, 73.8, 71.8, 68.5, 67.2, 67.1, 63.5, 60.4, 59.3, 58.2, 57.4, 15.8; HRMS  $m/z$  (M+H) calcd for  $\text{C}_{33}\text{H}_{42}\text{NO}_7$  564.2961, found 564.2964.



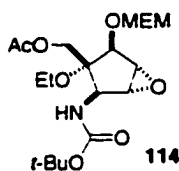
**Amino alcohol 111:** MEM ether **105** (44 mg, 0.08 mmol) was dissolved in MeOH (4.0 mL) and cooled to 0 °C. Pd/C (10%, 62 mg, 0.06 mmol),  $\text{Pd}(\text{OAc})_2$  (62 mg, 0.28 mmol), and  $\text{HCO}_2\text{NH}_4$  (0.18 mg, 2.80 mmol) were added. The reaction mixture stirred from 0 °C to room temperature overnight. The reaction mixture was filtered through celite and rinsed with water (10 mL),  $\text{CH}_2\text{Cl}_2$  (10 mL) and EtOAc

(10 mL). The solution was concentrated to a white solid which was dissolved in ether and aqueous NaOH (0.1 N). The layers were separated and the aqueous layer was washed with ether. The combined organic layers were dried with Na<sub>2</sub>SO<sub>4</sub>, filtered, and concentrated to give bibenzyl as a white solid. The aqueous layer was extracted with CH<sub>2</sub>Cl<sub>2</sub> (6x10 mL) and EtOAc (6x10 mL). The combined layers were dried with Na<sub>2</sub>SO<sub>4</sub>, filtered and concentrated to give amino alcohol **111** (10 mg, 0.04 mmol, 47%) as a clear oil which was used without further purification. **Amino alcohol 111**: <sup>1</sup>H NMR δ 4.84 (d, J = 6.8 Hz, 1H), 4.81 (d, J = 7.6 Hz, 1H), 4.00 (m, 1H), 3.97 (s, 1H), 3.74 (m, 5H), 3.57 (m, 2H), 3.43 (s, 1H), 3.40 (s, 3H), 3.35 (s, 1H), 2.43 (m, 3H), 1.21 (t, J = 6.8 Hz, 3H); <sup>13</sup>C NMR δ 95.7, 86.2, 86.1, 71.9, 67.3, 63.6, 62.5, 60.2, 59.8, 59.3, 57.9, 16.3; IR (neat) ν 3374 cm<sup>-1</sup>; HRMS *m/z* (M+H) calcd for C<sub>12</sub>H<sub>23</sub>NO<sub>6</sub> 278.1604, found 278.1611.

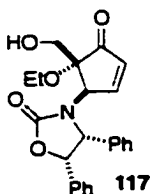


***t*-Butylcarbamate 113.** The amino alcohol **111** (30 mg, 0.11 mmol) was dissolved in CH<sub>2</sub>Cl<sub>2</sub> (2.0 mL) and (Boc)<sub>2</sub>O (26 mg, 0.12 mmol) then NaOH (1N, 0.10 mL, 0.10 mmol) were added. The reaction mixture stirred at room temperature overnight then was diluted with CH<sub>2</sub>Cl<sub>2</sub> and saturated aqueous NaHCO<sub>3</sub>. The layers were separated and the aqueous layer was extracted with CH<sub>2</sub>Cl<sub>2</sub> (5x), dried with Na<sub>2</sub>SO<sub>4</sub>, filtered, and concentrated in vacuo to a yellow oil. Preparative thin layer chromatography with hexane/EtOAc (1/1) gave carbamate **113** as a clear oil (27 mg, 0.07 mmol, 66%). **Carbamate 113**: <sup>1</sup>H NMR δ 4.87 (d, J = 7.2 Hz, 1H), 4.79 (d, J = 6.9 Hz, 1H), 4.60 (bd, J = 10.8 Hz, 1H), 4.18 (d, J = 5.4 Hz, 1H), 4.09 (s, 1H), 3.6-3.9 (m, 10H), 3.40 (s, 3H), 2.11 (bd, J = 9.0 Hz, 1H), 1.43 (s, 9H), 1.23 (t, J = 6.9 Hz, 3H);

$^{13}\text{C}$  NMR  $\delta$  155.3, 95.2, 85.9, 83.0, 80.3, 71.9, 67.5, 60.3, 59.8, 59.3, 57.7, 56.9, 28.5, 16.0; IR (neat)  $\nu$  3452, 1709  $\text{cm}^{-1}$ ; HRMS  $m/z$  (M+H) calcd for  $\text{C}_{17}\text{H}_{31}\text{NO}_8$  378.2128, found 378.2129.



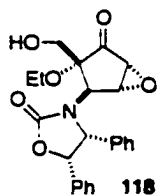
**Acetate 114:** *t*-Butylcarbamate **113** (27 mg, 0.07 mmol) was dissolved in  $\text{CH}_2\text{Cl}_2$  (2.0 mL) and cooled to 0  $^\circ\text{C}$ . Pyridine (0.006 mL, 0.07 mmol) was added and the reaction mixture was stirred for 10 min before acetic anhydride (0.01 mL, 0.11 mmol) and DMAP (4 mg, 0.03 mmol) were added. The reaction mixture was allowed to warm to room temperature overnight then was diluted with  $\text{CH}_2\text{Cl}_2$  and brine. The layers were separated and the aqueous layer was extracted with  $\text{CH}_2\text{Cl}_2$  (5x). The combined organic layers were washed with brine, dried with  $\text{Na}_2\text{SO}_4$ , filtered, and concentrated in vacuo. Preparative thin layer chromatography with hexane/EtOAc (3/2) gave acetate **114** as a clear oil (20 mg, 0.05 mmol, 66%). **Acetate 114:**  $^1\text{H}$  NMR  $\delta$  4.86 (d,  $J = 7.2$  Hz, 1H), 4.78 (d,  $J = 7.2$  Hz, 1H), 4.57 (d,  $J = 11.1$  Hz, 1H), 4.46 (d,  $J = 12.3$  Hz, 1H), 4.20 (m, 2H), 4.09 (s, 1H), 3.82 (m, 1H), 3.3-3.7 (m, 7H), 3.40 (s, 3H), 2.13 (s, 3H), 1.43 (s, 9H), 1.18 (t,  $J = 7.2$  Hz, 3H);  $^{13}\text{C}$  NMR  $\delta$  171.0, 154.9, 95.1, 84.4, 82.9, 80.2, 71.9, 67.5, 61.5, 60.1, 59.31, 59.25, 57.5, 57.1, 21.1, 15.8; IR (neat)  $\nu$  3450, 1743, 1710  $\text{cm}^{-1}$ ; HRMS  $m/z$  (M+H) calcd for  $\text{C}_{19}\text{H}_{33}\text{NO}_9$  420.2234, found 420.2241.



**Primary alcohol 117.** Cyclopentenone **88** (30 mg, 0.06 mmol) was dissolved in  $\text{CH}_2\text{Cl}_2$  (0.5 mL) in a 10 mL Schlenk flask and cooled to  $-78$   $^\circ\text{C}$ .  $\text{BCl}_3$  was slowly added down the side of the flask. After 5 min the

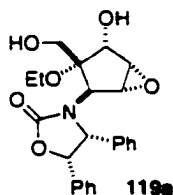
reaction mixture was quenched with MeOH (1.0 mL), removed from the cold bath and stirred for 10 min. Saturated aqueous NaHCO<sub>3</sub> was added and the aqueous layer was extracted with CH<sub>2</sub>Cl<sub>2</sub> (5x). The combined organic layers were dried with MgSO<sub>4</sub>, filtered, and concentrated to a yellow oil. Flash column chromatography with hexane/EtOAc/CH<sub>2</sub>Cl<sub>2</sub> (3/1/1) gave **117** as a white solid (19 mg, 0.05 mmol, 77%).

**Primary alcohol 117:** <sup>1</sup>H NMR δ 7.13 (m, 6H), 7.00 (m, 3H), 6.94 (bs, 1H), 6.06 (dd, J = 1.8, 4.8 Hz, 1H), 5.95 (d, J = 8.0 Hz, 1H), 5.39 (s, 1H), 5.08 (d, J = 7.6 Hz, 1H), 4.02 (m, 2H), 3.47 (m, 2H), 2.51 (m, 1H), 1.17 (t, 6.8 Hz, 3H); <sup>13</sup>C NMR δ 203.8, 158.8, 158.4, 136.2, 134.7, 133.9, 129.0, 128.8, 128.3, 128.2, 126.2, 85.4, 81.0, 65.3, 63.9, 61.0, 58.9, 15.7; IR (neat) ν 3450, 1748, 1720 cm<sup>-1</sup>; HRMS *m/z* (M+H) calcd for C<sub>23</sub>H<sub>24</sub>NO<sub>5</sub> 394.1654, found: 394.1657.

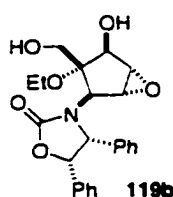


**Epoxy ketone 118.** Cyclopentenone **117** (0.67 g, 1.70 mmol) was dissolved in THF (20 mL) and water (10 mL) and cooled to 0 °C. NaOCl (5.25%, 2.3 g, 1.60 mmol) was added in small portions over 1.5 h. After 6 h the reaction mixture was quenched with 5% aqueous Na<sub>2</sub>S<sub>2</sub>O<sub>3</sub>. After stirring for 30 min at 0 °C the mixture was diluted with CH<sub>2</sub>Cl<sub>2</sub>. The layers were separated and the aqueous layer was extracted with CH<sub>2</sub>Cl<sub>2</sub> (5x). The combined organic layers were washed with brine, dried with MgSO<sub>4</sub>, filtered, and concentrated to a yellow oil. Flash column chromatography with hexane/EtOAc (6/1 to 3/1) afforded the epoxy ketone **118** (0.33 g, 0.79 mmol, 46%) as a white solid and recovered cyclopentenone **117** (56 mg, 0.14 mmol, 8%). **Epoxy ketone 118:** <sup>1</sup>H NMR δ 7.14 (m, 6H), 6.94 (m, 4H), 5.92 (d, J = 8.4 Hz, 1H), 8.4 Hz, 1H), 4.14 (bs, 1H), 4.08 (d, J = 12.0 Hz, 1H), 3.86 (m, 1H), 3.79 (s, 1H), 3.58 (s, 1H),

3.18 (m, 1H), 3.03 (m, 1H), 2.88 (m, 1H), 0.93 (t,  $J = 7.2$  Hz, 3H);  $^{13}\text{C}$  NMR  $\delta$  203.6, 159.7, 134.0, 129.3, 128.7, 128.6, 128.5, 128.3, 126.2, 81.0, 67.4, 63.1, 60.7, 57.1, 55.7, 55.0, 15.4; IR (neat)  $\nu$  3429, 1751  $\text{cm}^{-1}$ ; HRMS  $m/z$  (M+H) calcd for  $\text{C}_{23}\text{H}_{24}\text{NO}_6$  410.1604, found: 410.1608.



**Epoxy diol 119a.**  $\text{CeCl}_3 \cdot 7\text{H}_2\text{O}$  (38 mg, 0.10 mmol) was added to a solution of epoxy ketone 118 (30 mg, 0.07 mmol) in methanol (2.0 mL) at  $0^\circ\text{C}$  and the reaction mixture stirred for 30 min.  $\text{NaBH}_4$  (4 mg, 0.10 mmol) was added in one portion. After stirring for 2.5 h, 10% AcOH in methanol was added and the reaction mixture was stirred vigorously at  $0^\circ\text{C}$  for an additional 30 min. The mixture was diluted with  $\text{CH}_2\text{Cl}_2$  and water and the layers were separated. The aqueous layer was extracted with  $\text{CH}_2\text{Cl}_2$  (5x). The combined organic layers were washed with water, dried with  $\text{Na}_2\text{SO}_4$ , filtered and concentrated a white solid. Recrystallization from EtOAc/hexane or flash column chromatography with 10% aqueous neutral alumina (3-6% MeOH in  $\text{CH}_2\text{Cl}_2$ ) gave the epoxy diol **119a** (27 mg, 0.07 mmol, 90%). **Epoxy diol 119a:**  $^1\text{H}$  NMR  $\delta$  7.14 (m, 6H), 6.95 (m, 2H), 6.90 (m, 2H), 5.86 (d,  $J = 8.1$  Hz, 1H), 4.97 (d,  $J = 7.6$  Hz, 1H), 4.27 (bs, 1H), 4.62 (d,  $J = 10.4$  Hz, 1H), 3.89 (d,  $J = 3.6$  Hz, 2H), 3.55 (bs, 1H), 3.2-3.4 (m, 3H), 3.12 (d,  $J = 10.8$  Hz, 1H), 2.04 (m, 1H), 1.10 (t,  $J = 6.4$  Hz, 3H);  $^{13}\text{C}$  NMR  $\delta$  158.5, 134.1, 129.3, 128.8, 128.4, 128.3, 126.1, 85.5, 80.5, 76.0, 62.9, 60.5, 58.8, 56.8, 54.0, 15.8; IR (neat)  $\nu$  3467, 1745  $\text{cm}^{-1}$ ; HRMS  $m/z$  (M+H) calcd for  $\text{C}_{23}\text{H}_{26}\text{NO}_6$  412.1760, found: 412.1760. The relative stereochemistry was determined by X-ray crystallography.



**Epoxy diol 119b.** Epoxy ketone **118** (25 mg, 0.06 mmol) was dissolved in THF (3.8 mL) in a 10 mL pressure tube and cooled to  $-28\text{ }^{\circ}\text{C}$ . DIBAL (1.0 M in hexanes, 0.16 mmol) was added and the reaction mixture was shaken vigorously. After 15 h 10% aqueous AcOH was added and the reaction mixture stirred at room temperature for 1 h before it was diluted with  $\text{CH}_2\text{Cl}_2$ . The layers were separated and the aqueous layer was extracted with  $\text{CH}_2\text{Cl}_2$  (5x). The combined organic layers were washed with water, dried with  $\text{Na}_2\text{SO}_4$ , filtered, and concentrated. Flash column chromatography on deactivated neutral alumina (10%  $\text{H}_2\text{O}$ ) with methanol in  $\text{CH}_2\text{Cl}_2$  (3-6%) afforded a 2:1 mixture of alcohols **119a**:**119b** (13 mg, 0.03 mmol, 52%). **Epoxy diol 119b**:  $^1\text{H NMR}$   $\delta$  7.14 (m, 6H), 6.95 (m, 2H), 6.90 (m, 2H), 5.90 (d,  $J = 8.1\text{ Hz}$ , 1H), 5.25 (d,  $J = 8.4\text{ Hz}$ , 1H), 4.15 (d,  $J = 8.4\text{ Hz}$ , 2H), 3.89 (m, 3H), 3.1-3.6 (m, 3H), 2.44 (m, 1H), 1.10 (t,  $J = 6.6\text{ Hz}$ , 3H); HRMS  $m/z$  ( $\text{M}+\text{H}$ ) calcd for  $\text{C}_{23}\text{H}_{26}\text{NO}_6$  412.1760, found: 412.1761.

## VI. References

- 
- <sup>1</sup> Stryer, L. *Biochemistry* 4th ed.: W.H. Freeman: New York, 1995.
- <sup>2</sup> Berecibar, A.; Grandjean, C.; Siriwardena, A. *Chem. Rev.* **1999**, 779.
- <sup>3</sup> Ando, O.; Satake, H.; Itoi, K.; Sato, A.; Nakajima, M.; Takahasi, S.; Haruama, H.; Ohkuma, Y.; Kinoshita, T.; Enokita, R. *J. Antibiot.* **1991**, 44, 1165.
- <sup>4</sup> Kobayashi, Y.; Miyazaki, H.; Shiozaki, M. *J. Org. Chem.* **1994**, 59, 813.
- <sup>5</sup> a) Ogawa, S.; Uchida, C.; Yuming, Y. *J. Chem. Soc., Chem. Commun.* **1992**, 886; b) Ogawa, S.; Uchida, C. *J. Chem. Soc., Perkin Trans, 1.* **1992**, 1939.
- <sup>6</sup> Uchida, C.; Yamagishi, T.; Ogawa, S. *J. Chem. Soc., Perkin Trans, 1.* **1994**, 589.
- <sup>7</sup> Ledford, B.E.; Carreira, E.M. *J. Am. Chem. Soc.* **1995**, 117, 11811.
- <sup>8</sup> Li, J.; Lang, F.; Ganem, B. *J. Org. Chem.* **1998**, 63, 3403.
- <sup>9</sup> Storch de Gracia, I.; Dietrich, H.; Bobo, S.; Chiara, J.L. *J. Org. Chem.* **1998**, 63, 5883.
- <sup>10</sup> Storch de Gracia, I.; Bobo, S.; Martín-Ortega, M.D.; Chiara, J.L. *Org. Lett.* **1999**, 1, 1705.
- <sup>11</sup> Boiron, A.; Zillig, P.; Faber, D.; Giese, B. *J. Org. Chem.* **1998**, 6, 5877.
- <sup>12</sup> Knapp, S.; Purandare, A.; Rupitz, K.; Withers, S.G. *J. Am. Chem. Soc.* **1994**, 116, 7461.
- <sup>13</sup> Seepersaud, M.; Al-Abed, Y. *Tetrahedron Lett.* **2001**, 42, 1471.
- <sup>14</sup> Crimmins, M.T.; Tabet, E.A. *J. Org. Chem.* **2001**, 66, 4012.
- <sup>15</sup> a) Söderberg, B.C.; Hegedus, L.S.; Sierra, M.A. *J. Am. Chem. Soc.* **1990**, 113, 4364; b) Hegedus, L.S.; Bates, R.W.; Söderberg, B.C. *J. Am. Chem. Soc.* **1990**, 923; c) Söderberg, B.C.; Hegedus, L.S. *J. Org. Chem.* **1991**, 56, 2209.

- 
- <sup>16</sup> a) Aumann, R.; Fisher, E.O. *Angew. Chem. Int. Ed. Engl.* **1967**, *6*, 879; b) Casey, C.P.; Cyr, C.R.; Boggs, R.A. *Synth. Inorg. Met-Org. Chem.* **1973**, *3*, 249; c) Bao, J.; Wulff, W.D.; Dominy, J.B.; Fumo, M.J.; Grant, E.B.; Rob, A. C.; Whitcomb, M.C.; Yeung, S.-M.; Ostrander, R.L.; Rheingold, A.L. *J. Am. Chem. Soc.* **1996**, *118*, 3392; d) Kreissl, F.R. In *Transition Metal Carbene Complexes*; Seyforth, D.E., Ed.; Verlag Chemie: Weinheim, 1983.
- <sup>17</sup> a) Semmelhack M.F.; Lee, G.R. *Organometallics* **1987**, *6*, 1839; b) Hegedus, L.S.; Schwindt, M.A.; Lejon, T. *Organometallics* **1990**, *9*, 2914.
- <sup>18</sup> For reviews, see: a) Wulff, W. In *Comprehensive Organic Synthesis*; Trost, B.M.; Fleming, I.; Paquette, L.A., Eds.; Pergamon Press: Oxford, 1991; Vol. 6, pp 1065-1114; b) Dotz, K.H.; Fischer, H.; Hofmann, P.; Kreissel, F.R.; Schubert, U.; Weiss, K. *Transition Metal Carbene Complexes*; VCH: Deerfield Beach, 1983.
- <sup>19</sup> For a recent review, see: Hegedus, L.S. *Tetrahedron*, **1997**, *53*, 4105.
- <sup>20</sup> a) Reed, A. D.; Hegedus, L.S. *Organometallics* **1997**, *16*, 2313; b) Umbricht, G.; Hellman, M.D.; Hegedus, L.S. *J. Org. Chem.* **1998**, *63*, 5173.
- <sup>21</sup> a) Wen, X. Ph.D. Dissertation, Colorado State University, 1998; b) Wen, X.; Norling, H.; Hegedus, L.S. *J. Org. Chem.* **2000**, *65*, 2096.
- <sup>22</sup> Reed, A.D.; Hegedus, L.S. *Organometallics* **1997**, *16*, 2313.
- <sup>23</sup> Akiba, T.; Tamura, O.; Terashima, S. *Org. Synth.* **1997**, *75*, 45.
- <sup>24</sup> Li, K.; Hamann, L.G.; Koreeda, M. *Tetrahedron Lett.* **1992**, *33*, 6569.
- <sup>25</sup> Larock, R.C. *Comprehensive Organic Transformations*; VCH Publishers: New York, 1989; pp 129-131.

- 
- <sup>26</sup> a) Ito, Y.; Hirao, T.; Saegusa, T. *J. Org. Chem.* **1978**, *43*, 1011; b) Larock, R.C.; Hightower, T.R.; Kraus, G.A.; Hahn, P.; Zheng, D. *Tetrahedron Lett.* **1995**, *36*, 2423.
- <sup>27</sup> Trost, B.M.; Mikhail, G.K. *J. Am. Chem. Soc.* **1987**, *110*, 4124.
- <sup>28</sup> Reich, H.J.; Wollowitz, S.; Trend, J.E.; Chow, F.; Wendelborn, D.F. *J. Org. Chem.* **1978**, *43*, 1697.
- <sup>29</sup> Davis, F.A.; Stringer, O.D.; Billmers, J.M. *Tetrahedron Lett.* **1983**, *24*, 1213.
- <sup>30</sup> Nakato, T.; Tanka, T.; Oishi, T. *Tetrahedron Lett.* **1981**, *22*, 4723.
- <sup>31</sup> Brown, B., Colorado State University, unpublished results.
- <sup>32</sup> a) Langlois, N.; Mori, A. *Eur. J. Org. Chem.* **1999**, 3483; b) Inoue, M.; Furuyama, H.; Sakazaki, H.; HIRAMA, M. *Org. Lett.* **2001**, *3*, 2863.
- <sup>33</sup> Liu, D.-G.; Wang, B.; Lin, G.-Q. *J. Org. Chem.* **2000**, *65*, 9114.
- <sup>34</sup> Hu, Y.; Li, C.; Kulkarni, B.A.; Strobel, G.; Lobkovsky, E.; Torczynski, R.M.; Porco, J.A. *Org Lett.* **2001**, *3*, 1649.
- <sup>35</sup> The stereochemistry was determined with an X-ray crystal structure of **99**.
- <sup>36</sup> Brown, B.; Hegedus, L.S. *J. Org. Chem.* **2000**, *65*, 1865.
- <sup>37</sup> Black, T.H. *Aldrichimica Acta* **1983**, *16*, 3.
- <sup>38</sup> a) Davis, F.A.; McCauley, J.P.; Chattopadhyay, S.; Harakal, M.E.; Towson, J.C.; Watson, W.H.; Tavanaiepour, I. *J. Am. Chem. Soc.* **1987**, *109*, 3370; b) Davis, F.A.; Chattopadhyay, S.; Towson, J.C.; Lal, S.; Reddy, T. *J. Org. Chem.* **1988**, *53*, 2087.
- <sup>39</sup> Osborn, J.A.; Wilkinson, G. *Inorganic Synthesis* **1990**, *28*, 77.
- <sup>40</sup> *Encyclopedia of Reagents for Organic Synthesis*; Paquette, L.A., Ed.; John Wiley & Sons: Chichester, 1995; p 5536.

---

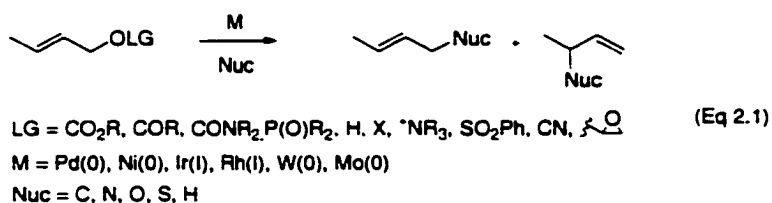
<sup>41</sup> a) Brown, H.C.; Weissman, P.N. *J. Am. Chem. Soc.* **1965**, *87*, 5614; b) Brown, H.C.;  
Deck, H.R. *J. Am. Chem. Soc.* **1965**, *87*, 5620.

## Chapter Two

### Effect of Adjacent Chiral Tertiary and Quaternary Centers on the Metal-Catalyzed Allylic Substitution Reaction

#### I. Introduction and Background

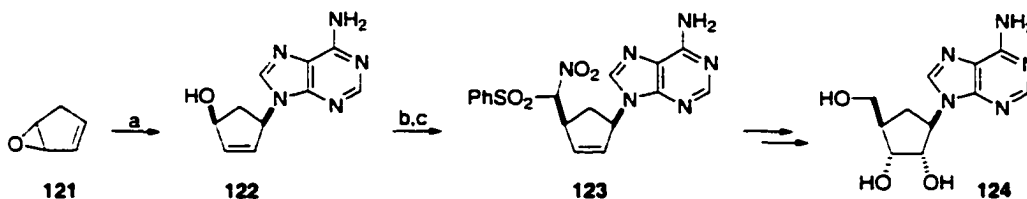
The metal-catalyzed allylic substitution reaction has been widely studied and has emerged as a powerful synthetic tool for the construction of carbon-carbon, carbon-heteroatom and carbon-hydrogen bonds (Eq 2.1).<sup>1</sup> A large variety of allylic substrates and nucleophiles undergo the reaction catalyzed by a wide range of metal complexes. However, the vast majority of studies have been conducted with palladium-catalysts. The transformation permits the use of configurationally stable and easily-handled allylic substrates such as acetates and carbonates, which helps overcome limitations imposed by the use of more highly activated allyl halides or sulfonate esters.



The metal-catalyzed substitution reaction has made a significant impact on synthetic chemistry, particularly the area of nucleosides. Because of their role as antivirals, antibiotics, and anti-cancer agents, the synthesis of nucleosides and their analogs has been the focus of a great deal of attention in recent years.<sup>2</sup> Trost has pioneered the use of  $\pi$ -allylpalladium chemistry in this endeavor.<sup>3</sup> Palladium-catalyzed substitution was used to introduce both the nucleoside base and side chain in Trost's

synthesis of aristeromycin **124** (Scheme 2.1). Subsequently, this methodology has been featured in a number of strategies towards the synthesis of carbovir, abacavir and analogs.<sup>3</sup>

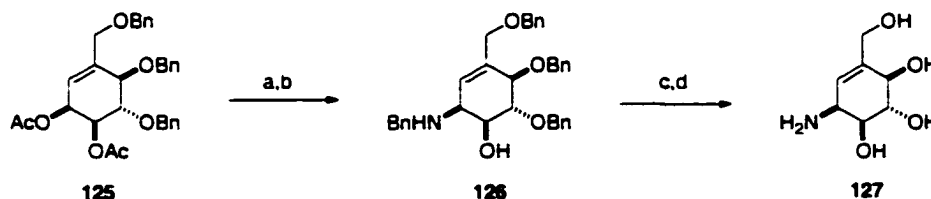
### Scheme 2.1



(a) Pd(OAc)<sub>2</sub>, P(O-Pr)<sub>3</sub>, adenine; (b) ClCO<sub>2</sub>Me; (c) Pd<sub>2</sub>(dba)<sub>3</sub>, PPh<sub>3</sub>, LiCH(NO<sub>2</sub>)SO<sub>2</sub>Ph

Shing and coworkers also applied the allylic amination reaction to their synthesis of valienamine **127**, an  $\alpha$ -glycosidase inhibitor (Scheme 2.2).<sup>4</sup> Reaction of the advanced intermediate **125** with benzylamine and a catalytic amount of Pd(PPh<sub>3</sub>)<sub>4</sub> followed by deacetylation gave the desired allylic amine **126** with complete regio- and stereoselectivity in 58% yield for the two steps. Protecting group manipulation afforded the natural product.

### Scheme 2.2



(a) Pd(PPh<sub>3</sub>)<sub>4</sub>, BnNH<sub>2</sub>, CH<sub>3</sub>CN, reflux; (b) NaOMe, MeOH (c) NH<sub>3</sub>, Na<sup>+</sup>, THF; (d) Ac<sub>2</sub>O, py.

The utility of the palladium-catalyzed transformation was greatly amplified with the development of the enantioselective version utilizing chiral ligands.<sup>5</sup> A few of the many ligands that have been developed are shown in Figure 2.1.

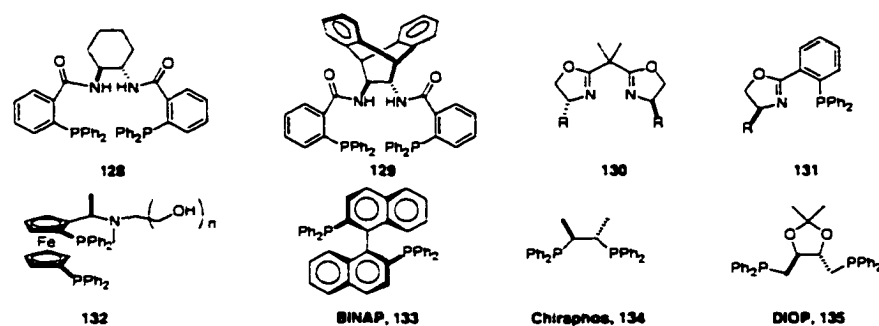
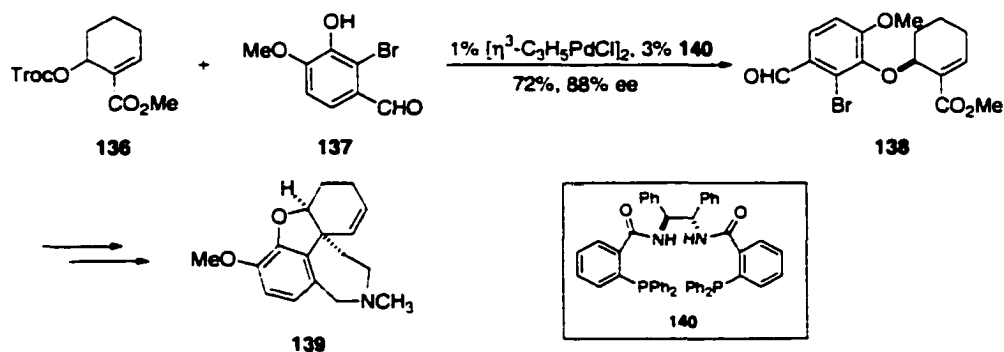


**Figure 2.1**

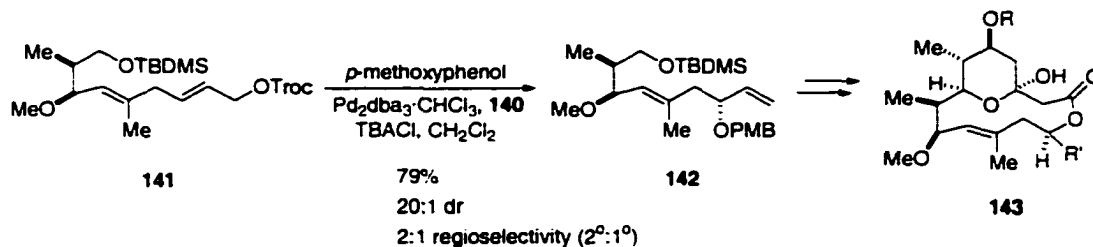
A number of recent syntheses have featured the asymmetric allylic substitution reaction. One example is Trost's synthesis of (-)-galanthamine **139**, a selective acetylcholinesterase inhibitor (Scheme 2.3).<sup>6</sup> Good enantioselectivity was observed in the formation of the aryl ether linkage of **138** even though the phenol was *ortho*-disubstituted.

**Scheme 2.3**



The synthesis of the macrolide portion of deschlorocallipeltoside A **143**, a potential cancer drug, also relied on the enantioselective introduction of an ether linkage via palladium-catalyzed asymmetric alkoxylation (Scheme 2.6).<sup>7</sup> Control of both the regio- and stereochemistry was possible with the use of the chiral ligand **140**.

## Scheme 2.4



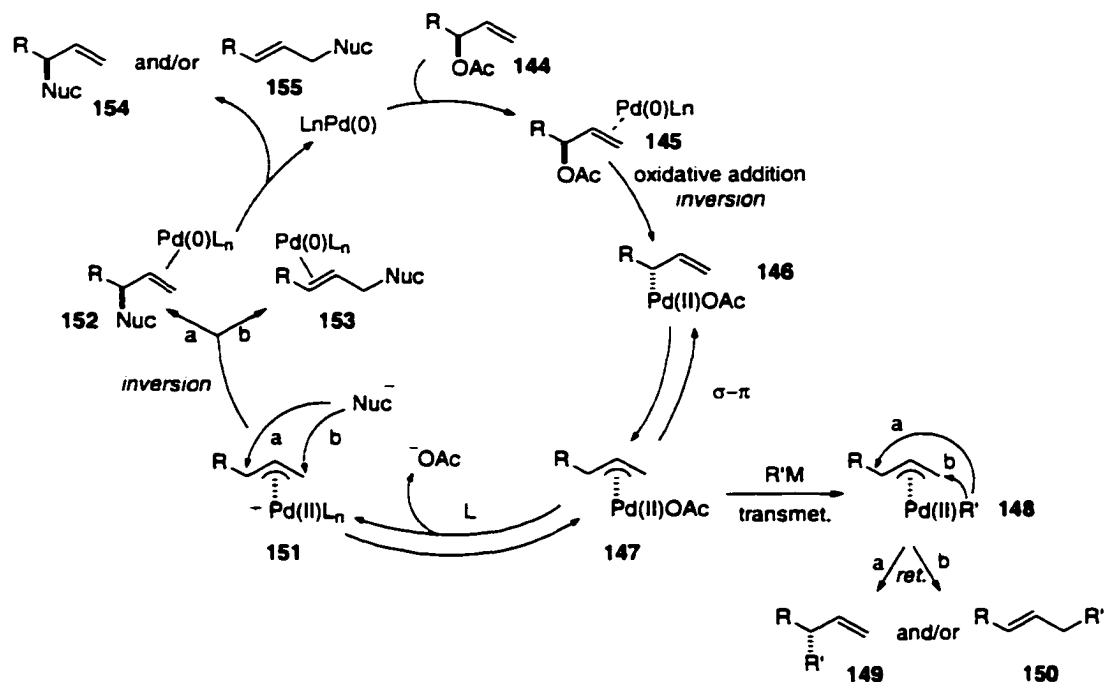
The development of enantioselective allylations catalyzed by other metal complexes is still in its infancy. There have been a few reports of moderate to good enantioselectivities with molybdenum,<sup>8</sup> tungsten,<sup>9</sup> rhodium, and iridium<sup>10</sup> complexes and there will no doubt be more focus in this area in the future.

### I.A Palladium-Catalyzed Reaction

#### I.A.1 Mechanism.

Undoubtedly, the majority of studies involving the allylic alkylation reaction have been conducted with palladium catalysts. The proposed mechanism is shown below (Scheme 2.5).<sup>11</sup> Initial complexation of the metal to the olefin (**145**) is followed by oxidative addition in which palladium displaces the leaving group in an  $S_N2$  type fashion to give an  $\eta^1$ -allylpalladium(II) complex **146** with inversion of stereochemistry. The  $\sigma$ -complex is in equilibrium with an  $\eta^3$ -allylpalladium intermediate **147**. In the presence of a main-group metal such as zinc, aluminum, boron, or tin, transmetalation in which  $R'$  is delivered directly to palladium occurs to give **148**. Reductive elimination then delivers  $R'$  to the allyl ligand on the same face as the metal, resulting in overall inversion of stereochemistry. The regiochemistry depends on the main-group metal used.

## Scheme 2.5



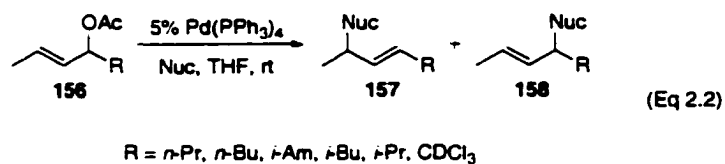
Alternatively, when the  $\eta^3$ -allylpalladium intermediate **147** is formed in the presence of excess ligand, a highly electrophilic cationic  $\pi$ -allylpalladium complex **151** is formed which reacts with a wide range of nucleophiles. Attack at the less-substituted allylic terminus usually dominates; however, a number of factors affect the regiochemistry and this will be discussed in more detail later. The nucleophile attacks on the face opposite the palladium, resulting in overall retention of stereochemistry. This selectivity is opposite that observed with classical alkylations for which an inversion pathway operates, making palladium-catalyzed allylic substitution a useful complement. Finally, decomplexation of the metal regenerates palladium(0) and gives the substituted product(s) **154** and **155**.

Control of regiochemistry is very important when the intermediate  $\pi$ -allylpalladium intermediate formed is non-symmetrically substituted. In most cases the

palladium-catalyzed reaction favors attack at the less-substituted allylic terminus. However, regioselectivity can vary<sup>12</sup> depending on the nucleophile,<sup>13</sup> the ligand,<sup>14</sup> remote electronic effects in the substrate,<sup>15</sup> and through the use of tethered directing groups.<sup>16</sup> These factors will be discussed in detail below.

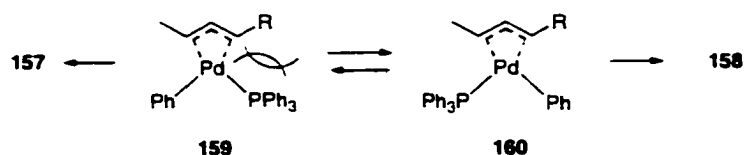
### I.A.2 Nucleophile Effects on Regioselectivity

Keinan and coworkers systematically studied the regioselectivities of a variety of nucleophiles with 1,3-dialkyl-substituted allylic substrates **156** (Eq 2.2).<sup>13</sup> The stabilized nucleophiles morpholine, 2-methyl-cyclohex-1-en-tributylstannyleneol, and dimethyl sodiomalonate displayed a high degree of selectivity for attack at the less-hindered terminus (**157**, 80-100%). This great preference was presumably due to the steric differences in the alkyl chains even though in some cases the differences were quite subtle (Me versus *n*-Pr). Electronic factors were not thought to be a factor since two alkyl groups should have similar donor/acceptor properties.



Alternatively, phenylzinc chloride, which reacts via the transmetalation/reductive elimination pathway, attacked the more-hindered terminus to give **158** with nearly complete selectivity (>99%). It was suggested that the intermediate formed prior to reductive elimination assumed a square planar conformation with the large phosphine ligand positioned *cis* to the smaller alkyl group (Scheme 2.6).<sup>13</sup>

## Scheme 2.6

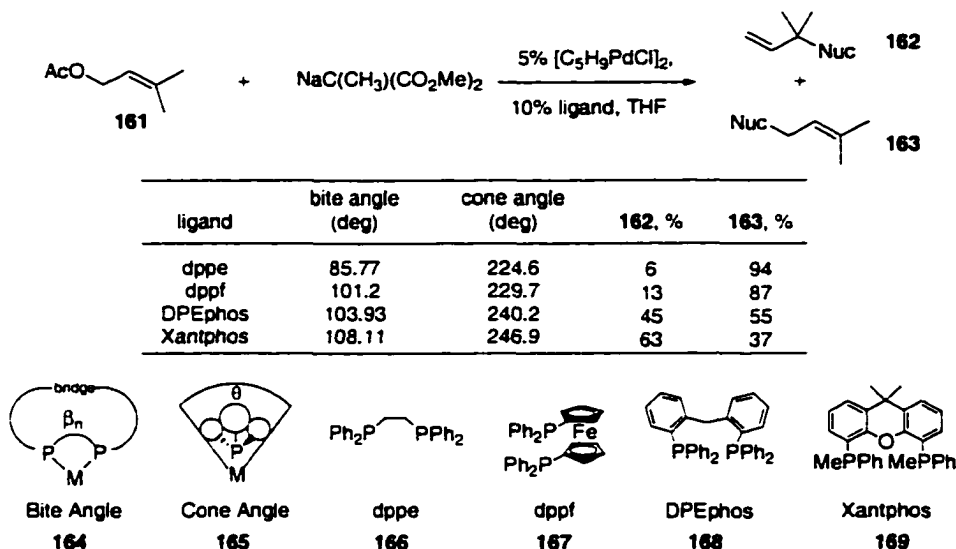


Conversely, aryl and vinyl tin reagents preferentially attacked the *less-substituted* terminus of acyclic allyl acetates<sup>17</sup> and the *less-hindered* terminus of cyclic allyl esters.<sup>18</sup> Although the mechanism for the Stille reaction has been examined in great detail,<sup>19</sup> the specifics for cross-coupling of organotin reagents with  $\pi$ -allylpalladium intermediates have not yet been uncovered. As a result, the differences in selectivity exhibited by organozinc and organotin reagents are not understood.

### I.A.3 Ligand Effects on Regioselectivity

One of the main advantages of metal-catalyzed reactions is the ability to adjust both the steric and electronic properties of the ancillary ligands to fine-tune the reactivity of the catalyst. Great success has been achieved in controlling the regioselectivity of the allylic alkylation reaction using this strategy. With the aid of X-ray crystallography, Van Leeuwen and coworkers observed that an increase in the bite angle (**164**) of chelating (P,P)- ligands resulted in an increase in the cone angle (**165**) and a preference for attack at the more-substituted allylic terminus of 3-methyl-2-butenyl-1- acetate (Scheme 2.7).<sup>14a</sup>

## Scheme 2.7



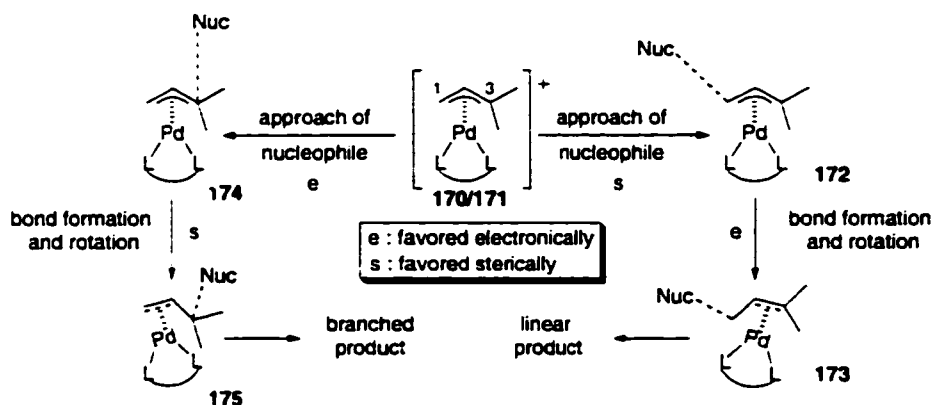
Use of ligands with small bite angles led to relatively few steric interactions between the ligand and the allyl moiety, and therefore resulted in less-activated intermediates and slower reaction rates. In this case, the steric differences between the two allylic termini determined the site of nucleophilic attack. As the bite angle and consequently the cone angle of the ligand increased, steric interactions between the ligand and the *anti*-substituent on the allyl moiety became more significant. Distortion of the intermediate **170** towards  $\eta^1, \eta^2$ -type coordination **171** occurred in which the Pd-C3 bond distance was elongated and the C2-C3 distance became shorter (Eq 2.3).<sup>20</sup>



The intermediate **171** became more activated towards nucleophilic attack and there was less back-bonding to the substituted terminus of the allyl ligand which resulted in an electronic preference for attack at the more-substituted carbon.<sup>21</sup> Additionally, the

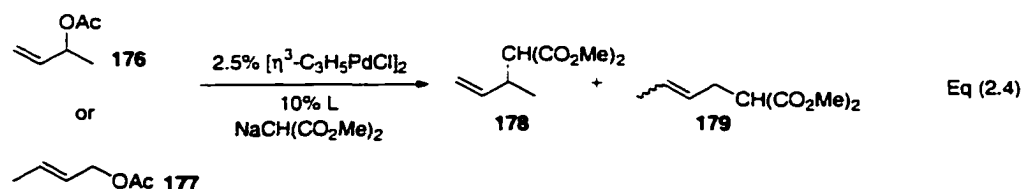
steric interactions in the resulting palladium-olefin complex were minimized when the branched product was formed (Scheme 2.8). This was consistent with the observation that nucleophiles preferentially attacked the longer Pd-C bond.<sup>22</sup>

**Scheme 2.8**



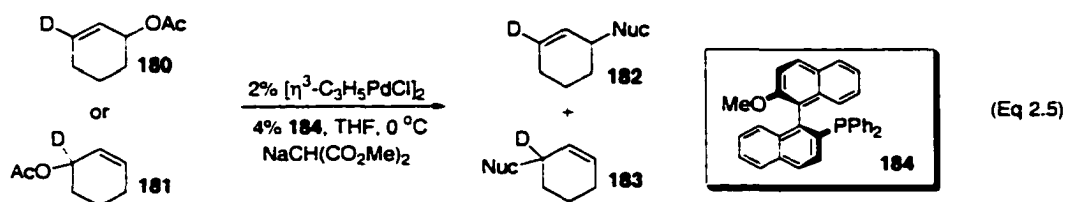
Åkermark and coworkers reported that in the amination of  $\eta^3$ -(3-methylbutenyl)palladium complexes electronics of the ligand determined the regioselectivity.<sup>23</sup> Acceptor ligands such as triphenylphosphine, 1,5-cyclooctadiene, and triphenylphosphite increased the rate of allylic amination compared with donor ligands such as bipyridine as well as directing the nucleophile to the more-substituted allylic terminus. They also observed a downfield  $^{13}\text{C}$  shift of C3, which corresponded with an increase in the percentage of branched product formed. This suggested that the  $^{13}\text{C}$  NMR shift was correlated with positive charge buildup on the substituted carbon.

Tricyclohexylphosphine ( $\text{PCy}_3$ ) has also been used to control the regiochemistry of the allylic alkylation reaction.<sup>14b</sup> Reaction of dimethyl sodiomalonate with butenyl acetate **176** and  $\text{PCy}_3$  favored formation of the branched product (11.5:1 **178**:**179**) which contrasted those results observed with  $\text{PPh}_3$  (1:2 **178**:**179**) (Eq 2.4).



Interestingly, the product distribution changed dramatically when the regioisomeric allyl acetate **177** was used (1.3:1 **178**:**179**). It was postulated that the acetate leaving group did not act as a simple spectator ion, but was intimately associated with the  $\pi$ -allyl intermediate, leading to what has been referred to as a “memory effect”.<sup>24</sup> However, the details of the interactions with  $\text{PCy}_3$  are still unclear.

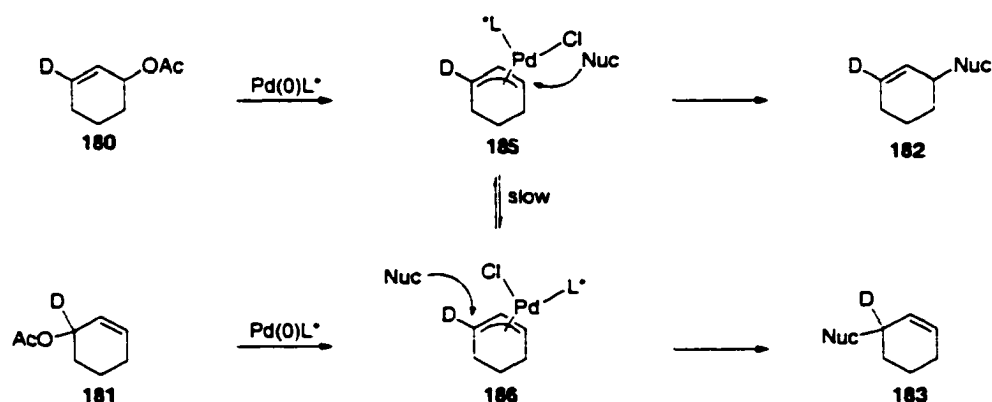
Other examples in which the original position of the leaving group affected the regiochemistry have been reported. Hayashi and coworkers showed that by using 2-(diphenylphosphino)-2'-methoxy-1,1'-binaphthyl (MeO-MOP, **184**) in the palladium-catalyzed allylic alkylation of unsymmetrically-substituted substrates, retention of regiochemistry of the allylic ester resulted.<sup>25</sup>  $\gamma$ - and  $\alpha$ -substituted allyl acetates **180** and **181**, which would be expected to give the same  $\eta^3$ -allylpalladium intermediate, were subjected to identical reaction conditions but afforded different product ratios. High selectivity for attack at the carbon originally substituted with the acetate was observed in both cases (Eq 2.5). Allylic acetate **180** gave an 88:12 mixture of **182**:**183**, while



the regioisomeric **181** afforded the opposite ratio (12:88). Other ligands including dppe and  $\text{PPh}_3$  led to a 1:1 mixture of **182**:**183**. The reactive intermediate formed with dppe

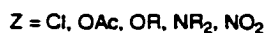
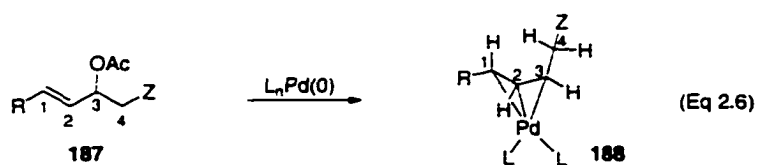
and  $\text{PPh}_3$  was a cationic bisphosphine complex. On the contrary, NMR studies suggested that with two equivalents of MeO-MOP (to Pd) a neutral monophosphine complex (**185** or **186**) was formed due to the steric bulk of **184** preventing coordination of two molecules to palladium (Scheme 2.9). Exchange of the coordination sites between Cl and the ligand was found to be slow based on a magnetization saturation transfer technique in  $^1\text{H}$  NMR spectroscopy.<sup>23</sup> The *trans*-effect suggests that nucleophilic attack should occur opposite the phosphine ligand because the electron density of the allyl moiety is slightly more localized *cis* to the phosphine compared with the halide.<sup>26</sup> Experimental results supported this hypothesis.

**Scheme 2.9**

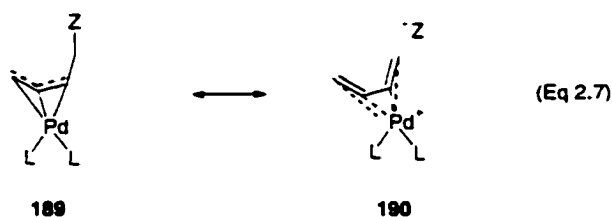


#### I.A.4. Substrate Electronics Effects on Regioselectivity

As was observed with bidentate ligands with large bite angles, electronic interactions with  $\beta$ -substituents on the allylic substrate also led to a distortion in the bonding between palladium and the allyl ligand.<sup>27</sup> When the ligand was a donor to moderate acceptor and Z was an electron-withdrawing group, the Pd-Cl bond length was longer than the Pd-C3 bond length (Eq 2.6). Nucleophilic attack usually occurs at the terminus with the longer Pd-C bond length and indeed, attack occurred predominately



at C1. Also, the C4-Z bond was antiperiplanar to the Pd-C3 bond and was longer and weaker than a normal C4-Z bond. It was postulated that donation from the HOMO of palladium into the LUMO of C4 would result in the observed bond elongation (Eq 2.7). Consistent with this hypothesis, strong acceptor ligands which bring about an increase in the HOMO-LUMO gap and consequently a decrease in orbital interactions, diminished the  $\beta$ -substituent effect.

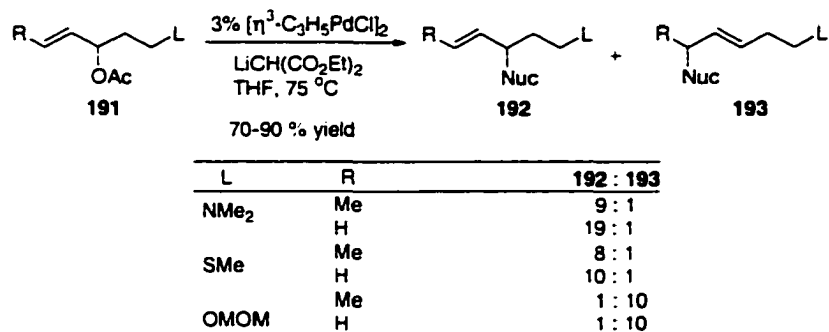


### I.A.5 Use of Tethers to Control Regioselectivity

Kraft and coworkers established that the presence of a thioether or tertiary amine in a substrate successfully reversed the regioselectivity of the allylic alkylation reaction.<sup>16b</sup> Reaction of substrate **191** with diethyl lithiomalonate resulted in a high preference for attack at the terminus proximal to the heteroatom, favoring branched (**192**) over linear (**193**) product formation (when R = H). It was observed that lengthening the chain between the allylic moiety and the heteroatom, increasing the steric bulk of the

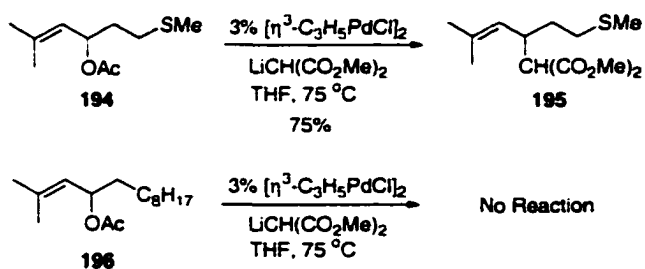
nucleophile or the alkyl groups on the tertiary amine, and using an ether-substituted substrate decreased the selectivity for the internal position (Scheme 2.10).

**Scheme 2.10**



The presence of the tethered heteroatom not only influenced the regioselectivity of the reaction, but also increased the reactivity. Di-substitution at the terminus distal to the heteroatom (**194**) led to exclusive attack at the internal position (**195**) while no reaction was observed with the analogous substrate **196** lacking the thioether. In the latter case the starting material was recovered unchanged (Scheme 2.11).

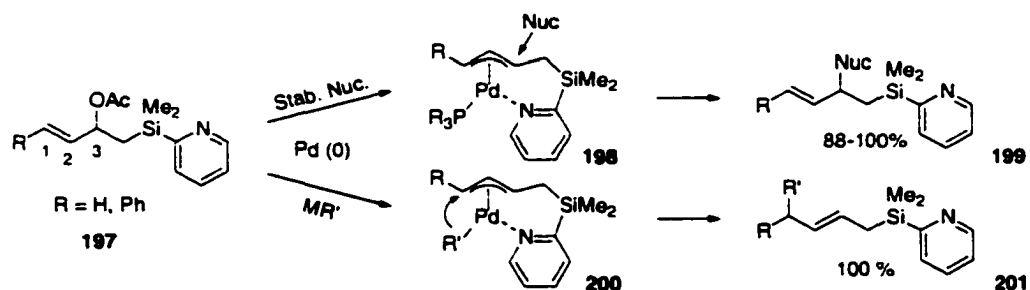
**Scheme 2.11**



The use of a tether to control the regioselectivity was also explored by Yoshida and coworkers using the removable 2-pyridyldimethylsilyl directing group (2-pyMe<sub>2</sub>Si).<sup>16a</sup> Stabilized nucleophiles attacked the terminus proximal to the pyridyl group while organotin nucleophiles (MR') exclusively attacked the distal terminus (Scheme

2.12). X-ray crystal structure data of the  $\pi$ -allyl intermediate revealed that the pyridyl group occupied a coordination site on palladium *trans* to C1 in a pseudo square planar geometry and that the allyl moiety was distorted (**198**). The Pd-C1 bond was substantially shorter than the Pd-C3 bond due to the *trans* effect.<sup>27</sup> Stabilized nucleophiles preferentially attack the carbon with the longer palladium-carbon bond, which in this example was Pd-C3. In comparison, Szabo observed that  $\beta$ -silyl groups directed stabilized nucleophiles to the terminus remote from the silyl group,<sup>15a</sup> suggesting that the coordination with the pyridyl group was indeed responsible for the observed regioselectivity.

**Scheme 2.12**



The selectivity displayed by organotin nucleophiles was opposite that observed with the stabilized nucleophiles.<sup>16a</sup> Although stabilized nucleophiles directly attacked the allyl moiety, the organotin first attacked the metal center (**200**). Because the pyridyl group already occupied one coordination site, this transmetalation step was completely regioselective and reductive elimination gave the observed product. The pyridyl group was removed following a three step protocol in reasonable yield.

## **I.B Molybdenum-Catalyzed Reactions**

### **I.B.1 General Reactivity**

Trost pioneered the extension of the metal-catalyzed allylic alkylation reaction to include molybdenum catalysts.<sup>28</sup> A high degree of chemoselectivity was observed as ketones, esters, acetals, alkyl halides, and allylic or vinylic silicon substituents<sup>29</sup> were tolerated. Higher catalyst loadings were required for the molybdenum-catalyzed reactions (10-15%) compared to palladium (1-5%). However, molybdenum catalysts are less expensive and often air stable, which helps compensate for the lower turnover observed.

A mechanism similar to the palladium-catalyzed reaction has been proposed involving the formation of an  $\eta^3$ -allylmolybdenum intermediate. However, since molybdenum is more electropositive than palladium, electronic factors affect the reactivity more significantly. The regioselectivity of the molybdenum-catalyzed reaction is dependent on a number of factors including the steric bulk of the nucleophile, the base, the electronics of the substrate, the solvent, and the ligands on the metal. However, using standard conditions, small nucleophiles attack the more-substituted terminus while larger nucleophiles preferentially attack the less-substituted position of the allyl system.

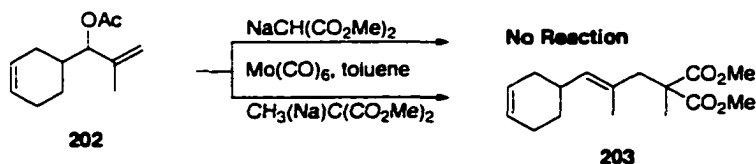
### **I.B.2 Nucleophile Effects on Reactivity and Regioselectivity**

The steric bulk and reactivity of the nucleophile influences the regioselectivity of the molybdenum-catalyzed reaction. Trost and coworkers observed that small nucleophiles such as dimethyl malonate displayed a high degree of selectivity for addition to the more-substituted end of the allyl system derived from a number of different substrates.<sup>28</sup> The electronic preference for the substituted terminus outweighed

the steric interactions. Alternatively, highly reactive, sterically demanding nucleophiles, such as dimethyl methylmalonate and substituted  $\beta$ -ketoesters, reacted exclusively at the less-substituted terminus. In these examples sterics prevailed over electronics. A number of nucleophiles with moderate steric bulk and decreased reactivity, including non-substituted  $\beta$ -ketoesters and both substituted and non-substituted 1,3-diketones displayed varying regioselectivities depending on subtle changes in the substrate.<sup>30</sup> Therefore, regioselectivity based on the nucleophile alone cannot be predicted and a case-by-case investigation is required.

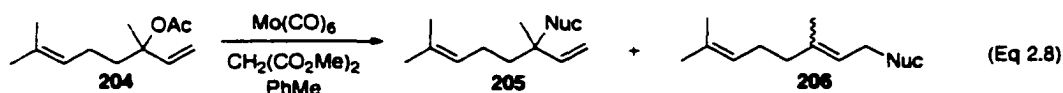
The choice of nucleophile also had a profound effect on the overall reactivity. The allylic acetate **202** was allowed to react under the same conditions with two different nucleophiles and major differences were observed (Scheme 2.13).<sup>28</sup> Dimethyl methylmalonate gave a 73% yield of **203** resulting from addition to the terminal end. No reaction was observed with dimethyl malonate and starting material was recovered in good yield. Accordingly, when dimethyl malonate was added to the reaction with dimethyl methylmalonate no reaction was observed. Formation of an alternative catalyst such as  $(OC)_{6-n}Mo(CHE_2)_n$  or  $(OC)_5Mo(CHE_2)^-$ , which would be less electrophilic than the parent compound  $Mo(CO)_6$ , could reduce its ability to coordinate with the olefin, therefore inhibiting oxidative addition. Because dimethyl methylmalonate was so sterically bulky, attack at the metal center was prevented and the reaction proceeded as expected. Alternatively, if oxidative addition did take place, the resulting  $\pi$ -allyl complex may not have been electrophilic enough to allow nucleophilic attack.

## Scheme 2.13



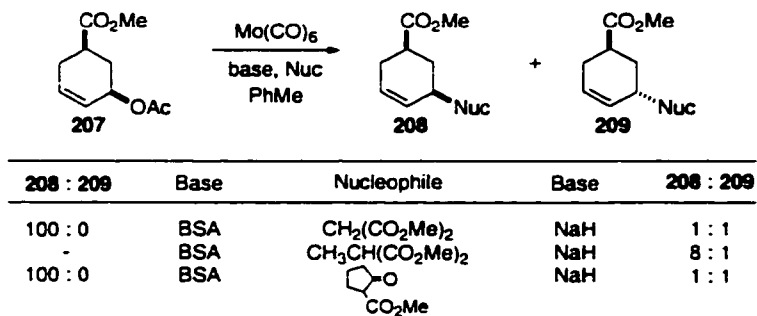
### I.B.3 Base Effects on Reactivity, Regio- and Stereoselectivity

A moderate effect on regioselectivity and reactivity was observed when the base was varied in the reaction of dimethyl malonate and acetate **204** (Eq 2.8).<sup>28</sup> Bis(trimethylsilyl)acetamide (BSA), which was capable of coordinating to the metal, gave the highest selectivity for attack at the substituted allylic terminus (97:3 **205**:**206**, 82% yield) and the fastest reaction (1.5 h), while the more strongly-coordinating base 1,8-diazabicyclo[5.4.0]undec-7-ene (DBU) poisoned the catalyst. Potassium hydride led to reduced regioselectivity compared with sodium hydride (80:20, 82% yield versus 85:15, 80% yield) and a faster reaction (2h versus 3h).



The choice of base had a much more pronounced effect on the *stereochemistry* of the reaction. Exclusive formation of **208**, resulting from retention of configuration was observed with BSA regardless of the nucleophile.<sup>28</sup> Alternatively, with sodium hydride a 1:1 mixture of products was formed with dimethyl malonate and 2-carbomethoxycyclopentanone, while dimethyl methylmalonate gave **208** selectively (Scheme 2.14).

## Scheme 2.14

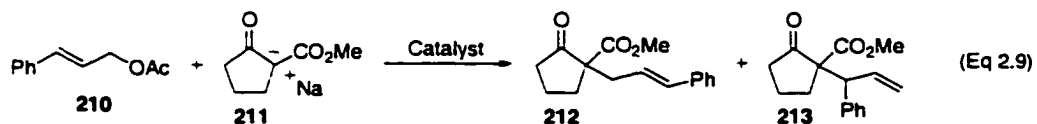


Possibly, dimethyl malonate reacted with the molybdenum hexacarbonyl resulting in an alternative catalyst such as  $(OC)_5Mo[CH(CO_2Me)_2]^-$ , which would have led to an intermediate in which malonate was bound to the molybdenum. Subsequent intramolecular delivery of the malonate from the metal to the allyl ligand would explain the formation of **209** from net inversion of stereochemistry. BSA can itself coordinate to the molybdenum, inhibiting attack by the malonate ion, and thereby shutting down the pathway to **209**. The increased steric bulk of the methyl-substituted malonate prevented attack at the metal center. Because this nucleophile could only react at the allylic terminus, overall retention of configuration resulted.

### I.B.4 Ligand Effects on Reactivity, Regio and Stereoselectivity

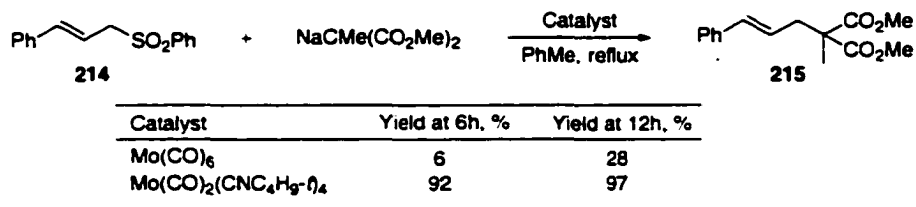
As was the case in the palladium-catalyzed reaction, ligands play a crucial role in controlling the reactivity, regio- and stereoselectivity of the molybdenum-mediated allylic substitution reaction. Trost and Merlic conducted a study in which they systematically varied the amount of  $\sigma$ -donating and  $\pi$ -accepting abilities of a number of imine and isonitrile ligands bound to molybdenum.<sup>31</sup> Two ligands generated notable results.  $Mo(CO)_3(CH_3CN)bpy$  efficiently catalyzed the reaction between (E)-cinnamyl acetate and 2-carbomethoxycyclopentanone and gave the opposite regioselectivity as that

observed with  $\text{Mo}(\text{CO})_6$  (30:70 versus 100:0 **212:213**). The replacement of one of the carbon monoxide ligands with the highly dissociable acetonitrile increased the rate of the reaction considerably as compared with the parent complex  $\text{Mo}(\text{CO})_4\text{bpy}$  (9 h versus 36h) (Eq 2.9).



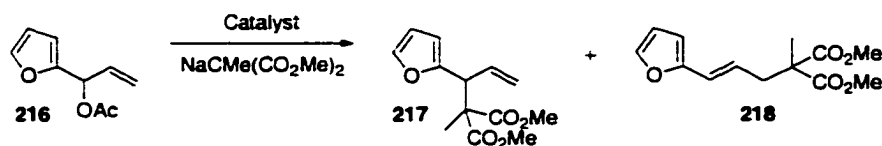
Additionally, the complex  $\text{Mo}(\text{CO})_2(\text{CNC}_4\text{H}_9\text{-}t)_4$  (**MoBI4**) effected a dramatic increase in reactivity compared with  $\text{Mo}(\text{CO})_6$  in the alkylation of (*E*)-cinnamyl phenylsulfone with dimethyl sodiomethylmalonate (Scheme 2.15).

### Scheme 2.15



Unlike  $\text{Mo}(\text{CO})_6$ , **MoBI4** tolerated the presence of acetylenes and improved yields with ethyl cyanoacetate.<sup>32</sup> With a number of substrates **MoBI4** gave high yields and preferential attack at the allylic terminus *opposite* that favored with  $\text{Mo}(\text{CO})_6$  (Scheme 2.16)<sup>31</sup> Attack at the less-substituted carbon predominated because of the increased steric hindrance created by the bulky *tert*-butylisocyanide ligands. Additionally, unreactive or poorly reactive substrates with molybdenum hexacarbonyl underwent alkylation nicely with **MoBI4**.  $\text{Mo}(\text{CO})_3(\text{CH}_3\text{CN})\text{bpy}$  displayed comparable reactivity to molybdenum hexacarbonyl but improved regioselectivities.<sup>33</sup>

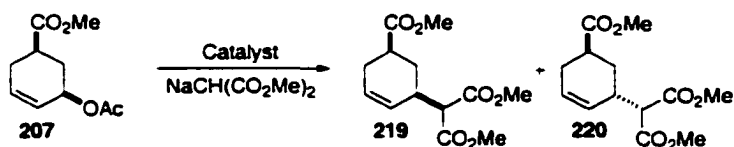
### Scheme 2.16



Catalyst	Time, h	217 : 218	Yield, %
Mo(CO) <sub>3</sub> (CH <sub>3</sub> CN)bpy	1.5	13 (E) : 87	73
Mo(CO) <sub>6</sub>	1	38 (E:Z 7 : 1) : 62	73
MoBI <sub>4</sub>	1	78 (E :Z 9 : 1) : 22	90

Improved stereoselectivity was also observed with MoBI<sub>4</sub>, favoring net retention of configuration.<sup>31</sup> Although reaction of **207** with molybdenum hexacarbonyl and dimethyl sodiomalonate gave a 1:1 mixture of stereoisomers, MoBI<sub>4</sub> gave almost exclusive formation of **219** resulting from net retention (Scheme 2.17).

### Scheme 2.17



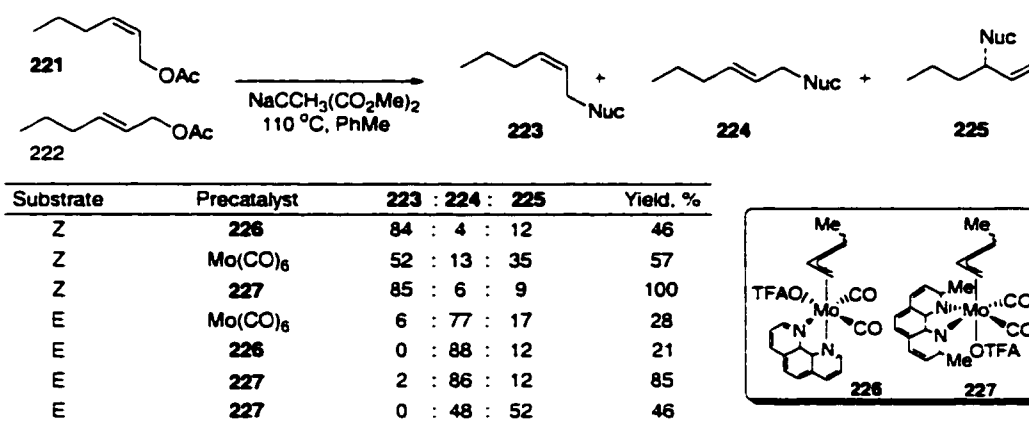
Catalyst	time, h	219 : 220	Yield, %
Mo(CO) <sub>6</sub>	48	1 : 1	50
MoBI <sub>4</sub>	24	99 : 1	70

The replacement of CO with isonitrile ligand(s) led to dramatic improvements. Presumably, because the isonitriles are both good  $\sigma$ -donors and  $\pi$ -acceptors they have the ability to stabilize both low and high oxidation states involved in the catalytic cycle.<sup>31</sup> As better  $\sigma$ -donors, isonitrile ligands are able to promote ionization leading to the cationic intermediate more readily. Also, because isonitriles are less volatile than CO they remain in solution better and can dissociate and associate as required. The improved chemo- and

stereoselectivity resulted from the isonitrile ligands better ligating ability which prevented replacement of a neutral ligand by another molecule such as malonate anion.

Phenanthroline derivatives also acted as ligands in the molybdenum-catalyzed alkylation reaction. Åkermark and coworkers prepared numerous substituted phenanthroline ligands and compared their resulting selectivities and reactivities.<sup>34</sup> One of the most active and successful precatalysts was dmphen  $\eta^3$ -allyl complex **227**. When **227** was reacted with (Z)- and (E)-1-acetoxy-2-hexene and dimethyl sodiomethylmalonate, retention of configuration about the double bond and attack at the less-substituted allylic terminus was favored (Scheme 2.18). Complex **227** displayed improved regioselectivity and yield compared with  $\text{Mo}(\text{CO})_6$  and increased yield compared with the parent phen compound **226**. Interestingly, the reaction with dimethyl sodiomalonate and the (E)-substrate was much slower with **227** and an approximately 1:1 mixture of regioisomers resulted.

**Scheme 2.18**



<sup>a</sup> $\text{NaCH}(\text{CO}_2\text{Me})_2$

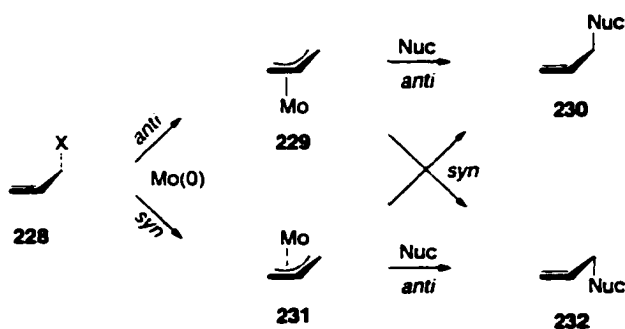
### I.B.5 Solvent Effects on Reactivity

Because molybdenum is more Lewis acidic than palladium, Lewis-basic solvents can render molybdenum complexes inactive. A number of solvents were screened in the reaction of sodium 2-carbomethoxycyclopentanone and allyl acetate with  $\text{Mo}(\text{CO})_4\text{bpy}$ .<sup>28b</sup> Toluene and dioxane were the most compatible and both resulted in 70% yield. DME, THF, diglyme and benzene all resulted in less than 10% yield. More recently  $\text{CH}_2\text{Cl}_2$  displayed compatibility with  $(\text{DMF})_3\text{Mo}(\text{CO})_3$ <sup>39</sup> and THF has been used in a number of asymmetric alkylations.<sup>8a,8c</sup>

### I.B.6 Mechanistic Considerations : *syn-syn* versus *anti-anti*

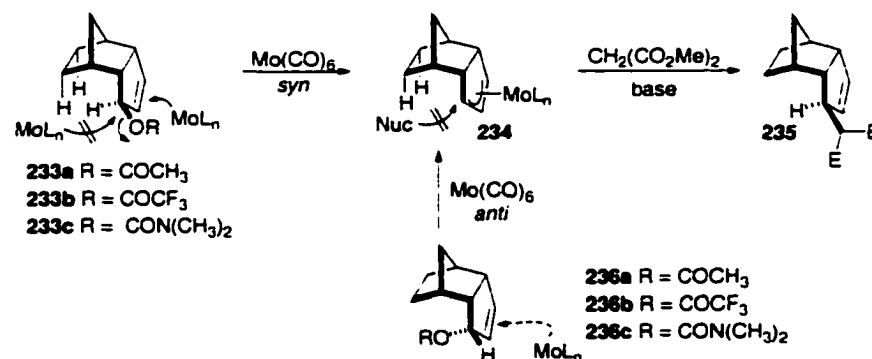
The details of the mechanism for the molybdenum-catalyzed allylic substitution reaction are less understood than for the palladium-catalyzed reaction. Analogy to the palladium-catalyzed reaction would suggest that a double inversion involving molybdenum attacking the face opposite the leaving group then nucleophilic attack on the side opposite the metal leads to the observed retention of configuration. However, recent studies have suggested that an alternative *syn-syn* mechanism may play an important role in the molybdenum-mediated reaction (Scheme 2.19).

**Scheme 2.19**



Liebeskind and Faller first reported that the stoichiometric reaction produced  $\eta^3$ -allylmolybdenum complexes via a *syn* pathway.<sup>35</sup> More recently, Kocovský and coworkers reported the first evidence for this pathway in the catalytic reaction (Scheme 2.20).<sup>36</sup>

Scheme 2.20

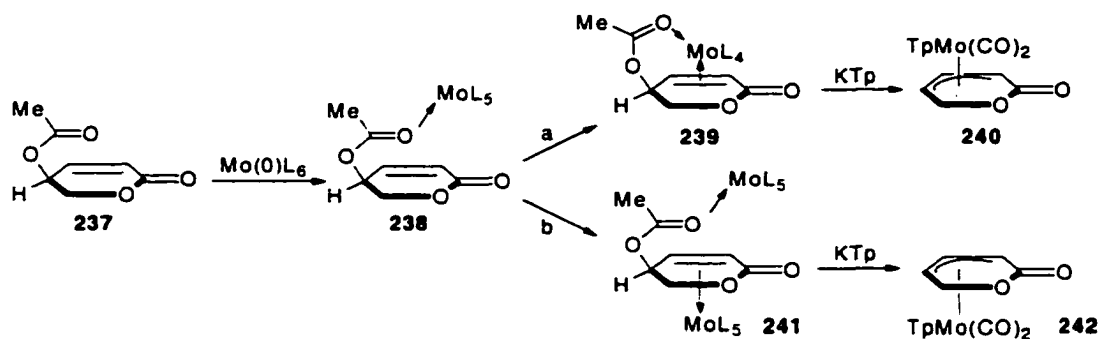


It was previously established that **233a** did not react in the palladium-catalyzed allylic substitution reaction.<sup>37</sup> Alternatively, **236a** underwent a clean reaction with PhZnCl/Pd(0) but was unreactive with LiCH(CO<sub>2</sub>Me)<sub>2</sub>/Pd(0). Because the *endo* face of **233a** was so sterically hindered, *anti* addition was prevented but occurred readily with substrate **236a**. Transmetalation/reductive elimination follows a *syn* mechanism, therefore PhZnCl reacted whereas malonate ion, which required *anti* addition to the allyl intermediate, did not. These results suggested that substrates **233a** and **236a** would be useful in probing the mechanism of molybdenum(0) catalysts. Both substrates were allowed to react with dimethyl malonate and BSA or NaH with catalytic Mo(CO)<sub>6</sub>.<sup>36</sup> Allylic acetate **233a** reacted successfully (92-96% conversion after 6h) while **236a** was isolated unchanged with BSA/CH<sub>2</sub>(CO<sub>2</sub>Me)<sub>2</sub> and reacted very slowly with NaCH(CO<sub>2</sub>Me)<sub>2</sub> (9% after 6h).

The leaving group was varied to determine whether increasing electron density on the carbonyl oxygen would facilitate coordination to molybdenum and thus accelerate oxidative addition following the *syn* pathway.<sup>36</sup> Epimeric trifluoroacetates **233b** and **236b** and dimethylcarbamates **233c** and **236c** were subjected to the previously described reaction conditions. Consistent with the *syn* pathway, trifluoroacetate **233b** (which has a non-nucleophilic carbonyl oxygen)<sup>38</sup> reacted three times slower than the acetate and the Lewis basic carbamate **233c** reacted 2.5 times faster. Conversely, trifluoroacetate **236b** accelerated the reaction as compared with acetate **236a**, and reacted even without catalyst while carbamate **236c** was practically inert. These observations suggested that precoordination of the molybdenum catalyst with the leaving group accelerated formation of the reactive  $\pi$ -allylmolybdenum intermediate following the *syn* mechanism.

More recently, Liebeskind discovered that slight modifications in the reaction conditions led to oxidative addition by *either* inversion or retention of configuration (Scheme 2.21).<sup>39</sup> Because of its lack of steric bias, lactone **237** was chosen as the substrate for the formation of  $\pi$ -allylmolybdenum complexes **240** and **242**.<sup>40</sup> Studies revealed that oxidative addition with inversion was favored at high concentrations of  $(\text{DMF})_3\text{Mo}(\text{CO})_3$  and low temperatures. The retention pathway was favored by changing solvents from  $\text{CH}_2\text{Cl}_2$  to THF, at low effective concentrations of  $(\text{DMF})_3\text{Mo}(\text{CO})_3$  or by using  $(\text{toluene})\text{Mo}(\text{CO})_3$ .

## Scheme 2.21



Catalyst	Solvent	Temp., °C	Major Product, %ee	Yield, %
1 eq. (DMF) <sub>3</sub> Mo(CO) <sub>3</sub>	CH <sub>2</sub> Cl <sub>2</sub>	22	<b>242</b> , 32	93
2 eq. (DMF) <sub>3</sub> Mo(CO) <sub>3</sub>	CH <sub>2</sub> Cl <sub>2</sub>	-40	<b>242</b> , 84	57
1 eq. (DMF) <sub>3</sub> Mo(CO) <sub>3</sub>	THF	22	<b>240</b> , 88	86
1 eq. (toluene)Mo(CO) <sub>3</sub>	CH <sub>2</sub> Cl <sub>2</sub>	22	<b>240</b> , >95	60-70
1 eq. (DMF) <sub>3</sub> Mo(CO) <sub>3</sub> <sup>a</sup>	CH <sub>2</sub> Cl <sub>2</sub>	22	<b>240</b> , 94	86

<sup>a</sup> Catalyst added dropwise to substrate.

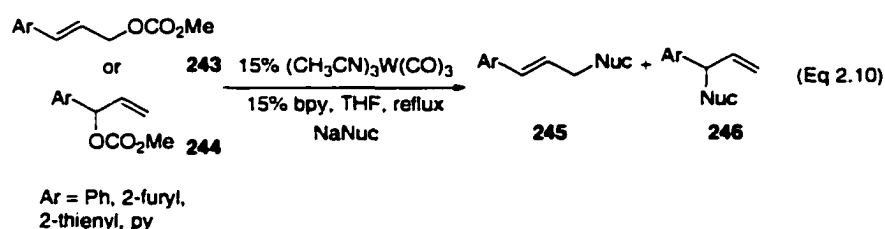
The pathway outlined in Scheme 2.21 may help to explain these observations. Initial complexation of Mo(0) to the carbonyl oxygen of the leaving group would give the common intermediate **238**. At low catalyst concentrations or when ligand dissociation is facile, as is the case with (toluene)Mo(CO)<sub>3</sub>, chelation to the olefin to form intermediate **239** then oxidative addition with retention would occur (path a). However, at high catalyst concentrations another molecule of Mo(0)L<sub>n</sub> could coordinate to the olefin on the opposite face the first due to sterics, giving **241**. This would lead to oxidative addition with inversion, as was observed (path b).

## I.C Tungsten-Catalyzed Reactions

### I.C.1 General Reactivity

Tungsten(0) complexes also catalyze the allylic alkylation reaction.<sup>41</sup> Tungsten is even more sensitive to electronic factors than molybdenum and as a result is highly regioselective for the more-substituted terminus of the allyl moiety. Tungsten(0)

catalyzed the reaction of substrates **243** and **244** with a wide range of nucleophiles including dimethyl malonate and dimethyl methylmalonate, sulphone-stabilized nucleophiles as well as cyclic  $\beta$ -ketoesters in high yields (60-90%) (Eq 2.10). In the majority of cases, regioselectivity was very high (>85:15) favoring attack at the substituted terminus. Only when the steric bulk of the nucleophile became extreme was there a decrease in selectivity;  $\text{NaCH}(\text{SO}_2\text{Ph})_2$  gave a 53:47 mixture of **245**:**246**. Limited studies revealed that retention of stereochemistry predominated.<sup>41a</sup>



The reaction tolerated alkyl halides and alkynes, but was extremely sensitive to the steric environment of the olefin.<sup>41a</sup> Substrate **247**, bearing the phenyl group, underwent a clean reaction with dimethyl sodiomalonate. Replacement of the aryl group with a cyclohexane completely shut down the reaction (Figure 2.2).<sup>41d</sup>

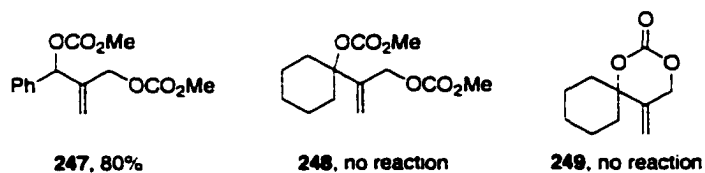
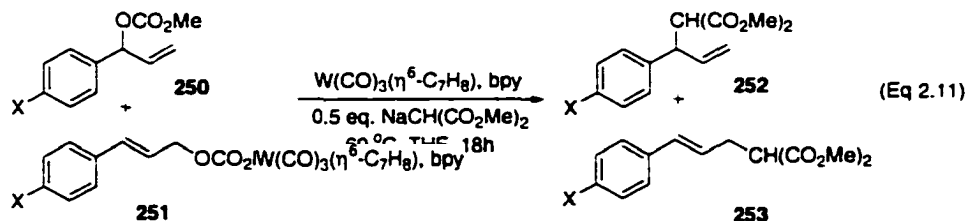


**Figure 2.2**

Additionally, Lloyd-Jones and coworkers demonstrated that the regioselectivity was independent of the original position of the leaving group (both **250** and **251** gave a 28:1 mixture of **252**:**253** in 84-85% yield).<sup>41c</sup> Conversely, the relative *reactivity* was

dependent on the regiochemistry and electronic properties of the starting material. Substrate **250** reacted six times faster than linear **251**. Also, when the electronics of X were varied (X = H, CF<sub>3</sub>, Br, Cl, Ph, CH<sub>3</sub>) the substrate bearing the more electron-withdrawing substituent was consumed more efficiently (Eq 2.11).



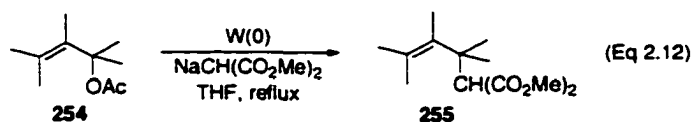
Trost and coworkers studied how intrinsic electronic properties of the substrate affected the regiochemistry of the tungsten-catalyzed reaction.<sup>41b</sup> MO calculations and frontier orbital considerations predicted the positive charge build-up on each of the carbons of the allyl system for a variety of substrates. The predictions were in good agreement with experimental observations in which attack at the carbon bearing the largest carbonium ion character predominated. The tungsten-catalyzed reaction displayed greater sensitivity to electronics than sterics.

An unusual characteristic of the tungsten-catalyzed allylic substitution reaction was that the order of addition was important.<sup>41d</sup> Trost found that the tungsten catalyst had to be combined with the *nucleophile* prior to addition of the electrophile, suggesting the active catalyst was actually an anionic species. No further direct evidence has been gathered.

### I.C.2 Ligand Effects on Reactivity

As with both palladium and molybdenum, the ligands on tungsten have a dramatic effect on the stability, reactivity, and selectivity of the resulting complexes. No reaction

was observed between allyl acetate **254** and dimethyl sodiomalonate in the presence of tungsten hexacarbonyl.<sup>41a</sup> Slow reaction (31%, 6h) resulted with  $(\text{CH}_3\text{CN})_3\text{W}(\text{CO})_3$  and addition of phosphine ligands poisoned the catalyst. The best results were observed with the addition of the strong  $\sigma$ -donating 2,2'-bipyridyl (bpy) to  $(\text{CH}_3\text{CN})_3\text{W}(\text{CO})_3$  (65% in 18h) (Eq 2.12). A more stable catalyst was formed by replacing acetonitrile with propionitrile or cycloheptatriene.



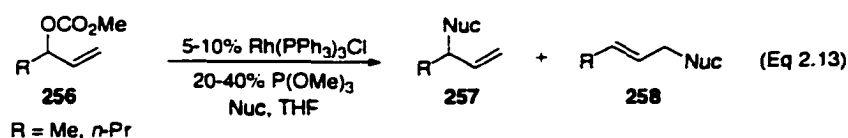
Utilization of substituted 1,10-phenanthroline ligands in the tungsten-catalyzed reaction by Åkermark and coworkers allowed for the efficient conversion of (Z)-substrates to (Z)-products.<sup>42</sup>

## I.D Rhodium-Catalyzed Allylic Substitution Reactions

### I.D.1 General Reactivity

Evans pioneered the development of the rhodium-catalyzed allylic substitution reaction, which accommodates a wide range of nucleophiles including stabilized carbon<sup>43</sup> and nitrogen<sup>44</sup> anions and phenols.<sup>45</sup> Attack at the more-substituted terminus with retention of stereochemistry predominates. For example, reaction of allylic carbonate **256** (R = Me) with dimethyl sodiomalonate and lithium *N*-toluenesulfonyl benzylamine gave a 42:1 mixture of **257**:**258** in 99% in the former case and >99:1 in 86% yield in the latter. Similarly, a wide range of *ortho*-substituted phenols reacted with the allylic carbonate **256** (R = *n*-Pr) with impressive selectivity (11:1 to >99:1 **257**:**258**) and good

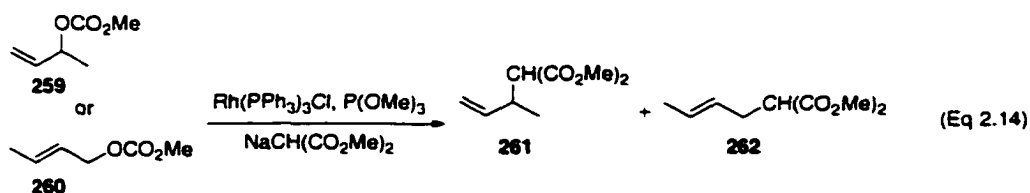
yields (80-95%) (Eq 2.13). Takeuchi reported similar results employing  $[\text{Rh}(\text{COD})\text{Cl}]_2/\text{P}(\text{OPh})_3$  as the catalyst with stabilized carbon nucleophiles.<sup>46</sup>



The rhodium-catalyzed substitution reaction has proven useful in the formation of quaternary carbon stereogenic centers of  $\gamma$ -lactones<sup>47</sup> and the preparation of dihydroquinoline, dihydrobenzo[*b*]indoline,<sup>44b</sup> and dihydrobenzo[*b*]furan derivatives.<sup>45</sup>

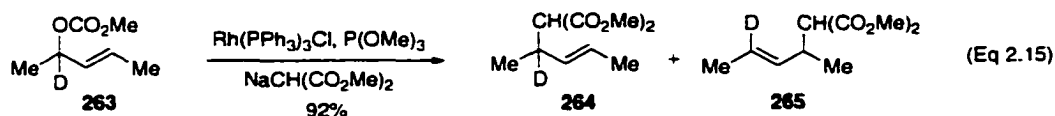
### I.D.2 Mechanism

Although nucleophilic attack predominately occurred at the more-substituted allylic terminus, both Evans and Takeuchi reported that the regioselectivity was dependent upon the position of the leaving group in the starting material. For example, allylic carbonates **259** and **260** led to strikingly different ratios of **261** and **262** (42:1, 99% and 2:1, 83% respectively).<sup>43</sup> If a common  $\eta^3$ -allyl intermediate was formed, as with palladium, the original position of the carbonate would be inconsequential (Eq 2.14).



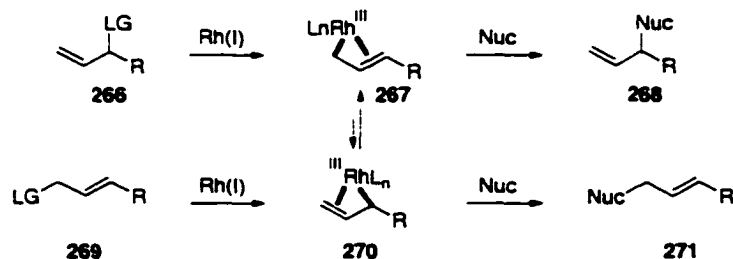
Additionally, reaction of deuterated allylic acetate **263**, whose allylic termini should be indistinguishable based on sterics or electronics, led to >19:1 preference for **264** (Eq 2.15).<sup>43</sup> This experiment provided more evidence suggesting the rhodium-

catalyzed allylic substitution reaction does not proceed through a symmetrical  $\pi$ -allyl intermediate.



Evans proposed an alternative mechanism to account for these results (Scheme 2.22).<sup>43</sup> He suggested that initial  $S_N2'$  displacement<sup>48</sup> of the carbonate **266** on the face opposite the leaving group would give the *enyl* intermediate **267** involving discrete  $\sigma$  and  $\pi$  bonds. If nucleophilic attack were faster than isomerization to **270** the regiochemistry of the starting material would be maintained, which is in agreement with the experimental

#### Scheme 2.22



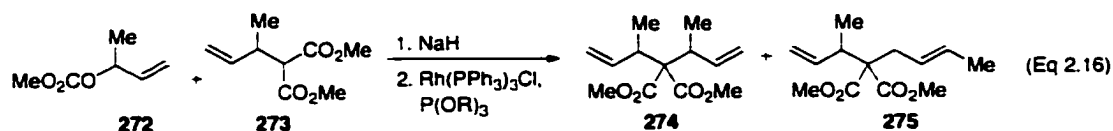
results. Linear carbonate **269** would similarly give *enyl* intermediate **270**. Steric interactions between the ligands on rhodium and the allyl substituent **R** were sufficient enough that isomerization to **267** competed with nucleophilic attack. Thus, a mixture of products was formed. The discrete  $\sigma$ - and  $\pi$ -metal carbon interactions in the *enyl* intermediate are consistent with the observed retention of configuration. An intermediate  $\sigma$ -allyl rhodium species, which was proposed by Takeuchi,<sup>46</sup> would lead to racemization due to the fast rotation around a C-C bond.

### I.D.3 Counterion Effects on Reactivity and Regioselectivity

Both the allylic amination and etherification reactions displayed sensitivity to the counterion used. Lithium *N*-toluenesulfonyl amide gave the best rate and regioselectivity as compared with the sodium and potassium salts.<sup>44</sup> Previous observations that classical nitrogen nucleophiles led to poor yields and competitive elimination suggested that a balance between nucleophilicity and basicity was required. The improved results observed with the lithium salt presumably stemmed from its diminished basicity and increased solubility. Alternatively, poor turnover and selectivity were observed with the potassium and lithium ions in the reaction with substituted phenols.<sup>45</sup> The sodium ion gave superior results and the best regioselectivity occurred at low temperature (0 °C versus 30 °C).

### I.D.3 Ligand Effects on Reactivity

The choice of ligand for the rhodium-catalyzed substitution reaction is essential for good reactivity. Traditional phosphine ligands render the catalyst inactive, but trialkyl or triaryl phosphites have displayed good reactivity, presumably because of their increased  $\pi$ -accepting ability. Evans found that by increasing the electron-withdrawing nature of the ligand from  $\text{P}(\text{OEt})_3$  to  $\text{P}(\text{OCH}_2\text{CF}_3)_3$  the yield as well as regioselectivity improved (9:1 **274**:**275**, 79% versus 21:1, 91% respectively) (Eq 2.16).<sup>43</sup>



Takeuchi also found that the ratio of ligand to rhodium was important.<sup>46</sup> A P/Rh ratio of 3/1 was optimum (90% yield, 74:26 **274**:**275**) for the reaction of (*E*)-2-hexenyl

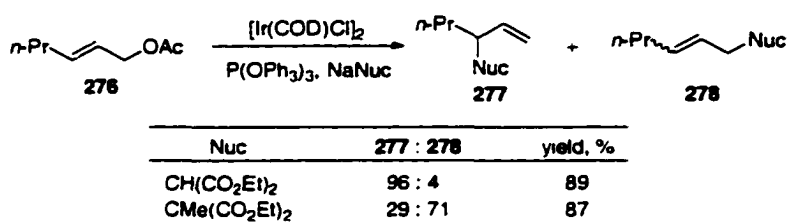
acetate with diethyl sodiomalonate and  $[\text{Rh}(\text{COD})\text{Cl}]_2$  while decreasing the ratio caused a decrease in reactivity and selectivity.

## I.E Iridium-Catalyzed Reaction

### I.E.1 General Reactivity

Takeuchi and coworkers discovered that iridium(I) could efficiently catalyze the allylic alkylation<sup>49</sup> and amination<sup>50</sup> reactions. General trends in stereo- and regioselectivities resembled that observed with molybdenum, as attack at the more-substituted terminus dominated with relatively small stabilized malonates and reversed selectivity with large nucleophiles such as dimethyl methylmalonate was observed (Scheme 2.23). Retention of stereochemistry predominated regardless of the nucleophile.

### Scheme 2.23

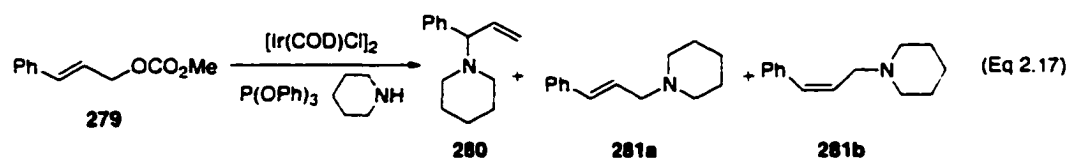


### I.E.2 Ligand Effects on Reactivity and Regioselectivity

The choice of ligand and ligand to metal ratio ( $\text{P}/\text{Ir}$ ) had a profound effect on the reactivity and selectivity of the alkylation reaction.<sup>49</sup> Triphenylphosphite was the superior ligand as it gave excellent yields and regioselectivities for attack at the more-substituted terminus at room temperature. Triphenylphosphite has good  $\pi$ -acceptor abilities, and therefore promotes carbonium ion character at the more-substituted terminus. High selectivity was preserved with other aryl phosphite ligands, however reactivity suffered. Alternatively, the alkyl phosphites  $\text{P}(\text{OEt})_3$  and  $\text{P}(\text{O}i\text{-Pr})_3$  rendered

the reaction basically unselective (Scheme 2.23, Nuc = CH(CO<sub>2</sub>Me)<sub>2</sub>; 59:41 and 53:47 **277:278** respectively) and phosphines were unreactive, most likely due to their diminished acceptor abilities.

The optimum P/Ir ratio was 1 or 2 for both the alkylation and amination reactions.<sup>49,50</sup> In the former case, P/Ir of 3 led to a sluggish reaction which did not go to completion. However, in the latter reaction a complete reversal of regioselectivity was observed. With P/Ir of 1 and 2, attack at the more-substituted terminus predominated (92:8 **280:281** for both in 89 and 84% yield respectively). The selectivity was reversed when P/Ir was 3 (11:89, 75% yield) (Eq 2.17). <sup>31</sup>P NMR studies suggested that the catalytically-active complex was a monophosphite species when P/Ir was 1 or 2.<sup>50</sup> The major catalyst may have been a bisphosphite species when P/Ir was 3 and because the steric bulk around iridium would be increased substantially, attack at the unsubstituted terminus would be favored.



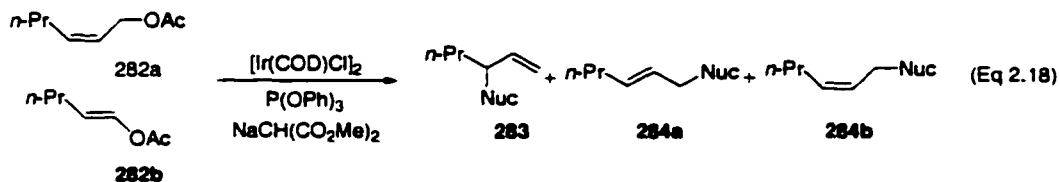
### I.E.3 Leaving Group Effects on Reactivity

The *position* of the leaving group had no consequence on the regioselectivity of the iridium-catalyzed reaction, suggesting a  $\pi$ -allyl iridium intermediate was formed.<sup>49,50</sup> Conversely, the *nature* of the leaving group did affect the reactivity of the substrates. The observed order of reactivity in the alkylation of 3-methyl-2 butenyl substrates was (EtO)<sub>2</sub>PO<sub>2</sub> ~ CF<sub>3</sub>CO<sub>2</sub> > MeO<sub>2</sub>CO > AcO. Interestingly, allylic alcohols have served as useful substrates in the alkylation reaction. Yields for a range of allylic alcohols with

diethyl sodiomalonate were high (71-100%) with regioselectivities all greater than 90:10 branched:linear. Experiments suggested that initial transesterification with the malonate was then followed by oxidative addition.<sup>49</sup>

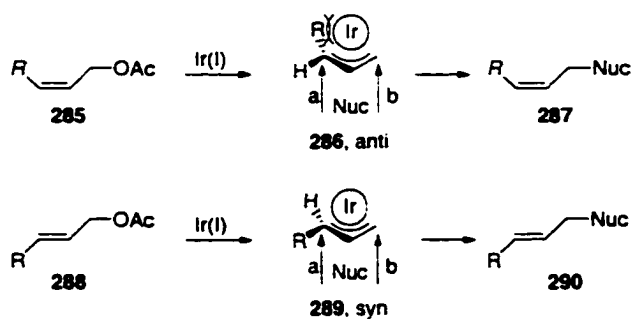
#### I.E.4 Olefin Geometry Effects on Regio and Stereoselectivity

Loss of olefin geometry was observed in the palladium-catalyzed allylic substitution reaction of (*Z*)-allylic esters.<sup>51</sup> Importantly, retention of configuration of the alkene was possible with iridium catalysts.<sup>49,50</sup> Also, the regioselectivity was opposite that observed with (*E*)-olefins, as attack at the less-substituted terminus predominated. (*Z*)-2-hexenyl acetate reacted with dimethyl sodiomalonate to give (*Z*)-**284b** as the major product (25:5:70 **283:284a:284b**, 81%) while (*E*)-2-hexenyl acetate reacted to give high selectivity for **283**. (96:4 **283:284**, 89%) (Eq 2.18). Selectivity for the *Z*-product was improved with the use of a bulky phosphite ligand such as tris(2-*tert*-butyl-4-methylphenyl)phosphite (3:7:90 **283:284a:284b**, 85%).



The observation that the stereochemistry of the olefin was preserved implied that the *syn-anti* isomerization was slower than nucleophilic attack, which contrasted with the palladium-catalyzed reaction.<sup>52</sup> The divergence in regioselectivity observed for (*E*)- and (*Z*)-olefins may have resulted from differences in both steric and electronic factors. Oxidative addition of the *Z*-alkene led to an *anti*  $\pi$ -allyl iridium complex and the *E*-alkene gave the *syn* complex (Scheme 2.24).

## Scheme 2.24



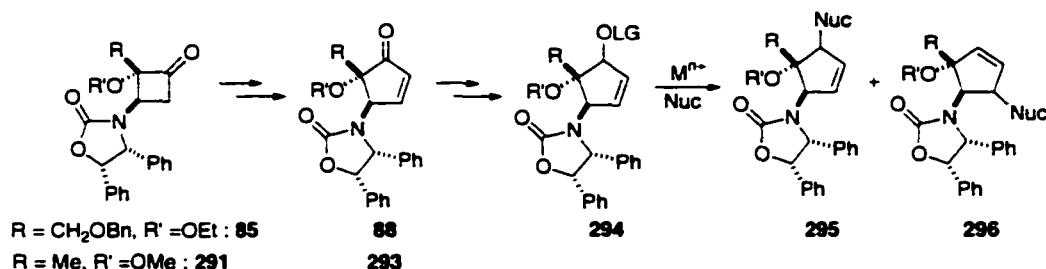
If the nucleophile approached the substituted terminus of the *anti* intermediate (path a), R was forced into close contact with the ligands on iridium, therefore destabilizing this transition state. Steric factors prevailed in this example, and attack occurred predominately on the less-substituted terminus (path b). Consistent with this argument, increasing the steric bulk of the ligand increased the selectivity. Conversely, nucleophilic attack at the substituted terminus of the *syn* complex did not create unfavorable steric interactions. Therefore, because the substituted carbon had the most carbonium ion character, the nucleophile added to this end. Addition to alkyl-substituted substrates was less regioselective than aryl-substituted substrates due to the smaller electronic differences induced.

## II. Rationale

As described above, the metal-catalyzed allylic substitution reaction has vast utility in the area of synthetic chemistry. However, to date, few studies have been conducted on highly sterically congested cyclic systems, which are prevalent in many natural products. Studies towards the synthesis of trehalamine<sup>53</sup> provided an efficient route to cyclopentenone **88**. 1,2-Reduction and acylation would provide a substrate for

the metal-catalyzed allylic substitution reaction, which would allow for the study of the effect of highly substituted  $\beta$ -positions (Scheme 2.25). Specifically, studies were

**Scheme 2.25**



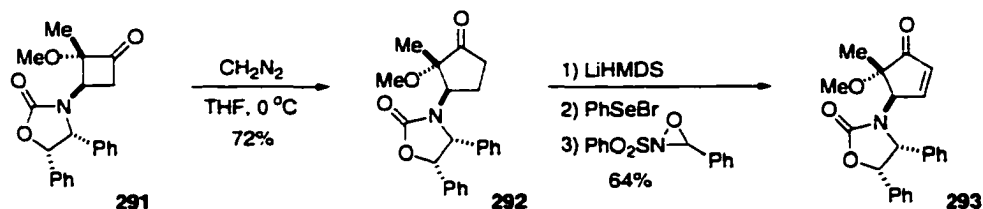
directed towards probing the effects of chiral tertiary and quaternary centers adjacent to the  $\pi$ -system of an allylic substrate on the regio- and stereoselectivity as well as the overall reactivity of the process. Also, metal complexes including palladium, iridium, rhodium, tungsten, and molybdenum were compared as catalysts. Because the (methyl)(methoxy)cyclobutanone **291** was more easily synthesized than the (benzyloxymethyl)(ethoxy)cyclobutanone **85** and because characterization would be more straightforward, experiments were carried out on this series.

### III. Results and Discussion

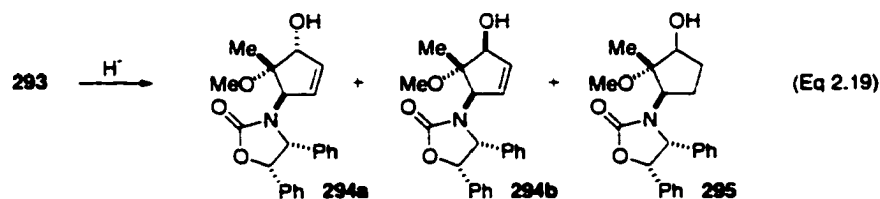
#### III.A Preparation of Starting Materials

Synthesis of the substrates to be used in these studies followed the strategy described in chapter one (Scheme 2.26). Ring expansion of cyclobutanone **291** with diazomethane to cyclopentanone **292** proceeded in 72% yield.<sup>54</sup>  $\alpha$ -Selenation followed by oxidation and spontaneous elimination gave cyclopentenone **293** in 64% yield. The use of Davis' oxaziridine and pyridine was essential for the oxidation as hydrogen peroxide led to decomposition.<sup>54</sup>

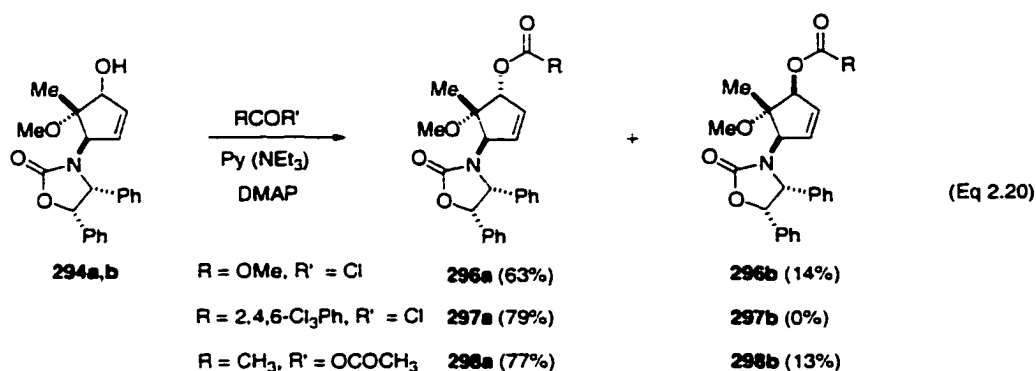
### Scheme 2.26



With cyclopentenone **293** in hand, gaining access to both epimers of the allylic alcohol was the next challenge. DIBAL-H reduction in THF gave a 1:2 mixture of **294a**:**294b** in 56% yield while reduction with Luche conditions provided complementary selectivity (4.5:1, 95%).  $\text{K}^-$  (potassium tri-*sec*-butylborohydride) and KS-selectride (potassium trisiamylborohydride) and led to decomposition and cyclopentanol **295** was formed by over-reduction with  $\text{LiAl}(\text{O}i\text{-Bu})_3$  (Eq 2.19). Separation of the diastereomeric alcohols was difficult at this stage, so the mixture was carried forward.



The leaving group affects the reactivity of the allylic substitution reaction considerably, therefore a variety of groups were installed. The traditionally used epimeric acetates were prepared as well as the more-activated methyl carbonates. The diethylphosphate esters proved unstable and attempts to form the sterically bulky trichlorobenzoyl esters led to isolation of only **297a**. Alcohol **294b** was presumably too sterically congested to react and was recovered unchanged (Eq 2.20).



### III.B Palladium-Catalyzed Reactions

#### III.B.1 Reaction of **296a** and **297a** with Stabilized Anions

A number of steps involved in the mechanism for the palladium-catalyzed reaction could potentially be affected by the steric hindrance created by the  $\beta$ -substituents of substrates **296**, **297**, and **298**. Approach of the metal for complexation to the olefin should be accessible. However, oxidative addition with the neopentyl leaving group is required and in substrates **296a**, **297a**, and **298a** attack will occur on the same face as the large methyl and oxazolidinone groups. Subsequent nucleophilic attack on the  $\pi$ -allylpalladium intermediate is similarly hindered, especially for the complexes derived from substrates with  $\beta$ -leaving groups as the nucleophile must approach on the same side as both large groups. Therefore, selection of a catalyst possessing the correct balance of nucleophilicity and electrophilicity was required to promote both oxidative addition *and* nucleophilic attack.

A variety of palladium complexes were surveyed in the reaction between substrate **296a** and dimethyl sodiomalonate (Eq 2.21). Commonly used palladium catalysts Pd(PPh<sub>3</sub>)<sub>4</sub> and [ $\eta^3$ -C<sub>3</sub>H<sub>5</sub>PdCl]<sub>2</sub>/PPh<sub>3</sub> as well as the more electrophilic sources Pd<sub>2</sub>dba<sub>3</sub>·CHCl<sub>3</sub> (with and without PPh<sub>3</sub> and AsPh<sub>3</sub>) and [ $\eta^3$ -C<sub>3</sub>H<sub>5</sub>PdCl]<sub>2</sub>/P(OEt)<sub>3</sub> proved

unreactive as did  $\text{PdCl}_2(\text{PPh}_3)_2/\text{DIBAL}$ . Bidentate ligands increase reactivity and influence regioselectivity and so were screened next.<sup>55</sup> Although  $[\eta^3\text{-C}_3\text{H}_5\text{PdCl}]_2/\text{dppm}$  was unreactive, dppe, which has a slightly larger bite angle (85 versus 72), led to reaction, albeit incomplete. The reactivity, conversion, and yield continued to increase as the bite angle increased. Exclusive attack at the less-hindered terminus was observed, although, surprisingly, the stereoselectivity varied. Although **299a**, resulting from retention of configuration, was always the major product, increasing amounts of epimer **299b** were isolated as the bite angle of the ligand increased. Presumably this was the result of nucleophilic attack of Pd(0) on the  $\pi$ -allylpalladium intermediate, a phenomenon that has been observed previously by Bäckvall.<sup>56</sup> The observation that a three-fold increase in the concentration of Pd(0) led to a significant increase in the amount of **299b** formed supports this hypothesis (Table 2.1, last entry).

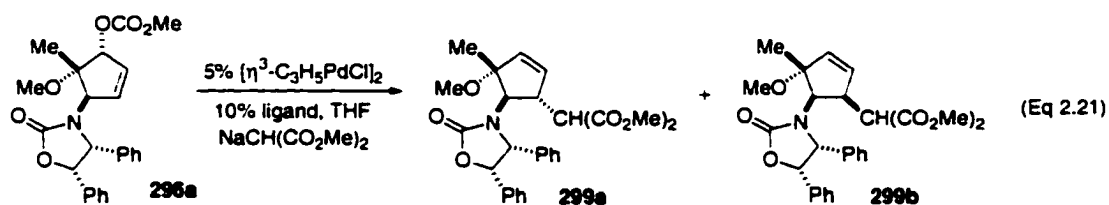


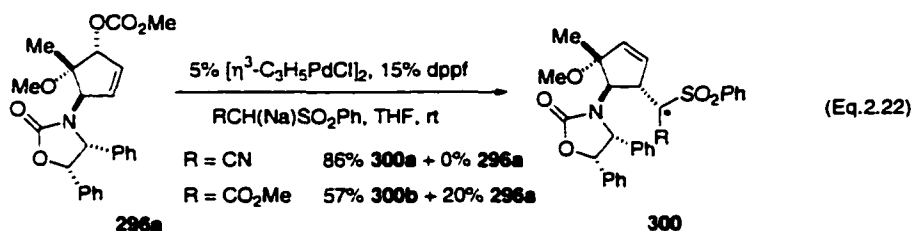
Table 2.1. Effect of Bite Angle of Bidentate Ligands

Ligand	$\beta_n$ (deg)	<b>296a</b> (%)	<b>299a</b> (%)	<b>299b</b> (%)
dppm	72	100	0	0
dppe	85	21	49	0
dppp	91	4	83	5
dppf	96	0	92	7
dppb	98	0	82	17
dppb <sup>a</sup>	98	0	54	33

<sup>a</sup> 17%  $[\eta^3\text{-C}_3\text{H}_5\text{PdCl}]_2$ , 40% dppb

The use of dppf appeared promising because it improved the reactivity and maintained a high degree of stereoselectivity. Indeed,  $\text{PhSO}_2\text{CH}_2\text{CN}$  and

PhSO<sub>2</sub>CH<sub>2</sub>CO<sub>2</sub>Me underwent clean reaction with **296a** at room temperature in good to excellent yield to give a mixture of diastereomers (Eq 2.22). Unfortunately, efforts to employ these conditions with other nucleophiles led to recovered starting material and heating seemed to decompose the catalyst. Therefore, more general conditions were sought.



The combination of  $[\eta^3\text{-C}_3\text{H}_5\text{PdCl}]_2$  and dppe in DMSO catalyzed the reaction between carbonate **296a** and trichlorobenzoate **297a** and a wide range of nucleophiles (Eq 2.23, Table 2.2) whereas acetates **298a** and **298b** proved unreactive. Exclusive attack at the less-hindered terminus with retention of stereochemistry was observed with all stabilized nucleophiles. The bulky sulphone-stabilized nucleophiles were reactive, although required higher temperatures, as did the cyclic  $\beta$ -ketoester and 1,3-diketone. Stabilized nitrogen nucleophiles were prone to attack at the carbonyl carbon, therefore the bulky trichlorobenzoyl ester served as the starting material in these cases. Higher temperatures were required when using **297a**, in part because oxidative addition was not as facile as with carbonate **296a**, which underwent oxidative addition at room temperature (entries 1, 2, 6). The lithium enolate reacted to give only the mono-alkylated product. Steric effects most likely prevented dialkylation. The stabilized sulfur nucleophile, sodium benzene sulfinate reacted in only 30 minutes to give a single product in moderate yield.

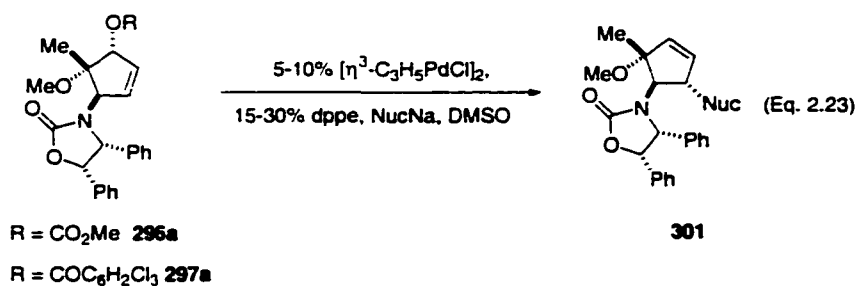
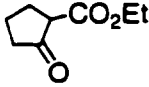


Table 2.2. Palladium-Catalyzed Nucleophilic Substitution Reactions of **296a** or **297a**

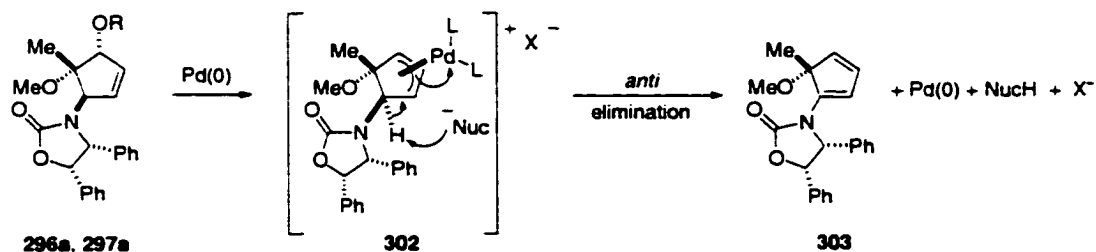
Nucleophile	Temp., °C	Time, hr.	%, Product <sup>a</sup>	Recovered	
				<b>296a</b> % <sup>a</sup>	or <b>297a</b> % <sup>a</sup>
1. (MeO <sub>2</sub> C) <sub>2</sub> CH <sub>2</sub>	23	1	51 <b>299a</b>	0	-
2. (MeO <sub>2</sub> C) <sub>2</sub> CHCH <sub>3</sub>	23	0.2	55 <b>301a</b>	8	-
3. PhSO <sub>2</sub> CH <sub>2</sub> CN	50	36	0 <b>300a</b>	56	-
4. PhSO <sub>2</sub> CH <sub>2</sub> CO <sub>2</sub> Me	70	14	27 <b>300b</b>	0	-
5. (PhSO <sub>2</sub> ) <sub>2</sub> CH <sub>2</sub>	100	12	21 <b>301b</b>	0	-
6. CH <sub>3</sub> COPh <sup>d</sup>	23	5	44 <b>301c</b>	0	-
7. (CH <sub>3</sub> CO) <sub>2</sub> CH <sub>2</sub>	60	24	33 <b>301d</b>	23	-
8.  CO <sub>2</sub> Et	70	12	41 <b>301e</b>	0	-
9. PhSO <sub>2</sub> H	60	0.5	64 <b>301f</b>	0	-
10. Succinimide	70-120	48	8 <b>301g</b>	-	20
11. TsNH <sub>2</sub>	70	12	62 <b>301h</b>	-	0
12. Ac <sub>2</sub> NH	70	48	3 <b>301i</b>	-	0
13. BnNHTs	40-90	36	4 <b>301j</b>	-	0
14. Phthalimide <sup>c</sup>	60	24	0 <b>301k</b>	-	56

<sup>a</sup>Yields are for isolated, purified products. <sup>d</sup>Lithium anion. <sup>c</sup>Potassium anion.

Although a wide range of nucleophiles underwent the substitution reaction, yields were often disappointing and with phthalimide and bis(phenylsulfonyl)methane anions as well as NaCN, NaN<sub>3</sub>, TMSN<sub>3</sub>, BuSH, and primary and secondary amines no reaction was observed. Oxidative addition had occurred, as products were isolated with some nucleophiles. Thus, attack on the π-allylpalladium intermediate appeared to be the difficult step. Decomposition of the reactive intermediates and/or the products under the reaction conditions occurred when the nucleophilic attack was slow, resulting in low mass balances. For example, allowing the reaction of **296a** with dimethyl sodiomethylmalonate to proceed for 0.5 h at room temperature led to 10% isolated

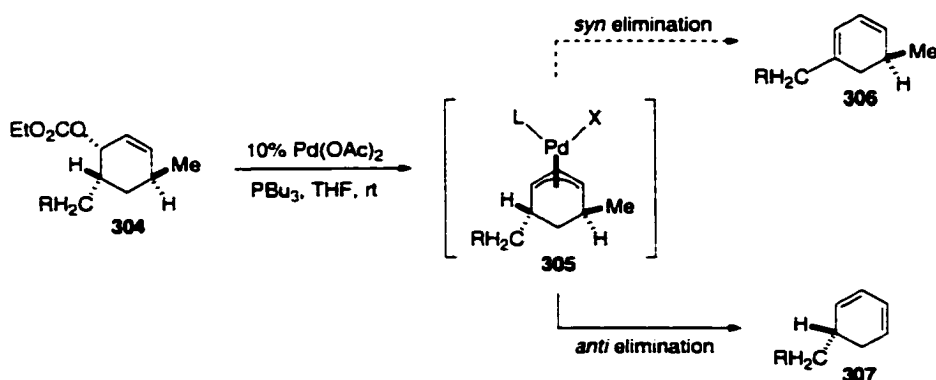
product as well as the diene elimination product **303**. Stopping the reaction after 10 minutes led to 55% product and 8% recovered starting material.

### Scheme 2.27



One possible mode of decomposition was base-promoted *anti* elimination of the elements  $LnPdX-H$  from the  $\pi$ -allylpalladium intermediate (Scheme 2.27). Evidence of similar *anti* elimination of allylic carbonates and acetates to form 1,3-dienes has been well-documented.<sup>57</sup> In a compelling example, the cyclic carbonate **304** was subjected to palladium (0) at 0 °C and afforded *exclusively* **307** (Scheme 2.28) resulting from *anti*-elimination.

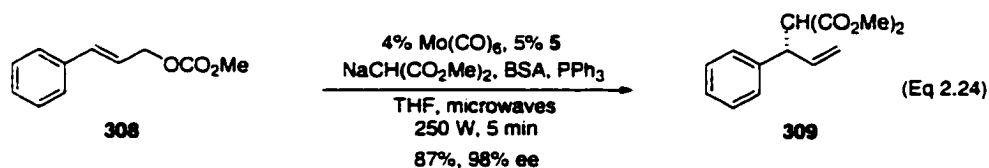
### Scheme 2.28



The product may also be decomposed by reversal of nucleophilic addition, followed by decomposition of the intermediate as was previously described. Salaun and

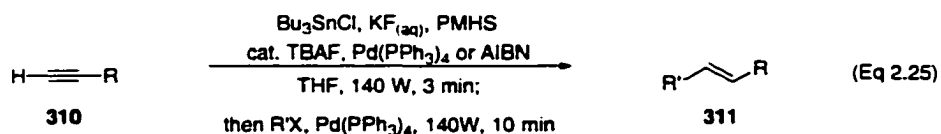
coworkers have reported this type of reversibility in the cyclization of 1,4-dichlorobut-2-ene with the anions of  $\alpha$ -substituted carbonitriles.<sup>58</sup>

It was apparent that longer reaction times led to increased decomposition. Consequently, microwave heating was investigated because of its recent success at improving the yields and decreasing reaction times of the metal-catalyzed allylic substitution reaction<sup>59</sup> as well as a wide range of other organic reactions.<sup>60</sup> Larhed, Moberg and coworkers demonstrated that microwave heating could promote the molybdenum-catalyzed asymmetric alkylation reaction (Eq 2.24).<sup>59</sup> Without microwave heating the addition of dimethyl malonate to cinnamyl carbonate required 2-3 hours, 10 mol%  $\text{Mo}(\text{EtCN})_3(\text{CO})_3$ , and inert conditions. The same transformation could be carried out with 4% of the commercially available, stable  $\text{Mo}(\text{CO})_6$  in only five minutes with microwave heating. Excellent yields and selectivity were maintained.



Although microwave reactors have been specifically designed for use in organic synthesis they are often very expensive (\$45-50,000 for a single reaction unit).<sup>61</sup> As a result, the majority of publications on microwave-assisted synthesis have been performed in domestic microwave ovens. Unfortunately, the inability to strictly control the heating and temperatures in domestic microwaves can sometimes lead to irreproducible results or even explosions. Nevertheless, when caution is taken, exceptional results have been obtained using this affordable and readily available tool. Malecza and coworkers accomplished a microwave-assisted, one-pot hydrostannylation/Stille coupling in a

fraction of the time required with conventional heating using a domestic microwave (Eq 2.25).<sup>62</sup>



Following Maleczka's protocol,<sup>62</sup> reactions with substrates **296** and **297** were run in a sealed pressure tube using a Sharp 700W microwave oven which was placed in a fume hood. Special O-rings were required and care was taken to maintain the integrity of the pressure tubes. To obtain the most consistent heating possible, the pressure tube was placed in the exact same position for each run. A limited survey of ligands and solvents was conducted (Table 2.3). It is clear that the optimal conditions were different for each nucleophile. For example, a dramatic improvement in yield was observed upon switching from dppe/DMSO to dppf/THF with BnN(Na)Ts (entries 16, 17) while the reverse was true for sodium diacetamide (entries 13, 14). With MeO<sub>2</sub>CCH(Na)SO<sub>2</sub>Ph, the amount of decomposition was minimized with dppf/THF versus dppe/DMSO as a large amount of starting material was recovered with a comparable yield of product (entries 7, 8). Solubility was an issue with NaCH(SO<sub>2</sub>Ph)<sub>2</sub> in THF and accordingly BSA was added, however no reaction was observed. A connection between both anion insolubility and long reaction times and the formation of a black precipitate was observed. Decomposition of the Pd(0) precursor may have occurred if activation by the nucleophile was slow because it was not sufficiently solubilized or after prolonged heating.

Table 2.3 Microwave Heating of Substrates **296a** and **297a**

SM	Nucleophile	Ligand	Solvent	Time, min	Power, W	Product %	Other	
1	<b>296a</b>	NaCH(SO <sub>2</sub> Ph) <sub>2</sub>	dppe	DMSO	6	210	<b>301b</b> 16	0
2	<b>296a</b>	NaCH(SO <sub>2</sub> Ph) <sub>2</sub>	dppe	CH <sub>3</sub> CN	4	210	<b>301b</b> 0	SM
				6	280			
3	<b>296a</b>	CH <sub>2</sub> (SO <sub>2</sub> Ph) <sub>2</sub> + BSA	dppe	DMSO	8	210	<b>301b</b> 0	SM
4	<b>296a</b>	NaCH(SO <sub>2</sub> Ph) <sub>2</sub>	dppe	DMSO	2		<b>301b</b> 0	SM +
				9	210			decomp
5	<b>296a</b>	NaCH(SO <sub>2</sub> Ph) <sub>2</sub>	dppf	THF	6	210	<b>301b</b> 32	0
6	<b>296a</b>	NaCH(SO <sub>2</sub> Ph) <sub>2</sub>	dppb	DMSO	12	70	<b>301b</b> 0	SM
7	<b>296a</b>	MeO <sub>2</sub> CCH(Na)SO <sub>2</sub> Ph	dppe	DMSO	3	210	<b>300b</b> 46	0
8	<b>296a</b>	MeO <sub>2</sub> CCH(Na)SO <sub>2</sub> Ph	dppf	THF	3x3	210	<b>300b</b> 43	~50
9	<b>297a</b>	NaNHTs	dppe	DMSO	5	140	<b>301h</b> 44	0
10	<b>297a</b>	NaNHTs	dppe	DMSO	4	70	<b>301h</b> 8	32% SM
				3	140			
11	<b>297a</b>	NaNHTs	dppf	THF	6	210	<b>301h</b> 0	decomp
12	<b>297a</b>	NaNHTs	dppb	DMSO	6	70	<b>301h</b> 10	8% SM
				3	140			
13	<b>297a</b>	NaNAC <sub>2</sub>	dppe	DMSO	3	210	<b>301i</b> 46	0
14	<b>297a</b>	NaNAC <sub>2</sub>	dppf	THF	6	210	<b>301i</b> 17	0
15	<b>297a</b>	BnN(Na)Ts	dppe	DMSO	2	140	<b>301j</b> 0	SM
				2x3	210			
16	<b>297a</b>	BnN(Na)Ts	dppe	DMSO	5	210	<b>301j</b> 37	0
17	<b>297a</b>	BnN(Na)Ts	dppf	THF	6	210	<b>301j</b> 86	0
18	<b>297a</b>	Na-Succinimide	dppe	DMSO	2	210	<b>301g</b> 29	0
19	<b>297a</b>	Na-Succinimide	dppf	THF	5x2	210	<b>301g</b> 0	SM
20	<b>297a</b>	K-Pthalimide	dppe	DMSO	5	210	<b>301k</b> 63	0

In most cases, yields were dramatically improved compared with conventional oil bath heating, as were the reaction times which were reduced to just minutes (Table 2.4). Importantly, for the first time reaction involving potassium phthalimide was observed in 64% yield. Although the reactivity was enhanced with microwave heating, the regio- and stereoselectivities were the same as with conventional heating.

Table 2.4. Results Comparing Microwave and Conventional Heating

Substrate	Nucleophile	Conventional	Microwave Heating <sup>d</sup>	
		Heating <sup>a</sup>	dppe/DMSO <sup>a</sup>	dppf/THF <sup>c</sup>
<b>296a</b>	PhSO <sub>2</sub> CH <sub>2</sub> CO <sub>2</sub> Me <sup>d</sup>	48 h, 40-70 °C	3 min.	3 x 3 min.
		27% <b>300b</b>	46% <b>300b</b>	93% <b>300b</b>
<b>297a</b>	Succinimide <sup>d</sup>	48 h, 40-70 °C	5 min.	5 x 2 min.
		8% <b>301g</b>	29% <b>301g</b>	0% <b>301g</b>
<b>297a</b>	Ac <sub>2</sub> NH <sup>d</sup>	48 h, 40-70 °C	2 min.	6 min.
		3% <b>301i</b>	46% <b>301i</b>	24% <b>301i</b>
<b>297a</b>	TsNHBn <sup>d</sup>	48 h, 40-90 °C	5 min.	6 min.
		4% <b>301j</b>	37% <b>301j</b>	86% <b>301j</b>
<b>297a</b>	Phthalimide <sup>e</sup>	no reaction	5 min.	-
			63% <b>301k</b>	-

<sup>a</sup> **296a** or **297a** (20 mg), 5% [η<sup>3</sup>-C<sub>3</sub>H<sub>5</sub>PdCl]<sub>2</sub>, 15% dppe, 1.5 eq. nucleophile anion in 0.4 ml DMSO. <sup>b</sup>210 W. <sup>c</sup>15% dppf and 0.4 ml THF. <sup>d</sup>Na anion. <sup>e</sup>K anion.

Yields could not be optimized further because when high powers or long reaction times were used, the reaction produced a black precipitate, possibly due to the thermal instability of the catalyst system.<sup>62</sup> Alternatively, reducing the power led to recovered starting material. Clearly, there was a small window in the power/reaction time combination that would achieve reaction but minimize decomposition.

The success observed with microwave heating can be attributed to the fact that in a pressurized system, temperatures far above the conventional boiling point of the solvent can be reached very rapidly, a phenomenon which is called superheating.<sup>60</sup> Additionally, the heating is uniform throughout the reaction mixture. In comparison, traditional heating often creates a temperature gradient leading to local overheating and consequently product, substrate or reagent decomposition. Because a large amount of energy can be put into the system uniformly and is required for only a short time, decomposition is minimized.

Microwaves, which for domestic microwave ovens are 12.2 cm and 2.450 GHz, produce heat by two major mechanisms.<sup>60</sup> The dipolar polarization mechanism involves rotation of the dipolar moment of a substance in an attempt to align itself with the oscillating electric field. The resulting friction and collisions causes energy to be lost from the dipole and produces dielectric heat. This is why solvents with a higher dielectric constant are able to produce heat more efficiently. For example DMSO has a dielectric constant ( $\epsilon_s$ ) of 47 so should heat more readily than THF ( $\epsilon_s = 7.6$ ). Additionally, heat is created by the conduction mechanism where ions in a solution follow the applied field, which increases the collision rate and as a result kinetic energy is

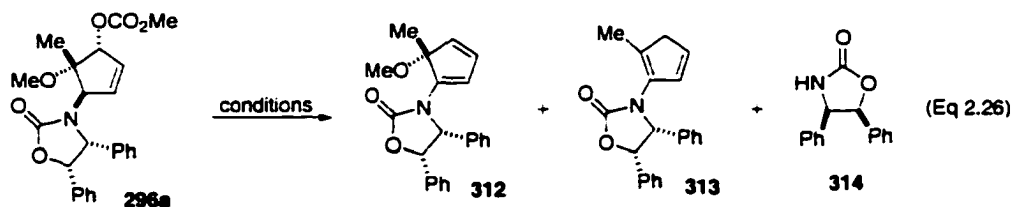
converted to heat. Accordingly, the use of the sodium or potassium salts of the nucleophiles increased the amount of heat produced.

### III.B.2 Alkylation of **296a** via Transmetallation

Inherent limitations in the alkylation of allylic esters via transmetallation have minimized the utility of this transformation. Nucleophilic ligands are required because oxidative addition of allylic esters is more difficult than for allylic halides. However, electron-rich ligands suppress transmetallation, as does the presence of ester anions, which bind tightly to palladium.

Nevertheless, introduction of a group via transmetallation provides complementary stereoselectivity and, depending on the metal, reversed regioselectivity to stabilized anions. Therefore, substrate **296a** was subjected to a variety of conditions to promote allylic alkylation via transmetallation. Not surprisingly, standard conditions failed to effect reaction. (*p*-MeOPh)SnBu<sub>3</sub> and the more readily transferable (*p*-MeOPh)SnMe<sub>3</sub><sup>63</sup> were unreactive with  $[\eta^3\text{-C}_3\text{H}_5\text{PdCl}]_2/\text{dppe}$  or Pd(PPh<sub>3</sub>)<sub>4</sub> in DMSO or THF. Furthermore, although the addition of lithium chloride<sup>17d</sup> and copper salts<sup>64</sup> has been shown to promote Stille couplings, only starting material was observed when these were combined with the above conditions. Me<sub>3</sub>SnPh was examined next due to the higher transferability of the phenyl group. However, reaction with Pd(PPh<sub>3</sub>)<sub>4</sub> and the ligandless palladium(0) source Pd<sub>2</sub>dba<sub>3</sub>·CHCl<sub>3</sub>, which should further facilitate transmetallation,<sup>17d</sup> led to recovered starting material. The absence of phosphine ligands may have rendered the catalyst unable to promote oxidative addition in such a sterically hindered environment. Interestingly, the addition of AsPh<sub>3</sub> to Pd<sub>2</sub>dba<sub>3</sub>·CHCl<sub>3</sub> with (CH<sub>2</sub>CH)SnBu<sub>3</sub>, LiCl and **296a** led to formation of **313** via loss of methoxide (eq 2.26).

This product was also observed with  $\text{Pd}(\text{PPh}_3)_4$  and both  $(\text{CH}_2\text{CH})\text{SnBu}_3$  and  $\text{PhMgBr}/\text{ZnCl}_2$ . It seemed that both catalyst systems were able to promote oxidative addition, but elimination of methanol from the  $\pi$ -allylpalladium intermediate followed. A ligand with more  $\pi$ -acceptor character was needed so that transmetalation would occur before decomposition.



Tri(2-furyl)phosphonium salts enhance the rate of coupling of allylic halides and organostannanes (45-fold rate increase over  $\text{PPh}_3$ ).<sup>17c</sup> This ability has been attributed to the substantial electron-withdrawing ability of the furan ring. Unfortunately, reaction with  $\text{Me}_3\text{SnPh}$ ,  $[\eta^3\text{-C}_3\text{H}_5\text{PdCl}]_2$  in HMPA led to recovery of starting material and switching to sodium tetraphenylborate ( $\text{NaBPh}_4$ ) resulted in decomposition to an unidentifiable mixture. Further examination of transmetalation with  $\text{NaBPh}_4$  led to starting material with  $\text{Pd}(\text{PPh}_3)_4$ ,  $[\eta^3\text{-C}_3\text{H}_5\text{PdCl}]_2/\text{P}(\text{OMe})_3$  and  $\text{Pd}_2\text{dba}_3\cdot\text{CHCl}_3/\text{dppe}$  and elimination product **312** with  $[\eta^3\text{-C}_3\text{H}_5\text{PdCl}]_2/\text{dppf}$  in THF or  $\text{C}_6\text{H}_6$  with and without maleic anhydride (Eq 2.26).<sup>65</sup> When only enough  $\text{NaBPh}_4$  was added to activate the  $[\eta^3\text{-C}_3\text{H}_5\text{PdCl}]_2/\text{dppf}$  in THF and the reaction mixture was refluxed for two days, only starting material was recovered, suggesting the borate was responsible for the decomposition. Therefore, a less-basic organometallic reagent was sought.

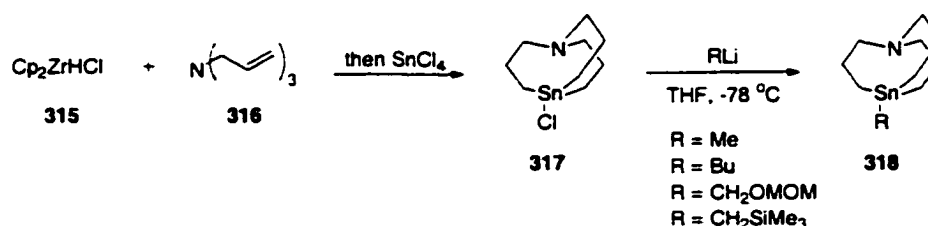
Benzylzinc bromide, generated from zinc dust and benzyl bromide, is a neutral and transferable group.<sup>66</sup> However, decomposition was the major pathway with this

reagent as well. In one case an unidentifiable mixture resulted ( $([\eta^3\text{-C}_3\text{H}_5\text{PdCl}]_2/\text{dppf}$ , THF, reflux) and a second set of conditions led to isolation of free oxazolidinone **314** ( $\text{Pd}(\text{acac})_2$ ,  $\text{PPh}_3$ , THF, reflux).

The nature of the leaving group affects the Stille reaction.<sup>67</sup> Halides and triflates are more subject to oxidative addition and the resulting  $\pi$ -allylpalladium complexes more prone to transmetalation than with esters. Therefore, allylic alcohol **294a** was transformed into the corresponding allylic chloride. Unfortunately, attempts to promote alkylation resulted in elimination product **312** and conditions required to form the triflate led to decomposition.

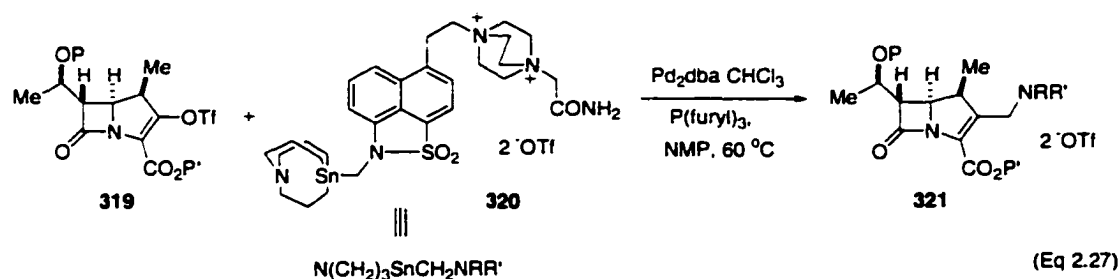
It seemed that the steric hindrance around palladium in the reactive intermediate was too great to allow for transmetalation. In 1992 Vedejs and coworkers published the facile preparation of stannatranes,<sup>68</sup> originally reported by Tzschach,<sup>69</sup> which were successful at promoting the Stille Coupling of alkyl and alkyloxy groups which are traditionally difficult to transfer (Scheme 2.29).

**Scheme 2.29**

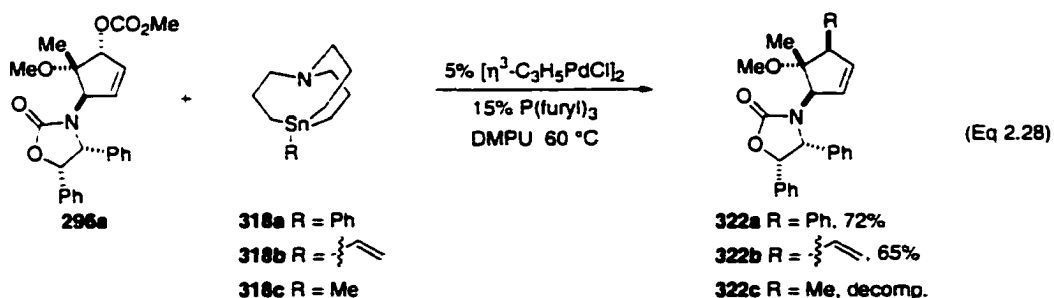


More recently Jensen and coworkers at Merck Research Laboratories found that typical Suzuki and Stille Coupling conditions failed in an attempt to couple an enol triflate with a sulfonamide substituted  $\text{sp}^3$  carbon.<sup>70</sup> However, with the use of a

stannatrane the entire side chain could be introduced in one step (Eq 2.27). Also, the stannatrane could be recovered as chloride **317** following a simple workup procedure.



These impressive results suggested that the use of a stannatrane might promote reaction with substrate **296a**. The methyl, phenyl, and vinyl stannatrane were prepared from stannatrane chloride **317** and the corresponding organolithium reagent in modest yield (65, 49 and 56% respectively). Fortunately, both the aryl and vinyl stannatrane underwent clean reaction with **296a** in DMPU or HMPA. As was expected, the reaction occurred with inversion of stereochemistry, but the regioselectivity was opposite that observed in the alkylation by stabilized nucleophiles (Eq 2.28).<sup>71</sup> Unfortunately, attempts to recover the stannatrane following the procedure of Jensen et al. were unsuccessful, possibly due to stronger Sn-OCO<sub>2</sub>Me or Sn-OMe bond formed compared with Sn-OTf. Only decomposition was observed with methyl stannatrane presumably due to decomposition of the  $\pi$ -allylpalladium intermediate due to slow transmetalation.



Two factors are thought to be responsible for the improved reactivity observed with the stannatranes: the unusually long exocyclic Sn-C bond length (on average 0.1 Å longer than a typical alkylstannane),<sup>72</sup> and internal tin-nitrogen coordination. A crystal structure of **318c** revealed that the distance between Sn and N was 2.624 Å and that the nitrogen was perfectly aligned to donate into the metal, thereby stabilizing the electron-deficient tin center formed in the transition state. The increased length of the Sn-C bond minimized the steric interactions and thereby facilitated transmetalation. The stannatranes provide a valuable tool for promoting Stille-type couplings with both difficult-to-transfer functionalities and sterically hindered substrates.

### III.B.3 Reactions of Epimeric Allylic Carbonate **296b**

A comparison of the epimeric allylic carbonates **296a** and **296b** revealed significant differences in reactivity (Table 2.5). Oxidative addition was expected to be more facile with substrate **296b** because of the decreased steric hindrance on the bottom face of the molecule. However, nucleophilic attack should be even more hindered. Reaction of **296b** with dimethyl sodiomalonate and  $[\eta^3\text{-C}_3\text{H}_5\text{PdCl}]_2/\text{dppf}$  in DMSO resulted in decomposition. As was expected, the use of *dppf*, which promotes nucleophilic attack, allowed for facile product formation with dimethyl malonate in good yield. Reaction with phenylstannatrane resulted in decomposition, which was surprising, since both oxidative addition and transmetalation would occur on the less-sterically demanding side.

Electronic interactions between palladium and an antiperiplanar electron-withdrawing  $\beta$ -substituents (such as OR) of  $\eta^3$ -allylpalladium intermediates led to

lengthening and weakening of the C-O bond, facilitating the loss of the  $\beta$ -substituent.<sup>15.73</sup>

The isolation of free oxazolidinone is consistent with this observation.

Conditions	<b>296a</b>	<b>296b</b>
NaCH(CO <sub>2</sub> Me) <sub>2</sub> DMSO, dppe, rt	51% <b>299a</b> 30 min	22% <b>299b</b> 30 min
NaCH(CO <sub>2</sub> Me) <sub>2</sub> THF, dppe, rt	92% <b>299a</b> >5 h	88% <b>299b</b> 2h
N(CH <sub>2</sub> ) <sub>3</sub> SnPh, DMPU, 60°C	73% <b>322a</b> 12 h	decomposition <sup>a</sup>

<sup>a</sup>70% free oxazolidinone recovered.

### III.C Reaction of **296a** and **296b** With Other Metal Catalysts

As rhodium catalysts demonstrated a high degree of reactivity in previous studies, efforts were initially focused on the application of rhodium complexes to the allylic alkylation of **296a** and **296b**. However, with the standard metal complexes, ligands and a wide range of nucleophiles, counterions and solvents, in almost every case starting material was recovered (Eq 2.29). Also, addition of the noncoordinating-ion PF<sub>6</sub> (entry 19) in efforts to form a more reactive intermediate led to starting material, as did reactions subjected to microwave heating (entries 17, 18). Since, in most cases, starting material was recovered it appeared that oxidative addition had not occurred. Oxidative addition should be more facile with substrate **296b** because attack on the face opposite the leaving group in an S<sub>N</sub>2' type manner should be relatively accessible. Indeed, it appears that with **296b**, RhClPPh<sub>3</sub>/P(OMe)<sub>3</sub>, and dimethyl sodiomalonate in toluene at 110 °C (entry 11) oxidative addition was possible, as only 42% starting material was

recovered along with some free oxazolidinone **314**. However, subjecting **296b** to other conditions led to recovered starting material.

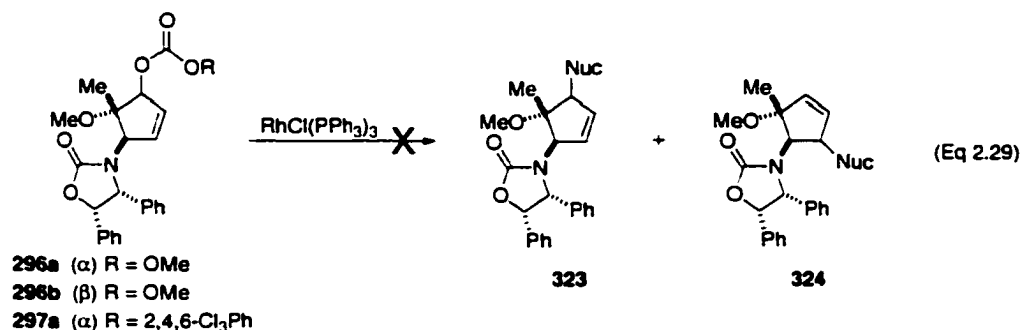


Table 2.6 Rhodium-Catalyzed Allylic Substitution

Entry	Substrate	Ligand	Nucleophile	Solvent	Result
1	<b>296a</b>	P(OPh) <sub>3</sub>	NaCH(CO <sub>2</sub> Me) <sub>2</sub>	THF	<b>296a</b>
2 <sup>a</sup>	<b>296a</b>	P(OPh) <sub>3</sub>	NaCH(CO <sub>2</sub> Me) <sub>2</sub>	THF	<b>296a</b>
3	<b>296a</b>	P(OPh) <sub>3</sub>	NaCH(CO <sub>2</sub> Me) <sub>2</sub>	PhMe	<b>296a</b>
4	<b>296a</b>	P(OPh) <sub>3</sub>	CH <sub>2</sub> (CO <sub>2</sub> Me) <sub>2</sub> /BSA	CH <sub>2</sub> Cl <sub>2</sub>	<b>296a</b>
5	<b>296a</b>	P(OMe) <sub>3</sub>	NaCH(CO <sub>2</sub> Me) <sub>2</sub>	THF	<b>296a</b>
6	<b>296a</b>	P(OMe) <sub>3</sub>	NaCH(CO <sub>2</sub> Me) <sub>2</sub>	CH <sub>3</sub> CN	<b>296a</b>
7	<b>296a</b>	P(OPh) <sub>3</sub>	NaCH(CO <sub>2</sub> Me) <sub>2</sub>	Cl(CH <sub>2</sub> ) <sub>2</sub> Cl	<b>296a</b>
8	<b>296a</b>	P(OPh) <sub>3</sub>	NaCH(CO <sub>2</sub> Me) <sub>2</sub>	dioxane	<b>296a</b>
9 <sup>a</sup>	<b>296a</b>	P(OPh) <sub>3</sub>	NaCH(CO <sub>2</sub> Me) <sub>2</sub>	dioxane	<b>296a</b>
10	<b>296b</b>	P(OPh) <sub>3</sub>	NaCH(CO <sub>2</sub> Me) <sub>2</sub>	THF	<b>296b</b>
11	<b>296b</b>	P(OPh) <sub>3</sub>	NaCH(CO <sub>2</sub> Me) <sub>2</sub>	PhMe	<b>296b+314</b>
12	<b>297a</b>	P(OPh) <sub>3</sub>	NaNHTs	PhMe	<b>297a</b>
13	<b>296a</b>	P(OMe) <sub>3</sub>	NaCH(CO <sub>2</sub> Me) <sub>2</sub>	THF	<b>296a</b>
14	<b>296a</b>	P(OPh) <sub>3</sub>	TsN(Li)Bn	THF	<b>296a</b>
15	<b>296a</b>	P(OPh) <sub>3</sub>	TsN(Li)Bn	dioxane	<b>296a</b>
16 <sup>d</sup>	<b>296a</b>	P(OPh) <sub>3</sub>	NaCH(CO <sub>2</sub> Me) <sub>2</sub>	PhMe	<b>296b</b>
17 <sup>c</sup>	<b>296a</b>	P(OPh) <sub>3</sub>	NaCH(CO <sub>2</sub> Me) <sub>2</sub>	THF	<b>296a+294a</b>
18 <sup>b,c</sup>	<b>296a</b>	P(OPh) <sub>3</sub>	NaCH(CO <sub>2</sub> Me) <sub>2</sub>	THF	<b>296a</b>
19 <sup>b,d</sup>	<b>296a</b>	P(OPh) <sub>3</sub>	NaCH(CO <sub>2</sub> Me) <sub>2</sub>	THF	<b>296a</b>
20 <sup>b</sup>	<b>296a</b>	P(OPh) <sub>3</sub>	NaCH(CO <sub>2</sub> Me) <sub>2</sub>	EtOH	<b>296a+294a</b>

<sup>a</sup> Stoichiometric RhCl(PPh<sub>3</sub>)<sub>3</sub>, <sup>b</sup> [Rh(COD)Cl]<sub>2</sub>, <sup>c</sup> Microwave heating <sup>d</sup> NH<sub>4</sub>PF<sub>6</sub>

General success on relatively simple substrates has also been achieved with molybdenum catalysts, therefore attention was next focused in this direction (Eq 2.30,

Table 2.7). However, again the standard reaction conditions led to starting material with only a few exceptions.

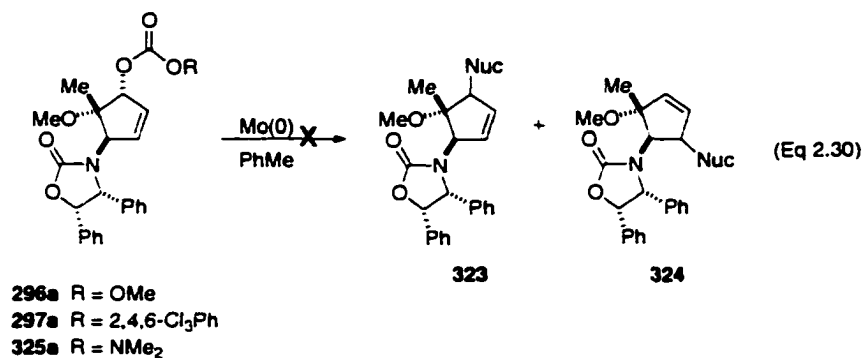
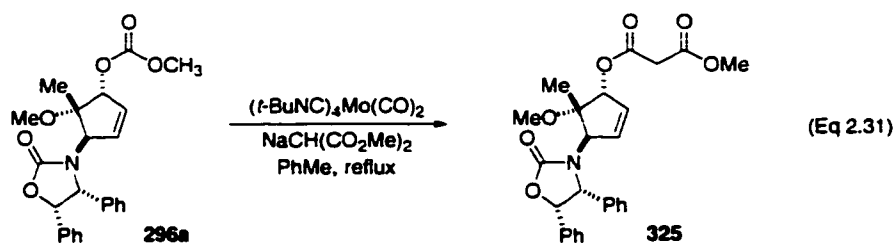


Table 2.7 Molybdenum-Catalyzed Allylic Substitution

Entry	Substrate	Nucleophile	Mo(0)	Result
1	<b>296a</b>	CH <sub>2</sub> (CO <sub>2</sub> Me) <sub>2</sub> , NaH	( <i>t</i> -BuNC) <sub>4</sub> Mo(CO) <sub>2</sub>	<b>325</b>
2	<b>296a</b>	CH <sub>2</sub> (SO <sub>2</sub> Ph) <sub>2</sub> , NaH	( <i>t</i> -BuNC) <sub>4</sub> Mo(CO) <sub>2</sub>	<b>296a</b>
3	<b>296a</b>	PhSO <sub>2</sub> CH <sub>2</sub> CO <sub>2</sub> Me, NaH	( <i>t</i> -BuNC) <sub>4</sub> Mo(CO) <sub>2</sub>	<b>296a</b>
4	<b>296a</b>	CH <sub>3</sub> CH(CO <sub>2</sub> Me) <sub>2</sub> , NaH	( <i>t</i> -BuNC) <sub>4</sub> Mo(CO) <sub>2</sub>	<b>296a</b>
5	<b>297a</b>	TsNH <sub>2</sub> , NaH	( <i>t</i> -BuNC) <sub>4</sub> Mo(CO) <sub>2</sub>	<b>297a + 294a</b>
6	<b>326a</b>	CH <sub>2</sub> (CO <sub>2</sub> Me) <sub>2</sub> , NaH	( <i>t</i> -BuNC) <sub>4</sub> Mo(CO) <sub>2</sub>	<b>326a</b>
7	<b>296a</b>	CH <sub>2</sub> (CO <sub>2</sub> Me) <sub>2</sub> , NaH	Mo(CO) <sub>6</sub>	<b>296a</b>
8	<b>296a</b>	CH <sub>2</sub> (CO <sub>2</sub> Me) <sub>2</sub> , BSA	( <i>t</i> -BuNC) <sub>4</sub> Mo(CO) <sub>2</sub>	<b>296a + 314</b>
9	<b>296a</b>	CH <sub>2</sub> (CO <sub>2</sub> Me) <sub>2</sub> , BSA	Mo(CO) <sub>6</sub>	<b>296a + 314</b>
10	<b>296a</b>	CH <sub>3</sub> CH(CO <sub>2</sub> Me) <sub>2</sub> , BSA	Mo(CO) <sub>6</sub>	<b>296a + 314</b>
11	<b>296a</b>	CH <sub>2</sub> (CO <sub>2</sub> Me) <sub>2</sub> , NaH	Mo(CO) <sub>6</sub>	<b>296a</b>
12	<b>296a</b>	CH <sub>2</sub> (CO <sub>2</sub> Me) <sub>2</sub> , NaH	( <i>t</i> -BuNC) <sub>4</sub> Mo(CO) <sub>2</sub>	<b>296a</b>

Subjecting **296a** to (*t*-BuNC)<sub>4</sub>Mo(CO)<sub>2</sub> and dimethyl sodiomalonate in refluxing toluene gave **325**, resulting from transesterification with dimethyl malonate (Eq 2.31). Similar transformations have been observed in the iridium-catalyzed alkylation of allylic alcohols.



Because the nature of the leaving group significantly affects the reactivity in molybdenum-catalyzed reactions and because the methyl carbonate had participated in transesterification, other leaving groups were examined. The aryl ester **297a** should suppress transesterification and dimethyl carbamate **326a** (prepared from alcohol **294a** and dimethylcarbamoyl chloride) should promote oxidative *syn* addition due to the coordinating ability of the carbonyl oxygen, as was demonstrated by Takeuchi. Unfortunately, these substrates also gave no reaction.

Varying the steric bulk of the nucleophile induced differences in reactivity. However, the use of a wide range of nucleophiles led to starting material. Strikingly different results were observed by varying the base. With sodium hydride, starting material was observed in all cases except the example shown in equation 2.20. In contrast, BSA with both  $\text{Mo}(\text{CO})_6$  and  $(t\text{-BuNC})_4\text{Mo}(\text{CO})_2$  and dimethyl malonate and the more bulky dimethyl methylmalonate, led to isolation of free oxazolidinone **314** along with recovered starting material. Silylation of the oxazolidinone may facilitate its elimination.

Because iridium and tungsten complexes are less reactive than the rhodium and molybdenum complexes only limited studies were conducted with these metals. Carbonate **296a** was reacted with both  $[\text{Ir}(\text{COD})\text{Cl}]_2/\text{P}(\text{OPh})_3$ , and  $(\text{EtCN})_3\text{W}(\text{CO})_3/\text{bpy}$  and dimethyl sodiomalonate but led to recovered starting material.

#### **IV. Conclusions**

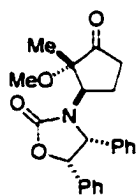
The chiral adjacent tertiary and quaternary centers have a dramatic effect on the reactivity of the metal-catalyzed allylic substitution reaction of **296a**, **296b**, and **297a**. Promotion of oxidative addition and nucleophilic attack required careful selection of reaction conditions. Microwave heating improved yields and reaction times. The substrates were inert to standard conditions for transmetalation, however **296a** underwent smooth reaction with vinyl and phenyl stannatranes. Stabilized nucleophiles exclusively attacked the less-hindered terminus, while transmetalation with the stannatranes occurred at the opposite end. Stereoselectivity was dependent on the bidentate ligand used, although retention of stereochemistry predominated with the stabilized nucleophiles and inversion with the stannatranes.

## V. Experimental Section

**Materials.** The following compounds were prepared according to literature procedures: cyclobutanone **291**,<sup>74</sup>  $[\eta^3\text{-C}_3\text{H}_5\text{PdCl}]_2$ ,<sup>75</sup>  $\text{Pd}(\text{PPh}_3)_4$ ,<sup>76</sup>  $\text{N}[(\text{CH}_2)_3]_3\text{SnCl}$  (**317**),<sup>68</sup>  $\text{N}[(\text{CH}_2)_3]_3\text{SnMe}$  (**318c**),<sup>69b</sup> phenyllithium,<sup>77</sup> and vinylolithium.<sup>78</sup>

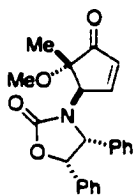
**General Procedures.** The procedures from Chapter One were followed with these additions: DMSO and DMPU were distilled from  $\text{CaH}_2$ . Microwave reactions were carried out in a Sharp 700 W microwave oven (model R-220BW) in pressure tubes purchased from Ace Glass (Ace catalog No. 8648-23) and fitted with Teflon plugs (Ace catalog No. 5846-48) and Teflon encapsulated O-rings (Ace catalog No. 7855-818).

**Extreme caution** should be taken when heating a sealed tube in a microwave oven. High pressures and temperatures are generated which have led to *explosions*. In the event of such explosions, glass shards may penetrate the walls of the oven. Thus, all reactions should be run in a fume hood with a blast shield in place.



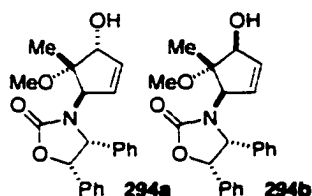
**Cyclopentanone 292.** A freshly prepared solution of diazomethane (prepared by slow addition of Diazald (10 g, 47 mmol) in 90 mL  $\text{Et}_2\text{O}$  to 10 g KOH in 18 mL water and 20 mL 95% ethanol at 65 °C and co-distillation of  $\text{Et}_2\text{O}$ /diazomethane)<sup>79</sup> was poured into a 500 mL Erlenmeyer flask containing cyclobutanone **291** (3.4 g, 9.8 mmol) in THF (90 mL). (*Extreme caution* is required when working with diazomethane because it can be *explosive* on heating at 100 °C or on contact with rough surfaces or solids. Scratched or ground glassware should be avoided.)<sup>79</sup> The reaction mixture stood for 5 h at 0 °C. Argon was bubbled through until

the yellow color dissipated then the solvent was removed under reduced pressure. Flash chromatography with hexane/EtOAc (4/1 to 2/1) gave **292** as a white solid (2.6 g, 7.0 mmol, 72%). **Cyclopentanone 292:**  $^1\text{H NMR}$   $\delta$  7.12 (m, 6H), 6.91 (m, 4H), 5.86 (d,  $J = 7.5$  Hz, 1H), 4.98 (d,  $J = 7.8$  Hz, 1H), 4.41 (t,  $J = 7.5$  Hz, 1H), 3.27 (s, 3H), 2.1-2.4 (m, 2H), 1.93-2.05 (m, 1H), 1.59-1.71 (m, 1H), 1.37 (s, 3H);  $^{13}\text{C NMR}$   $\delta$  213.3, 158.7, 135.4, 134.0, 128.8, 128.6, 128.3, 128.1, 127.7, 126.3, 83.8, 80.6, 65.5, 56.9, 51.8, 34.8, 22.9, 14.9; IR (neat)  $\nu$  1749  $\text{cm}^{-1}$ ; Anal. Calcd for  $\text{C}_{22}\text{H}_{23}\text{NO}_4$ : C, 72.31; H, 6.34; N, 3.83. Found: C, 72.12; H, 6.25; N, 3.78.



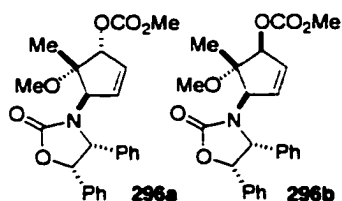
**Cyclopentenone 293.** Cyclopentanone **292** (2.00 g, 5.47 mmol) in THF (12 mL) was added slowly to a solution of LiHMDS [prepared from *n*-BuLi (5.52 mmol) and HMDS (2.65 mL, 12.6 mmol) in THF (10 mL) at 0 °C] at -78 °C and this reaction mixture stirred for 2.5 h. Phenylselenyl bromide (1.42 g, 6.00 mmol) in THF (10 mL) was added via syringe pump over 20 min. After 1.5 h the reaction mixture was quenched with saturated aqueous  $\text{NH}_4\text{Cl}$ . The layers were separated and the aqueous layer was extracted with  $\text{CH}_2\text{Cl}_2$  (3x 25 mL). The combined organic layers were dried with  $\text{MgSO}_4$ , filtered, and concentrated in vacuo. The orange oil was passed through a plug of silica gel eluting with hexane/EtOAc (10/1 to 2/1). The selenide was dissolved in  $\text{CHCl}_3$  (88 mL) and cooled to 0 °C. Pyridine (1.31 mL, 16.2 mmol) then the Davis oxaziridine (4.38 g, 16.8 mmol) were added and the reaction mixture stirred vigorously for 35 min. The reaction was quenched with water and the layers were separated. The aqueous layer was extracted with  $\text{CH}_2\text{Cl}_2$  (3x50 mL). The combined organic layers were washed with brine, dried with  $\text{MgSO}_4$  and concentrated in

vacuo. Immediate flash chromatography with hexane/EtOAc(10/1 to 2/1) gave the cyclopentenone **293** (1.27 g, 3.50 mmol, 64%) as a white solid. See ref 54 for spectral data.



**Allylic alcohols 294a, 294b.** Cyclopentenone **293** (367 mg, 1.01 mmol) was dissolved in MeOH (30 mL) and cooled to 0 °C.  $\text{CeCl}_3 \cdot 7\text{H}_2\text{O}$  (535 mg, 1.44 mmol) was added and the reaction mixture stirred for 0.5 h before  $\text{NaBH}_4$  (51 mg, 1.33 mmol) was added in portions. The reaction stirred for an additional 2.5 h then 10% AcOH in methanol was added. The mixture stirred vigorously for 0.5 h at 0 °C. The layers were separated and the aqueous layer was extracted with  $\text{CH}_2\text{Cl}_2$  (5x). The combined organic layers were washed with brine, dried with  $\text{MgSO}_4$ , filtered and concentrated in vacuo. Column chromatography using hexane/EtOAc (3/1) gave a 4:1 mixture of diastereomeric allylic alcohols **294a:294b** (348 mg, 0.96 mmol, 95%) as a white solid which was used without further purification. Analytical samples of the allylic alcohols were prepared by preparative thin layer chromatography with hexane/EtOAc (3/2). **Allylic alcohol 294a:**  $^1\text{H NMR}$   $\delta$  7.09 (m, 6H), 6.98(m, 4H), 5.81 (d,  $J = 7.2$  Hz, 1H), 5.72 (d,  $J = 6.0$  Hz, 1H), 5.08 (m, 1H), 5.00 (m, 1H), 4.59 (d,  $J = 7.2$  Hz, 1H), 4.55 (d,  $J = 1.5$  Hz, 1H), 3.47 (s, 3H), 3.12 (d,  $J = 9.6$  Hz, 1H), 1.54 (s, 3H);  $^{13}\text{C NMR}$   $\delta$  158.5, 138.6, 136.6, 133.9, 128.5, 128.4, 128.3, 128.1, 126.3, 82.6, 80.8, 64.5, 63.0, 51.4, 16.9; IR (neat)  $\nu$  3508, 1733  $\text{cm}^{-1}$ ; Anal. Calcd for  $\text{C}_{22}\text{H}_{23}\text{NO}_4$ : C, 72.31; H, 6.34; N, 3.83. Found: C, 72.45; H, 6.20; N, 3.83. **Allylic alcohol 294b:**  $^1\text{H NMR}$   $\delta$  7.11 (m, 6H), 6.94 (m, 4H), 6.00 (d,  $J = 6.0$  Hz, 1H), 5.83 (d,  $J = 8.1$  Hz, 1H), 5.51 (dd,  $J = 2.1, 5.4$  Hz, 1H), 5.08 (d,  $J = 8.4$  Hz, 1H), 4.41 (bs, 1H), 4.31

(bs, 1H), 3.16 (s, 3H), 1.42 (s, 3H);  $^{13}\text{C}$  NMR  $\delta$  158.3, 136.6, 135.6, 134.5, 130.3, 128.7, 128.4, 128.2, 128.1, 126.2, 87.6, 80.8, 80.1, 65.8, 64.5, 51.0, 14.3; IR (neat)  $\nu$  1728, 3416  $\text{cm}^{-1}$ ; HRMS  $m/z$  (M+H) calcd for  $\text{C}_{22}\text{H}_{24}\text{NO}_4$  366.1705, found 366.1702.

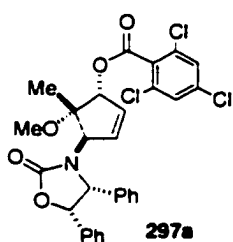
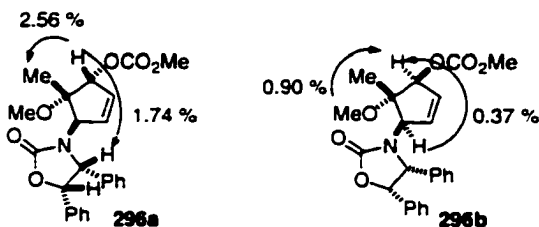


**Allylic carbonates 296a, 296b.** Pyridine (0.04 mL, 0.50 mmol) was added to a mixture of allylic alcohols **294a, 294b** (0.13 g, 0.36 mmol) in  $\text{CH}_2\text{Cl}_2$  (5.0 mL) at 0 °C. After 0.5 h methyl chloroformate (0.04 mL, 1.4 mmol) then DMAP (14 mg, 0.12 mmol) were added and the mixture stirred at 0 °C to room temperature overnight. The reaction mixture was quenched with water and the layers were separated. The aqueous layer was extracted with  $\text{CH}_2\text{Cl}_2$  (4x) and the combined organic layers were washed with brine, dried with  $\text{MgSO}_4$ , filtered, and concentrated in vacuo. Flash chromatography with hexane/EtOAc (3/1) gave allylic carbonate **296a** (82 mg, 63%) and **296b** (18 mg, 14%).

**Allylic carbonate 296a:**  $^1\text{H}$  NMR  $\delta$  7.09 (m, 7H), 6.99 (m, 2H), 6.82 (bs, 1H), 5.83 (d,  $J = 7.6$  Hz, 1H), 5.73 (dt,  $J = 1.8, 6.0$  Hz, 1H), 5.47 (dd,  $J = 1.8, 3.4$  Hz, 1H), 5.34 (dt,  $J = 2.0, 6.0$  Hz, 1H), 5.14 (d,  $J = 2.4$  Hz, 1H), 4.67 (d,  $J = 7.6$  Hz, 1H), 3.82 (s, 3H), 3.38 (s, 3H), 1.58 (s, 3H);  $^{13}\text{C}$  NMR  $\delta$  158.2, 156.0, 136.4, 133.8, 133.0, 132.4, 128.5, 128.3, 128.1, 127.5, 126.3, 85.5, 83.4, 80.7, 64.9, 64.8, 55.2, 52.0, 18.4; IR (neat)  $\nu$  1744  $\text{cm}^{-1}$ ; Anal. Calcd for  $\text{C}_{24}\text{H}_{25}\text{NO}_6$ : C, 68.07; H, 5.95; N, 3.31. Found: C, 67.90; H, 5.88; N, 3.30.

**Allylic carbonate 296b:**  $^1\text{H}$  NMR  $\delta$  7.08 (m, 6H), 6.93 (m, 3H), 6.50 (bs, 1H), 5.83 (d,  $J = 7.5$  Hz, 1H), 5.74 (dt,  $J = 2.1, 5.7$  Hz, 1H), 5.35 (dd,  $J = 2.7, 6.0$  Hz, 1H), 5.31 (d,  $J = 2.4$  Hz, 1H), 5.01 (t,  $J = 1.8$  Hz, 1H), 4.82 (d,  $J = 7.5$  Hz, 1H), 3.89 (s, 3H), 3.43 (s, 3H), 1.46 (s, 3H)  $^{13}\text{C}$  NMR  $\delta$  158.3, 155.3, 136.9, 135.7, 134.1, 131.5, 128.5, 128.4, 128.2, 128.1,

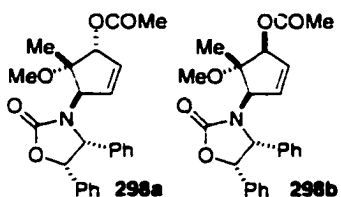
126.3, 86.9, 84.7, 80.8, 64.1, 63.6, 55.4, 51.6, 13.9; IR (neat)  $\nu$  1752  $\text{cm}^{-1}$ ; HRMS  $m/z$  (M+H) calcd for  $\text{C}_{24}\text{H}_{26}\text{NO}_6$  424.1760, found 424.1756. The stereochemistry was assigned on the basis of the following NOE data.



**Allylic ester 297a.** 2,4,6-trichlorobenzoyl chloride (0.10 mL, 0.64 mmol), DMAP (53 mg, 0.43 mmol), triethylamine (0.09 mL, 0.65 mmol), and  $\text{CH}_2\text{Cl}_2$  (3 mL) were combined in a flame dried 10 mL round bottomed flask equipped with a reflux condenser and stir bar.

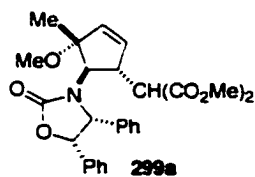
This reaction mixture stirred at room temperature for five min then a mixture 4:1 of allylic alcohols **294a** and **294b** (0.16 g, 0.43 mmol) in  $\text{CH}_2\text{Cl}_2$  (2 mL) was added dropwise. The reaction mixture was heated at reflux overnight then diluted with  $\text{CH}_2\text{Cl}_2$  and water. The layers were separated and the aqueous layer was extracted with  $\text{CH}_2\text{Cl}_2$  (3x). The combined organic layers were washed with brine, dried with  $\text{MgSO}_4$ , filtered and concentrated in vacuo to an oily yellow solid. Flash chromatography with hexane/EtOAc (10/1 to 2/1) gave allylic ester **297a** (0.15 g, 0.26 mmol, 60%) and unreacted **294b** (29 mg, 0.08 mmol, 19%). **Allylic ester 297a:**  $^1\text{H}$  NMR  $\delta$  7.35 (s, 2H), 7.11 (m, 6H), 6.99 (m, 2H), 6.86 (bs, 2H), 5.90 (dd,  $J = 1.7, 3.5$  Hz, 1H), 5.87 (d,  $J = 7.5$  Hz, 1H), 5.84 (dt,  $J = 1.8, 6.3$  Hz, 1H), 5.40 (ddd,  $J = 1.5, 2.7, 6.3$  Hz, 1H), 5.16 (m, 1H), 4.72 (d,  $J = 7.2$  Hz, 1H), 3.37 (s, 3H), 1.65 (s, 3H);  $^{13}\text{C}$  NMR  $\delta$  164.3, 158.3, 136.5, 136.4, 133.8, 133.4, 132.9, 132.1, 128.6, 128.3, 128.1, 126.3, 84.0, 83.6, 80.8, 64.9, 64.8,

51.9, 18.0; IR (neat)  $\nu$  1740  $\text{cm}^{-1}$ ; Anal. Calcd for  $\text{C}_{29}\text{H}_{24}\text{Cl}_3\text{NO}_5$ : C, 60.80; H, 4.22; N, 2.45. Found: C, 60.75; H, 4.28 N, 2.44.



**Allylic acetates 298a, 298b.** A 4:1 mixture of alcohols **294a** and **294b** (0.73 g, 2.0 mmol) and DMAP (0.49 g, 4.0 mmol) were dissolved in  $\text{CH}_2\text{Cl}_2$  (10 mL). Acetyl chloride (0.57 mL, 8.0 mmol) was added slowly and the reaction mixture was stirred overnight at room temperature. The reaction mixture was quenched with 1N HCl and extracted with  $\text{CH}_2\text{Cl}_2$  (3x). The combined organic layers were washed with saturated aqueous  $\text{NaHCO}_3$ , dried with  $\text{MgSO}_4$ , filtered and concentrated. Flash column chromatography with hexane/EtOAc (3/1 to 3/2) gave acetate **298a** (0.62 g, 1.5 mmol, 76%) and acetate **298b** (90 mg, 0.23 mmol, 11%). **Allylic acetate 298a:**  $^1\text{H}$  NMR  $\delta$  6.97 (m, 10H), 5.83 (d,  $J = 6.6$  Hz, 1H), 5.64 (d,  $J = 11.1$ , 2H), 5.29 (bs, 1H), 5.15 (s, 1H), 4.67 (d,  $J = 6.6$  Hz, 1H), 3.38 (s, 3H), 2.12 (s, 3H), 1.55 (s, 3H);  $^{13}\text{C}$  NMR  $\delta$  171.0, 158.1, 136.4, 133.6, 133.0, 132.2, 128.3, 128.1, 127.9, 127.2, 126.1, 83.7, 81.9, 80.7, 64.56, 64.60, 51.9, 21.3, 18.3; IR (neat)  $\nu$  1740  $\text{cm}^{-1}$ ; HRMS  $m/z$  (M+H) calcd for  $\text{C}_{24}\text{H}_{25}\text{NO}_5$  408.1811, found 408.1820. **Allylic acetate 298b:**  $^1\text{H}$  NMR  $\delta$  7.08 (m, 7H), 6.98 (m, 2H), 6.60 (bs, 1H), 5.83 (d,  $J = 7.5$  Hz, 1H), 5.68 (d,  $J = 5.7$  Hz, 1H), 5.48 (d,  $J = 2.4$  Hz, 1H), 5.31 (dd,  $J = 2.4, 5.7$  Hz, 1H), 5.01 (s, 1H), 4.78 (d,  $J = 7.8$  Hz, 1H), 3.41 (s, 3H), 2.20 (s, 3H), 1.41 (s, 3H);  $^{13}\text{C}$  NMR  $\delta$  169.7, 158.0, 136.6, 134.4, 133.8, 131.9, 128.3, 128.2, 128.1, 128.0, 126.1, 87.1, 81.0, 80.8, 64.2, 63.9, 51.5, 21.5, 14.2; IR (neat)  $\nu$  1747  $\text{cm}^{-1}$ ; HRMS  $m/z$  (M+H) calcd for  $\text{C}_{24}\text{H}_{25}\text{NO}_5$  408.1811, found 408.1827.

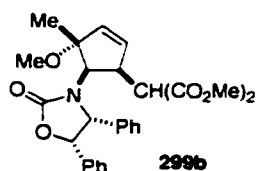
**General Procedure for the Allylic Substitutions. Procedure A:** Allylic carbonate **296a**, **296b** or ester **297a** (0.04 to 0.05 mmol),  $[\eta^3\text{-C}_3\text{H}_5\text{PdCl}]_2$  (5-10%), and the bidentate ligand (15-30%) were combined in a 10 mL Schlenk flask which was purged with Ar for ten min. DMSO or THF (0.4 mL) was added and the reaction mixture stirred at room temperature for 10 min before the nucleophile (1-3 eq.) was added via syringe. After the said amount of time the reaction mixture was diluted with diethyl ether and saturated aqueous  $\text{NH}_4\text{Cl}$ . The layers were separated and the aqueous layer was extracted with ether (3x). The combined organic layers were washed with brine, dried with  $\text{Na}_2\text{SO}_4$ , filtered and concentrated in vacuo. The products were purified with flash column chromatography on silica gel. **Procedure B:** Allylic carbonate **296a** or ester **297a** (0.04 to 0.05 mmol),  $[\eta^3\text{-C}_3\text{H}_5\text{PdCl}]_2$  (5-10%), and dppe or dppf (15-30%) were combined in a 10 mL pressure tube fitted with a septum which was then purged with Ar for ten min. DMSO or THF (0.4 mL) was added and the reaction mixture was shaken so that everything dissolved, then allowed to stand at room temperature for 10 min before the nucleophile (1-3 eq) was added via syringe. The pressure tube was sealed with a Teflon plug and placed in the center of the microwave in a large beaker and irradiated for the said amount of time. The pressure tube was then immediately placed in a beaker containing cold water to stop the reaction, then the reaction was worked following the protocol of **Procedure A**.



**Dimethyl malonate addition product 299a. Procedure A**

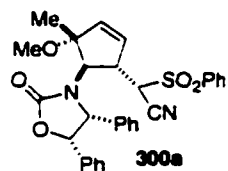
**(dppe/DMSO):** From 20 mg (0.05 mmol) allylic carbonate **296a**,  $[\eta^3\text{-C}_3\text{H}_5\text{PdCl}]_2$  (6%), dppe (16%), dimethyl sodiomalonate (0.14

mmol) in DMSO at room temperature for 0.2 h gave **299a** (11 mg, 0.02 mmol, 51%) after column chromatography with hexane/EtOAc (5/1 to 2/1). **Procedure A (dppe/THF):** From 21 mg (0.05 mmol) allylic carbonate **296a**,  $[\eta^3\text{-C}_3\text{H}_5\text{PdCl}]_2$  (5%), dppe (11%), dimethyl sodiomalonate (0.15 mmol) in THF at room temperature for 14 h gave **299a** (12 mg, 0.04 mmol, 49%) and recovered **296a** (4 mg, 0.01 mmol, 21%). **Procedure A (dppp/THF):** From 21 mg (0.05 mmol) allylic carbonate **296a**,  $[\eta^3\text{-C}_3\text{H}_5\text{PdCl}]_2$  (5%), dppp (11%), dimethyl sodiomalonate (0.15 mmol) in THF at room temperature for 14 h gave **299a** (20 mg, 0.04 mmol, 83%), **299b** (1 mg, 0.003 mmol, 5%), and recovered **296a** (1 mg, 0.002 mmol, 4%). **Procedure A (dppb/THF):** From 21 mg (0.05 mmol) allylic carbonate **296a**,  $[\eta^3\text{-C}_3\text{H}_5\text{PdCl}]_2$  (5%), dppb (11%), dimethyl sodiomalonate (0.15 mmol) in THF at room temperature for 14 h gave **299a** (20 mg, 0.04 mmol, 82%) and **299b** (4 mg, 0.009 mmol, 17%). **Procedure A (dppf/THF):** From 21 mg (0.05 mmol) allylic carbonate **296a**,  $[\eta^3\text{-C}_3\text{H}_5\text{PdCl}]_2$  (5%), dppf (11%), dimethyl sodiomalonate (0.15 mmol) in THF at room temperature for 14 h gave **299a** (22 mg, 0.05 mmol, 92%) and **299b** (2 mg, 0.004 mmol, 7%). **Dimethyl malonate addition product 299a.**  $^1\text{H NMR}$   $\delta$  6.94–7.14 (m, 10H), 5.91 (d,  $J = 8.1$  Hz, 1H), 5.78 (m, 2H), 5.04 (d,  $J = 7.5$  Hz, 1H), 4.48 (bs, 1H), 3.71 (s, 3H), 3.58 (s, 3H), 3.50 (bs, 1H), 3.30 (bs, 1H), 3.01 (bs, 3H), 1.47 (s, 3H);  $^{13}\text{C NMR}$   $\delta$  168.6, 168.5, 158.2, 136.6, 135.9, 134.6, 132.3, 128.6, 128.4, 128.1, 128.0, 126.1, 89.1, 80.1, 66.2, 60.5, 52.8, 52.7, 52.6, 50.6, 43.5, 21.7; IR (neat)  $\nu$  1748  $\text{cm}^{-1}$ ; HRMS  $m/z$  ( $\text{M}+\text{H}$ ) calcd for  $\text{C}_{27}\text{H}_{30}\text{NO}_7$  480.2022, found 480.2004



**Dimethyl malonate addition product 299b. Procedure A:** From

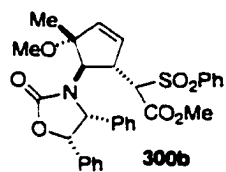
20 mg (0.05 mmol) allylic carbonate **296b**,  $[\eta^3\text{-C}_3\text{H}_5\text{PdCl}]_2$  (6%), dppf (15%), dimethyl sodiomalonate (0.16 mmol) in THF at room temperature for 2h gave **299b** (19 mg, 0.04 mmol, 88%) after column chromatography with hexane/EtOAc (3/1).  $^1\text{H NMR}$   $\delta$  7.10 (m, 7H), 6.99 (m, 2H), 6.89 (bs, 1H), 5.82 (d,  $J = 7.2$  Hz, 1H), 5.60 (dt,  $J = 2.2, 6.0$  Hz, 1H), 5.13 (d,  $J = 1.6$  Hz, 1H), 5.05 (dt,  $J = 2.0, 6.2$  Hz, 1H), 4.79 (d,  $J = 7.2$  Hz, 1H), 3.81 (s, 3H), 3.76 (s, 3H), 3.56 (m, 1H), 3.51 (m, 1H), 3.42 (s, 3H), 1.38 (s, 3H);  $^{13}\text{C NMR}$   $\delta$  168.8, 168.7, 158.4, 136.7, 133.9, 133.7, 128.5, 128.4, 128.2, 128.1, 126.4, 89.6, 80.8, 64.9, 64.4, 53.2, 52.9, 52.5, 50.8, 49.7, 16.0; IR (neat)  $\nu$  1751  $\text{cm}^{-1}$ ; HRMS  $m/z$  (M+H) calcd for  $\text{C}_{27}\text{H}_{30}\text{NO}_7$  480.2022, found 480.2008.



**(Phenylsulfonyl)acetonitrile addition product 300a. Procedure A:**

From 21 mg (0.05 mmol) allylic carbonate **296a**,  $[\eta^3\text{-C}_3\text{H}_5\text{PdCl}]_2$  (5%), dppe (12%), sodium (phenylsulfonyl) acetonitrile (0.15 mmol) in THF at room temperature for 5 h gave **300a** as inseparable 2:1 mixture of diastereomers (23 mg, 0.04 mmol, 86%) after column chromatography with hexane/EtOAc (2/1). The product ratio was determined by integration of the methoxy methyl resonances in the  $^1\text{H NMR}$  spectrum: Major isomer, 3.26 (s); Minor isomer, 2.75 (s). Major isomer:  $^1\text{H NMR}$   $\delta$  7.74 (m, 3H), 7.61 (m, 2H), 7.1-7.3 (m, 6H), 6.99 (m, 4H), 6.08 (s, 2H), 5.94 (d,  $J = 7.2$  Hz, 1H), 5.05 (d,  $J = 7.5$  Hz, 1H), 4.78 (d,  $J = 7.8$  Hz, 1H), 3.74 (d,  $J = 4.5$  Hz, 1H), 3.60 (dd,  $J = 3.9, 7.5$  Hz, 1H), 3.26 (s, 3H), 1.56 (s, 3H), 1.51 (s, 3H). Minor isomer:  $^1\text{H NMR}$   $\delta$  8.08 (d,  $J = 7.2$  Hz, 2H), 7.75 (m, 3H), 7.01-7.27 (m, 10H), 6.08 (s, 1H), 5.93 (d,  $J = 7.6$

Hz, 1H), 5.72 (d,  $J = 6.0$  Hz, 1H), 5.32 (d,  $J = 8.4$  Hz, 1H), 4.67 (bs, 1H), 4.19 (d,  $J = 5.2$  Hz, 2H), 2.75 (s, 3H), 1.38 (s, 3H); IR (neat)  $\nu$  1747  $\text{cm}^{-1}$ ; HRMS  $m/z$  (M+H) calcd for  $\text{C}_{30}\text{H}_{29}\text{N}_2\text{O}_5\text{S}$  529.1797, found 529.1781.



**Methyl phenylsulfonylacetate addition product 300b. Procedure**

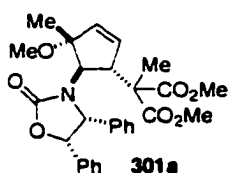
**A (dppe, DMSO):** From 20 mg (0.05 mmol) allylic carbonate **296a**,  $[\eta^3\text{-C}_3\text{H}_5\text{PdCl}]_2$  (5%), dppe (15%), sodium methyl phenylsulfonylacetate (0.15 mmol) in DMSO at 70 °C for 14 h gave **300b** as an inseparable 1:1 mixture of diastereomers (7 mg, 0.01 mmol, 27%) after column chromatography with hexane/EtOAc (6/1 to 3/1). The product ratio was determined by integration of the methoxy methyl resonances in the  $^1\text{H}$  NMR spectrum: 3.58 (s); 3.52 (s).

**Procedure A (dppf, THF):** From 21 mg (0.05 mmol) allylic carbonate **296a**,  $[\eta^3\text{-C}_3\text{H}_5\text{PdCl}]_2$  (6%), dppe (19%), sodium methyl phenylsulfonylacetate (0.14 mmol) in THF at room temperature for 48 h gave **300b** as a 1:1 mixture of diastereomers (16 mg, 0.03 mmol, 57%) and recovered **296a** (4 mg, 0.01 mmol, 20%).

**Procedure B (dppe, DMSO):** From 20 mg (0.05 mmol) allylic carbonate **296a**,  $[\eta^3\text{-C}_3\text{H}_5\text{PdCl}]_2$  (7%), dppe (15%), sodium methyl phenylsulfonylacetate (0.14 mmol) in DMSO and irradiating for 3 min at 210 W gave **300b** as a 1:1 mixture of diastereomers (12 mg, 0.02 mmol, 46%).

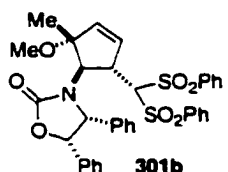
**Procedure B (dppf, THF):** From 21 mg (0.05 mmol) allylic carbonate **296a**,  $[\eta^3\text{-C}_3\text{H}_5\text{PdCl}]_2$  (5%), dppf (10%), sodium methyl phenylsulfonylacetate (0.14 mmol) in THF and irradiating for 3 x 3 min at 210 W gave **300b** as a 1:1 mixture of diastereomers (12 mg, 0.02 mmol, 43%) and recovered **296a** (10 mg, 0.02 mmol, 50%).  $^1\text{H}$  NMR  $\delta$  7.82 (d,  $J = 7.5$  Hz), 7.71 (m), 7.56 (m), 6.92-7.17 (m), 5.8-6.0 (m), 5.14 (m), 5.06 (m), 4.46 (m),

4.15 (d,  $J = 7.2$  Hz), 3.97 (d,  $J = 6.6$  Hz), 3.78 (m), 3.45-3.68 (m), 3.34 (m), 2.95 (m), 1.60 (bs), 1.44 (m); IR (neat)  $\nu$  1747  $\text{cm}^{-1}$ ; HRMS  $m/z$  (M+H) calcd for  $\text{C}_{31}\text{H}_{32}\text{NO}_7\text{S}$  562.1900, found 562.1881.



**Dimethyl methylmalonate addition product 301a. Procedure A .**

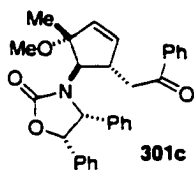
From 20 mg (0.05 mmol) allylic carbonate **296a**,  $[\eta^3\text{-C}_3\text{H}_5\text{PdCl}]_2$  (5%), dppe (15%), sodium dimethyl methylmalonate anion (0.14 mmol) in DMSO at room temperature for 0.2 h **301a** (13 mg, 0.03 mmol, 55%) after column chromatography with hexane/EtOAc (6/1 to 3/1). Several attempts to remove an unidentified impurity were unsuccessful.  $^1\text{H}$  NMR  $\delta$  7.07 (m, 10H), 5.90 (d,  $J = 9.3$  Hz, 1H), 5.75 (dd,  $J = 1.5, 6.3$  Hz, 1H), 5.67 (dd,  $J = 2.1, 6.0$  Hz, 1H), 5.02 (d,  $J = 8.7$  Hz, 1H), 4.69 (dt,  $J = 1.8, 7.5$  Hz, 1H), 3.82 (s, 3H), 3.79 (s, 3H), 3.63 (d,  $J = 8.1$  Hz, 1H), 2.40 (s, 3H), 1.37 (s, 3H).



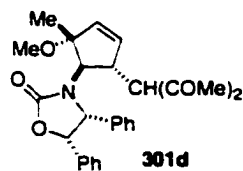
**Bis(phenylsulfonyl)methane addition product 301b. Procedure A:**

From 30 mg (0.07 mmol) allylic carbonate **296a**,  $[\eta^3\text{-C}_3\text{H}_5\text{PdCl}]_2$  (5%), dppe (14%), sodium bis(phenylsulfonyl) methane anion (0.20 mmol) in DMSO at 100  $^\circ\text{C}$  for 12 h gave **301b** (10 mg, 0.02 mmol, 21%) after column chromatography with hexane/EtOAc (3/1 to 1/1).  $^1\text{H}$  NMR  $\delta$  7.88 (d,  $J = 9.6$  Hz, 2H), 7.80 (m, 2H), 7.71 (m, 2H), 7.57 (m, 4H), 7.11 (m, 5H), 7.02 (m, 5H), 5.98 (d,  $J = 8.4$  Hz, 1H), 5.72 (s, 2H), 5.46 (d,  $J = 8.7$  Hz, 1H), 4.99 (d,  $J = 8.4$  Hz, 1H), 4.65 (m, 2 H), 2.76 (s, 3H), 1.42 (s, 3H);  $^{13}\text{C}$  NMR  $\delta$  158.2, 139.3, 139.2, 136.6, 135.3, 135.0, 134.9, 130.0, 129.6, 129.5, 129.4, 129.3, 128.7, 128.1, 128.0, 127.9, 126.2, 88.9, 83.4, 80.0,

68.0, 61.1, 50.9, 41.3, 22.4; IR (neat)  $\nu$  1749, 2360  $\text{cm}^{-1}$ ; HRMS  $m/z$  (M+H) calcd for  $\text{C}_{35}\text{H}_{34}\text{NO}_7\text{S}_2$  644.1777, found 644.1767.

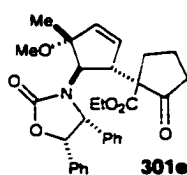


**Acetophenone addition product 301c. Procedure A.** From 20 mg (0.05 mmol) allylic carbonate **296a**,  $[\eta^3\text{-C}_3\text{H}_5\text{PdCl}]_2$  (5%), dppe (19%), lithium enolate of acetophenone (0.07 mmol) in DMSO at room temperature for 5 h gave **301c** (10 mg, 0.02 mmol, 44%) after column chromatography with hexane/EtOAc (2/1).  $^1\text{H}$  NMR  $\delta$  7.68 (d,  $J = 8.1$  Hz, 2H), 7.53 (m, 1H), 7.40 (t,  $J = 7.8$  Hz, 2H), 7.04 (m, 7H), 6.91 (t,  $J = 7.5$  Hz, 2H), 6.79 (m, 1H), 5.95 (d,  $J = 7.2$  Hz, 1H), 5.77 (m, 2H), 5.04 (d,  $J = 7.2$  Hz, 1H), 4.44 (d,  $J = 7.5$  Hz, 1H), 3.28 (s, 3H), 3.14 (m, 1H), 2.76 (d,  $J = 6.6$  Hz, 2H), 1.51 (s, 3H);  $^{13}\text{C}$  NMR  $\delta$  176.7, 158.7, 136.6, 136.3, 135.1, 134.9, 134.3, 133.3, 128.6, 128.4, 128.1, 128.0, 126.1, 89.3, 80.6, 65.4, 62.6, 51.0, 42.3, 40.2, 21.4; IR (neat)  $\nu$  1746, 1684  $\text{cm}^{-1}$ ; HRMS  $m/z$  (M+H) calcd for  $\text{C}_{30}\text{H}_{30}\text{NO}_4$  468.2175, found 468.2195.



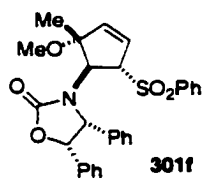
**Acetylacetonone addition product 301d. Procedure A:** From 19 mg (0.05 mmol) allylic carbonate **296a**,  $[\eta^3\text{-C}_3\text{H}_5\text{PdCl}]_2$  (5%), dppe (18%), sodium enolate of acetylacetonone (0.14 mmol) in DMSO at room temperature to 60  $^\circ\text{C}$  over 24 h gave **301d** (7 mg, 0.02 mmol, 33%) and recovered **296a** (4 mg, 0.01 mmol, 23%) after column chromatography with hexane/EtOAc (2/1).  $^1\text{H}$  NMR  $\delta$  7.10 (m, 6H), 7.03 (m, 4H), 5.89 (d,  $J = 7.6$  Hz, 1H), 5.81 (d,  $J = 6.0$  Hz, 1H), 5.69 (dd,  $J = 1.8, 6.2$  Hz, 1H), 4.90 (d,  $J = 7.6$  Hz, 1H); 4.07 (bs, 1H), 3.58 (d,  $J = 6.4$  Hz, 2H), 2.97 (bs, 3H), 2.13 (s, 3H), 1.93 (bs, 3H), 1.41 (s, 3H);  $^{13}\text{C}$  NMR  $\delta$  203.7, 203.0,

158.2, 136.5, 136.0, 134.5, 133.2, 128.9, 128.6, 128.4, 128.1, 128.0, 126.1, 88.9, 80.2, 70.5, 66.1, 62.1, 50.6, 44.3, 31.3, 29.6, 20.3; IR (neat)  $\nu$  1750, 1699  $\text{cm}^{-1}$ ; HRMS  $m/z$  (M+H) calcd for  $\text{C}_{27}\text{H}_{30}\text{NO}_5$  448.2124, found 448.2118.



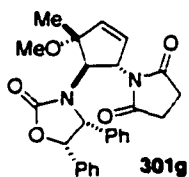
**Ethyl 2-oxocyclopentanecarboxylate addition product 301e.**

**Procedure A.** From 20 mg (0.05 mmol) allylic carbonate **296a**,  $[\eta^3\text{-C}_3\text{H}_5\text{PdCl}]_2$  (5%), dppe (16%), sodium ethyl 2-oxocyclopentanecarboxylate anion (0.13 mmol) in DMSO at 70 °C for 12 h gave **301e** (10 mg, 0.02 mmol, 41%) as an inseparable mixture of diastereomers after column chromatography with hexane/EtOAc (3/1).  $^1\text{H}$  NMR of mixture  $\delta$  7.05 (m), 5.99 (dd,  $J = 1.8, 6.3$  Hz), 5.7 (m), 5.71 (d,  $J = 2.1, 6.3$  Hz), 6.68 (m), 5.52 (m), 5.10 (d,  $J = 9.0$  Hz), 4.64 (d,  $J = 7.2$  Hz), 4.2–4.4 (m), 3.91 (m), 3.69 (d,  $J = 6.3$  Hz), 3.23 (s), 3.21 (s), 2.60 (m), 2.53 (s), 2.45 (s), 1.84–2.35 (m), 1.23–1.44 (m); IR (neat)  $\nu$  1752  $\text{cm}^{-1}$ ; HRMS  $m/z$  (M+H) calcd for  $\text{C}_{30}\text{H}_{33}\text{NO}_6$  503.2308, found 503.2310.

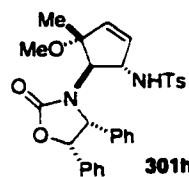


**Benzenesulfinic acid addition product 301f. Procedure A:** From 20 mg (0.05 mmol) allylic carbonate **296a**,  $[\eta^3\text{-C}_3\text{H}_5\text{PdCl}]_2$  (7%), dppe (14%), sodium benzenesulfinate (0.14 mmol) in DMSO at 60 °C for 0.5 h gave **301f** (15 mg, 0.03 mmol, 64%) after column chromatography with hexane/EtOAc (3/1).  $^1\text{H}$  NMR  $\delta$  7.89 (d,  $J = 7.2$  Hz, 2H), 7.67 (m, 1H), 7.56 (m, 2H), 7.15 (m, 6H), 6.97 (m, 4H), 5.84 (dd,  $J = 1.8, 6.3$  Hz, 1H), 5.76 (d,  $J = 8.4$  Hz, 1H), 5.67 (dd,  $J = 1.8, 6.0$  Hz, 1H), 5.60 (m, 1H), 5.51 (bs, 1H), 4.00 (m, 1H), 2.24 (bs, 3H), 1.46 (s, 3H);  $^{13}\text{C}$  NMR  $\delta$  158.5, 141.6, 137.1, 135.3, 134.4, 133.1, 129.8, 129.6, 129.2, 129.0, 128.2,

128.1, 128.0, 126.3, 125.3, 90.1, 79.7, 69.0, 67.8, 57.6, 50.1, 22.9; IR (neat)  $\nu$  1755  $\text{cm}^{-1}$ ;  
Anal. Calcd for  $\text{C}_{28}\text{H}_{27}\text{NO}_5\text{S}$ : C, 68.69; H, 5.56; N, 2.86. Found: C, 68.69; H, 5.32 N,  
2.87.

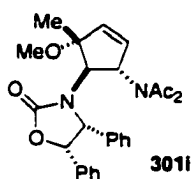


**Succinimide addition product 301g. Procedure A:** From 20 mg (0.03 mmol) allylic ester **297a**,  $[\eta^3\text{-C}_3\text{H}_5\text{PdCl}]_2$  (10%), dppe (32%), sodium succinimide anion (0.08 mmol) in DMSO at 70-120  $^\circ\text{C}$  for 48 h gave **301g** (1 mg, 0.003 mmol, 8%) and recovered **297a** (4 mg, 0.01 mmol, 20%) after column chromatography with hexane/EtOAc (6/1 to 3/1). **Procedure B:** From 27 mg (0.05 mmol) allylic ester **297a**,  $[\eta^3\text{-C}_3\text{H}_5\text{PdCl}]_2$  (7%), dppe (16%), sodium succinimide (0.01 mmol) in DMSO and irradiating for 2 min at 210 W gave **301g** (6 mg, 0.01 mmol, 29%).  
 $^1\text{H}$  NMR  $\delta$  7.09 (m, 6H), 6.92 (m, 2H), 6.85(m, 2H), 5.96 (dd,  $J = 2.4, 6.4$  Hz, 1H), 5.83 (d,  $J = 7.2$  Hz, 1H), 5.73 (d,  $J = 8.8$  Hz, 1H), 5.55 (dd,  $J = 1.8, 6.2$  Hz, 1H), 5.19 (dt,  $J = 1.8, 8.4$  Hz, 1H), 4.99 (d,  $J = 7.6$  Hz, 1H), 3.27 (s, 3H), 2.3-2.5 (m, 4H), 1.49 (s, 3H);  $^{13}\text{C}$  NMR  $\delta$  176.9, 176.5, 158.2, 138.2, 135.0, 134.1, 129.6, 128.8, 128.3, 128.13, 128.08, 126.3, 88.0, 80.8, 66.3, 57.4, 55.2, 51.4, 27.9(2C), 22.5; IR (neat)  $\nu$  1750, 1703  $\text{cm}^{-1}$ ;  
HRMS  $m/z$  ( $\text{M}+\text{H}$ ) calcd for  $\text{C}_{26}\text{H}_{27}\text{N}_2\text{O}_5$  447.1920, found 447.1909.

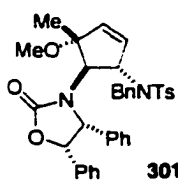


***p*-Toluenesulfonamide addition product 301h.** From 31 mg (0.06 mmol) allylic ester **297a**,  $[\eta^3\text{-C}_3\text{H}_5\text{PdCl}]_2$  (6%), dppe (16%), sodium *p*-toluenesulfonamide anion (0.17 mmol) in DMSO at 70  $^\circ\text{C}$  for 12 h gave **301h** (17 mg, 0.03 mmol, 62%) after column chromatography with hexane/EtOAc (4/1).  
 $^1\text{H}$  NMR  $\delta$  7.80 (d,  $J = 8.4$  Hz, 2H), 7.36 (d,  $J = 8.4$  Hz, 1H), 7.11 (m, 6H), 6.97(m, 4H),

5.84 (d,  $J = 8.4$  Hz, 1H), 5.77 (dd,  $J = 1.6, 6.0$  Hz, 1H), 5.43 (dd,  $J = 1.8, 6.2$  Hz, 1H), 5.28 (d,  $J = 8.8$  Hz, 1H), 5.07 (bt, 8.07.2 Hz, 1H), 4.80 (d,  $J = 8.8$  Hz, 1H), 3.66 (d,  $J = 6.0$  Hz, 1H), 2.60 (s, 3H), 2.45 (s, 3H), 1.43 (s, 3H);  $^{13}\text{C}$  NMR  $\delta$  158.4, 144.1, 139.0, 137.3, 135.4, 134.6, 131.0, 130.2, 130.0, 129.2, 128.8, 128.1, 128.0, 127.5, 126.3, 87.2, 79.7, 68.8, 67.3, 56.5, 50.1, 21.8, 21.5; IR (neat)  $\nu$  3259, 1738  $\text{cm}^{-1}$ ; HRMS  $m/z$  (M+H) calcd for  $\text{C}_{29}\text{H}_{31}\text{N}_2\text{O}_5\text{S}$  519.1954, found 519.1935.

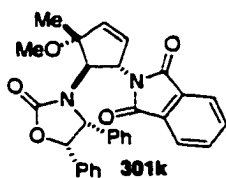


**Diaceamide addition product 301i. Procedure A:** From 20 mg (0.03 mmol) allylic ester **297a**,  $[\eta^3\text{-C}_3\text{H}_5\text{PdCl}]_2$  (6%), dppe (16%), sodium diacetamide anion (0.07 mmol) in DMSO at 70 °C for 48 h gave **301i** (1 mg, 0.001 mmol, 3%) after column chromatography with hexane/EtOAc (6/1 to 1/1). **Procedure B (dppe, DMSO):** From 20 mg (0.04 mmol) allylic ester **297a**,  $[\eta^3\text{-C}_3\text{H}_5\text{PdCl}]_2$  (5%), dppe (10%), sodium diacetamide anion (0.10 mmol) in DMSO and irradiating for 2 min at 210 W gave **301i** (7 mg, 0.02 mmol, 46%). **Procedure B (dppf, THF):** From 20 mg (0.03 mmol) allylic ester **297a**,  $[\eta^3\text{-C}_3\text{H}_5\text{PdCl}]_2$  (10%), dppf (33%), sodium diacetamide anion (0.07 mmol) in THF and irradiating for 6 min at 210 W gave **301i** (4 mg, 0.01 mmol, 24%).  $^1\text{H}$  NMR  $\delta$  7.24 (bs, 1H), 7.09 (m, 6H), 7.03(m, 2H), 6.74 (bs, 1H), 5.79 (d,  $J = 7.2$  Hz, 1H), 5.50 (dt,  $J = 2.4, 6.0$  Hz, 1H), 5.40 (d,  $J = 7.2$  Hz, 1H), 5.01 (s, 1H), 4.96 (dt,  $J = 2.4, 6.4$  Hz, 1H), 4.77 (t,  $J = 2.4$  Hz, 1H), 3.54 (s, 3H), 2.47 (s, 6H), 1.36 (s, 3H);  $^{13}\text{C}$  NMR  $\delta$  175.2 (2C), 158.4, 137.9, 134.2, 132.4, 128.4, 128.0, 126.4, 90.6, 81.1, 73.9, 65.6, 63.4, 51.4, 15.3; IR (neat)  $\nu$  1736, 1688  $\text{cm}^{-1}$ ; HRMS  $m/z$  (M+H) calcd for  $\text{C}_{26}\text{H}_{29}\text{N}_2\text{O}_5$  449.2076, found 449.2057.



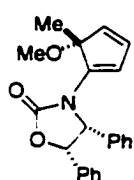
**Benzyl toluenesulfonamide addition product 301j. Procedure A:**

From 20 mg (0.03 mmol) allylic ester **297a**,  $[\eta^3\text{-C}_3\text{H}_5\text{PdCl}]_2$  (10%), dppe (30%), sodium benzyl toluenesulfonamide anion (0.07 mmol) in DMSO at 40-90 °C for 36 h gave **301j** (1 mg, 0.002 mmol, 4%) after column chromatography with hexane/EtOAc (15/1 to 3/1). **Procedure B (dppe, DMSO):** From 20 mg (0.04 mmol) allylic ester **297a**,  $[\eta^3\text{-C}_3\text{H}_5\text{PdCl}]_2$  (9%), dppe (20%), sodium benzyl toluenesulfonamide anion (0.11 mmol) in DMSO and irradiating for 5 min at 210 W gave **301j** (8 mg, 0.01 mmol, 37%). **Procedure B (dppf, THF):** From 21 mg (0.04 mmol) allylic ester **297a**,  $[\eta^3\text{-C}_3\text{H}_5\text{PdCl}]_2$  (10%), dppf (31%), sodium benzyl toluenesulfonamide anion (0.07 mmol) in THF (0.75 mL) and irradiating for 6 min at 210 W gave **301j** (19 mg, 0.03 mmol, 86%).  $^1\text{H NMR}$   $\delta$  7.82 (d,  $J = 8.4$  Hz, 2H), 7.37 (m, 3H), 7.24 (m, 4H), 7.03 (m, 8H), 6.80 (dd,  $J = 1.3, 8.1$  Hz, 2H), 5.91 (d,  $J = 7.5$  Hz, 1H), 5.87 (d,  $J = 9.3$  Hz, 1H), 5.70 (dd,  $J = 2.3, 6.2$  Hz, 1H), 5.39 (dd,  $J = 1.8, 6.3$  Hz, 1H), 4.97 (d,  $J = 9.0$  Hz, 1H), 4.85 (d,  $J = 15.9$  Hz, 1H), 4.04 (d,  $J = 16.2$  Hz, 1H), 3.46 (d,  $J = 6.9$  Hz, 1H), 2.46 (s, 3H), 2.02 (s, 3H), 1.39 (s, 3H);  $^{13}\text{C NMR}$   $\delta$  158.2, 143.9, 139.9, 139.8, 138.6, 137.0, 135.8, 134.6, 130.2, 129.21, 129.15, 129.0, 128.42, 128.36, 128.0, 127.9, 127.8, 127.7, 127.6, 126.2, 86.5, 79.5, 69.5, 64.5, 60.3, 49.7, 49.0, 22.8, 21.8; IR (neat)  $\nu$  1753  $\text{cm}^{-1}$ ; Anal. Calcd for  $\text{C}_{36}\text{H}_{36}\text{N}_2\text{O}_5\text{S}$ : C, 71.03; H, 5.96; N, 4.60. Found: C, 71.17; H, 5.85 N, 4.55.

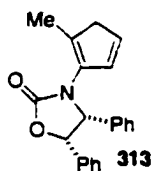


**Phthalimide addition product 301k. Procedure B:** From 20 mg (0.04 mmol) allylic ester **297a**,  $[\eta^3\text{-C}_3\text{H}_5\text{PdCl}]_2$  (10%), dppe (20%), potassium phthalimide (0.08 mmol) in DMSO and irradiating for 5

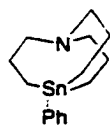
min at 210 W gave **301k** (11 mg, 0.02 mmol, 63%) after column chromatography with hexane/EtOAc (3/1 to 1/1).  $^1\text{H NMR}$   $\delta$  7.73 (s, 4H), 7.07 (m, 6H), 6.92 (m, 2H), 6.80 (m, 2H), 5.98 (dd,  $J = 2.0, 6.4$  Hz, 1H), 5.81 (d,  $J = 7.2$  Hz, 1H), 5.70 (dd,  $J = 1.6, 6.4$  Hz, 1H), 5.65 (d,  $J = 8.4$  Hz, 1H), 5.44 (d,  $J = 8.8$  Hz, 1H), 5.01 (d,  $J = 7.6$  Hz, 1H), 3.25 (s, 3H), 1.55 (s, 3H);  $^{13}\text{C NMR}$   $\delta$  167.7 (2C), 158.2, 137.9, 134.5, 134.3, 131.9, 130.4, 128.5, 128.1, 128.0, 126.3, 123.5, 87.8, 80.6, 66.8, 58.8, 53.9, 51.2, 22.7; IR (neat)  $\nu$  1749, 1712  $\text{cm}^{-1}$ ; HRMS  $m/z$  (M+H) calcd for  $\text{C}_{30}\text{H}_{27}\text{N}_2\text{O}_5$  495.1920, found 495.1914.



**Diene 303.**  $^1\text{H NMR}$   $\delta$  7.11 (m, 7H), 6.98 (m, 2H), 6.80 (m, 2H), 6.62 (d,  $J = 1.5$  Hz, 1H), 6.28 (m, 1H), 5.92 (d,  $J = 7.5$  Hz, 1H), 5.70 (d,  $J = 7.5$  Hz, 1H), 5.61 (d,  $J = 5.7$  Hz, 1H), 3.26 (s, 3H), 1.02 (s, 3H);  $^{13}\text{C NMR}$   $\delta$  155.7, 142.7, 135.8, 134.9, 134.0, 133.7, 131.3, 130.9, 128.5, 128.23, 128.17, 126.9, 126.6, 117.7, 89.3, 81.2, 64.1, 53.1, 22.3; IR (neat)  $\nu$  1758  $\text{cm}^{-1}$ .



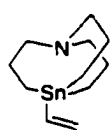
**Diene 313.** The cyclopentadiene was isolated as a mixture of olefinic isomers.  $^1\text{H NMR}$   $\delta$  7.07 (m, 6H), 7.02 (m, 2H), 6.90 (m, 4H), 5.9-6.3 (m, 3H), 5.39 (m, 1H), 2.7-3.1 (m, 2H), 2.05 (m, 3H); HRMS  $m/z$  (M+H) calcd for  $\text{C}_{21}\text{H}_{19}\text{NO}_2$  317.1416, found 317.1417.



**318a**

**Phenyl stannatrane 318a.** Phenyllithium (2.06 mmol) was added slowly to a suspension of stannatrane chloride **317** (0.20 g, 0.68 mmol) in THF (8 mL) at  $-78$   $^{\circ}\text{C}$ . After the final addition the reaction mixture stirred at  $-78$   $^{\circ}\text{C}$  for 2 h then was poured into a mixture of hexanes/water (3 mL each). The layers were separated

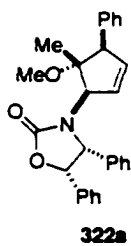
and the organic layer was washed with brine, dried with  $\text{Na}_2\text{SO}_4$ , filtered, and concentrated to give **318a** (0.11 g, 0.33 mmol, 49%) and biphenyl as a light yellow oil. The mixture was used without further purification. Distillation and chromatography on silica gel or deactivated basic alumina led to no separation in the former case and decomposition in the latter.  $^1\text{H}$  NMR (for methylene protons only) ( $\text{C}_6\text{D}_6$ )  $\delta$  2.02 (t,  $J$  = 5.8 Hz, 6H), 1.51 (m, 6H), 0.88 (t,  $J$  = 6.8 Hz, 6H);  $^{13}\text{C}$  NMR (for methylene carbons only)  $\delta$  54.9, 23.5, 7.0.



**Vinyl stannatrane 318b.** Vinyl lithium (0.68 mmol) was added slowly to a suspension of stannatrane chloride **317** (0.10 g, 0.34 mmol) in THF (4 mL) at  $-78$  °C. After the final addition the reaction mixture stirred at  $-78$  °C for 6 h then was poured into a mixture of hexanes/water (3 mL each). The layers were separated and the organic layer was washed with brine, dried with  $\text{Na}_2\text{SO}_4$ , filtered and concentrated to give **318b** (57 mg, 0.19 mmol, 56%) and tetrabutylstannane as a light yellow oil. The mixture was used as is and an analytical sample was obtained by distillation.  $^1\text{H}$  NMR ( $\text{C}_6\text{D}_6$ )  $\delta$  6.90 (dd,  $J$  = 10.5, 15.6 Hz, 1H), 6.36 (dd,  $J$  = 3.2, 10.7 Hz, 1H), 5.85 (dd,  $J$  = 3.0, 15.6 Hz, 1H), 2.00 (t,  $J$  = 4.2 Hz, 6H), 1.47 (m, 6H), 0.79 (t,  $J$  = 5.0 Hz, 6H);  $^{13}\text{C}$  NMR  $\delta$  151.3, 130.6, 55.0, 23.8, 7.2.

**General Procedure for Allylic Substitutions with Stannatranes.** Allylic carbonate **296a** (0.04 to 0.09 mmol),  $[\eta^3\text{-C}_3\text{H}_5\text{PdCl}]_2$  (2-3%), and  $\text{P}(\text{furyl})_3$  (13-14%) were combined in the reaction flask and purged with Ar for ten min. DMPU (0.2 mL) was added and the reaction mixture stirred at room temperature for 10 min before the

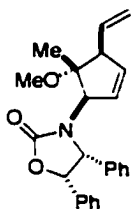
stannatrane (1-3 eq) was added via syringe as a solution in DMPU (0.2 mL). After 6 h a second portion of  $[\eta^3\text{-C}_3\text{H}_5\text{PdCl}]_2$  (2-3%) and  $\text{P}(\text{furyl})_3$  (13-14%) were added. After an additional 6h the reaction mixture was diluted with diethyl ether and water. The layers were separated and the organic layer was washed with brine, dried with  $\text{Na}_2\text{SO}_4$ , filtered and concentrated in vacuo.



**322a**

**Phenyl addition product 322a.** From 30 mg (0.07 mmol) allylic carbonate **296a**,  $[\eta^3\text{-C}_3\text{H}_5\text{PdCl}]_2$  (5%),  $\text{P}(\text{furyl})_3$  (27%), and phenyl stannatrane (0.10 mmol) in DMPU at 60 °C gave **322a** (20 mg, 0.05 mmol, 65%) and recovered **296a** (2 mg, 0.01, 7%) after preparative chromatography with hexane/EtOAc

(3/2).  $^1\text{H NMR}$   $\delta$  7.38 (m, 5H), 7.14 (m, 5H), 7.07 (m, 3H), 6.91 (m, 2H), 5.79 (dt,  $J = 2.1, 6.0$  Hz, 1H), 5.63 (d,  $J = 7.2$  Hz, 1H), 5.28 (bs, 1H), 5.25 (dt,  $J = 2.7, 6.0$  Hz, 1H), 4.61 (d,  $J = 7.5$  Hz, 1H), 4.00 (bs, 1H), 3.53 (s, 3H), 0.99 (s, 3H);  $^{13}\text{C NMR}$   $\delta$  158.3, 140.3, 136.8, 135.3, 133.9, 129.0, 128.6, 128.4, 128.2, 128.0, 127.4, 126.4, 90.6, 80.7, 65.8, 64.2, 59.4, 51.0, 18.3; IR (neat)  $\nu$  1749  $\text{cm}^{-1}$ ; HRMS  $m/z$  (M+H) calcd for  $\text{C}_{28}\text{H}_{28}\text{NO}_3$  426.2069, found 426.2055.

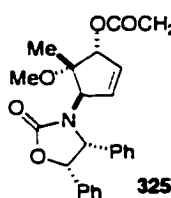


**322b**

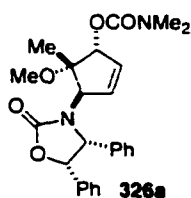
**Vinyl addition product 322b.** From 39 mg (0.09 mmol) allylic carbonate **296a**,  $[\eta^3\text{-C}_3\text{H}_5\text{PdCl}]_2$  (6%),  $\text{P}(\text{furyl})_3$  (28%), and vinyl stannatrane (0.14 mmol) in DMPU at 60 °C gave **322b** (17 mg, 0.05 mmol, 49%) and recovered **296a** (6 mg, 0.02 mmol, 16%) after preparative chromatography with

hexane/EtOAc (3/2).  $^1\text{H NMR}$   $\delta$  7.10 (m, 6H), 6.96 (m, 3H), 6.60 (bs, 1H), 5.92 (m, 1H), 5.74 (d,  $J = 7.2$  Hz, 1H), 5.70 (m, 1H), 5.26 (d,  $J = 10.2$  Hz, 1H), 5.07 (m, 2H), 5.01 (d,  $J$

= 17.4 Hz, 1H), 4.60 (d, J = 7.8 Hz, 1H), 3.43 (s, 3H), 3.29 (d, J = 5.4 Hz, 1H), 1.37 (s, 3H);  $^{13}\text{C}$  NMR  $\delta$  158.5, 137.6, 137.0, 135.6, 134.0, 128.4, 128.3, 128.2, 128.2, 128.0, 126.4, 116.8, 88.8, 80.8, 65.5, 64.0, 57.3, 50.9, 16.9; IR (neat)  $\nu$  1747  $\text{cm}^{-1}$ ; HRMS  $m/z$  (M+H) calcd for  $\text{C}_{24}\text{H}_{26}\text{NO}_3$  376.1913, found 376.1912.



**Transesterification product 325.**  $\text{Mo}(t\text{-BuNC})_4\text{Mo}(\text{CO})_2$  then allylic carbonate **296a** (15 mg, 0.04 mmol) in PhMe (0.6 mL) were added to a solution of dimethyl sodiomalonate (0.06 mmol) in PhMe (0.15 mL). The reaction mixture stirred was sealed and heated at 100-120  $^\circ\text{C}$  overnight. The reaction mixture was cooled to room temperature, diluted with ether, washed with 10% aqueous KOH (2x) and brine. The organic layer was dried with  $\text{Na}_2\text{SO}_4$ , filtered and concentrated to an off-white solid. Flash column chromatography with hexane/EtOAc (3/1 to 1/1) gave **325** (7 mg, 0.02 mmol, 44%) as a white solid and recovered carbonate **296a** (5 mg, 34%). **Transesterification product 325.**  $^1\text{H}$  NMR  $\delta$  7.09 (m, 6H), 6.98 (m, 3H), 6.85 (bs, 1H), 5.84 (d, J = 7.2 Hz, 1H), 5.71 (dt, J = 2.0, 6.4 Hz, 1H), 5.66 (d, J = 1.6 Hz, 1H), 5.33 (m, 1H), 5.15 (m, 1H), 4.67 (d, J = 7.6 Hz, 1H), 3.76 (s, 3H), 3.46 (m, 2H), 3.37 (s, 3H), 1.56 (s, 3H);  $^{13}\text{C}$  NMR  $\delta$  167.0, 166.9, 158.3, 136.5, 133.8, 133.1, 132.4, 128.6, 128.3, 128.1, 126.3, 83.8, 82.8, 80.8, 64.82 (2C), 52.8, 52.0, 41.5, 18.2; IR (neat)  $\nu$  1749  $\text{cm}^{-1}$ ; LRMS  $m/z$  (M+H) calcd for  $\text{C}_{26}\text{H}_{28}\text{NO}_7$  466.2, found 466.2.



**Carbamate 326a.** A 4:1 mixture of epimeric alcohols **294a** and **294b** (31 mg, 0.08 mmol) in DMF (0.5 mL) was added to a slurry of NaH (7 mg, 0.17 mmol) in DMF (0.5 mL) at 0 °C in a 10 mL round bottom flask equipped with a bubbler. The reaction stirred for 30 min then the carbamyl chloride (0.03 mL, 0.27 mmol) was added dropwise. The reaction mixture stirred from 0 °C to room temperature over night then at 50 °C for 48 h. The mixture was diluted with diethyl ether and water. The layers were separated and the aqueous layer was extracted with ether (3x). The combined organic layers were dried with MgSO<sub>4</sub>, filtered and concentrated. Flash column chromatography with hexane/EtOAc (3/1 to 1/1) afforded carbamate **326a** (21 mg, 0.05 mmol, 58%) as a white solid. **Carbamate 326a.** <sup>1</sup>H NMR δ 7.07 (m, 7H), 6.97 (m, 2H), 6.80 (bs, 1H), 5.82 (d, J = 7.5 Hz, 1H), 5.72 (d, J = 6.0 Hz, 1H), 5.58 (d, J = 1.8 Hz, 1H), 5.23 (dd, J = 2.1, 6.0 Hz, 1H), 5.17 (s, 1H), 4.66 (d, J = 7.5 Hz, 1H), 3.39 (s, 3H), 2.95 (s, 6H), 1.55 (s, 3H); <sup>13</sup>C NMR δ 158.3, 156.3, 136.6, 134.2, 133.7, 131.3, 128.4, 128.2, 128.1, 128.0, 126.2, 83.8, 82.5, 80.7, 64.6, 64.5, 52.1, 36.8, 36.3, 18.3; IR (neat) ν 1746, 1703 cm<sup>-1</sup>; HRMS *m/z* (M+H) calcd for C<sub>25</sub>H<sub>27</sub>N<sub>2</sub>O<sub>5</sub> 436.1998, found 436.2000.

---

## VI. References

- <sup>1</sup> a) Godleski, S.A. In *Comprehensive Organic Synthesis*; Trost, B.M., Fleming, I., Eds.: Pergamon Press: New York, 1991; Vol. 4, Chapter 3.3; b) Davies, J.A. In *Comprehensive Organometallic Chemistry II*; Wilkinson, B.; Stone, F.G.A.; Abel, E.W., Eds.: Pergamon Press: Oxford, 1995; Vol. 9, p 291; c) Harrington, P.J. In *Comprehensive Organometallic Chemistry II*; Wilkinson, G.; Stone, F.G.A.; Abel, E.W., Eds., Pergamon Press: Oxford, 1995; Vol. 12, p 798; d) Tsuji, J. *Palladium Reagents and Catalysts. Innovations in Organic Synthesis*; John Wiley: Chichester, 1995.
- <sup>2</sup> For review, see: a) Crimmins, M.T. *Tetrahedron* **1998**, *54*, 9229; b) Marquez, V.E. *Adv. Antiviral Drug Design* **1996**, *2*, 89.
- <sup>3</sup> a) Trost, B.M.; Li, L.; Guile, S.D. *J. Am. Chem. Soc.* **1992**, *114*, 8745; b) Evans, C.T.; Roberts, S.M.; Shoberu, K.A.; Sutherland, A.G. *J. Chem. Soc. Perkin Trans. 1*, **1992**, 589; c) Popescu, A.; Hornfeldt, A.-B.; Gronowitz, S.; Johansson, N.G. *Nucleosides and Nucleotides* **1995**, *14*, 1233; d) Saville-Stones, E.A.; Turner, R.M.; Lindell, S.D.; Jennings, N.S.; Head, J.C.; Carver, D.S. *Tetrahedron* **1994**, *50*, 6695; e) Crimmins, M.T.; King, B.W. *J. Org. Chem.* **1996**, *61*, 4192.
- <sup>4</sup> Kiok, S.H.-L.; Lee, C.C.; Shing, T.K.M. *J. Org. Chem.* **2001**, *66*, 7184.
- <sup>5</sup> a) Trost, B.M.; van Vranken, D.L. *Chem. Rev.* **1996**, *96*, 395; b) Trost, B.M. *Acc. Chem. Res.* **1996**, *29*, 355.
- <sup>6</sup> Trost, B.M.; Toste, F.D. *J. Am. Chem. Soc.* **2000**, *122*, 11262.
- <sup>7</sup> Trost, B.M.; Gunzner, J.L. *J. Am. Chem. Soc.* **2001**, *123*, 9449.

- 
- <sup>8</sup> a) Trost, B.M.; Hachiya, I. *J. Am. Chem. Soc.* **1998**, *120*, 1104; b) Trost, B.M.; Hildbrand, S.; Dogra, K. *J. Am. Chem. Soc.* **1999**, *121*, 10416; c) Glorius, F.; Pfaltz, A. *Org. Lett.* **1999**, *1*, 141.
- <sup>9</sup> Lloyd-Jones, G.C.; Pfaltz, A. *Angew. Chem. Int. Ed.* **1995**, *34*, 462.
- <sup>10</sup> Selvakumar, K.; Valentini, M.; Pregosin, P.S. *Organometallics* **1999**, *18*, 4591.
- <sup>11</sup> Hegedus, L.S. *Transition Metals in the Synthesis of Complex Organic Molecules*; University Science Books: Mill Valley, 1994; Chapter 9.
- <sup>12</sup> For a detailed discussion see: Trost, B.M.; Toste, F.D. *J. Am. Chem. Soc.* **1999**, *121*, 4545.
- <sup>13</sup> a) Keinan, E.; Roth, Z. *J. Org. Chem.* **1983**, *48*, 1772; b) Keinan, E.; Sahai, M. *J. Chem. Soc., Chem. Commun.* **1984**, 648.
- <sup>14</sup> a) van Haaren, R.J.; Goubitz, K.; Fraanje, J.; van Strijdonck, G. P. F.; Oevering, H.; Coussens, B.; Reek, J.N.H.; Kamer, P.C.J.; van Leeuwen, P. W. N. M. *Inorg. Chem.* **2001**, *40*, 3363; b) Blacker, A. J.; Clarke, M.L.; Loft, M.S.; Williams, J.M.J. *Org. Lett.* **1999**, *1*, 1969; c) Amatore, C.; Jutland, A.; Barki, M.A.M.; Meyer, G.; Mottier, L. *Eur. J. Inorg. Chem.* **2001**, 873; d) Åkermark, B.; Hansson, S.; Krakenberger, B.; Zetterberg, K.; Vitagliano, A. *Chemica Scripta* **1986**, 525.
- <sup>15</sup> a) Szabo, K.J. *Chem. Soc. Rev.* **2001**, *30*, 136; b) Branchadell, V.; Moreno-Mañas, M.I.; Pajuelo, F.; Pleixats, R. *Organometallics* **1999**, *18*, 4934.
- <sup>16</sup> a) Itami, K.; Koike, T.; Yoshida, J.-i. *J. Am. Chem. Soc.* **2001**, *123*, 6957; b) Kraft, M.E.; Fu, Z.; Procter, M.J.; Wilson, A.M.; Dasse, O.A.; Hirosawa, C. *Pure Appl. Chem.* **1998**, *70*, 1083; c) Farthing, C.N.; Kocovsky, P. *J. Am. Chem. Soc.* **1998**, *120*, 6661.

- 
- <sup>17</sup> a) Takamashi, S.-i.; Mori, K. *Liebigs Ann. Chem.Rec.* **1997**, 825; b) Castaño, A.M.; Ruano, M.; Echavarren, A.M. *Tetrahedron Lett.* **1996**, 37, 6591; c) Farina, V.; Baker, S.R.; Benigni, D.A.; Sapino, C., Jr. *Tetrahedron Lett.* **1988**, 29, 5739; d) Del Valle, L.; Stille, J.K.; Hegedus, L.S. *J. Org. Chem.* **1990**, 55, 3019; e) Fiaud, J.-C.; Legros, J.-Y. *J. Org. Chem.* **1987**, 52, 1907.
- <sup>18</sup> Hoke, M.E.; Brescia, M.-R.; Bogaczyk, S.; DeShong, P.; King, B.; Crimmins, M.T. *J. Org. Chem.* **2002**, 67, 327.
- <sup>19</sup> a) Casado, A.L.; Espinet, P.; Gallego, A.M. *J. Am. Chem. Soc.* **2000**, 122, 11771; b) Casado, A.L.; Espinet, P. *J. Am. Chem. Soc.* **1998**, 120, 8978.
- <sup>20</sup> a) van Haaren, R.J.; Goubitz, K.; Fraanje, J.; van Strijdonck, G.P.F.; Oevering, H.; Coussens, B.; Reek, J.N.H.; Kamer, P.C.J.; van Leeuwen, P.W.N.M. *Inorg. Chem.* **2001**, 40, 3363; b) Kamer, P.C.J.; van Leeuwen, P.W.N.M.; Reek, J.N.H. *Acc. Chem. Res.* **2001**, 34, 895.
- <sup>21</sup> Åkermark, B.; Hansson, S.; Krakenberger, B.; Vitagliano, A.; Zetterberg, K. *Organometallics* **1984**, 3, 679.
- <sup>22</sup> a) Helmchen, G.; Pfaltz, A. *Acc. Chem. Res.* **2000**, 33, 336; b) Pfaltz, A. *Acc. Chem. Res.* **1993**, 26, 339; c) Matt, P.V.; Lloyd-Jones, G.C.; Minidis, A.B.E.; Pfaltz, A.; Macko, L.; Neuburger, M.; Zehnder, M.; Rügger, H.; Pregosin, P.S. *Helv. Chim. Acta.* **1995**, 78, 265.
- <sup>23</sup> Åkermark, B.; Hansson, S.; Krakenberger, B.; Zetterberg, K.; Vitagliano, A. *Chemica Scripta* **1986**, 525.
- <sup>24</sup> Carfagna, C.; Galarina, R.; Linn, K.; Lopez, J.A.; Mealli, C.; Musco, A. *Organometallics* **1993**, 12, 3019.

- 
- <sup>25</sup> Hayashi, T.; Kawatsua, M.; Uozumi, Y. *J. Am. Chem. Soc.* **1998**, *120*, 1681.
- <sup>26</sup> The general trend for the *trans* effect is:  $\text{PR}_3 > \text{Cl} > \text{C}_5\text{H}_5\text{N}$ . For details, see: a) Appleton, T.G.; Clark, H.C.; Manzer, L.E. *Coord. Chem. Rev.* **1973**, *10*, 335; b) Blochl, P.E.; Togni, A. *Organometallics* **1996**, *15*, 4125; c) Ward, T.R. *Organometallics* **1996**, *15*, 2836.
- <sup>27</sup> a) Szabo, K.J. *Chem. Soc. Rev.* **2001**, *30*, 136; b) Branchadell, V.; Moreno-Mañas, M.I.; Pajuelo, F.; Pleixats, R. *Organometallics* **1999**, *18*, 4934.
- <sup>28</sup> a) Trost, B.M.; Lautens, M. *J. Am. Chem. Soc.* **1987**, *109*, 1469; b) Trost, B.M.; Lautens, M. *Tetrahedron* **1987**, *43*, 4817.
- <sup>29</sup> In the palladium-catalyzed reaction, allylic and vinylic silicon substituents often protodesilylate.
- <sup>30</sup> The reactivity is based on the  $\text{pK}_a$  of the nucleophile, which is reflective of the relative stability of the anion.
- <sup>31</sup> Trost, B.M.; Merlic, C.A. *J. Am. Chem. Soc.* **1990**, *112*, 9590.
- <sup>32</sup> Polyalkylation, a common problem with cyano-stabilized anions, was also observed in 38%.
- <sup>33</sup> Regioselectivity depended on the degree of substitution of the  $\pi$ -allyl intermediate.
- <sup>34</sup> Sjogren, M.P.T.; Frisell, H.; Åkermark, B.; Norrby, P.; Eriksson, L.; Vitagliano, A. *Organometallics* **1997**, *16*, 942.
- <sup>35</sup> a) Rubio, A.; Liebeskind, L.S. *J. Am. Chem. Soc.* **1993**, *115*, 891; b) Faller, J.W.; Linebarrier, D. *Organometallics* **1988**, *7*, 1670.
- <sup>36</sup> Dvorák, D.; Starý, I.; Kocovský, P. *J. Am. Chem. Soc.* **1995**, *117*, 6130.

- 
- <sup>37</sup> a) Stary, I.; Kocovský, P. *J. Am. Chem. Soc.* **1989**, *111*, 4981; b) Fiaud, J.-C.; Legros, J.-Y. *J. Org. Chem.* **1987**, *52*, 1907.
- <sup>38</sup> Kocovský, P.; Pour, M. *J. Org. Chem.* **1990**, *55*, 5580.
- <sup>39</sup> Ward, Y.D.; Villanueva, L.A.; Alfred, G.D.; Liebeskind, L.S. *J. Am. Chem. Soc.* **1996**, *118*, 897.
- <sup>40</sup> The hydridotris(1-pyrazoyl)borate ligand (Tp) was required for isolation. For details see: Ward, Y.D.; Villanueva, L.A.; Alfred, G.D.; Payne, S.C.; Semones, M.A.; Liebeskind, L.S. *Organometallics* **1995**, *14*, 4132.
- <sup>41</sup> a) Trost, B.M.; Hung, M.-H. *J. Am. Chem. Soc.* **1983**, *105*, 7757; b) Trost, B.M.; Hung, M.-H. *J. Am. Chem. Soc.* **1984**, *106*, 6837; c) Trost, B.M.; Lautens, M.; Hung, M.-H. *J. Am. Chem. Soc.* **1984**, *106*, 7641; d) Trost, B.M.; Tometzki, G.B.; Hung, M.-H. *J. Am. Chem. Soc.* **1987**, ; e) Lehmann, J.; Lloyd-Jones, G.C. *Tetrahedron* **1995**, *51*, 8863.
- <sup>42</sup> Frisell, H.; Åkermark, B. *Organometallics* **1995**, *14*, 561.
- <sup>43</sup> Evans, P.A.; Nelson, J.D. *J. Am. Chem. Soc.* **1998**, *120*, 5581.
- <sup>44</sup> Evans, P.A.; Robinson, J.E.; Nelson, J.D. *J. Am. Chem. Soc.* **1999**, *121*, 6761; b) Evans, P.A.; Robinson, J.E.; Moffett, K.K. *Org. Lett.* **2001**, *3*, 3269.
- <sup>45</sup> Evans, P.A.; Leahy, D.K. *J. Am. Chem. Soc.* **2000**, *122*, 5012.
- <sup>46</sup> Takeuchi, R.; Kitamura *New J. Chem.* **1998**, 659.
- <sup>47</sup> Evans, P.A.; Kennedy, L.J. *Org. Lett.* **2000**, *2*, 2213.
- <sup>48</sup> Reaction of a series of primary carbonates revealed that as the substitution at the distal terminus increased, the reactivity decreased. This observation supported an S<sub>N</sub>2' versus S<sub>N</sub>2 type displacement.
- <sup>49</sup> Takeuchi, R.; Kashio, M. *J. Am. Chem. Soc.* **1998**, *120*, 8647.

---

<sup>50</sup> Takeuchi, R.; Ue, N.; Tanabe, K.; Yamashita, K.; Shiga *J. Am. Chem. Soc.* **2001**, *123*, 9525.

<sup>51</sup> Sjögren, M.P.T.; Hansson, S.; Åkermark, B.; Vitagliano, A. *Organometallics* **1994**, *13*, 1963; b) Trost, B.M.; Verhoeven, T.R. *J. Am. Chem. Soc.* **1980**, *102*, 4730.

<sup>52</sup> For an example of palladium-catalyzed reaction with retention of (Z)-configuration, see: Sjögren, M.P.T.; Hansson, S.; Åkermark, B.; Vitagliano, A.; *Organometallics* **1994**, *13*, 19963.

<sup>53</sup> Wen, X.; Norling, H.; Hegedus, L.S. *J. Org. Chem.* **2000**, *65*, 2096.

<sup>54</sup> Heileman, M.J.; Hegedus, L.S. *Synthesis* **2001**, 1356.

<sup>55</sup> For a review, see: van Leeuwen, P.W.N.M.; Kramer, P.C.J.; Reek, J.N.H.; Dierkes, P. *Chem. Rev.* **2000**, 1356.

<sup>56</sup> Granberg, K.L.; Bäckvall, J.-E. *J. Am. Chem. Soc.* **1992**, *114*, 6858.

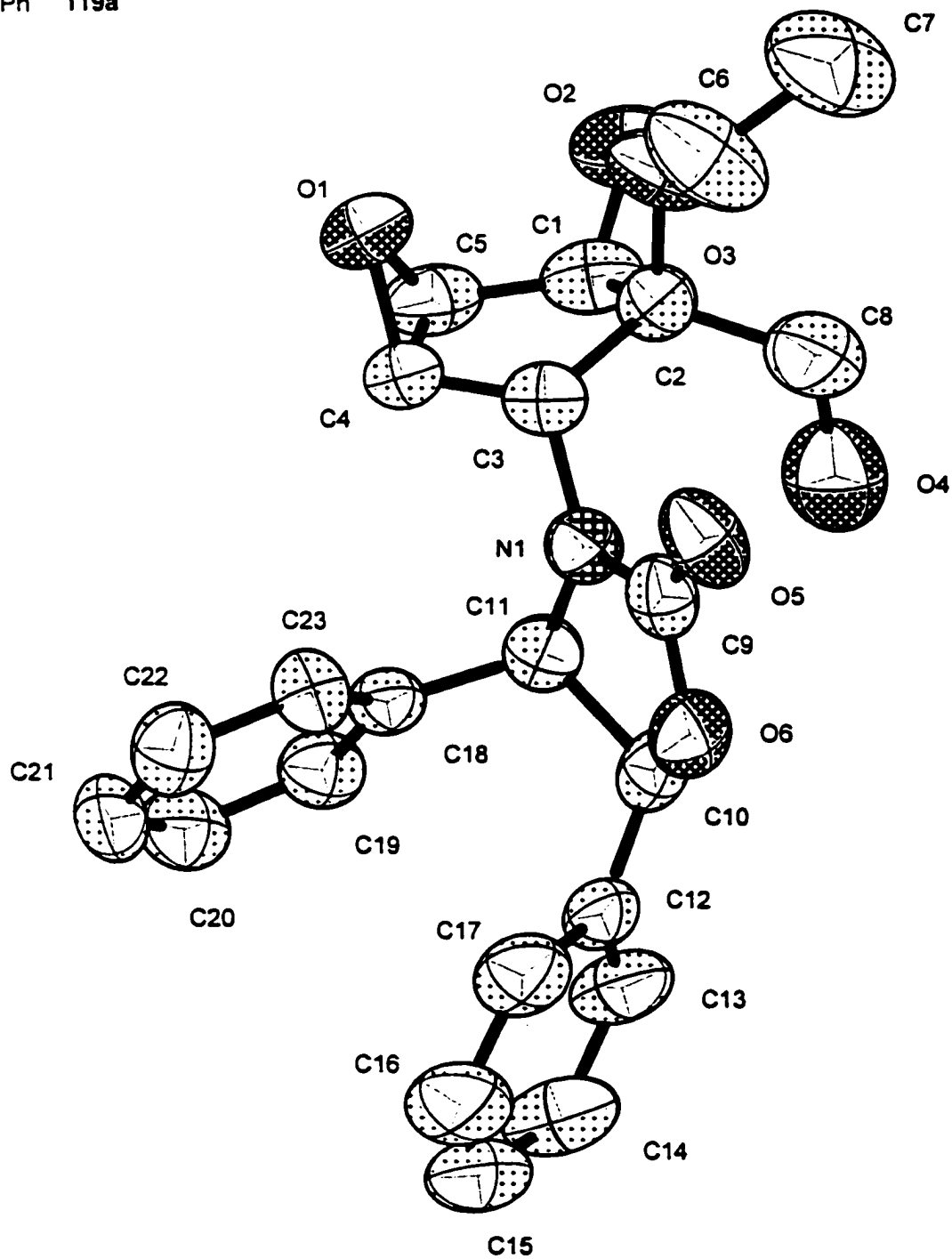
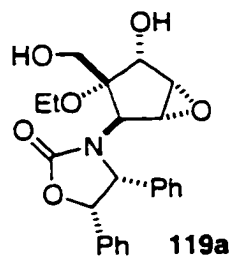
<sup>57</sup> a) Takacs, J.M.; Lawson, E.C.; Clement, F. *J. Am. Chem. Soc.* **1997**, *119*, 5956; b) Andersson, P.G.; Schab, S. *Organometallics* **1995**, *14*, 1; c) Schwarz, I.; Braun, M. *Chem. Eur. J.* **1999**, *5*, 2300.

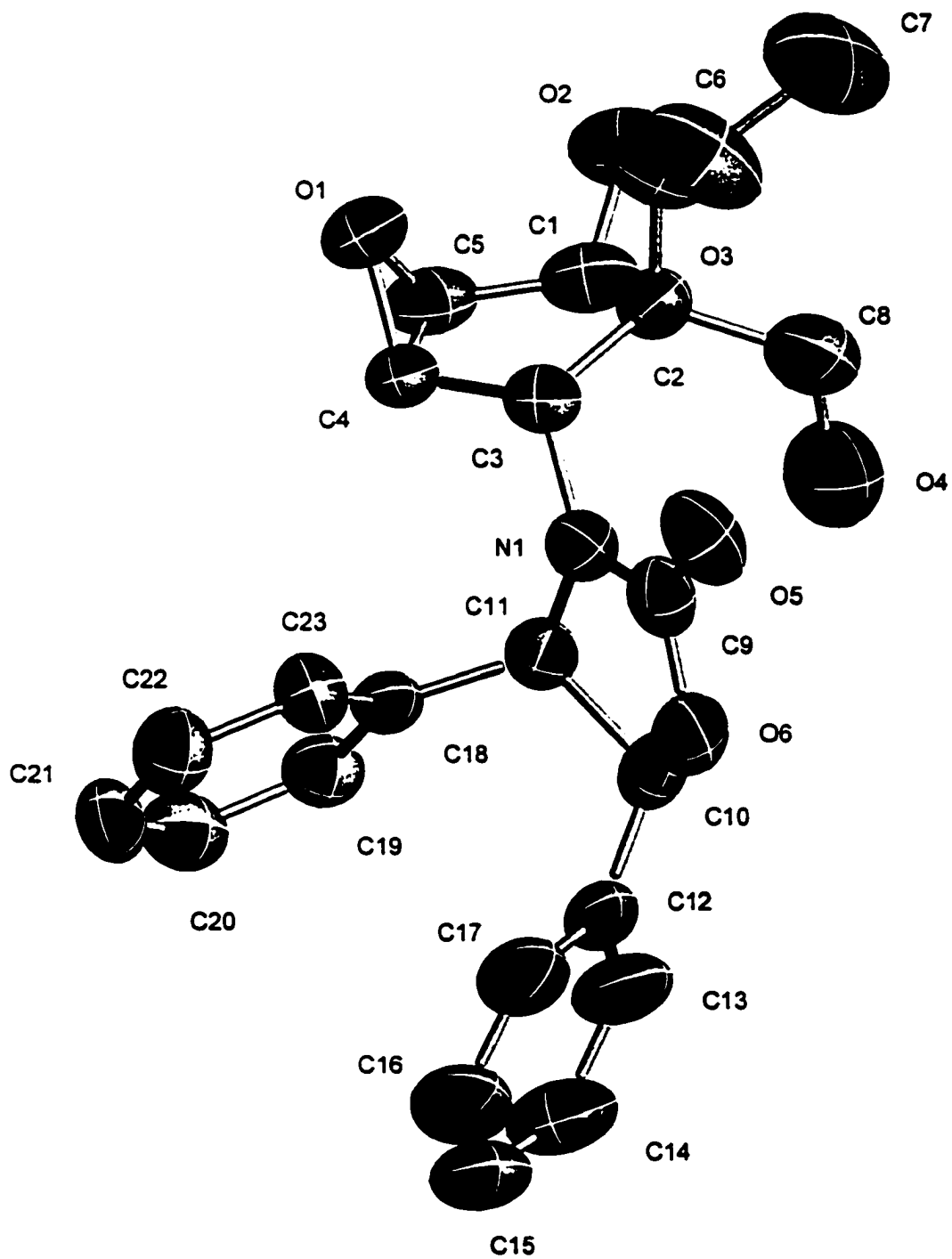
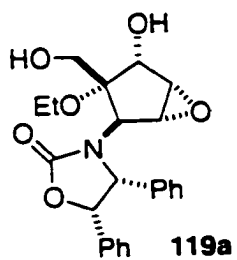
<sup>58</sup> Dorizon, P.; Su, G.; Ludvig, G.; Nikitina, L.; Paugam, R.; Ollivier, J.; Salaün, J. *J. Org. Chem.* **1999**, *64*, 4712.

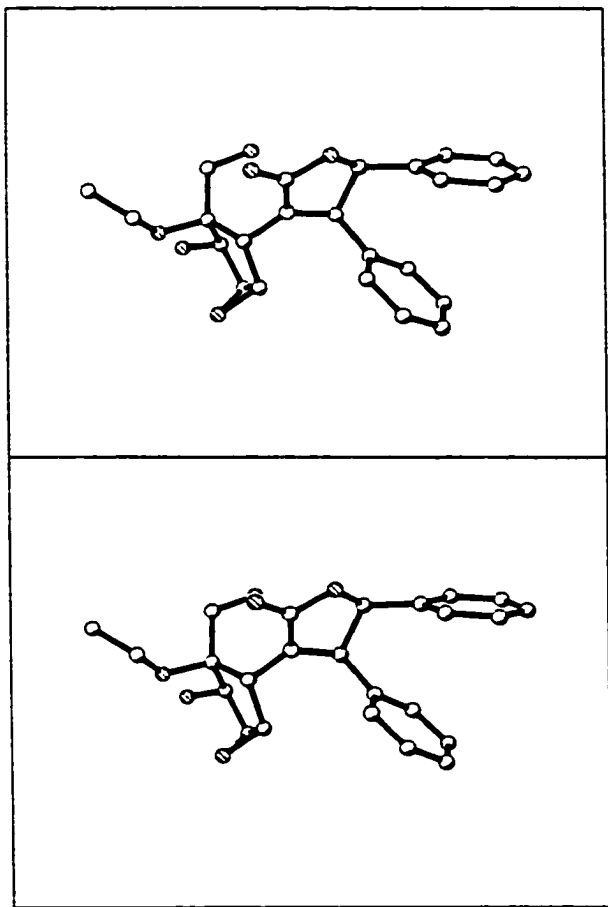
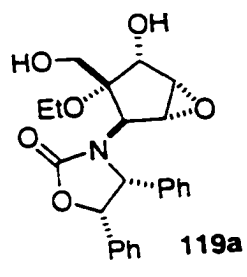
<sup>59</sup> a) Kaiser, N.K.; Brenberg, U.; Larhed, M.; Moberg, C.; Hallberg, A. *Angew. Chem. Int. Ed.* **2000**, *39*, 3596; b) Brenberg, U.; Lutsenko, S.; Kaiser, N.; Larhed, M.; Hallberg, A.; Moberg, C. *Synthesis* **2000**, 1004; c) Brenberg, U.; Larhed, M.; Moberg, C.; Hallberg, A. *J. Org. Chem.* **1999**, *64*, 1082.

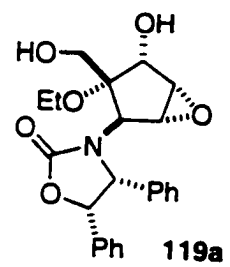
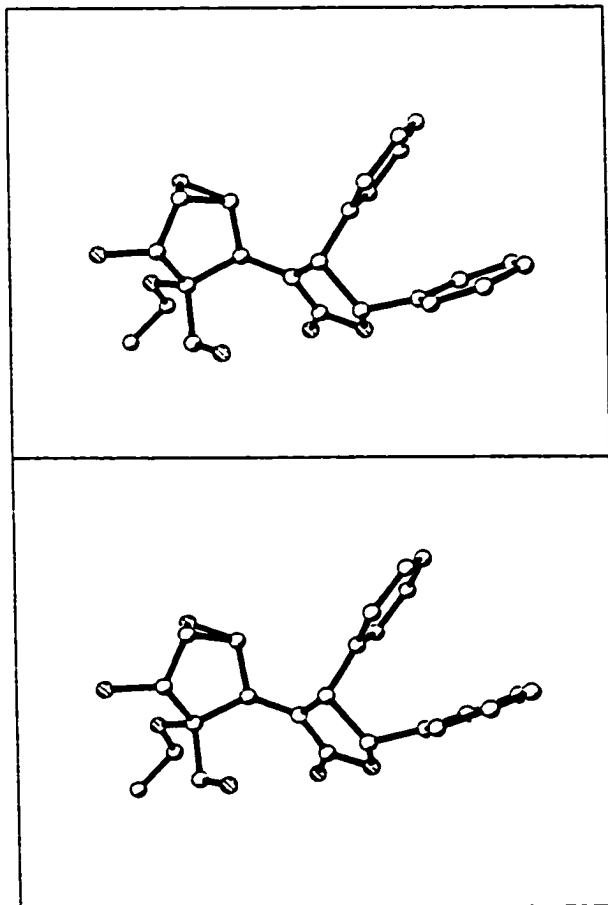
- 
- <sup>60</sup> For recent reviews, see: a) Lidström, P.; Tierney, J.; Wathey, B.; Westman, J. *Tetrahedron*, **2001**, *57*, 9225, b) Caddick, S. *Tetrahedron* **1995**, *51*, 10403; c) Mingos, D. *Res. Chem. Intermed.* **1994**, *20*, 85.
- <sup>61</sup> Based on a quote from Personal Chemistry.
- <sup>62</sup> Maleczka, R.E., Jr.; Lavis, J.M.; Clark, D.H.; Gallagher, W.P. *Org. Lett.* **2000**, *2*, 3655.
- <sup>63</sup> Stille, J.K. *Angew. Chem. Int. Ed.* **1986**, *25*, 508.
- <sup>64</sup> Han, X.; Stoltz, B.M.; Corey, E.J. *J. Am. Chem. Soc.* **1999**, *121*, 7600.
- <sup>65</sup> The addition of maleic anhydride facilitates reductive elimination. For details, see: Kurosawa, H.; Kajimaru, H.; Miyoshi, M.; Ohnishi, H.; Ikea, I. *J. Mol. Cat.* **1992**, *74*, 481.
- <sup>66</sup> Minsker, D.L.; Ibragimov, A.G.; Dzhemilev, U.M. *J. Org. Chem.* **1984**, *20*, 873.
- <sup>67</sup> Casado, A.L.; Espinet, P.; Gallego, A.M. *J. Am. Chem. Soc.* **2000**, *122*, 11771.
- <sup>68</sup> Vedejs, E.; Haight, A.R.; Moss, W.O. *J. Am. Chem. Soc.* **1992**, *114*, 6556.
- <sup>69</sup> a) Jurkschat, K.; Tzschach, A. *J. Organomet. Chem.* **1986**, *315*, 45; b) Jurkschat, K.; Tzschach, A. *J. Organomet. Chem.* **1984**, *272*, C13.
- <sup>70</sup> Jensen, M.S.; Yang, C.; Hsiao, Y.; Rivera, N.; Wells, K.M.; Chung, J.Y.L.; Yasuda, N.; Hughes, D.L.; Reider, P.J. *Org. Lett.* **2000**, *2*, 1081.
- <sup>71</sup> The stereo- and regiochemistry were confirmed with an X-ray crystal structure of **217b**.
- <sup>72</sup> Krebs, B.; Henkel, G.; Dartmann, M. *Acta Crystallog. Sec. C. : Struct. Commun.* **1989**, *45*, 1010.
- <sup>73</sup> Robinson, S.D.; Shaw, B.L. *J. Chem. Soc.* **1963**, 4806.
- <sup>74</sup> Brown, B.; Hegedus, L.S. *J. Org. Chem.* **2000**, *65*, 1865;

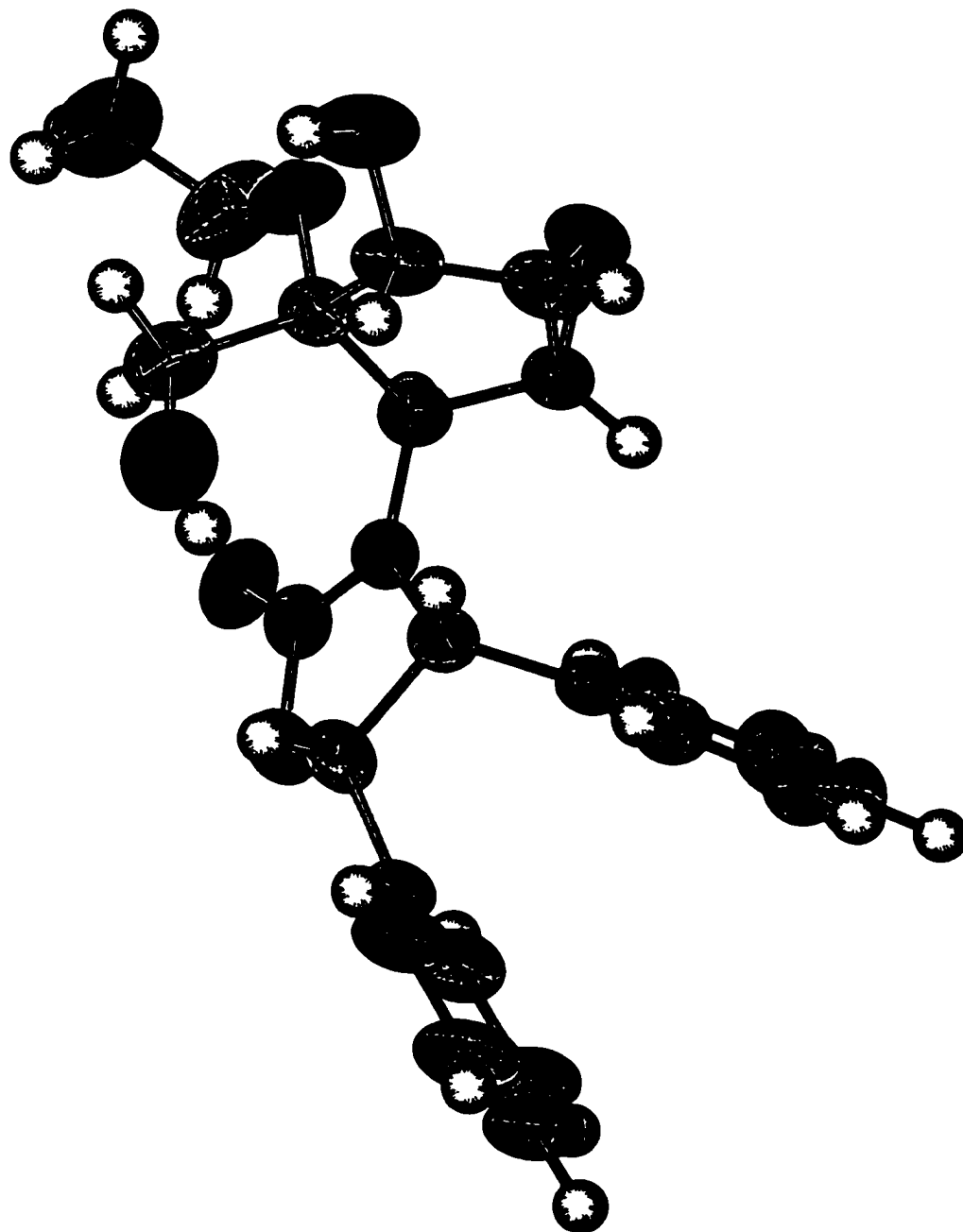
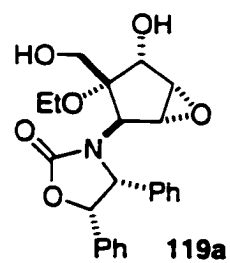
- 
- <sup>75</sup> Auburn, P.R.; Mackenzie, P.B.; Bosnich, B. *J. Am. Chem. Soc.* **1985**, *107*, 2033.
- <sup>76</sup> Heck, R.F. *Palladium Reagents in Organic Synthesis*; Academic Press: London, 1985.
- <sup>77</sup> Komiya, S. *Synthesis of Organometallic Compounds. A Practical Guide*; Wiley & Sons: New York, 1997; p 324.
- <sup>78</sup> Wakefield, B.J. *Organolithium Methods*; Academic Press: New York, 1988; p 46.
- <sup>79</sup> Black, T.H. *Aldrichimica Acta* **1983**, *16*, 3.











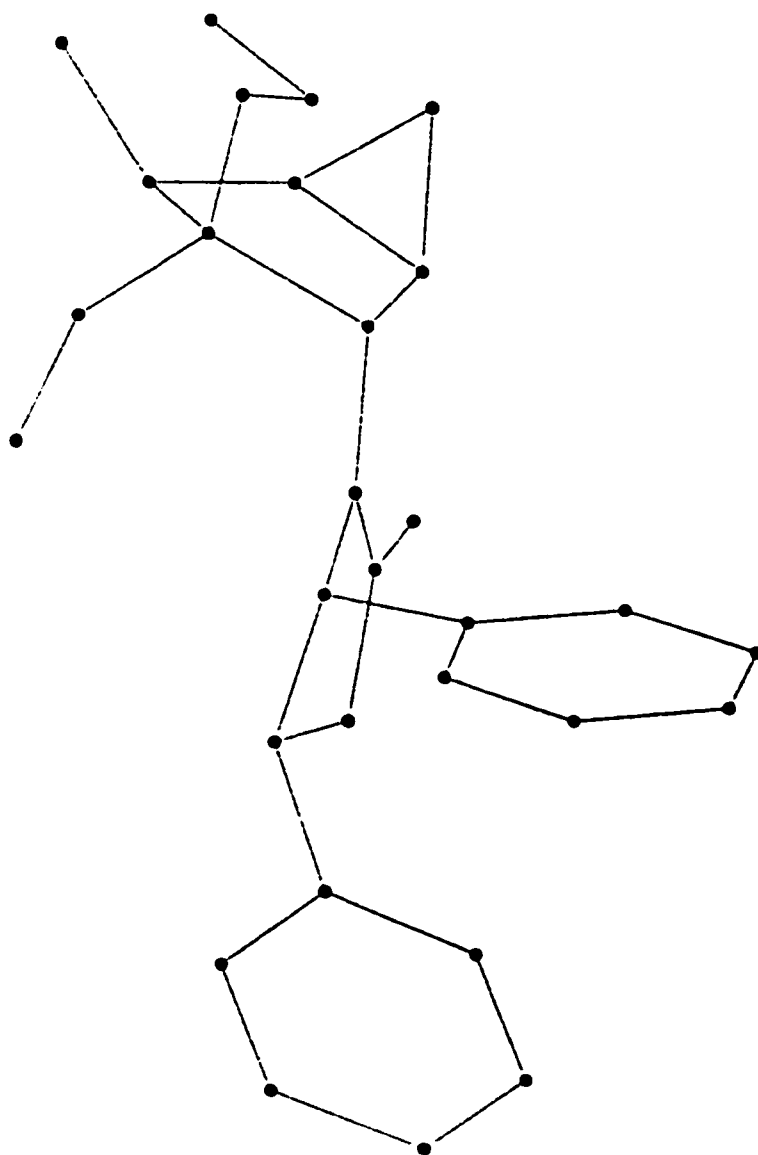
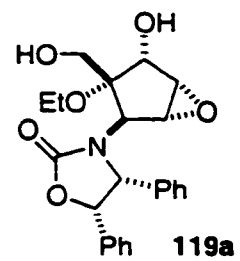
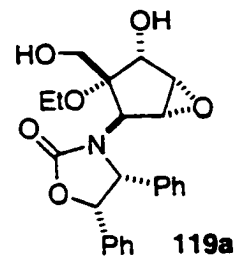


Table 1. Crystal data and structure refinement for lsh104m.

Identification code	lsh104m
Empirical formula	$C_{23}H_{25}NO_6$
Formula weight	411.44
Temperature	298(2) K
Wavelength	0.71073 Å
Crystal system	Monoclinic
Space group	P2(1)/c
Unit cell dimensions	$a = 9.2996(10)$ Å $\alpha = 90^\circ$ $b = 10.1462(11)$ Å $\beta = 98.607(2)^\circ$ $c = 21.694(2)$ Å $\gamma = 90^\circ$
Volume, Z	$2023.9(4)$ Å <sup>3</sup> , 4
Density (calculated)	$1.350$ Mg/m <sup>3</sup>
Absorption coefficient	$0.098$ mm <sup>-1</sup>
Absorption correction	SADABS
F(000)	872
Crystal size	0.3 x 0.2 x 0.2mm
$\theta$ range for data collection	2.99 to 23.29°
Limiting indices	$-10 \leq h \leq 10$ , $-11 \leq k \leq 11$ , $-24 \leq l \leq 24$
Reflections collected	12596
Independent reflections	2914 ( $R_{int} = 0.0999$ )
Completeness to $\theta = 23.29^\circ$	99.8 %
Refinement method	Full-matrix least-squares on $F^2$
Data / restraints / parameters	2914 / 0 / 275
Goodness-of-fit on $F^2$	0.960
Final R indices [ $I > 2\sigma(I)$ ]	$R1 = 0.0711$ , $wR2 = 0.1737$
R indices (all data)	$R1 = 0.1506$ , $wR2 = 0.2080$
Extinction coefficient	0.003(2)
Largest diff. peak and hole	0.834 and -0.242 eÅ <sup>-3</sup>



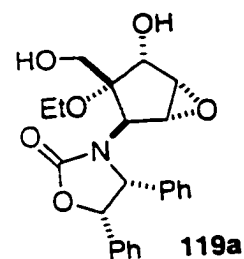


Table 2. Atomic coordinates [ $\times 10^4$ ] and equivalent isotropic displacement parameters [ $\text{\AA}^2 \times 10^3$ ] for lsh104m.  $U(\text{eq})$  is defined as one third of the trace of the orthogonalized  $U_{ij}$  tensor.

	x	y	z	$U(\text{eq})$
C(1)	7775(5)	282(5)	5010(3)	60(2)
C(2)	7473(5)	1780(5)	4945(2)	50(1)
C(3)	7773(5)	2334(5)	5628(2)	48(1)
C(4)	7629(5)	1137(5)	6030(2)	58(2)
C(5)	7588(5)	-57(5)	5660(3)	64(2)
C(6)	5296(8)	3156(6)	4622(3)	100(2)
C(7)	4653(8)	3377(7)	3984(3)	116(3)
C(8)	8302(7)	2431(6)	4473(3)	79(2)
C(9)	9308(7)	4297(5)	5710(2)	52(1)
C(10)	11611(5)	3507(5)	5977(2)	56(1)
C(11)	10512(5)	2409(5)	6103(2)	46(1)
C(12)	12875(6)	3717(5)	6477(2)	55(1)
C(13)	14153(6)	3030(6)	6458(3)	73(2)
C(14)	15275(6)	3103(7)	6943(4)	85(2)
C(15)	15158(8)	3864(7)	7457(3)	88(2)
C(16)	13916(8)	4571(7)	7476(3)	87(2)
C(17)	12790(6)	4517(6)	6984(3)	70(2)
C(18)	10567(5)	2151(4)	6792(2)	43(1)
C(19)	11556(5)	1259(5)	7084(2)	55(1)
C(20)	11756(6)	1102(5)	7729(3)	65(2)
C(21)	10939(7)	1836(6)	8076(3)	68(2)
C(22)	9928(6)	2725(6)	7794(3)	67(2)
C(23)	9752(5)	2877(5)	7151(2)	54(1)
N(1)	9163(4)	3004(4)	5805(2)	47(1)
O(1)	6285(4)	458(4)	5852(2)	70(1)
O(2)	6938(4)	-470(4)	4546(2)	78(1)
O(3)	5980(4)	1882(3)	4705(2)	68(1)
O(4)	9787(5)	2262(4)	4597(2)	96(1)
O(5)	8381(4)	5092(4)	5512(2)	71(1)
O(6)	10710(4)	4664(3)	5881(2)	63(1)

Table 3. Bond lengths [Å] and angles [°] for lsh104m.

C(1)-O(2)	1.403(6)	C(1)-C(5)	1.486(7)
C(1)-C(2)	1.549(7)	C(2)-O(3)	1.412(5)
C(2)-C(8)	1.523(7)	C(2)-C(3)	1.569(6)
C(3)-N(1)	1.461(5)	C(3)-C(4)	1.513(7)
C(4)-O(1)	1.429(5)	C(4)-C(5)	1.450(7)
C(5)-O(1)	1.438(6)	C(6)-O(3)	1.440(7)
C(6)-C(7)	1.441(8)	C(8)-O(4)	1.378(6)
C(9)-O(5)	1.211(6)	C(9)-N(1)	1.338(6)
C(9)-O(6)	1.354(6)	C(10)-O(6)	1.439(6)
C(10)-C(12)	1.492(6)	C(10)-C(11)	1.564(6)
C(11)-N(1)	1.454(5)	C(11)-C(18)	1.510(6)
C(12)-C(17)	1.378(7)	C(12)-C(13)	1.383(7)
C(13)-C(14)	1.369(8)	C(14)-C(15)	1.373(9)
C(15)-C(16)	1.366(8)	C(16)-C(17)	1.380(7)
C(18)-C(19)	1.375(6)	C(18)-C(23)	1.380(6)
C(19)-C(20)	1.393(7)	C(20)-C(21)	1.366(7)
C(21)-C(22)	1.379(7)	C(22)-C(23)	1.387(7)
O(2)-C(1)-C(5)	115.1(5)	O(2)-C(1)-C(2)	113.2(4)
C(5)-C(1)-C(2)	105.6(4)	O(3)-C(2)-C(8)	106.8(4)
O(3)-C(2)-C(1)	105.1(4)	C(8)-C(2)-C(1)	112.6(4)
O(3)-C(2)-C(3)	110.4(4)	C(8)-C(2)-C(3)	116.3(4)
C(1)-C(2)-C(3)	105.1(4)	N(1)-C(3)-C(4)	111.9(4)
N(1)-C(3)-C(2)	116.2(4)	C(4)-C(3)-C(2)	103.8(4)
O(1)-C(4)-C(5)	59.9(3)	O(1)-C(4)-C(3)	112.3(4)
C(5)-C(4)-C(3)	110.4(4)	O(1)-C(5)-C(4)	59.3(3)
O(1)-C(5)-C(1)	114.4(4)	C(4)-C(5)-C(1)	109.6(4)
O(3)-C(6)-C(7)	111.8(5)	O(4)-C(8)-C(2)	114.1(5)
O(5)-C(9)-N(1)	128.7(5)	O(5)-C(9)-O(6)	121.3(5)
N(1)-C(9)-O(6)	110.0(5)	O(6)-C(10)-C(12)	111.6(4)
O(6)-C(10)-C(11)	103.0(4)	C(12)-C(10)-C(11)	116.1(4)
N(1)-C(11)-C(18)	114.3(4)	N(1)-C(11)-C(10)	99.8(4)
C(18)-C(11)-C(10)	111.7(4)	C(17)-C(12)-C(13)	118.2(5)
C(17)-C(12)-C(10)	122.1(5)	C(13)-C(12)-C(10)	119.5(5)
C(14)-C(13)-C(12)	120.6(6)	C(13)-C(14)-C(15)	120.7(6)
C(16)-C(15)-C(14)	119.4(6)	C(15)-C(16)-C(17)	120.2(6)
C(12)-C(17)-C(16)	120.9(6)	C(19)-C(18)-C(23)	118.4(5)
C(19)-C(18)-C(11)	119.5(4)	C(23)-C(18)-C(11)	121.7(4)
C(18)-C(19)-C(20)	121.2(5)	C(21)-C(20)-C(19)	119.3(5)
C(20)-C(21)-C(22)	120.7(5)	C(21)-C(22)-C(23)	119.3(5)
C(18)-C(23)-C(22)	121.1(5)	C(9)-N(1)-C(11)	112.1(4)
C(9)-N(1)-C(3)	121.4(4)	C(11)-N(1)-C(3)	126.5(4)
C(4)-O(1)-C(5)	60.8(3)	C(2)-O(3)-C(6)	120.2(4)
C(9)-O(6)-C(10)	109.4(4)		

Symmetry transformations used to generate equivalent atoms:

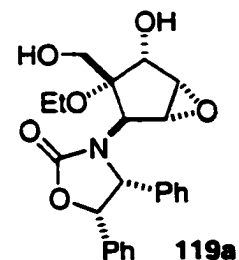
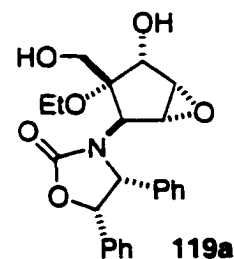


Table 4. Anisotropic displacement parameters [ $\text{\AA}^2 \times 10^3$ ] for 1sh104m.

The anisotropic displacement factor exponent takes the form:

$$-2\pi^2 [ (ha^*)^2 U_{11} + \dots + 2hka^* b^* U_{12} ]$$

	U11	U22	U33	U23	U13	U12
C(1)	46(3)	53(4)	80(4)	-15(3)	7(3)	1(3)
C(2)	52(3)	48(3)	51(3)	-8(3)	13(3)	-3(3)
C(3)	45(3)	47(3)	52(3)	-5(3)	6(2)	1(3)
C(4)	47(3)	71(4)	54(3)	9(3)	0(3)	-15(3)
C(5)	45(3)	51(4)	91(5)	10(3)	-5(3)	-2(3)
C(6)	130(6)	67(4)	88(5)	3(4)	-30(4)	30(4)
C(7)	117(6)	99(6)	117(6)	24(5)	-34(5)	13(5)
C(8)	74(4)	95(5)	67(4)	-10(4)	5(3)	-8(4)
C(9)	75(4)	41(4)	41(3)	-2(3)	10(3)	-4(3)
C(10)	65(3)	55(4)	52(3)	-8(3)	25(3)	-13(3)
C(11)	52(3)	41(3)	47(3)	-7(2)	10(2)	-2(3)
C(12)	59(4)	61(3)	48(3)	-12(3)	16(3)	-24(3)
C(13)	57(4)	79(4)	85(4)	-32(3)	22(4)	-23(3)
C(14)	55(4)	88(5)	111(6)	-17(4)	13(4)	-15(3)
C(15)	69(5)	105(6)	86(5)	-16(4)	2(4)	-37(4)
C(16)	86(5)	99(5)	75(5)	-38(4)	14(4)	-30(4)
C(17)	73(4)	65(4)	74(4)	-20(3)	19(3)	-18(3)
C(18)	41(3)	41(3)	45(3)	-4(2)	5(2)	-5(2)
C(19)	55(3)	51(3)	59(4)	-1(3)	4(3)	-1(3)
C(20)	67(4)	55(4)	68(4)	9(3)	-2(3)	1(3)
C(21)	88(4)	68(4)	47(3)	12(3)	4(3)	-15(4)
C(22)	76(4)	68(4)	61(4)	-1(3)	22(3)	-2(3)
C(23)	61(3)	56(3)	46(3)	2(3)	9(3)	5(3)
N(1)	52(3)	41(3)	47(3)	2(2)	5(2)	2(2)
O(1)	52(2)	82(3)	77(3)	7(2)	8(2)	-19(2)
O(2)	72(3)	62(3)	99(3)	-38(2)	7(2)	-2(2)
O(3)	71(3)	53(2)	72(2)	-8(2)	-18(2)	10(2)
O(4)	110(4)	92(3)	90(3)	-5(3)	25(3)	-1(3)
O(5)	104(3)	49(2)	55(2)	5(2)	-2(2)	12(2)
O(6)	81(3)	44(2)	63(2)	4(2)	11(2)	-14(2)



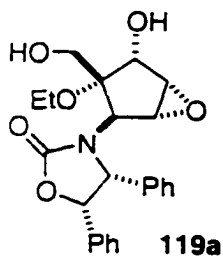
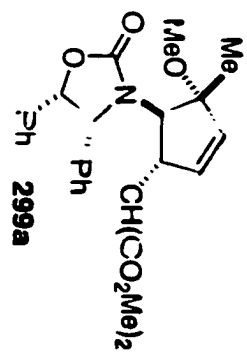
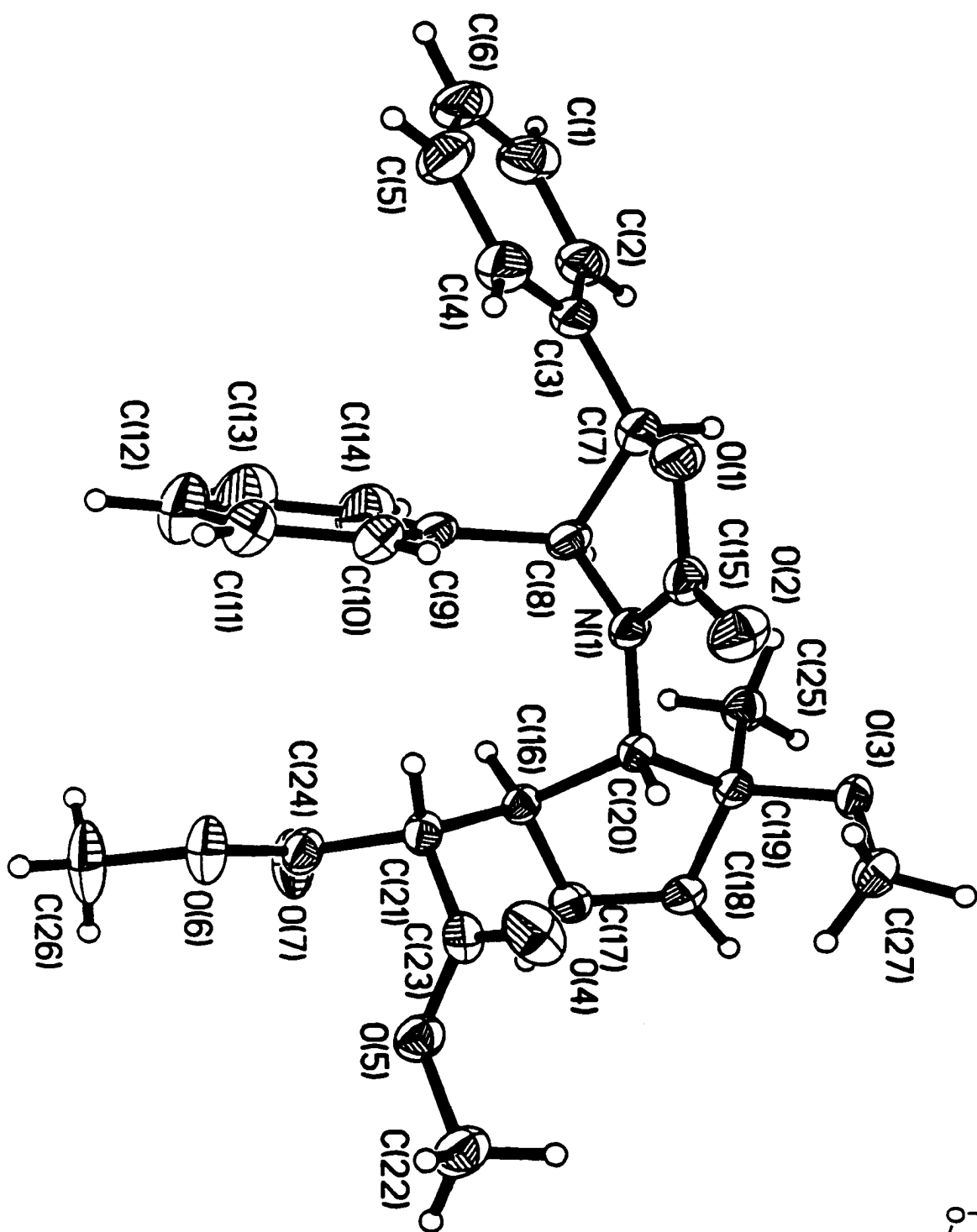
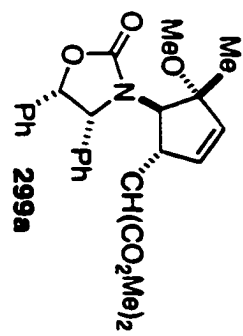
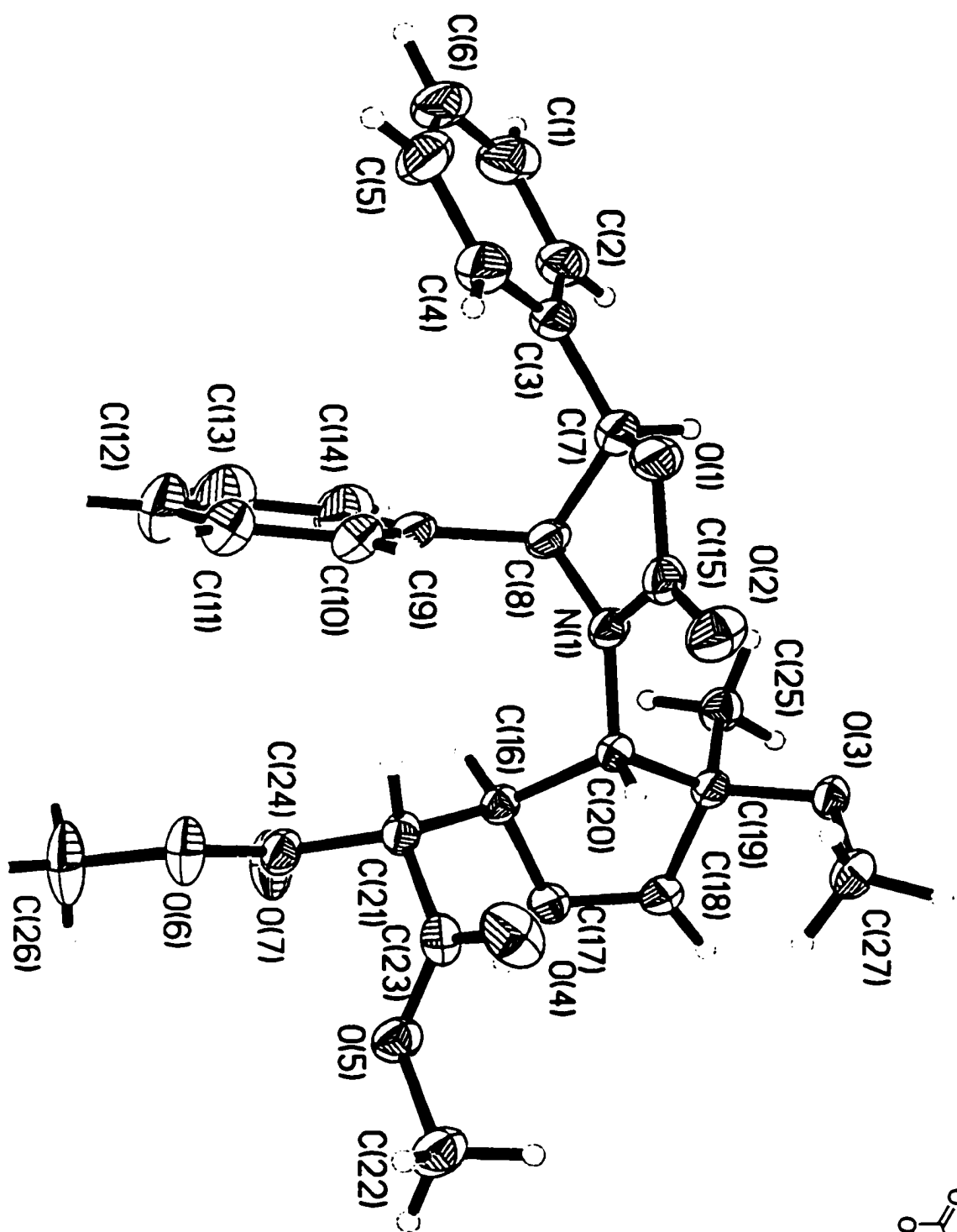
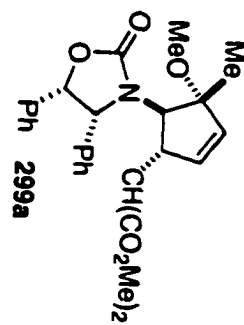
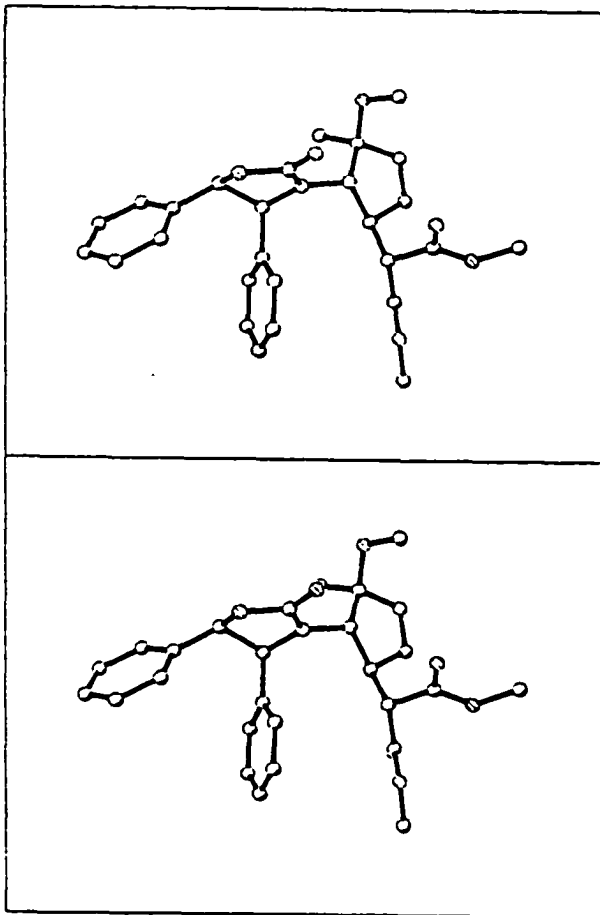


Table 5. Hydrogen coordinates (  $\times 10^4$  ) and isotropic displacement parameters ( $\text{\AA}^2 \times 10^3$ ) for lsh104m.

	x	y	z	U(eq)
H(1)	8800	141	4971	72
H(3)	6992	2952	5682	58
H(4)	8094	1130	6466	70
H(5)	8020	-869	5850	77
H(6A)	6015	3835	4748	120
H(6B)	4549	3222	4888	120
H(7A)	3999	2668	3847	174
H(7B)	5404	3417	3726	174
H(7C)	4126	4194	3955	174
H(8A)	7952	2074	4063	95
H(8B)	8090	3368	4461	95
H(10)	11978	3300	5587	67
H(11)	10705	1595	5887	56
H(13)	14250	2515	6112	87
H(14)	16126	2631	6925	102
H(15)	15918	3899	7788	106
H(16)	13828	5089	7822	104
H(17)	11964	5028	6994	84
H(19)	12100	751	6847	66
H(20)	12438	505	7922	77
H(21)	11066	1734	8507	82
H(22)	9370	3218	8031	80
H(23)	9074	3479	6960	65
H(2)	7376	-550	4247	117
H(4A)	10169	2945	4741	144







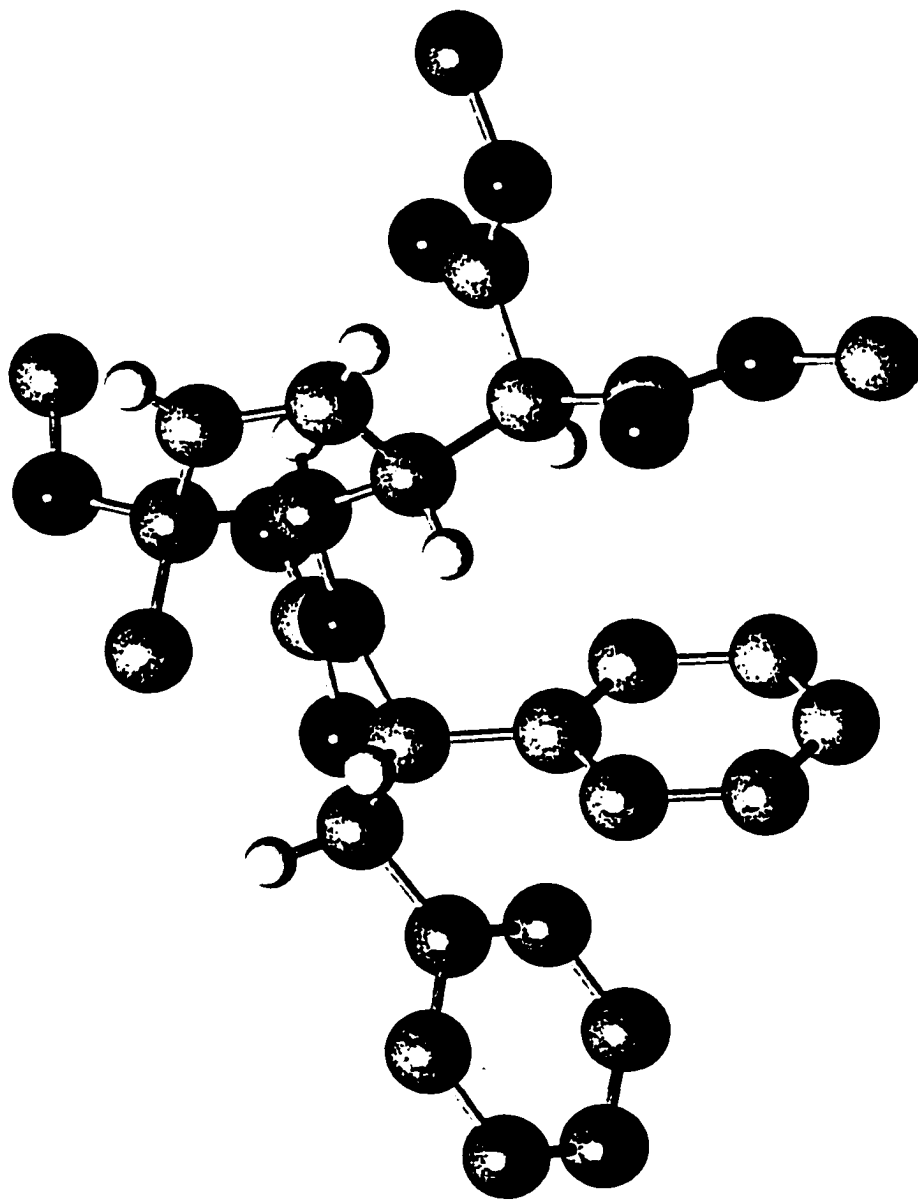
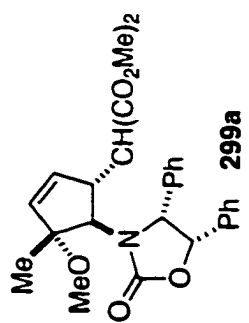
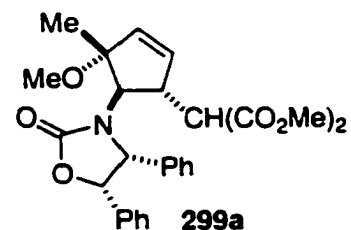


Table 1. Crystal data and structure refinement for lh43.

Identification code	lh43
Empirical formula	$C_{27}H_{29}NO_7$
Formula weight	479.51
Temperature	170(2) K
Wavelength	0.71073 Å
Crystal system	Triclinic
Space group	P-1
Unit cell dimensions	$a = 6.727(3) \text{ \AA}$ $\alpha = 89.816(9)^\circ$ $b = 12.865(6) \text{ \AA}$ $\beta = 86.777(12)^\circ$ $c = 14.511(7) \text{ \AA}$ $\gamma = 77.296(10)^\circ$
Volume, Z	1223.1(10) Å <sup>3</sup> , 2
Density (calculated)	1.302 Mg/m <sup>3</sup>
Absorption coefficient	0.094 mm <sup>-1</sup>
Absorption correction	SADABS
F(000)	508
Crystal size	0.50 x 0.30 x 0.28mm
$\theta$ range for data collection	1.41 to 28.35°
Limiting indices	-7 ≤ h ≤ 8, -16 ≤ k ≤ 16, -19 ≤ l ≤ 13
Reflections collected	8366
Independent reflections	5741 ( $R_{int} = 0.0379$ )
Completeness to $\theta = 28.35^\circ$	94.2 %
Refinement method	Full-matrix least-squares on $F^2$
Data / restraints / parameters	5741 / 0 / 321
Goodness-of-fit on $F^2$	0.986
Final R indices [ $I > 2\sigma(I)$ ]	$R1 = 0.0661$ , $wR2 = 0.1646$
R indices (all data)	$R1 = 0.1023$ , $wR2 = 0.1850$
Extinction coefficient	0.003(3)
Largest diff. peak and hole	0.380 and -0.271 eÅ <sup>-3</sup>



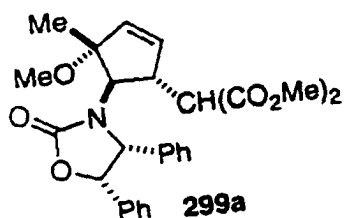


Table 2. Atomic coordinates [ $\times 10^4$ ] and equivalent isotropic displacement parameters [ $\text{\AA}^2 \times 10^3$ ] for 1h43.  $U(\text{eq})$  is defined as one third of the trace of the orthogonalized  $U_{ij}$  tensor.

	x	y	z	$U(\text{eq})$
C(1)	5332(4)	11970(2)	2615(2)	48(1)
N(1)	1275(2)	8457(1)	3627(1)	24(1)
O(1)	83(2)	10210(1)	3702(1)	35(1)
C(2)	4728(4)	11167(2)	3119(2)	37(1)
O(2)	-2067(2)	9156(1)	4133(1)	38(1)
C(3)	2883(3)	10903(2)	2979(2)	31(1)
O(3)	972(2)	7178(1)	5532(1)	26(1)
C(4)	1654(4)	11447(2)	2318(2)	39(1)
O(4)	-2471(2)	6494(1)	2936(1)	46(1)
C(5)	2283(4)	12250(2)	1813(2)	47(1)
O(5)	-558(2)	4975(1)	2339(1)	30(1)
C(6)	4106(5)	12519(2)	1970(2)	52(1)
O(6)	975(2)	6142(1)	652(1)	40(1)
C(7)	2288(3)	10045(2)	3565(2)	31(1)
O(7)	3746(3)	5406(1)	1403(1)	43(1)
C(8)	2920(3)	8887(2)	3185(2)	26(1)
C(9)	3039(4)	8804(2)	2138(2)	35(1)
C(10)	4941(5)	8560(2)	1667(2)	60(1)
C(11)	5056(8)	8522(3)	699(3)	94(1)
C(12)	3336(9)	8713(3)	220(2)	93(2)
C(13)	1458(7)	8944(2)	676(2)	68(1)
C(14)	1298(5)	8999(2)	1637(2)	44(1)
C(15)	-388(3)	9245(2)	3854(2)	29(1)
C(16)	2218(3)	6538(2)	3049(1)	22(1)
C(17)	2721(3)	5515(2)	3592(2)	24(1)
C(18)	2670(3)	5701(2)	4493(2)	25(1)
C(19)	2237(3)	6876(2)	4713(1)	23(1)
C(20)	1236(3)	7348(2)	3815(1)	20(1)
C(21)	842(3)	6507(2)	2239(1)	23(1)
C(22)	-2132(4)	4426(2)	2658(2)	37(1)
C(23)	-928(3)	6011(2)	2538(1)	27(1)
C(24)	2043(3)	5947(2)	1402(2)	28(1)
C(25)	4185(3)	7223(2)	4901(2)	28(1)
C(26)	2032(5)	5669(3)	-195(2)	60(1)
C(27)	-979(3)	6933(2)	5557(2)	32(1)

Table 3. Bond lengths [Å] and angles [°] for 1h43.

C(1)-C(6)	1.372(4)	C(1)-C(2)	1.384(4)
N(1)-C(15)	1.360(3)	N(1)-C(20)	1.457(2)
N(1)-C(8)	1.460(3)	O(1)-C(15)	1.361(3)
O(1)-C(7)	1.454(3)	C(2)-C(3)	1.382(3)
O(2)-C(15)	1.207(3)	C(3)-C(4)	1.387(3)
C(3)-C(7)	1.501(3)	O(3)-C(27)	1.414(3)
O(3)-C(19)	1.425(2)	C(4)-C(5)	1.391(4)
O(4)-C(23)	1.203(3)	C(5)-C(6)	1.376(4)
O(5)-C(23)	1.331(3)	O(5)-C(22)	1.450(3)
O(6)-C(24)	1.331(3)	O(6)-C(26)	1.449(3)
C(7)-C(8)	1.550(3)	O(7)-C(24)	1.203(3)
C(8)-C(9)	1.519(3)	C(9)-C(10)	1.389(4)
C(9)-C(14)	1.389(4)	C(10)-C(11)	1.403(5)
C(11)-C(12)	1.360(6)	C(12)-C(13)	1.366(6)
C(13)-C(14)	1.394(4)	C(16)-C(17)	1.515(3)
C(16)-C(21)	1.542(3)	C(16)-C(20)	1.543(3)
C(17)-C(18)	1.327(3)	C(18)-C(19)	1.507(3)
C(19)-C(25)	1.514(3)	C(19)-C(20)	1.560(3)
C(21)-C(24)	1.512(3)	C(21)-C(23)	1.512(3)
C(6)-C(1)-C(2)	120.5(3)	C(15)-N(1)-C(20)	120.31(17)
C(15)-N(1)-C(8)	111.23(17)	C(20)-N(1)-C(8)	128.44(16)
C(15)-O(1)-C(7)	108.20(15)	C(3)-C(2)-C(1)	120.6(2)
C(2)-C(3)-C(4)	119.0(2)	C(2)-C(3)-C(7)	118.0(2)
C(4)-C(3)-C(7)	122.9(2)	C(27)-O(3)-C(19)	116.29(16)
C(3)-C(4)-C(5)	119.8(3)	C(6)-C(5)-C(4)	120.6(3)
C(23)-O(5)-C(22)	115.72(17)	C(1)-C(6)-C(5)	119.5(2)
C(24)-O(6)-C(26)	115.08(19)	O(1)-C(7)-C(3)	111.33(18)
O(1)-C(7)-C(8)	102.86(16)	C(3)-C(7)-C(8)	117.19(19)
N(1)-C(8)-C(9)	113.63(18)	N(1)-C(8)-C(7)	99.07(16)
C(9)-C(8)-C(7)	114.19(17)	C(10)-C(9)-C(14)	119.1(3)
C(10)-C(9)-C(8)	119.1(3)	C(14)-C(9)-C(8)	121.7(2)
C(9)-C(10)-C(11)	119.2(4)	C(12)-C(11)-C(10)	120.9(4)
C(11)-C(12)-C(13)	120.3(3)	C(12)-C(13)-C(14)	120.1(4)
C(9)-C(14)-C(13)	120.4(3)	O(2)-C(15)-N(1)	128.1(2)
O(2)-C(15)-O(1)	122.46(18)	N(1)-C(15)-O(1)	109.45(18)
C(17)-C(16)-C(21)	114.77(16)	C(17)-C(16)-C(20)	101.39(16)
C(21)-C(16)-C(20)	113.82(16)	C(18)-C(17)-C(16)	111.87(17)
C(17)-C(18)-C(19)	111.97(18)	O(3)-C(19)-C(18)	114.17(16)
O(3)-C(19)-C(25)	103.71(16)	C(18)-C(19)-C(25)	110.77(16)
O(3)-C(19)-C(20)	113.69(16)	C(18)-C(19)-C(20)	100.77(16)
C(25)-C(19)-C(20)	114.11(17)	N(1)-C(20)-C(16)	115.89(16)
N(1)-C(20)-C(19)	116.07(16)	C(16)-C(20)-C(19)	104.64(15)
C(24)-C(21)-C(23)	111.88(16)	C(24)-C(21)-C(16)	111.64(16)
C(23)-C(21)-C(16)	110.55(17)	O(4)-C(23)-O(5)	123.9(2)
O(4)-C(23)-C(21)	123.7(2)	O(5)-C(23)-C(21)	112.40(17)
O(7)-C(24)-O(6)	123.9(2)	O(7)-C(24)-C(21)	125.1(2)
O(6)-C(24)-C(21)	111.02(17)		

Symmetry transformations used to generate equivalent atoms:

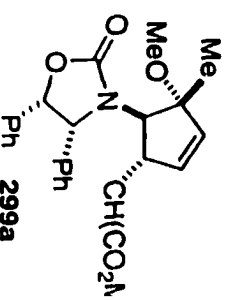
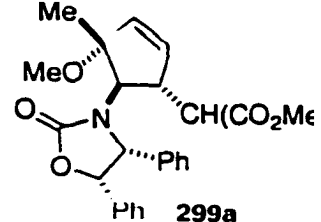


Table 4. Anisotropic displacement parameters [ $\text{\AA}^2 \times 10^3$ ] for 1h43

The anisotropic displacement factor exponent takes the form:

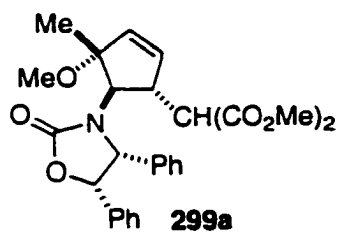
$$-2\pi^2 [ (ha^*)^2 U_{11} + \dots + 2hka^* b^* U_{12} ]$$



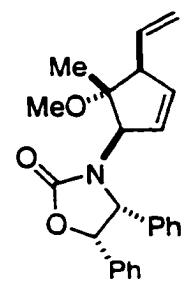
	U11	U22	U33	U23	U13	U12
C(1)	45(2)	35(1)	62(2)	-2(1)	22(1)	-13(1)
N(1)	25(1)	22(1)	23(1)	1(1)	7(1)	-4(1)
O(1)	38(1)	24(1)	39(1)	-1(1)	13(1)	-3(1)
C(2)	41(1)	29(1)	41(2)	-3(1)	8(1)	-7(1)
O(2)	31(1)	33(1)	45(1)	5(1)	14(1)	-1(1)
C(3)	39(1)	22(1)	30(1)	-1(1)	9(1)	-5(1)
O(3)	27(1)	32(1)	19(1)	-2(1)	5(1)	-10(1)
C(4)	45(1)	33(1)	38(1)	1(1)	3(1)	-6(1)
O(4)	27(1)	54(1)	55(1)	-24(1)	15(1)	-11(1)
C(5)	62(2)	34(1)	38(2)	12(1)	11(1)	1(1)
O(5)	27(1)	32(1)	31(1)	2(1)	4(1)	-9(1)
C(6)	68(2)	35(1)	51(2)	4(1)	31(2)	-14(1)
O(6)	37(1)	62(1)	19(1)	-4(1)	3(1)	-6(1)
C(7)	34(1)	30(1)	28(1)	1(1)	4(1)	-8(1)
O(7)	35(1)	62(1)	25(1)	-9(1)	5(1)	4(1)
C(8)	27(1)	22(1)	28(1)	4(1)	6(1)	-5(1)
C(9)	50(1)	21(1)	31(1)	0(1)	17(1)	-10(1)
C(10)	70(2)	50(2)	54(2)	-4(1)	38(2)	-10(1)
C(11)	125(4)	84(3)	64(3)	-9(2)	65(3)	-20(3)
C(12)	174(5)	75(3)	31(2)	-5(2)	32(3)	-38(3)
C(13)	132(3)	47(2)	31(2)	9(1)	-9(2)	-31(2)
C(14)	73(2)	33(1)	28(1)	9(1)	-2(1)	-17(1)
C(15)	33(1)	25(1)	25(1)	0(1)	8(1)	-2(1)
C(16)	21(1)	24(1)	20(1)	1(1)	3(1)	-5(1)
C(17)	23(1)	22(1)	26(1)	-1(1)	2(1)	-2(1)
C(18)	24(1)	23(1)	27(1)	4(1)	0(1)	-5(1)
C(19)	24(1)	24(1)	20(1)	1(1)	2(1)	-6(1)
C(20)	21(1)	22(1)	19(1)	0(1)	2(1)	-6(1)
C(21)	25(1)	24(1)	19(1)	1(1)	2(1)	-3(1)
C(22)	36(1)	45(1)	34(1)	6(1)	3(1)	-18(1)
C(23)	26(1)	35(1)	19(1)	-3(1)	-1(1)	-6(1)
C(24)	29(1)	34(1)	21(1)	2(1)	4(1)	-10(1)
C(25)	26(1)	35(1)	26(1)	1(1)	-1(1)	-11(1)
C(26)	61(2)	96(2)	19(1)	-14(1)	7(1)	-10(2)
C(27)	30(1)	39(1)	30(1)	-1(1)	10(1)	-14(1)

Table 5. Hydrogen coordinates ( $\times 10^4$ ) and isotropic displacement parameters ( $\text{\AA}^2 \times 10^3$ ) for lh43.

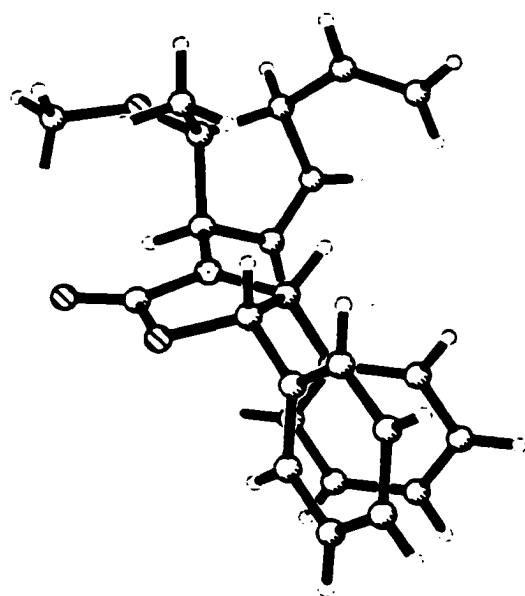
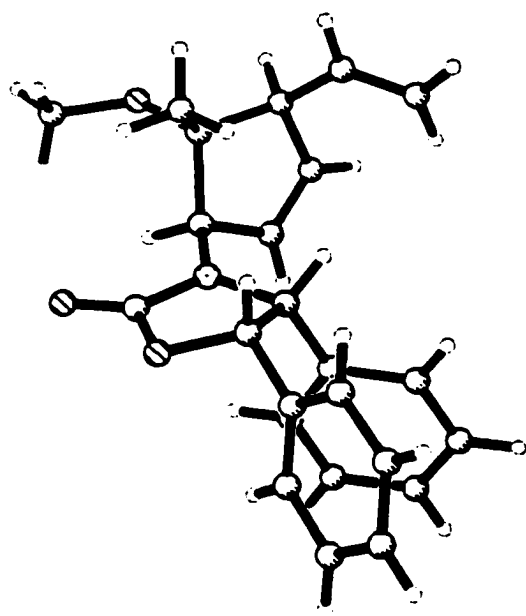
	x	y	z	U(eq)
H(1)	6606	12142	2717	57
H(2)	5588	10793	3565	45
H(4)	386	11272	2210	47
H(5)	1448	12615	1355	56
H(6)	4511	13081	1636	63
H(7)	2871	10065	4182	37
H(8)	4256	8523	3428	31
H(10)	6151	8421	1997	72
H(11)	6354	8360	375	113
H(12)	3441	8685	-436	112
H(13)	260	9067	338	82
H(14)	-11	9172	1952	53
H(16)	3520	6717	2804	26
H(17)	3035	4823	3320	29
H(18)	2882	5158	4945	30
H(20)	-235	7313	3888	24
H(21)	263	7260	2063	28
H(22A)	-2426	4549	3323	56
H(22B)	-1659	3661	2536	56
H(22C)	-3374	4699	2331	56
H(25A)	3880	7994	5013	42
H(25B)	5158	7047	4367	42
H(25C)	4779	6854	5446	42
H(26A)	3213	5983	-342	90
H(26B)	1103	5807	-699	90
H(26C)	2496	4899	-116	90
H(27A)	-1910	7476	5219	48
H(27B)	-1505	6920	6199	48
H(27C)	-874	6234	5269	48







322b



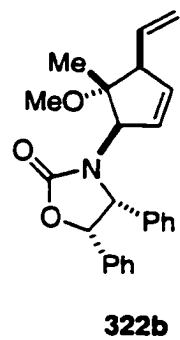
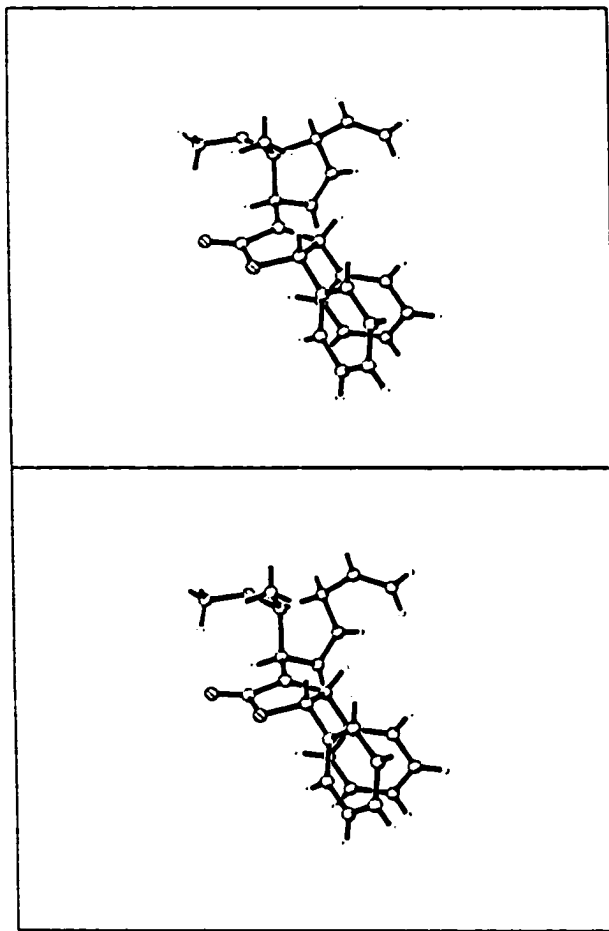
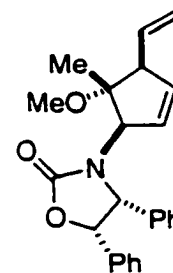


Table 1. Crystal data and structure refinement for hn4-076c.

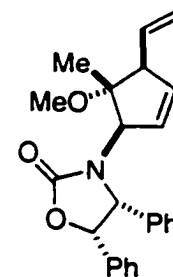
Identification code	lh103 (Norling-Hegedus)	
Empirical formula	C <sub>24</sub> H <sub>25</sub> N O <sub>3</sub>	
Formula weight	375.45	
Temperature	173(2) K	
Wavelength	0.71073 Å	
Crystal system	Orthorhombic	
Space group	Pbca	
Unit cell dimensions	a = 18.161(5) Å	α = 90°.
	b = 9.797(3) Å	β = 90°.
	c = 22.664(6) Å	γ = 90°.
Volume	4032.4(18) Å <sup>3</sup>	
Z	8	
Density (calculated)	1.237 Mg/m <sup>3</sup>	
Absorption coefficient	0.081 mm <sup>-1</sup>	
F(000)	1600	
Crystal size	0.02 x 0.20 x 0.38 mm <sup>3</sup>	
Theta range for data collection	3.19 to 23.31°.	
Index ranges	-20 ≤ h ≤ 20, -10 ≤ k ≤ 10, -24 ≤ l ≤ 25	
Reflections collected	22739	
Independent reflections	2898 [R(int) = 0.2521]	
Completeness to theta = 23.31°	99.6 %	
Absorption correction	None	
Refinement method	Full-matrix least-squares on F <sup>2</sup>	
Data / restraints / parameters	2898 / 0 / 254	
Goodness-of-fit on F <sup>2</sup>	0.921	
Final R indices [I > 2σ(I)]	R1 = 0.0694, wR2 = 0.1186	
R indices (all data)	R1 = 0.1607, wR2 = 0.1470	
Extinction coefficient	0.0122(11)	
Largest diff. peak and hole	0.192 and -0.178 e.Å <sup>-3</sup>	



322b

Table 2. Atomic coordinates ( $\times 10^4$ ) and equivalent isotropic displacement parameters ( $\text{\AA}^2 \times 10^3$ ) for hn4-076c.  $U(\text{eq})$  is defined as one third of the trace of the orthogonalized  $U^{ij}$  tensor.

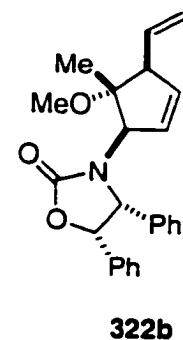
	x	y	z	$U(\text{eq})$
N(1)	6446(2)	1414(3)	3682(1)	29(1)
O(1)	7357(2)	376(3)	3211(1)	35(1)
O(2)	6723(2)	-836(3)	3886(1)	44(1)
O(3)	5759(2)	1468(3)	5194(1)	52(1)
C(1)	6821(2)	230(5)	3629(2)	32(1)
C(2)	7433(2)	1817(4)	3082(2)	32(1)
C(3)	6668(2)	2422(4)	3245(2)	29(1)
C(4)	5870(2)	1570(4)	4126(2)	32(1)
C(5)	5245(2)	2448(4)	3928(2)	35(1)
C(6)	5165(2)	3530(5)	4259(2)	37(1)
C(7)	5729(2)	3627(4)	4746(2)	39(1)
C(8)	6114(2)	2232(4)	4729(2)	38(1)
C(9)	6947(2)	2279(5)	4803(2)	50(1)
C(10)	6054(3)	146(5)	5310(2)	69(2)
C(11)	6199(2)	4858(5)	4715(2)	54(1)
C(12)	6201(2)	5777(6)	4318(3)	67(2)
C(13)	7715(2)	2022(4)	2465(2)	31(1)
C(14)	8300(3)	2890(4)	2366(2)	46(1)
C(15)	8557(3)	3119(5)	1796(3)	59(2)
C(16)	8240(3)	2465(5)	1329(2)	58(2)
C(17)	7670(3)	1566(5)	1430(2)	50(1)
C(18)	7414(2)	1348(5)	1992(2)	42(1)
C(19)	6133(2)	2559(4)	2736(2)	27(1)
C(20)	6134(2)	3744(5)	2409(2)	39(1)
C(21)	5693(3)	3890(5)	1917(2)	50(1)
C(22)	5242(3)	2839(6)	1747(2)	55(1)
C(23)	5227(2)	1654(5)	2067(2)	43(1)
C(24)	5675(2)	1516(4)	2562(2)	36(1)



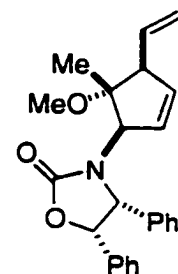
**322b**

Table 3. Bond lengths [Å] and angles [°] for hn4-076c.

N(1)-C(1)	1.351(5)
N(1)-C(3)	1.455(4)
N(1)-C(4)	1.460(5)
O(1)-C(1)	1.366(5)
O(1)-C(2)	1.449(4)
O(2)-C(1)	1.208(5)
O(3)-C(10)	1.426(5)
O(3)-C(8)	1.444(5)
C(2)-C(13)	1.503(6)
C(2)-C(3)	1.553(5)
C(3)-C(19)	1.515(5)
C(4)-C(5)	1.493(5)
C(4)-C(8)	1.575(5)
C(5)-C(6)	1.307(5)
C(6)-C(7)	1.510(5)
C(7)-C(11)	1.479(6)
C(7)-C(8)	1.536(5)
C(8)-C(9)	1.523(5)
C(11)-C(12)	1.273(6)
C(13)-C(18)	1.374(5)
C(13)-C(14)	1.378(6)
C(14)-C(15)	1.392(6)
C(15)-C(16)	1.364(6)
C(16)-C(17)	1.378(6)
C(17)-C(18)	1.373(5)
C(19)-C(24)	1.376(5)
C(19)-C(20)	1.378(5)
C(20)-C(21)	1.379(5)
C(21)-C(22)	1.372(6)
C(22)-C(23)	1.369(6)
C(23)-C(24)	1.391(5)
C(1)-N(1)-C(3)	112.5(3)
C(1)-N(1)-C(4)	120.8(4)

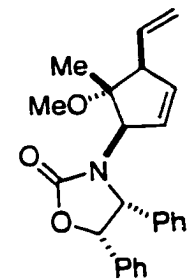


C(3)-N(1)-C(4)	126.7(3)
C(1)-O(1)-C(2)	108.0(3)
C(10)-O(3)-C(8)	116.0(3)
O(2)-C(1)-N(1)	128.7(4)
O(2)-C(1)-O(1)	122.0(4)
N(1)-C(1)-O(1)	109.3(4)
O(1)-C(2)-C(13)	110.5(3)
O(1)-C(2)-C(3)	103.8(3)
C(13)-C(2)-C(3)	118.4(3)
N(1)-C(3)-C(19)	113.6(3)
N(1)-C(3)-C(2)	98.7(3)
C(19)-C(3)-C(2)	115.2(3)
N(1)-C(4)-C(5)	113.3(3)
N(1)-C(4)-C(8)	116.1(3)
C(5)-C(4)-C(8)	103.8(3)
C(6)-C(5)-C(4)	112.3(4)
C(5)-C(6)-C(7)	113.3(4)
C(11)-C(7)-C(6)	114.1(4)
C(11)-C(7)-C(8)	117.5(4)
C(6)-C(7)-C(8)	103.5(3)
O(3)-C(8)-C(9)	112.3(4)
O(3)-C(8)-C(7)	103.8(3)
C(9)-C(8)-C(7)	115.0(4)
O(3)-C(8)-C(4)	107.1(3)
C(9)-C(8)-C(4)	112.8(3)
C(7)-C(8)-C(4)	105.1(3)
C(12)-C(11)-C(7)	127.7(5)
C(18)-C(13)-C(14)	118.4(4)
C(18)-C(13)-C(2)	121.7(4)
C(14)-C(13)-C(2)	119.9(4)
C(13)-C(14)-C(15)	120.6(5)
C(16)-C(15)-C(14)	120.2(5)
C(15)-C(16)-C(17)	119.3(5)
C(18)-C(17)-C(16)	120.4(5)
C(17)-C(18)-C(13)	121.0(4)
C(24)-C(19)-C(20)	118.2(4)



**322b**

C(24)-C(19)-C(3)	122.8(4)
C(20)-C(19)-C(3)	119.0(4)
C(19)-C(20)-C(21)	121.5(4)
C(22)-C(21)-C(20)	119.7(4)
C(23)-C(22)-C(21)	120.0(4)
C(22)-C(23)-C(24)	119.8(4)
C(19)-C(24)-C(23)	120.9(4)

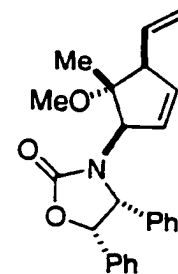


**322b**

---

Symmetry transformations used to generate equivalent atoms:

Table 4. Anisotropic displacement parameters ( $\text{\AA}^2 \times 10^3$ ) for hn4-076c. The anisotropic displacement factor exponent takes the form:  $-2\pi^2 [ h^2 a^{*2} U^{11} + \dots + 2 h k a^* b^* U^{12} ]$

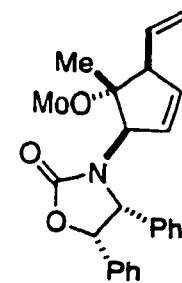


**322b**

	$U^{11}$	$U^{22}$	$U^{33}$	$U^{23}$	$U^{13}$	$U^{12}$
N(1)	32(2)	30(2)	25(2)	2(2)	-1(2)	5(2)
O(1)	35(2)	35(2)	33(2)	-2(2)	4(2)	9(2)
O(2)	58(2)	31(2)	44(2)	7(2)	6(2)	10(2)
O(3)	55(2)	65(2)	34(2)	8(2)	11(2)	11(2)
C(1)	35(3)	37(3)	24(3)	-10(2)	-10(2)	9(3)
C(2)	32(3)	33(3)	31(3)	-6(2)	-9(2)	-1(2)
C(3)	28(2)	30(3)	28(2)	-3(2)	0(2)	-3(2)
C(4)	30(3)	35(3)	30(3)	3(2)	4(2)	0(2)
C(5)	30(3)	35(3)	39(3)	-2(2)	-1(2)	-1(2)
C(6)	25(3)	43(3)	43(3)	0(3)	-3(2)	7(2)
C(7)	34(3)	46(3)	37(3)	-12(3)	2(2)	2(3)
C(8)	38(3)	48(3)	29(3)	-5(3)	-2(2)	5(2)
C(9)	36(3)	75(4)	40(3)	-15(3)	-12(2)	8(3)
C(10)	83(4)	76(4)	48(4)	30(3)	1(3)	10(3)
C(11)	38(3)	58(4)	66(4)	-8(3)	-4(3)	5(3)
C(12)	32(3)	86(4)	83(4)	28(4)	-8(3)	-11(3)
C(13)	21(2)	30(3)	42(3)	-2(2)	-4(2)	2(2)
C(14)	37(3)	41(3)	60(4)	-18(3)	9(3)	-1(2)
C(15)	49(3)	43(3)	86(4)	-12(3)	45(3)	-5(3)
C(16)	67(4)	58(4)	50(3)	9(3)	24(3)	17(3)
C(17)	43(3)	70(4)	38(3)	1(3)	7(3)	2(3)
C(18)	38(3)	53(3)	35(3)	6(3)	5(3)	-6(2)
C(19)	27(2)	28(3)	27(2)	0(2)	-1(2)	2(2)
C(20)	30(3)	47(3)	40(3)	2(3)	-2(2)	1(2)
C(21)	46(3)	53(4)	50(3)	17(3)	-3(3)	6(3)
C(22)	52(3)	74(4)	39(3)	13(3)	-16(3)	4(3)
C(23)	40(3)	53(4)	36(3)	-3(3)	-12(3)	-7(3)
C(24)	42(3)	34(3)	34(3)	2(2)	5(2)	2(2)

Table 5. Hydrogen coordinates ( $\times 10^4$ ) and isotropic displacement parameters ( $\text{\AA}^2 \times 10^3$ ) for hn4-076c.

	x	y	z	U(eq)
H(2A)	7804	2205	3361	38
H(3A)	6735	3329	3440	34
H(4A)	5668	643	4214	38
H(5A)	4942	2244	3598	42
H(6A)	4788	4189	4199	44
H(7A)	5453	3675	5127	47
H(9A)	7069	2705	5182	75
H(9B)	7164	2814	4481	75
H(9C)	7145	1349	4793	75
H(10A)	5778	-281	5633	104
H(10B)	6573	229	5423	104
H(10C)	6013	-420	4955	104
H(11A)	6540	4977	5029	65
H(12A)	5872	5713	3993	80
H(12B)	6531	6526	4347	80
H(14A)	8529	3336	2689	55
H(15A)	8954	3733	1732	71
H(16A)	8410	2628	939	70
H(17A)	7453	1093	1108	60
H(18A)	7022	722	2055	50
H(20A)	6444	4477	2524	47
H(21A)	5702	4716	1697	59
H(22A)	4941	2932	1406	66
H(23A)	4911	928	1952	52
H(24A)	5664	691	2782	44



322b

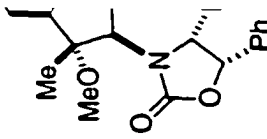


Table 6. Observed and calculated structure factors for hn4-076c

Observed										Calculated										Observed										Calculated									
h	k	l	10Fo	10Fc	10s	h	k	l	10Fo	10Fc	10s	h	k	l	10Fo	10Fc	10s	h	k	l	10Fo	10Fc	10s	h	k	l	10Fo	10Fc	10s	h	k	l	10Fo	10Fc	10s				
4	0	0	939	926	14	8	10	0	129	0	128	12	5	1	51	32	51	18	0	2	233	212	35	9	5	2	120	100	26	9	5	2	120	100	26				
6	0	0	559	583	25	2	1	1	384	412	16	13	5	1	127	131	32	19	0	0	152	84	68	10	5	2	177	182	18	10	5	2	177	182	18				
6	0	0	693	677	22	3	1	1	781	821	13	14	5	1	0	25	1	19	0	0	106	64	105	11	5	2	89	89	51	11	5	2	89	89	51				
10	0	0	235	198	26	4	1	1	987	1026	15	15	5	1	71	103	70	20	1	1	517	562	7	12	5	2	118	128	36	12	5	2	118	128	36				
12	0	0	855	835	36	5	1	1	116	114	13	16	5	1	70	5	70	14	0	0	1243	1288	26	13	5	2	206	204	19	13	5	2	206	204	19				
14	0	0	447	460	28	6	1	1	549	554	9	17	5	1	0	29	1	3	4	1	587	587	7	14	5	2	182	193	23	14	5	2	182	193	23				
16	0	0	222	248	46	7	1	1	668	718	9	0	6	1	215	189	16	16	0	0	359	360	7	15	5	2	154	176	30	15	5	2	154	176	30				
18	0	0	0	26	1	8	1	1	328	339	8	1	6	1	337	334	9	16	0	0	452	431	11	15	5	2	100	81	98	16	5	2	100	81	98				
20	0	0	518	522	32	9	1	1	353	360	8	2	6	1	244	252	11	16	0	0	323	325	8	16	5	2	167	181	41	16	5	2	167	181	41				
4	1	1	2777	2668	45	10	1	1	237	224	10	3	6	1	166	177	16	17	0	0	408	393	8	17	5	2	85	53	70	17	5	2	85	53	70				
6	1	1	643	647	16	11	1	1	283	301	10	4	6	1	317	328	10	18	0	0	69	4	46	18	6	6	140	141	17	18	6	6	140	141	17				
8	1	1	338	338	15	12	1	1	208	193	15	5	6	1	161	168	18	19	0	0	330	338	9	19	6	6	302	319	10	19	6	6	302	319	10				
10	1	1	260	267	14	13	1	1	276	279	14	6	6	1	424	409	9	20	0	0	86	17	37	20	6	6	64	36	64	20	6	6	64	36	64				
12	1	1	512	496	13	14	1	1	262	266	15	7	6	1	95	38	39	21	0	0	139	111	22	21	6	6	479	480	9	21	6	6	479	480	9				
14	1	1	153	123	44	15	1	1	231	200	19	8	6	1	81	47	73	22	0	0	263	267	13	22	6	6	73	92	73	22	6	6	73	92	73				
16	1	1	413	410	29	16	1	1	125	74	40	9	6	1	138	130	25	23	0	0	120	109	36	23	6	6	83	98	44	23	6	6	83	98	44				
18	1	1	233	225	34	17	1	1	75	15	74	10	6	1	163	160	22	24	0	0	201	182	22	24	6	6	131	110	24	24	6	6	131	110	24				
20	0	2	96	161	95	18	1	1	139	57	44	11	6	1	149	95	27	25	0	0	207	213	24	25	6	6	89	81	48	25	6	6	89	81	48				
2	2	2	2650	2635	21	19	1	1	0	54	1	12	6	1	44	12	44	26	0	0	37	40	37	26	6	6	180	154	19	26	6	6	180	154	19				
4	2	2	165	166	15	20	1	1	232	210	27	13	6	1	207	202	21	27	0	0	121	55	58	27	6	6	215	202	17	27	6	6	215	202	17				
6	2	2	659	675	17	1	3	2	582	633	6	14	6	1	106	86	59	28	0	0	106	82	106	28	6	6	127	113	35	28	6	6	127	113	35				
8	2	2	779	814	17	3	2	2	1065	1077	11	15	6	1	139	81	46	29	0	0	144	131	52	29	6	6	68	95	68	29	6	6	68	95	68				
10	2	2	65	7	65	4	2	2	1447	1505	24	16	6	1	114	79	72	30	0	0	742	814	6	30	6	6	97	59	76	30	6	6	97	59	76				
12	2	2	199	197	22	5	2	2	305	292	7	1	7	1	105	93	30	31	0	0	69	28	48	31	6	6	70	19	69	31	6	6	70	19	69				
14	2	2	84	69	84	6	2	2	1043	1049	15	2	7	1	26	21	26	32	0	0	601	630	7	32	6	6	0	51	1	32	6	6	0	51	1	32	6	6	
16	2	2	239	286	28	8	2	2	604	572	8	3	7	1	88	100	44	33	0	0	730	760	17	33	6	6	96	38	96	33	6	6	96	38	96				
18	2	2	0	35	1	9	2	2	565	558	8	4	7	1	212	190	15	34	0	0	298	301	7	34	6	6	79	12	52	34	6	6	79	12	52				
2	2	4	133	120	16	10	2	2	217	206	11	5	7	1	316	300	11	35	0	0	307	283	7	35	6	6	343	352	10	35	6	6	343	352	10				
4	2	4	272	269	13	11	2	2	420	425	9	6	7	1	130	106	29	36	0	0	272	278	9	36	6	6	215	218	15	36	6	6	215	218	15				
6	2	4	315	320	12	12	2	2	118	82	24	7	7	1	143	107	28	37	0	0	613	601	9	37	6	6	48	33	47	37	6	6	48	33	47				
8	2	4	447	425	12	13	2	2	182	156	16	8	7	1	160	123	24	38	0	0	44	40	43	38	6	6	68	8	67	38	6	6	68	8	67				
10	2	4	352	359	14	14	2	2	97	18	48	10	7	1	175	182	26	39	0	0	261	235	10	39	6	6	378	382	11	39	6	6	378	382	11				
12	2	4	839	830	22	15	2	2	33	25	32	11	7	1	115	92	50	40	0	0	174	155	16	40	6	6	245	230	16	40	6	6	245	230	16				
14	2	4	150	139	38	16	2	2	99	32	69	12	7	1	184	168	28	41	0	0	81	27	58	41	6	6	119	65	42	41	6	6	119	65	42				
16	2	4	159	116	49	17	2	2	0	17	1	13	7	1	212	163	27	42	0	0	102	33	35	42	6	6	31	62	31	42	6	6	31	62	31				
18	2	4	98	140	98	18	2	2	205	193	28	14	7	1	0	28	1	43	0	0	217	214	17	43	6	6	57	6	56	43	6	6	57	6	56				
2	2	6	92	75	41	19	2	2	199	166	31	15	7	1	67	28	66	44	0	0	185	200	24	44	6	6	0	87	1	44	6	6	0	87	1	44	6	6	
4	2	6	844	860	10	2	2	2	230	226	6	0	8	1	611	612	14	45	0	0	98	57	97	45	6	6	218	211	26	45	6	6	218	211	26				
6	2	6	186	164	16	2	2	2	556	586	6	1	8	1	103	125	41	46	0	0	235	256	23	46	6	6	96	45	95	46	6	6	96	45	95				
8	2	6	1067	1041	31	3	2	2	346	348	6	2	8	1	139	115	27	47	0	0	0	73	1	47	6	6	68	1	68	47	6	6	68	1	68				
10	2	6	186	168	18	4	2	2	223	224	8	3	8	1	61	54	61	48	0	0	758	829	6	48	6	6	203	203	25	48	6	6	203	203	25				
12	2	6	457	470	14	5	2	2	572	588	10	4	8	1	109	43	40	49	0	0	665	687	6	49	6	6	94	31	57	49	6	6	94	31	57				
14	2	6	356	365	16	6	2	2	540	534	9	5	8	1	93	89	60	50	0	0	955	992	9	50	6	6	82	51	81	50	6	6	82	51	81				
16	2	6	622	630	15	7	2	2	167	153	13	6	8	1	137	43	45	51	0	0	606	625	10	51	6	6	182	224	22	51	6	6	182	224	22				
18	2	6	170	86	41	8	2	2	581	588	8	7	8	1	87	8	87	52	0	0	148	146	11	52	6	6	200	230	23	52	6	6	200	230	23				
2	2	8	247	267	37	9	2	2	146	104	17	8	8	1	106	65	61	53	0	0	209	209	9	53	6	6	183	202	27	53	6	6	183	202	27				
4	2	8	510	519	12	10	2	2	284	267	10	9	8	1	150	156	36	54	0	0	267	259	9	54	6	6	118	43	43	54	6	6	118</						

Table 6. Observed and calculated structure factors for hn4-076c

h	k	l	10Fo	10Fc	10s	h	k	l	10Fo	10Fc	10s	h	k	l	10Fo	10Fc	10s	h	k	l	10Fo	10Fc	10s						
14	1	1	0	12	1	6	6	3	305	301	10	9	1	4	418	393	7	1	6	4	76	59	49	5	2	5	155	134	10
15	1	1	0	51	1	7	6	3	127	74	23	10	1	4	346	352	8	2	6	4	271	267	10	5	6	2	71	55	33
16	1	1	89	70	88	8	6	3	285	286	12	10	1	4	208	215	12	3	6	4	124	117	22	6	7	5	225	221	9
17	1	1	277	281	19	9	6	6	314	321	13	12	1	4	186	176	15	4	6	4	87	80	35	8	8	2	402	388	10
18	1	1	187	171	32	10	6	6	54	20	54	13	1	4	162	189	21	5	6	4	115	110	26	9	9	5	152	154	14
19	1	1	203	183	30	11	6	6	190	184	23	14	1	4	395	396	13	6	6	4	119	103	28	10	2	2	96	69	28
0	0	1	204	201	12	12	6	6	117	112	46	15	1	4	150	129	30	7	6	4	109	94	32	11	1	1	243	254	12
1	1	1	128	154	13	13	6	6	240	232	20	16	1	4	119	121	45	8	6	4	223	236	17	12	2	2	139	135	24
2	2	2	229	237	8	14	6	6	105	47	86	17	1	4	295	274	18	8	6	4	146	142	31	13	3	3	137	96	27
3	3	3	561	617	10	15	6	6	26	66	26	18	1	4	164	170	36	10	6	4	74	96	73	14	4	4	60	17	59
4	4	4	1637	1619	39	16	6	6	115	89	76	19	1	4	141	129	50	11	6	4	2	46	2	15	5	5	117	103	44
5	5	5	155	150	10	1	7	7	96	65	37	20	0	0	573	571	17	12	6	4	144	163	39	16	6	6	40	29	39
6	6	6	125	93	15	2	7	7	58	72	57	21	0	0	408	436	8	13	6	4	96	78	95	17	7	7	85	50	85
7	7	7	84	23	28	3	7	7	307	301	11	22	2	2	891	929	12	14	6	4	0	34	1	18	8	8	104	53	103
8	8	8	317	315	11	4	7	7	170	164	20	3	3	3	134	135	11	15	6	4	176	161	34	19	9	9	158	153	43
9	9	9	245	243	10	5	7	7	168	144	20	4	4	4	37	39	36	16	6	4	75	9	75	19	1	1	138	112	12
10	10	10	187	183	13	6	7	7	339	360	12	5	5	5	649	648	11	1	7	4	102	39	35	2	2	2	269	297	8
11	11	11	276	262	11	7	7	7	89	79	66	6	6	6	329	320	7	2	7	4	319	308	11	3	3	3	168	171	11
12	12	12	336	353	10	8	7	7	105	52	56	7	7	7	233	204	10	3	7	4	29	52	29	4	4	4	188	191	11
13	13	13	196	201	17	9	7	7	112	39	53	8	8	8	403	410	7	4	7	4	281	295	13	5	5	5	77	38	28
14	14	14	64	55	64	10	7	7	104	125	60	9	9	9	300	282	11	5	7	4	121	75	32	6	6	6	293	285	8
15	15	15	87	121	86	11	7	7	135	97	40	10	10	10	218	183	12	6	7	4	79	38	78	7	7	7	117	110	18
16	16	16	80	39	79	12	7	7	41	31	41	11	11	11	260	269	12	7	7	4	242	239	18	8	8	8	192	205	11
17	17	17	172	115	30	13	7	7	18	19	18	12	12	12	75	51	74	8	7	4	134	162	39	9	9	9	107	122	24
18	18	18	87	39	87	14	7	7	0	122	1	13	13	13	196	203	17	9	7	4	53	99	52	10	10	10	106	97	28
19	19	19	72	59	72	15	0	0	178	145	38	14	14	14	128	117	32	10	7	4	168	148	30	11	11	11	224	220	14
0	0	2	106	121	15	0	8	8	222	203	22	15	15	15	235	257	19	11	7	4	223	226	22	12	12	12	240	244	17
1	1	2	232	251	7	1	8	8	278	277	14	16	16	16	195	210	25	12	7	4	90	88	90	13	13	13	207	233	17
2	2	2	506	522	7	2	8	8	310	292	15	17	17	17	112	90	57	13	7	4	140	167	49	14	14	14	88	100	59
3	3	2	79	5	21	3	3	3	123	101	42	18	18	18	141	152	45	14	7	4	175	72	38	15	15	15	174	159	25
4	4	2	169	160	11	4	4	4	143	66	32	19	19	19	136	94	55	15	7	4	76	23	75	16	16	16	245	239	21
5	5	2	64	31	41	6	6	6	127	75	40	2	2	2	60	42	31	0	4	4	138	70	55	17	17	17	172	158	31
6	6	2	548	536	9	7	7	7	104	96	65	3	3	3	40	2	40	2	2	4	52	21	52	18	18	18	112	124	74
7	7	2	0	53	1	8	8	8	95	77	95	4	4	4	386	376	7	3	3	4	147	111	33	19	19	19	172	71	68
8	8	2	305	326	10	9	8	8	137	24	44	5	5	5	171	159	11	4	4	4	216	175	20	0	0	0	233	221	13
9	9	2	129	83	25	10	8	8	0	50	1	6	6	6	394	384	8	5	4	4	277	275	15	1	1	1	71	67	34
10	10	2	91	5	44	11	8	8	0	9	1	7	7	7	86	34	26	6	6	4	439	437	12	2	2	2	85	60	27
11	11	2	165	153	21	12	8	8	76	58	75	8	8	8	239	249	9	7	7	4	192	182	28	3	3	3	120	100	18
12	12	2	128	120	29	13	8	8	136	23	54	9	9	9	398	383	8	8	8	4	0	20	1	4	4	4	184	211	12
13	13	2	82	33	82	1	9	9	111	122	60	10	10	10	119	99	23	9	8	4	87	75	87	5	5	5	173	153	12
14	14	2	125	143	43	2	9	9	103	86	102	11	11	11	127	132	24	10	8	4	116	158	52	6	6	6	142	137	16
15	15	2	136	93	43	3	9	9	153	94	36	12	12	12	180	158	18	11	8	4	100	60	100	7	7	7	103	98	26
16	16	2	235	226	25	4	9	9	73	95	73	13	13	13	237	252	14	12	8	4	134	95	58	8	8	8	94	79	32
17	17	2	173	75	38	5	9	9	95	25	94	14	14	14	304	306	14	13	8	4	98	58	97	10	10	10	0	45	1
18	18	2	102	60	29	6	9	9	48	66	48	15	15	15	0	27	1	1	9	4	105	98	69	11	11	11	173	154	19
19	19	2	125	126	16	7	9	9	105	81	95	16	16	16	77	73	76	2	9	4	119	70	59	12	12	12	98	98	41
0	0	2	286	300	8	8	9	9	105	21	104	17	17	17	28	29	27	3	9	4	55	72	54	13	13	13	119	77	34
1	1	2	125	121	14	9	9	9	73	153	73	18	18	18	131	134	52	4	9	4	251	225	20	14	14	14	99	7	60
2	2	2	596	578	9	10	9	9	180	187	42	19	19	19	122	72	67	5	9	4	23	10	22	15	15	15	132	136	41
3	3	2	538	552	10	11	9	9	0	53	1	20	20	20	46	23	45	6	6	4	105	25	105	16	16	16	0	41	1
4	4	2	490	483	7	10	10	10	43	203	43	1	1	1	814	818	8	7	9	4	0	57	1	17	17	17	97	91	96
5	5	2	306	308	8	10	10	10	73	91	72	2	2	2	723	741	7	8	8	4	327	340	20	18	18	18	156	34	54
6	6	2	192	205	12	11	10	10	174	43	39	3	3	3	37	18	37	9	9	4	117	34	114	1	1	1	96	114	28
7	7	2	268	266	11	3	10	10	156	54	64	4	4	4	607	600	9	10	10	4	158	55	47	2	2	2	144	156	14
8	8	2	118	56	26	4	10	10	108	57	107	5	5	5	330	314	8	6	6	4	200	140	42	3	3	3	182	174	11
9	9	2	160	155	20	5	10	10	108	22	107	6	6	6	161	152	13	1	10	4	163	130	40	4	4	4	117	100	20
10	10	2	109	108	36	6	10	10	151	168	151	7	7	7	264	258	9	2	10	4	180	149	38	5	5	5	281	275	9
11	11	2	32	39	31	7	10	10	110	177	109	8																	

Table 6. Observed and calculated structure factors for h<sub>v</sub>-076c

h	k	l	10Fo	10Fc	10s	h	k	l	10Fo	10Fc	10s	h	k	l	10Fo	10Fc	10s	h	k	l	10Fo	10Fc	10s
1	7	5	124	57	31	2	2	6	94	96	17	15	6	6	25	44	24	3	3	7	167	152	13
2	7	7	328	327	12	3	2	6	101	94	17	16	6	6	0	58	1	6	8	7	609	623	15
3	7	5	103	21	39	4	2	6	274	260	8	1	7	6	34	37	34	4	4	7	442	435	15
4	7	7	85	37	79	5	2	6	546	528	10	2	7	6	77	69	76	5	5	7	548	543	10
5	7	7	131	110	32	6	6	6	626	617	12	3	7	6	126	144	33	6	6	7	410	407	10
6	7	7	217	160	19	7	6	6	74	48	33	4	7	6	0	30	1	7	7	7	82	40	41
7	7	7	40	29	40	8	6	6	283	277	8	5	7	6	86	12	75	8	8	7	210	217	12
8	7	7	150	157	33	9	6	6	648	652	11	6	7	6	84	45	83	9	9	7	643	647	13
9	7	7	153	152	36	10	6	6	82	66	37	7	7	6	117	35	43	10	10	7	261	257	12
10	7	7	83	19	83	11	6	6	64	68	63	8	7	6	205	182	23	11	11	7	337	338	11
11	7	7	114	111	57	12	6	6	80	13	62	9	7	6	30	18	30	12	12	7	161	129	23
12	7	7	267	245	20	13	6	6	217	204	16	10	7	6	339	352	16	13	13	7	163	166	27
13	7	7	46	13	46	14	6	6	0	36	1	11	7	6	138	182	41	14	14	7	64	43	64
14	7	7	157	41	41	15	6	6	350	365	14	12	7	6	123	78	53	15	15	7	299	316	21
15	7	7	427	465	18	16	6	6	120	19	52	13	7	6	157	121	39	16	16	7	118	36	83
16	7	7	222	224	19	17	6	6	153	88	38	14	7	6	94	2	93	17	17	7	0	29	1
17	7	7	181	189	25	18	6	6	98	89	97	15	8	6	133	119	49	18	18	7	664	657	14
18	7	7	220	206	20	19	6	6	124	18	63	16	8	6	100	10	58	19	19	7	90	9	31
19	7	7	80	74	79	20	6	6	292	299	7	2	8	6	158	126	30	20	20	7	124	79	19
20	7	7	238	235	19	21	6	6	85	81	23	3	8	6	106	115	58	21	21	7	463	464	8
21	7	7	82	65	81	22	6	6	476	487	11	4	8	6	137	86	36	22	22	7	172	166	14
22	7	7	228	224	23	23	6	6	288	267	9	5	8	6	263	250	18	23	23	7	112	77	24
23	7	7	205	240	28	24	6	6	662	659	17	6	8	6	0	39	1	24	24	7	37	42	36
24	7	7	147	131	42	25	6	6	137	124	14	7	8	6	109	109	72	25	25	7	63	63	62
25	7	7	54	25	53	26	6	6	68	68	42	8	8	6	244	259	22	26	26	7	110	83	27
26	7	7	49	21	48	27	6	6	124	99	18	9	8	6	181	174	34	27	27	7	226	222	14
27	7	7	124	49	63	28	6	6	402	394	9	10	8	6	0	29	1	28	28	7	220	215	16
28	7	7	103	91	103	29	6	6	58	55	57	11	8	6	125	127	58	29	29	7	260	265	16
29	7	7	115	134	51	30	6	6	151	154	21	12	8	6	156	119	42	30	30	7	114	142	42
30	7	7	90	59	89	31	6	6	170	150	20	13	9	6	96	130	95	31	31	7	81	57	81
31	7	7	107	11	79	32	6	6	163	152	23	14	9	6	107	51	68	32	32	7	257	245	19
32	7	7	121	73	56	33	6	6	146	112	27	15	9	6	226	237	25	33	33	7	71	103	70
33	7	7	77	52	77	34	6	6	128	123	39	16	9	6	133	110	51	34	34	7	134	119	50
34	7	7	113	32	68	35	6	6	0	62	1	17	9	6	166	198	35	35	35	7	0	19	1
35	7	7	104	47	103	36	6	6	116	112	66	18	9	6	0	39	1	36	36	7	184	184	12
36	7	7	93	105	93	37	6	6	143	82	60	19	9	6	100	97	100	37	37	7	191	201	13
37	7	7	0	26	1	38	6	6	674	667	14	20	9	6	0	61	1	38	38	7	0	26	1
38	7	7	44	17	43	39	6	6	797	791	10	21	9	6	170	168	64	39	39	7	309	293	11
39	7	7	361	319	27	40	6	6	68	69	42	22	9	6	149	148	60	40	40	7	162	116	18
40	7	7	0	0	1	41	6	6	264	252	11	23	9	6	0	9	1	41	41	7	223	238	15
41	7	7	94	75	93	42	6	6	195	207	13	24	9	6	159	119	43	42	42	7	120	81	27
42	7	7	118	100	72	43	6	6	417	391	9	25	9	6	347	328	19	43	43	7	34	93	34
43	7	7	244	178	27	44	6	6	327	336	8	26	9	6	55	4	54	44	44	7	83	93	83
44	7	7	0	57	1	45	6	6	229	220	11	27	9	6	143	85	54	45	45	7	57	65	56
45	7	7	57	89	57	46	6	6	94	113	31	28	9	6	132	64	77	46	46	7	202	200	20
46	7	7	0	16	1	47	6	6	115	88	26	29	9	6	98	29	98	47	47	7	351	355	14
47	7	7	945	1015	27	48	6	6	278	273	11	30	9	6	591	598	10	48	48	7	114	115	49
48	7	7	37	31	37	49	6	6	85	77	64	31	9	6	1244	1241	25	49	49	7	132	114	45
49	7	7	1051	1084	29	50	6	6	68	7	67	32	9	6	414	411	7	50	50	7	108	14	67
50	7	7	792	779	10	51	6	6	136	63	32	33	9	6	673	632	10	51	51	7	90	22	90
51	7	7	595	577	16	52	6	6	211	222	22	34	9	6	651	626	9	52	52	7	51	57	51
52	7	7	225	231	13	53	6	6	164	151	33	35	9	6	145	144	14	53	53	7	350	333	16
53	7	7	328	314	10	54	6	6	118	24	65	36	9	6	396	379	8	54	54	7	102	29	36
54	7	7	1122	1091	17	55	6	6	0	34	1	37	9	6	183	199	12	55	55	7	142	98	21
55	7	7	164	138	18	56	6	6	25	79	25	38	9	6	153	156	15	56	56	7	60	43	59
56	7	7	115	62	40	57	6	6	339	330	8	39	9	6	799	790	10	57	57	7	58	36	57
57	7	7	445	468	11	58	6	6	480	476	10	40	9	6	46	1	46	58	58	7	79	13	74
58	7	7	249	240	15	59	6	6	410	424	9	41	9	6	163	147	20	59	59	7	259	258	14
59	7	7	216	239	19	60	6	6	307	313	10	42	9	6	95	68	49	60	60	7	84	29	76
60	7	7	222	199	24	61	6	6	222	214	12	43	9	6	161	133	27	61	61	7	346	336	17
61	7	7	0	63	1	62	6	6	105	91	29	44	9	6	203	67	58	62	62	7	313	313	16
62	7	7	399	410	23	63	6	6	84	2	53	45	9	6	203	210	25	63	63	7	167	123	30
63	7	7	133	96	63	64	6	6	108	48	38	46	9	6	61	70	61	64	64	7	69	94	68
64	7	7	105	92	105	65	6	6	192	214	21	47	9	6	138	45	47	65	65	7	290	294	17
65	7	7	227	214	36	66	6	6	137	76	29	48	9	6	81	135	80	66	66	7	30	22	29
66	7	7	140	139	83	67	6	6	217	224	19	49	9	6	331	340	20	67	67	7	77	102	76
67	7	7	478	467	6	68	6	6	129	127	36	50	9	6	177	163	9	68	68	7	26	89	26
68	7	7	584	584	9	69	6	6	99	93	64	51	9	6	1209	1214	21	69	69	7	48	4	48
69	7	7	675	684	13	70	6	6	169	160	30	52	9	6	217	210	9	70	70	7	391	386	11
70	7	7	880	865	12	71	6	6	142	118	42	53	9	6	509	514	9	71	71	7	129	125	31
71	7	7	363	363	6	72	6	6	151	122	44	54	9	6	111	94	18	72	72	7	300	285	14
72	7	7																					

Table 6. Observed and calculated structure factors for hrX-076c

h	k	l	10Fo	10Fc	10s	h	k	l	10Fo	10Fc	10s	h	k	l	10Fo	10Fc	10s	h	k	l	10Fo	10Fc	10s	h	k	l	10Fo	10Fc	10s	h	k	l	10Fo	10Fc	10s						
8	3	8	139	170	18	12	8	8	103	89	103	17	4	9	97	18	96	17	0	10	172	106	54	14	5	10	100	108	99	14	5	10	100	108	99						
9	8	8	156	134	17	1	9	8	160	101	35	18	0	10	304	313	11	18	0	10	414	417	22	15	5	10	0	17	1	15	5	10	0	17	1						
10	3	8	106	53	32	2	9	8	161	186	36	2	5	9	129	140	22	1	1	10	352	352	7	16	5	10	52	59	51	16	5	10	52	59	51						
11	8	8	163	138	21	3	9	8	184	148	33	3	5	9	178	157	16	2	1	10	179	179	10	0	6	10	181	171	29	0	6	10	181	171	29						
12	3	8	0	18	1	4	9	8	53	35	52	4	5	9	139	117	22	2	1	10	334	336	7	1	6	10	62	80	61	1	6	10	62	80	61						
13	8	8	77	45	77	5	9	8	148	108	44	5	5	9	114	79	29	4	1	10	81	20	32	2	6	10	73	34	73	2	6	10	73	34	73						
14	8	8	96	26	74	6	9	8	105	36	105	6	5	9	77	52	76	5	1	10	12	3	12	3	6	10	145	111	28	3	6	10	145	111	28						
15	3	8	132	122	44	7	9	8	84	41	83	7	5	9	160	107	22	6	1	10	777	735	12	4	6	10	70	18	69	4	6	10	70	18	69						
16	8	8	89	114	88	8	9	8	0	2	1	8	5	9	165	155	23	6	1	10	84	63	33	5	6	10	405	408	21	5	6	10	405	408	21						
17	3	8	124	105	65	9	9	8	120	49	119	9	5	9	80	31	80	7	1	10	148	137	18	6	6	10	171	156	27	6	6	10	171	156	27						
18	8	8	0	19	1	10	8	8	0	31	1	10	5	9	311	318	17	8	1	10	175	188	15	6	6	10	182	215	23	6	6	10	182	215	23						
0	4	8	45	66	45	1	10	8	77	43	77	11	5	9	117	63	48	10	1	10	235	241	12	8	6	10	209	203	21	8	6	10	209	203	21						
1	4	8	332	336	9	2	10	8	193	180	36	12	5	9	315	303	16	11	1	10	98	92	36	9	6	10	88	35	88	9	6	10	88	35	88						
2	4	8	111	73	21	3	10	8	165	168	43	13	5	9	32	38	32	12	1	10	83	70	63	10	6	10	122	27	52	10	6	10	122	27	52						
3	4	8	200	201	12	4	1	9	129	144	69	14	5	9	124	122	52	13	1	10	401	407	12	11	6	10	258	273	22	11	6	10	258	273	22						
4	4	8	355	343	9	1	1	9	373	390	6	15	5	9	153	152	42	14	1	10	447	482	13	12	6	10	119	2	57	12	6	10	119	2	57						
5	4	8	162	150	17	2	1	9	353	373	6	16	5	9	0	21	1	15	1	10	0	100	1	13	6	10	268	223	22	13	6	10	268	223	22						
6	4	8	201	209	14	3	1	9	476	465	9	0	6	9	51	87	50	16	1	10	95	92	95	14	6	10	70	53	70	14	6	10	70	53	70						
7	4	8	105	70	33	4	1	9	382	351	7	1	6	9	271	267	14	17	1	10	138	119	50	1	7	10	220	230	19	1	7	10	220	230	19						
8	4	8	0	7	1	5	1	9	196	187	12	2	6	9	70	20	70	18	1	10	185	185	36	2	7	10	72	54	71	2	7	10	72	54	71						
9	4	8	323	332	12	6	1	9	125	112	18	3	6	9	95	61	45	0	2	10	120	45	24	3	7	10	89	62	88	3	7	10	89	62	88						
10	4	8	281	298	15	7	1	9	275	276	9	4	6	9	0	48	1	0	1	10	79	48	28	4	7	10	54	59	54	4	7	10	54	59	54						
11	4	8	177	160	23	8	1	9	748	719	10	5	6	9	142	110	27	2	2	10	424	412	8	5	7	10	54	98	53	5	7	10	54	98	53						
12	4	8	109	15	46	9	1	9	256	236	10	6	6	9	145	137	27	3	2	10	312	309	9	6	6	10	76	17	75	6	6	10	76	17	75						
13	4	8	0	1	1	10	1	9	392	383	8	7	6	9	162	151	25	4	4	10	50	8	50	7	7	10	67	98	66	7	7	10	67	98	66						
14	4	8	271	259	18	11	1	9	210	198	14	8	6	9	154	122	31	5	2	10	334	331	8	8	7	10	132	121	49	8	7	10	132	121	49						
15	4	8	0	25	1	12	1	9	125	146	28	9	6	9	170	165	28	6	2	10	82	33	33	9	7	10	274	290	23	9	7	10	274	290	23						
16	4	8	51	79	50	13	1	9	111	109	40	10	6	9	245	267	21	7	2	10	662	657	12	10	7	10	179	158	34	10	7	10	179	158	34						
17	4	8	99	6	98	14	1	9	238	240	19	11	6	9	118	31	58	8	2	10	151	133	18	11	7	10	129	85	56	11	7	10	129	85	56						
1	5	8	37	13	37	15	1	9	126	118	42	12	6	9	53	41	52	9	9	10	370	369	9	12	7	10	159	71	47	12	7	10	159	71	47						
2	5	8	498	516	9	16	1	9	187	203	28	13	6	9	166	9	35	10	2	10	151	134	20	13	7	10	139	54	52	13	7	10	139	54	52						
3	5	8	293	287	10	17	1	9	57	3	56	14	6	9	118	69	64	11	2	10	454	478	10	0	8	10	30	110	30	0	8	10	30	110	30	30					
4	5	8	209	199	13	18	0	9	73	65	72	15	6	9	49	62	49	12	2	10	111	113	50	1	8	10	147	119	35	1	8	10	147	119	35						
5	5	8	65	28	64	0	2	9	348	377	11	1	7	9	114	117	41	13	2	10	191	205	22	2	8	10	122	53	46	2	8	10	122	53	46						
6	5	8	143	124	25	1	1	9	414	417	8	2	7	9	263	267	17	14	2	10	129	120	39	3	8	10	99	45	69	3	8	10	99	45	69						
7	5	8	215	228	16	2	2	9	105	32	20	3	7	9	87	79	86	15	2	10	0	1	1	4	8	10	158	177	37	4	8	10	158	177	37						
8	5	8	70	84	69	3	2	9	320	315	9	4	7	9	248	243	19	16	2	10	95	89	95	5	8	10	149	127	39	5	8	10	149	127	39						
9	5	8	205	176	20	4	4	9	158	151	15	5	7	9	161	119	31	17	2	10	125	33	68	6	8	10	103	68	102	6	8	10	103	68	102						
10	5	8	409	410	17	5	5	9	120	93	19	6	7	9	167	144	28	18	2	10	293	273	24	7	8	10	174	209	45	7	8	10	174	209	45						
11	5	8	328	325	22	6	6	9	729	719	11	7	7	9	88	71	87	1	3	10	497	513	9	8	8	10	71	48	71	1	3	10	71	48	71						
12	5	8	326	342	16	7	2	9	81	68	35	8	7	9	316	320	18	2	3	10	403	403	11	9	8	10	0	52	1	9	8	10	0	52	1	9	8	10	0	52	1
13	5	8	0	35	1	8	8	9	126	110	20	9	7	9	105	7	75	3	3	10	100	63	26	10	8	10	140	30	67	10	8	10	140	30	67						
14	5	8	72	30	71	9	9	9	284	273	10	10	7	9	54	35	53	4	3	10	447	443	10	11	8	10	145	54	78	4	3	10	145	54	78						
15	5	8	0	69	1	10	1	9	145	126	20	11	7	9	110	30	78	5	3	10	294	291	10	1	9	10	69	93	69	1	9	10	69	93	69						
16	5	8	87	56	86	11	2	9	120	14	28	12	7	9	179	189	34	6	3	10	134	122	22	2	9	10	122	56	51	2	9	10	122	56	51						
0	6	8	152	107	34	12	2	9	267	285	14	13	7	9	31	30	30	7	7	10	42	89	42	3	9	10	139	175	44	3	9	10	139	175	44						
1	6	8	0	0	1	13	9	9	165	149	23	0	8	9	221	245	31	8	8	10	294	311	12	4	9	10	67	2	67	4	9	10	67	2	67						
2	6	8	115	94	31	14	2	9	284	296	16	1	1	9	0	61	1	9	3	10	339	326	15	5	9	10	82</														

Table 6. Observed and calculated structure factors for h<sub>n</sub>k-076c

h	k	l	10Fo	10Fc	10s	h	k	l	10Fo	10Fc	10s	h	k	l	10Fo	10Fc	10s	h	k	l	10Fo	10Fc	10s	h	k	l	10Fo	10Fc	10s	h	k	l	10Fo	10Fc	10s	
16	2	11	145	106	52	9	8	11	42	13	42	9	4	12	153	153	28	5	2	13	221	229	13	4	8	13	173	97	32	4	8	13	173	97	32	
17	1	11	133	79	64	10	8	11	164	93	56	10	4	12	427	438	14	5	2	13	163	154	19	5	8	13	128	100	69	5	8	13	128	100	69	
1	1	11	116	86	21	10	1	11	101	80	86	11	4	12	141	116	38	6	7	13	127	125	32	6	8	13	104	63	103	6	8	13	104	63	103	
2	3	11	101	115	25	2	3	9	11	14	40	12	4	12	147	147	36	8	2	13	124	115	32	8	7	13	149	107	61	8	7	13	149	107	61	
3	3	11	166	160	15	3	9	11	126	1	56	13	4	12	77	11	77	9	9	13	258	267	15	9	8	13	96	4	95	9	9	13	96	4	95	
4	5	11	427	416	11	4	5	9	11	0	44	14	4	12	98	95	98	10	2	13	149	155	28	10	1	13	157	105	41	10	1	13	157	105	41	
5	5	11	104	18	31	5	5	9	11	102	20	15	4	12	138	119	49	11	2	13	75	66	74	11	2	13	31	14	31	11	2	13	31	14	31	
6	6	11	0	36	1	6	6	9	11	65	7	16	4	12	168	120	42	12	2	13	0	39	1	12	2	13	124	18	59	12	2	13	124	18	59	
7	7	11	242	227	14	7	7	9	11	0	63	1	5	12	209	214	18	13	2	13	140	68	39	13	2	13	141	62	59	13	2	13	141	62	59	
8	8	11	68	21	67	0	0	12	95	140	54	2	5	12	110	90	38	14	2	13	118	36	59	14	2	13	995	966	42	14	2	13	995	966	42	
9	9	11	292	296	13	1	1	0	12	629	614	3	5	12	112	166	39	15	2	13	159	140	44	15	2	13	90	77	49	15	2	13	90	77	49	
10	11	11	896	920	20	2	2	0	12	227	229	4	5	12	399	400	12	16	2	13	26	27	26	16	2	13	179	170	19	16	2	13	179	170	19	
11	11	11	531	546	12	3	3	0	12	956	973	5	5	12	150	154	26	17	1	13	51	43	50	17	1	13	267	251	14	17	1	13	267	251	14	
12	11	11	297	303	16	4	4	0	12	186	166	6	5	12	165	95	27	18	2	13	88	108	37	18	2	13	160	154	23	18	2	13	160	154	23	
13	11	11	134	180	40	5	5	0	12	75	36	7	5	12	77	95	77	19	3	13	74	58	73	19	3	13	287	284	16	19	3	13	287	284	16	
14	11	11	180	126	28	6	6	0	12	275	287	8	5	12	343	337	17	20	4	13	236	235	13	20	4	13	384	391	15	20	4	13	384	391	15	
15	11	11	0	28	1	7	7	0	12	0	51	9	5	12	133	103	35	21	5	13	212	209	14	21	5	13	141	143	37	21	5	13	141	143	37	
16	11	11	241	212	27	8	8	0	12	125	100	10	5	12	142	24	40	22	6	13	159	161	21	22	6	13	25	19	25	22	6	13	25	19	25	
17	11	11	128	5	75	9	9	0	12	67	57	11	5	12	236	221	23	23	7	13	286	275	13	23	7	13	235	258	22	23	7	13	235	258	22	
0	0	11	562	569	15	10	10	0	12	72	17	12	5	12	187	179	31	24	8	13	50	28	50	24	8	13	207	174	24	24	8	13	207	174	24	
1	4	11	215	219	13	11	11	0	12	136	72	13	5	12	184	176	31	25	9	13	122	137	36	25	9	13	229	220	23	25	9	13	229	220	23	
2	4	11	125	91	22	12	12	0	12	140	94	14	5	12	187	137	32	26	10	13	215	229	20	26	10	13	138	118	52	26	10	13	138	118	52	
3	4	11	71	42	71	13	13	0	12	346	360	15	5	12	144	50	50	27	11	13	115	129	53	27	11	13	70	8	70	27	11	13	70	8	70	
4	4	11	30	65	29	14	14	0	12	245	168	16	6	12	146	62	46	28	12	13	226	232	22	28	12	13	68	38	68	28	12	13	68	38	68	
5	4	11	69	3	68	15	15	0	12	191	183	17	6	12	166	148	25	29	13	13	93	96	93	29	13	13	146	57	146	29	13	13	146	57	146	
6	4	11	449	458	13	16	16	0	12	241	193	18	6	12	135	89	32	30	14	13	192	182	29	30	14	13	51	97	50	30	14	13	51	97	50	
7	4	11	93	24	49	17	17	0	12	193	195	19	6	12	126	133	37	31	15	13	137	48	51	31	15	13	364	371	8	31	15	13	364	371	8	
8	4	11	216	195	17	1	1	1	12	231	233	2	6	12	0	34	1	32	16	0	13	191	103	39	2	1	14	258	248	10	2	1	14	258	248	10
9	4	11	0	24	1	2	2	1	12	106	62	3	6	12	244	228	20	3	1	14	99	47	87	3	1	14	160	135	15	3	1	14	160	135	15	
10	4	11	95	24	70	3	3	1	12	94	65	4	6	12	160	157	33	4	1	14	263	243	14	4	1	14	296	285	11	4	1	14	296	285	11	
11	4	11	0	85	1	4	4	1	12	220	185	5	6	12	516	540	14	5	1	14	94	97	50	5	1	14	56	5	55	5	1	14	56	5	55	
12	4	11	105	3	58	5	5	1	12	114	114	6	6	12	163	186	33	6	1	14	129	116	27	6	1	14	193	152	17	6	1	14	193	152	17	
13	4	11	119	95	48	6	6	1	12	164	174	7	6	12	75	75	74	7	1	14	218	226	16	7	1	14	172	169	20	7	1	14	172	169	20	
14	4	11	321	321	17	7	7	1	12	179	155	8	6	12	123	101	53	8	1	14	136	107	25	8	1	14	171	128	21	8	1	14	171	128	21	
15	4	11	123	12	55	8	8	1	12	76	57	9	6	12	143	29	44	9	1	14	20	4	20	9	1	14	101	68	43	9	1	14	101	68	43	
16	4	11	97	76	97	9	9	1	12	200	201	10	6	12	87	54	87	10	1	14	76	52	76	10	1	14	51	35	51	10	1	14	51	35	51	
1	5	11	84	30	61	10	1	1	12	424	402	11	6	12	191	159	33	11	1	14	186	186	22	11	1	14	215	219	18	11	1	14	215	219	18	
2	5	11	211	212	17	11	1	1	12	110	72	12	7	12	0	34	1	12	1	14	232	229	18	12	1	14	74	68	73	12	1	14	74	68	73	
3	5	11	50	51	49	12	1	1	12	251	255	13	7	12	145	146	32	13	1	14	295	291	17	13	1	14	0	38	1	13	1	14	0	38	1	
4	5	11	247	230	15	13	1	1	12	267	252	14	7	12	108	80	54	14	1	14	109	87	63	14	1	14	47	5	47	14	1	14	47	5	47	
5	5	11	113	95	35	14	1	1	12	0	21	1	4	12	222	230	21	15	1	14	93	117	92	15	1	14	92	94	92	15	1	14	92	94	92	
6	5	11	362	358	12	15	1	1	12	141	69	16	7	12	165	152	33	16	1	14	69	19	69	16	1	14	83	123	82	16	1	14	83	123	82	
7	5	11	84	84	70	16	1	1	12	1	1	1	7	12	0	31	1	17	1	14	116	92	64	17	1	14	199	170	20	17	1	14	199	170	20	
8	5	11	151	151	27	17	1	1	12	158	119	18	7	12	0	24	1	18	1	14	82	79	81	18	1	14	250	243	10	18	1	14	250	243	10	
9	5	11	138	136	34	0	0	2	12	338	341	19	7	12	199	195	35	19	1	14	99	40	51	19	1	14	135	156	20	19	1	14	135	156	20	
10	5	11	101	113	72	1	1	2	12	299	291	20	7	12	0	45	83	20	2	14	92	86	57	20	2	14	201	194	14	20	2	14	201	194	14	
11	5	11	76	58	76	2	2	2	12	63	0	21	7	12	0	17	1	21	2	14	62	25	61	21	2	14	85	14	46	21	2	14	85	14	46	
1																																				

Table 6. Observed and calculated structure factors for hr4-076c

h	k	l	10Fo	10Fc	10s	h	k	l	10Fo	10Fc	10s	h	k	l	10Fo	10Fc	10s	h	k	l	10Fo	10Fc	10s	h	k	l	10Fo	10Fc	10s	
13	4	14	150	105	42	6	3	15	101	56	48	6	1	16	102	119	67	3	8	16	43	36	42	1	8	17	124	139	67	
14	4	14	58	65	58	7	3	15	81	17	80	7	1	16	0	38	1	0	0	18	1008	1018	31	0	0	18	1008	1018	31	
15	4	14	157	156	44	8	3	15	170	146	25	8	1	16	219	226	19	4	8	16	32	42	31	0	0	18	333	341	15	
1	5	14	124	52	38	9	3	15	185	149	23	9	1	16	157	149	28	2	0	18	114	95	27	0	0	18	153	145	35	
2	5	14	132	116	35	10	3	15	254	250	18	10	1	16	0	25	1	3	0	18	57	51	56	2	0	18	250	276	20	
3	5	14	307	289	15	11	3	15	149	143	40	11	1	16	81	87	80	4	0	18	0	29	1	0	0	18	75	97	97	
4	5	14	52	58	51	12	3	15	232	233	23	12	1	16	254	227	19	5	0	18	234	234	16	4	0	18	89	57	88	
5	5	14	196	183	22	13	3	15	239	217	24	13	1	16	116	125	71	6	0	18	180	155	21	5	0	18	662	644	18	
6	5	14	108	39	62	14	3	15	0	35	1	14	1	16	0	51	1	7	0	18	25	7	25	6	0	18	140	100	54	
7	5	14	239	208	22	15	3	15	0	28	1	15	1	16	94	85	93	8	0	18	0	0	14	1	0	18	108	61	107	
8	5	14	330	324	16	0	4	15	120	74	60	0	2	16	87	2	87	9	0	18	80	54	79	8	0	18	293	271	25	
9	5	14	170	121	40	1	4	15	175	192	24	1	2	16	31	51	31	10	0	18	0	24	1	10	0	18	118	15	117	
10	5	14	376	369	16	2	4	15	0	27	1	2	2	16	0	72	1	11	0	18	128	23	42	10	0	18	95	31	95	
11	5	14	53	73	52	3	4	15	236	250	18	3	2	16	238	221	14	12	0	18	171	159	31	12	0	18	145	169	69	
12	5	14	180	152	35	4	4	15	0	73	1	4	2	16	73	38	72	13	0	18	118	63	57	13	0	18	89	90	89	
13	5	14	189	143	33	5	4	15	47	55	46	5	2	16	167	127	23	14	0	18	50	59	50	14	0	18	126	116	126	
14	5	14	172	231	72	6	4	15	124	11	41	6	2	16	109	99	43	15	0	18	53	28	52	1	1	18	159	154	22	
1	6	14	213	238	33	7	4	15	284	287	17	7	2	16	137	99	32	16	0	18	266	279	28	1	1	18	331	349	12	
2	6	14	217	216	22	8	4	15	225	230	19	8	2	16	116	18	67	17	0	18	212	214	19	3	1	18	341	341	12	
3	6	14	94	25	85	9	4	15	67	82	67	9	2	16	94	18	68	18	0	18	569	583	11	4	1	18	208	217	19	
4	6	14	63	48	63	10	4	15	59	65	59	10	2	16	30	154	29	19	0	18	105	74	42	5	1	18	306	288	14	
5	6	14	209	223	23	11	4	15	145	106	43	11	2	16	120	83	49	20	0	18	91	47	52	6	1	18	74	68	73	
6	6	14	151	135	34	12	4	15	140	95	50	12	2	16	117	60	56	21	0	18	260	263	21	7	1	18	171	139	29	
7	6	14	430	433	15	13	4	15	171	158	36	13	2	16	120	45	60	22	0	18	86	46	85	8	1	18	237	221	20	
8	6	14	161	61	37	14	4	15	0	81	25	1	14	2	16	101	62	100	9	0	18	107	77	50	9	1	18	83	102	83
9	6	14	101	70	101	1	5	15	81	85	80	15	2	16	0	67	1	10	0	18	156	156	27	10	1	18	263	277	19	
10	6	14	0	0	0	2	5	15	24	19	24	9	3	16	182	205	23	11	0	18	325	328	15	11	1	18	92	7	91	
11	6	14	67	33	67	3	5	15	265	270	18	3	3	16	240	250	17	12	0	18	254	243	20	12	1	18	157	78	65	
12	6	14	151	159	57	4	5	15	128	118	38	4	3	16	275	281	20	13	0	18	0	0	11	13	1	18	83	65	82	
1	7	14	0	22	1	5	5	15	159	145	30	5	4	16	127	67	32	14	0	18	0	13	1	14	1	18	106	70	106	
2	7	14	99	119	74	6	5	15	184	185	29	6	3	16	130	70	34	15	0	18	110	21	44	0	2	18	116	80	63	
3	7	14	134	99	41	7	5	15	111	125	57	7	3	16	267	271	16	16	0	18	97	98	56	2	2	18	254	270	17	
4	7	14	77	41	77	8	5	15	12	60	12	8	3	16	169	107	26	17	0	18	64	36	64	3	2	18	94	74	56	
5	7	14	137	40	47	9	5	15	41	65	41	9	3	16	127	103	39	18	0	18	210	226	21	4	2	18	169	161	25	
6	7	14	117	0	61	10	5	15	0	82	1	10	3	16	174	162	30	19	0	18	129	102	34	5	2	18	38	109	38	
7	7	14	0	34	1	11	5	15	118	122	75	11	3	16	157	118	38	20	0	18	126	119	39	6	2	18	201	226	23	
8	7	14	174	222	48	12	5	15	94	87	94	12	3	16	56	5	55	21	0	18	261	209	20	7	2	18	131	47	39	
9	7	14	44	225	44	13	6	15	0	33	1	13	3	16	52	31	51	22	0	18	98	52	63	8	2	18	96	3	73	
10	7	14	129	73	83	1	6	15	0	24	1	14	3	16	125	25	62	23	0	18	137	82	37	9	2	18	108	83	58	
11	8	14	55	22	55	2	6	15	251	258	19	0	4	16	278	296	23	24	0	18	134	105	40	10	2	18	155	105	36	
12	8	14	156	166	37	3	6	15	161	180	31	1	4	16	58	51	58	25	0	18	119	94	56	11	2	18	90	33	89	
13	8	14	224	225	25	4	6	15	164	172	41	2	4	16	142	145	32	26	0	18	0	45	1	12	2	18	123	143	64	
14	8	14	161	130	43	5	6	15	146	120	40	3	4	16	195	167	23	27	0	18	172	124	39	13	2	18	118	44	93	
15	8	14	151	86	40	6	6	15	198	200	31	4	4	16	292	311	16	28	0	18	131	121	55	13	3	18	174	95	26	
16	8	14	140	116	50	7	6	15	129	142	55	5	4	16	192	228	25	29	0	18	124	69	64	4	3	18	473	508	13	
1	8	14	160	27	54	8	6	15	258	188	26	6	4	16	130	103	41	30	0	18	104	68	55	5	3	18	335	343	14	
2	8	14	108	59	107	9	6	15	102	7	101	7	4	16	148	99	39	31	0	18	165	201	28	6	3	18	35	0	34	
3	8	14	0	0	0	10	6	15	134	88	75	8	4	16	319	312	16	32	0	18	50	32	50	7	3	18	42	72	41	
4	8	14	201	189	65	11	6	15	72	81	71	9	4	16	181	198	27	33	0	18	137	1	1	8	3	18	141	80	1	
5	8	14	170	154	15	1	7	15	56	36	56	10	4	16	81	51	80	34	0	18	110	106	54	9	3	18	205	174	26	
6	8	14	195	208	13	2	7	15	71	71	71	11	4	16	28	133	27	35	0	18	205	206	25	10	3	18	109	107	59	
7	8	14	211	171	13	3	7	15	196	179	27	12	4	16	227	266	28	36	0	18	394	418	16	11	3	18	115	86	60	
8	8	14	105	87	31	4	7	15	130	137	48	13	4	16	161	48	61	37	0	18	162	63	36	10	3	18	115	86	60	
9	8	14	0	47	1	5	7	15	25	11	24	1	5	16	0	52	1	38	0	18	74	94	74	11	3	18	190	129	34	
10	8	14	85	75	70	6	7	15	195	156	32	2	5	16	234	256	19	39	0	18	151	146	49	12	3	18	90	35	89	
11	8	14	93	17	50	7	7	15	115	107	82	3	5	16	111	26	50	40	0	18	88	58	87	13	3	18	152	95	151	
12	8	14	94	37	52	8	7	15	197	144	38	4	5	16	126	45	43	41	0	18</										

Table 6. Observed and calculated structure factors for h<sub>n</sub>-076c

h	k	l	10Fo	10Fc	10s	h	k	l	10Fo	10Fc	10s	h	k	l	10Fo	10Fc	10s	h	k	l	10Fo	10Fc	10s	h	k	l	10Fo	10Fc	10s
7	6	18	68	92	68	2	5	19	43	38	42	4	3	20	111	41	62	6	3	21	263	297	25	0	4	22	220	256	40
8	6	18	81	86	80	3	5	19	112	25	61	5	3	20	167	140	32	7	3	21	129	80	62	1	4	22	163	73	38
1	7	18	158	109	42	4	5	19	162	114	36	6	3	20	133	112	56	8	3	21	158	92	45	2	4	22	0	5	1
2	7	18	108	131	83	5	5	19	152	139	40	7	3	20	114	9	77	9	3	21	0	101	1	3	4	22	189	113	32
3	7	18	83	70	83	6	5	19	0	17	1	8	3	20	83	68	83	0	4	21	304	288	27	4	4	22	0	33	1
4	7	18	84	10	83	7	5	19	146	125	54	9	3	20	165	81	46	1	4	21	0	68	1	5	4	22	148	167	46
5	7	18	139	5	60	8	5	19	129	91	66	10	3	20	174	68	48	2	4	21	155	128	38	6	4	22	114	37	113
1	1	19	201	195	20	9	5	19	41	68	41	0	0	20	336	364	25	3	4	21	0	27	1	1	5	22	160	136	42
2	1	19	114	2	40	0	6	19	165	87	57	1	4	20	79	7	79	4	4	21	260	261	22	2	5	22	197	137	33
3	1	19	98	114	53	1	6	19	141	103	46	2	4	20	234	223	23	5	4	21	0	62	1	3	5	22	52	70	52
4	1	19	163	163	25	2	6	19	125	24	56	3	4	20	123	126	51	4	4	21	106	60	105	1	1	23	164	122	53
5	1	19	116	48	47	3	6	19	137	114	55	4	4	20	82	74	81	6	4	21	138	28	58	2	2	23	80	46	80
6	1	19	72	55	71	4	6	19	0	5	1	5	4	20	139	65	44	8	4	21	93	28	92	3	3	23	164	122	53
7	1	19	148	147	36	5	6	19	15	26	14	6	4	20	117	98	70	1	5	21	109	127	80	4	4	23	150	99	53
8	1	19	110	20	62	6	6	19	126	80	71	7	4	20	184	109	36	2	5	21	87	17	87	5	5	23	115	54	114
9	1	19	150	96	36	7	6	19	131	56	69	8	4	20	134	107	73	3	5	21	54	21	53	6	6	23	191	42	42
10	1	19	139	68	47	1	7	19	155	137	42	9	4	20	100	0	99	4	5	21	221	186	28	7	7	23	89	59	89
11	1	19	126	26	58	2	7	19	144	119	53	1	5	20	114	134	65	5	5	21	217	174	29	8	8	23	202	55	78
12	1	19	53	87	52	0	0	20	568	571	19	2	5	20	104	120	86	5	5	21	92	69	92	0	0	23	0	40	1
13	1	19	0	86	1	1	1	0	20	56	56	3	5	20	165	180	36	0	6	21	199	69	51	1	1	23	155	123	42
1	1	20	500	499	18	2	2	0	20	119	129	4	4	20	126	111	58	1	6	21	56	12	56	2	2	23	160	121	41
2	2	20	447	463	13	3	0	20	75	99	75	5	5	20	108	113	79	0	0	22	252	120	70	3	2	23	92	115	91
3	2	20	108	67	48	4	4	0	20	491	500	6	5	20	126	50	68	1	0	22	282	245	75	4	4	23	138	29	66
4	4	20	273	245	17	7	7	0	20	81	161	8	5	20	134	59	66	2	0	22	340	280	39	5	5	23	0	67	1
5	5	20	138	75	34	8	0	20	143	120	66	9	5	20	64	42	63	3	0	22	182	105	61	6	6	23	32	37	31
6	6	20	153	154	34	8	0	20	0	22	1	1	6	20	192	67	51	4	0	22	131	106	102	7	7	23	151	71	61
7	7	20	93	63	93	9	0	20	0	17	1	2	6	20	154	145	45	5	0	22	173	172	61	1	1	23	94	12	84
8	8	20	88	12	88	10	0	20	253	198	34	3	6	20	74	91	74	6	0	22	223	215	42	2	3	23	0	38	1
9	9	20	34	63	33	11	0	20	204	147	46	4	6	20	111	44	89	7	0	22	0	61	1	3	3	23	120	61	74
10	2	22	120	139	56	12	0	20	0	3	1	5	6	20	101	2	100	9	0	22	164	31	70	5	5	23	135	1	57
11	2	22	108	95	92	1	1	20	257	264	18	1	1	21	199	181	25	1	1	22	61	91	61	6	6	23	47	31	47
12	2	22	273	238	25	2	1	20	375	357	14	2	1	21	131	81	42	2	1	22	75	38	75	7	7	23	223	209	43
1	3	22	245	230	19	3	1	20	262	253	18	3	1	21	102	1	76	3	1	22	223	159	29	1	4	23	154	126	45
2	3	22	105	121	56	4	4	20	27	20	27	4	1	21	96	80	95	4	1	22	174	162	41	2	4	23	93	7	92
3	3	22	103	14	86	5	1	20	105	7	67	5	1	21	99	8	98	5	1	22	201	214	34	3	4	23	85	90	84
4	4	22	347	364	15	6	6	20	97	56	96	6	1	21	80	19	79	6	1	22	223	181	32	0	0	24	363	273	60
5	5	22	167	190	31	7	1	20	171	56	34	7	1	21	120	54	63	7	1	22	69	46	69	1	1	24	227	202	68
6	6	22	94	24	93	8	1	20	84	134	83	8	1	21	41	76	41	8	1	22	126	24	64	2	2	24	167	88	109
7	7	22	0	11	1	9	1	20	91	70	90	9	1	21	111	80	86	9	1	22	156	47	51	3	3	24	0	134	1
8	8	22	115	43	73	10	1	20	179	86	35	10	1	21	75	9	74	0	2	22	114	58	113	4	4	24	135	50	134
9	9	22	131	115	57	11	1	20	167	45	40	11	1	21	82	12	81	1	2	22	67	57	67	5	5	24	144	116	144
10	3	23	0	13	1	12	1	20	108	46	107	0	2	21	41	21	41	2	2	22	175	69	33	6	6	24	222	162	76
11	3	23	57	69	57	0	2	20	134	124	59	1	2	21	92	103	92	3	2	22	142	62	44	1	1	24	87	13	86
12	3	23	0	5	1	1	2	20	81	147	81	2	2	21	145	70	38	4	4	22	290	299	21	2	2	24	54	87	54
0	4	19	424	435	22	2	2	20	71	103	71	3	2	21	208	209	25	5	2	22	215	193	28	3	1	24	328	317	25
1	4	19	91	43	90	3	2	20	206	201	24	4	4	21	290	273	20	6	2	22	146	108	57	4	4	24	143	19	71
2	4	19	60	25	60	4	4	20	294	307	18	5	5	21	29	30	29	5	2	22	0	55	1	5	5	24	151	18	74
3	4	19	220	223	24	5	2	20	0	69	1	6	6	21	16	28	16	8	2	22	36	68	35	5	0	24	0	71	1
4	4	19	184	177	28	6	7	20	293	263	21	7	7	21	168	94	41	9	2	22	123	114	113	1	1	24	126	93	60
5	4	19	85	33	84	7	2	20	237	221	24	8	8	21	111	93	111	1	3	22	145	174	42	2	2	24	0	26	1
6	4	19	362	367	17	8	8	20	216	184	25	9	9	21	69	27	69	2	2	22	143	102	44	3	3	24	147	30	64
7	4	19	64	55	64	9	2	20	100	10	100	10	2	21	71	9	71	2	3	22	151	102	47	4	4	24	78	63	78
8	4	19	202	213	31	10	2	20	142	173	47	1	3	21	88	146	88	4	3	22	155	193	42	1	1	24	102	98	102
9	4	19	89	42	88	11	1	20	122	22	68	2	3	21	159	172	35	5	3	22	86	52	86	2	3	24	132	139	61
10	4	19	123	131	105	1	3	20	108	60	55	3	3	21	161	173	36	6	3	22	77	40	77	1	1	25	184	26	58
11	4	19	48	7	48	2	3	20	206	209	25	4	3	21	88	0	88	7	3	22	136	35	63	8	3	25	147	89	56
1	5	19	111	98	65	3	3	20	56	4	55	5	3	21	0	15	1	8	3	22	147	89	56						

